The design and synthesis of compounds that moderate nitric oxide levels

A thesis submitted to Keele University in partial fulfilment for the requirements for the degree of Doctor of Philosophy

By

Phillip Thomson

June 2016

Abstract

Nitric oxide (NO) is a potent biological messenger known to play key roles in many biological processes. Medical conditions such as angina, cancer and some neurodegenerative diseases have been shown to benefit from nitric oxide related therapy. The moderation of *in vivo* levels of nitric oxide is important when considering any lead compounds that exploit NO pathways. It has been theorised that conditions such as Alzheimer's and Parkinson's disease may benefit from a reduction in the levels of NO present in the brain. By inhibiting the nNOS enzyme in brain tissue it is possible to reduce the levels of NO and produce an effective way of treating a number of different neurodegenerative diseases. A series of novel, and chemically simple NOS inhibitors were sought out, building upon evidence alluded from three-dimensional structural docking studies performed using pymol and a 3D virtual environment facility.

In conditions that could benefit from a higher concentration of NO, such as angina and arteriosclerosis, the use of NO-donors is an attractive option. The synthesis of a series of novel NO-donors, based on a furoxan scaffold, of sufficient stability was achieved allowing NO release and vasodilatory studies to be conducted. Compound **94** induced 100% reversal of contraction in rat aortic, renal and pulmonary vessels and was able to release NO under both photochemical and oxidative conditions with an IC_{50} 0.25μM. The vasodilatory effect of compound **94** and other compounds in the series was found to be reproducible and reversible. When compared to the BNF listed NO donor, sodium nitroprusside (SNP, **9**), compound **94** produced a more sustainable relaxation with no fluctuations in vascular tone.

Mechanistically NO release was confirmed using mass spectroscopy and a nitric oxide analyser (NOA) through the application of ozone based chemiluminescence and provided interesting evidence towards the decomposition of this novel furoxan. In addition, a second series of novel NO donors based on the diazeniumdiolates was successfully synthesised alongside X-ray crystallography data, which is pertinent to the debate surrounding the reactivity of both the internal and terminal oxygens in the NONO moiety. These diazeniumdiolate based donors were also investigated using the NOA to identify the bet conditions for NO release, which were found to be light at 254nm.

Acknowledgements

Preface

The majority of the work conducted in this thesis has been carried out in the School of Physical and Geographical Sciences (Lennard-Jones Building- Shelton Laboratories). The biological data was obtained through collaboration with co-workers at Kingston University (UK).

The results seen within this work have been presented at the following conferences and seminars:

P. Thomson and R. J. Pearson, Novel series of NO-hybrids with a furoxan core- poster presentation, UK and Ireland Controlled Release (UKICRS) 2013 Symposium- Reading University, UK

P. Thomson and R. J. Pearson, The design and synthesis of novel C-diazeniumdiolate based NO-donors as potential vasodilatory agents- poster presentation, ISACS 14, Challenges in Organic Chemistry, Shanghai Institute of Organic Chemistry (SIOC), Shanghai, China. August 2014

P. Thomson, The design and synthesis of compounds that moderate nitric oxide levels- oral presentation, Keele University, May 2015.

Contents

Table of Figures

Tables of Schemes

Table of Graphs

Table of Tables

Chapter 1.0- Introduction

Nitric oxide (NO) is a small, gaseous diatomic radical made up of a single atom of nitrogen and oxygen. Before 1987 NO was only considered as a constituent in photochemical smog[1]. Areas of high sun-exposure such as Los Angeles can provide suitable energy for complex radical reactions to occur and the production of smog. Alternatively, NO can also be formed as a by-product of incomplete combustion in the internal combustion engine.

In 1987 it was discovered that NO was not just a nuisance to the environment but was also biologically active and vital to health. In 1869 Frederick Guthrie reported[2] that amyl nitrite when inhaled caused "an acceleration in the action of the heart" and induced a "throbbing in the arteries". It wasn't until 1988 that a major breakthrough in nitric oxide research occurred, when the Nobel Prize for medicine was awarded to three scientists, Furchgott, Ignarro and Murad for their discoveries concerning nitric oxide as signalling agent in the cardiovascular system.[3-6] Robert Fuchgott was researching vascular muscle relaxation and how acetylcholine induced this process. Furchgott conducted an experiment (shown in Fig.1) using rabbit aorta and found that the relaxation of the smooth aortic muscle, upon stimulation with noradrenaline, only occurred when endothelial cells were present. In the absence of the endothelial layer, smooth muscle cells continue to contract in the presence of noradrenaline. This led Furchgott to conclude that there must be a compound or factor inside the endothelial layer that produces this relaxation when exposed to a stimulant such as acetylcholine. He named this unknown substance the endothelium derived relaxation factor (EDRF).
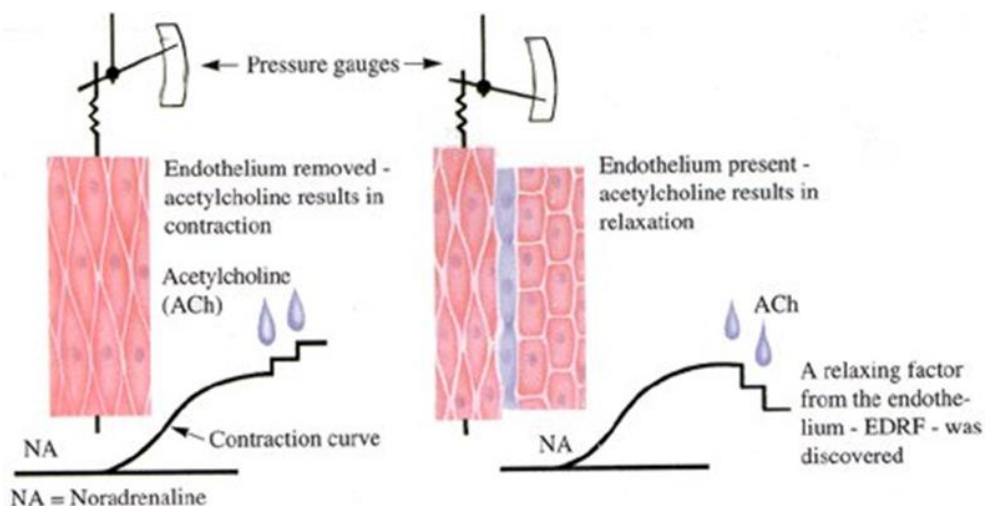
Figure 1: Furchgott's famous experiment: Using rat aorta with and without the endothelium to conclude that the factor EDRF produced vasodialation.[3]

Ignarro[5], who was also researching EDRF, conducted an experiment to see if the effect of nitrogylcerin, which has long been used for the treatment of angina, worked by the release of NO. By doing UV-Vis spectrophotometry (Fig. 2) on haemoglobin in the presence of EDRF and then in the presence of NO he found that the resulting maximum absorbance for the complex formed had exactly the same shift pattern and concluded that EDRF must be NO[3,5].
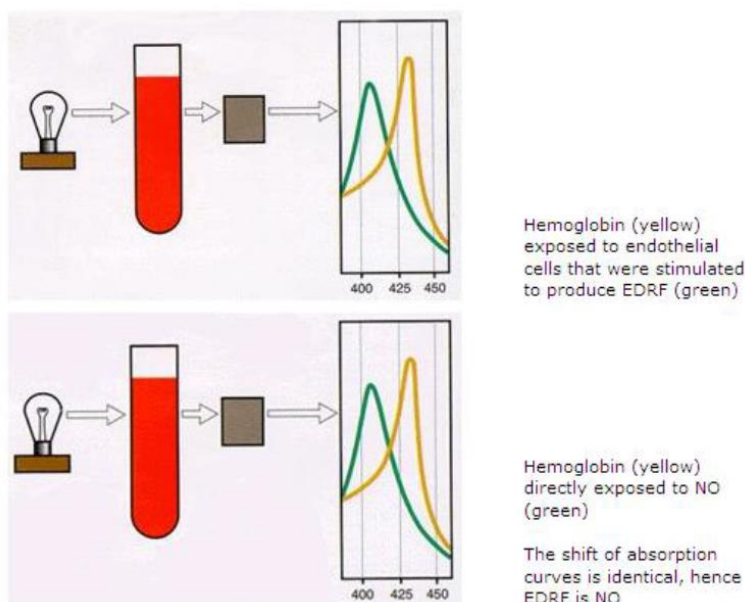
Figure 2: Experiment performed by Ignarro to show that NO and EDRF were the same compound[5].

Murad's research[6] was concerned with the mechanism by which nitroglycerin relaxed smooth muscle cells. He found that nitroglycerin activated an enzyme called guanylyl cyclase (GC), the key enzyme in smooth muscle relaxation, which produced cyclic guanosine monophosphate (cGMP), a compound known to be involved in the relaxation of smooth muscle.[3,6] Murad wanted to determine whether nitroglycerin acted via the release of nitric oxide, as suggested by Furchgott in an earlier publication, so he bubbled nitric oxide gas through a section of tissue containing the enzyme guanylyl cyclase and found that the concentration of cGMP increased thus suggesting that nitric oxide is involved in the activation of GC.

At a similar time it was concluded by a fourth scientist, Moncada, that EDRF was in fact the diatomic molecule nitric oxide as he found that the relaxation of endothelium tissue with EDRF was indistinguishable from the results produced by nitric oxide and thus EDRF had to be NO.[7,8]

1.0.1- Reactions of NO

Nitric oxide is formed from the combination of one atom of nitrogen and one atom of oxygen producing a compound with an unpaired electron. Therefore by definition NO is a radical species however, it isn't as reactive some radicals such as the hydroxyl radical.[9]

In the gas phase nitric oxide reacts with oxygen to produce nitrogen dioxide as a brown fuming, toxic gas (shown in scheme 1). This only occurs at high concentrations, not consistent with those found *in vivo* and as the half-life of NO[10] is quite short (approximately five seconds) it is unlikely that this reaction occurs in the body to any great extent.

$$2\ \overset{\bullet}{N}O\ + O_2 \longrightarrow 2\ NO_2$$
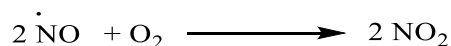
Scheme 1: Reaction nitric oxide with molecular oxygen to produce the toxic gas NO_2

A more likely pathway involves superoxide (O_2^-), a reactive oxygen species, found and produced in the electron transport chain in respiration, and produced in macrophages by the enzyme NADPH oxidase. Superoxide reacts with nitric oxide to produce a compound known as peroxynitrite ($ONOO^-$) as shown in scheme 2. Due to superoxide's being as a cytotoxic compound, the decomposition of NO actually performs a beneficial action by detoxifying superoxide.
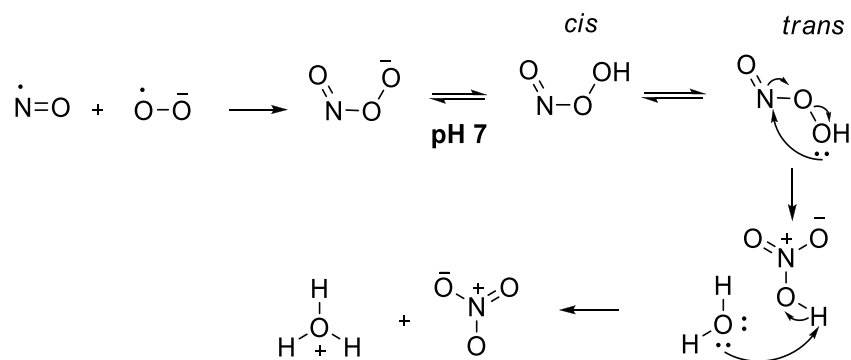
Scheme 2: Reaction of nitric oxide with superoxide anion: The *in vivo* metabolism of NO

Peroxynitrite ($ONOO^-$) is a stable anion and is initially produced as the *cis* isomer due to the creation of a ion-dipole interaction. Once protonated at a neutral pH it isomerises to the *trans* conformer, which rapidly decomposes to produce the nitrate anion (NO_3^-) and is then excreted in urine by the body. Peroxynitrite itself has been linked to a number of negative effects in the body and is believed to be a main contributor to DNA damage when it's overproduced. If superoxide concentrations increase by 10 fold the levels of peroxynitrite are seen to increase by a 100 fold thus creating quite high levels of a fairly strong oxidant. Regulation of this by-product and the constituent compounds is a constant battle that the body must respond to.

1.0.2- Biosynthesis of NO

Nitric oxide is produced in the body at the site of action by a class of enzymes known as the nitric oxide synthases which catalyse the conversion of L-arginine **1** to L-citrulline **2** through a five electron transfer process resulting in the production of nitric oxide. The L-citrulline **2** is then recycled back in to L-arginine **1** by reduced NADP to start the process again as shown below in scheme 3[11].
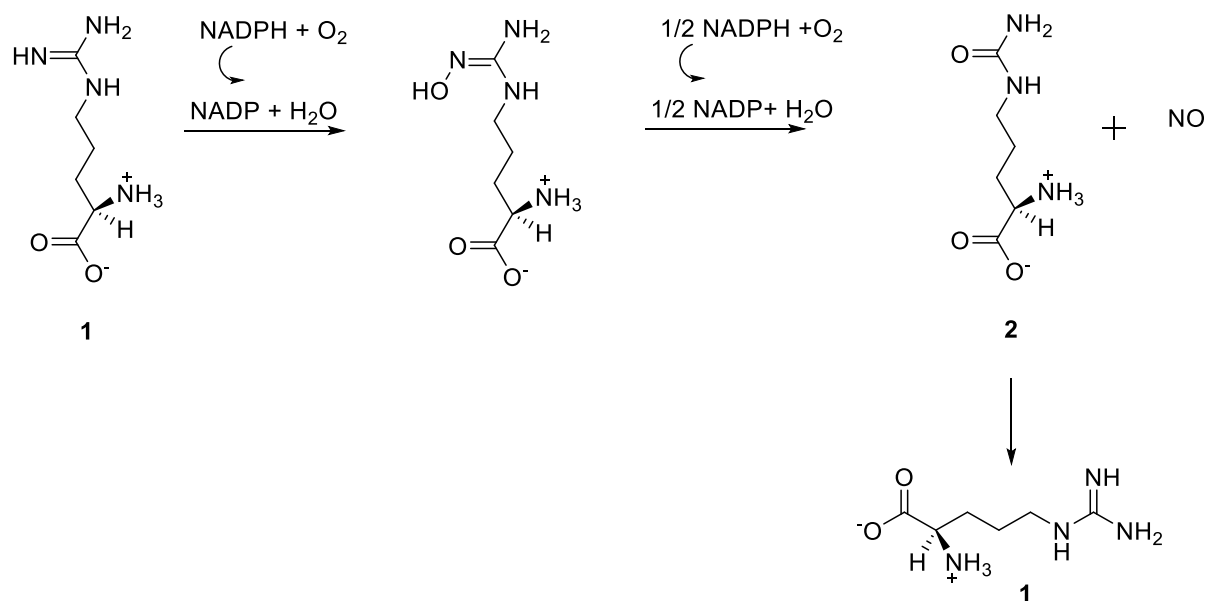
Scheme 3: Conversion of the simple amino acid L-Arginine to L-Citrulline and the production of NO, a reaction catalysed by the enzyme NOS. Adapted from A. R. Butler[1]

There are three types of NOS enzyme named after where they were originally discovered in the body, the endothelium, within neurons and the immune system. The three isoforms of NOS can be further divided into two different sub-classes: constitutive NOS and inducible NOS. Their location and actions are summarised in Table 1.

Properties	Constitutive		Inducible
	eNOS	nNOS	iNOS
Source	Endothelial cells	Neurons, cerebral tissue, skeletal muscles, nerve fibres	Hepatocytes, Macrophages, T-cells, Glial cells
Number of amino acids	1203	1554	1153
Stimulant required for activation	Acetylcholine	Glutamate	Cytokines
Dependence	Ca^{2+}	Ca^{2+}	Ca^{2+} independent
Primary Function	Vasodilation	Cell communication	Immune response

Table 1: Location and function of the three isoforms of the NOS enzyme. Adapted from P. Tripathi, 2007[12]

Constitutive NOS is comprised of the endothelial and neuronal NOS enzymes, and are both known to be calcium dependent. After either acetylcholine or glutamate has bound the protein calmodulin, calcium channels are opened providing an influx of Ca^{2+} ions into the cell which then activates the relevant NOS enzyme to catalyse the production of nitric oxide. NO then diffuses out of the tissue to carry out its various actions as described in Fig. 3. The activity of inducible NOS (iNOS) is independent of calcium concentration and instead is normally activated in response to an external stimulus, such as the initiation of an immune response.[12,13,14] Inducible NOS (iNOS) produces a much higher concentration of NO compared to the constitutive NOS enzymes and is involved in the 'flight or fight' mechanism.
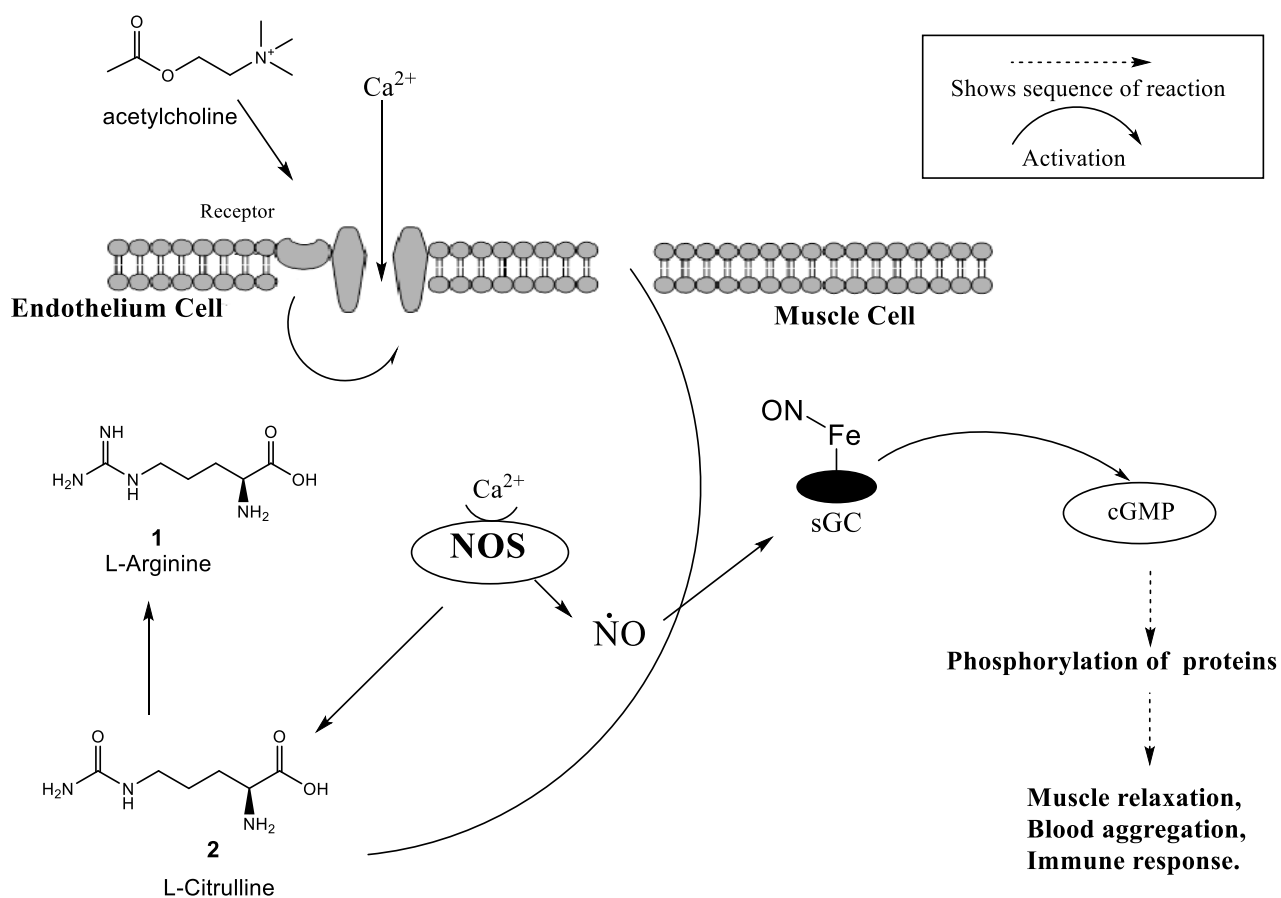
Figure 3: NO production within the endothelial cell that leads to a cascade of different reactions

One of the primary uses for nitric oxide in the body is as a vasodilator, increasing vascular blood flow by causing the relaxation of smooth muscle cells, as depicted in Fig. 3. Nitric oxide, produced by eNOS, binds to the haem centre of soluble guanylate cyclase **3** (sGC). It is the affinity of nitric oxide for iron (Fig. 4) that causes the activation of sGC catalysing the cyclisation reaction of guanosine-5'-triphosphate (GTP) to cyclic guanosine monophosphate or cGMP, which then initiates a cascade of reactions that eventually lead to the relaxation of smooth muscle cells and the reduction of blood pressure.[1, 15]
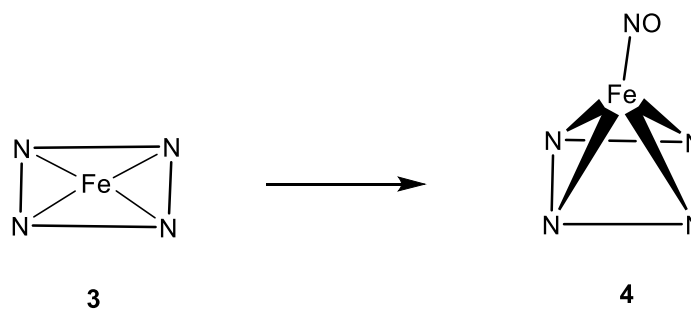
Figure 4: The ferric centre of guanylate cyclase and its activation when NO binds (adapted from A. R. Butler, 2003[1])

1.0.3- Biological roles of NO

Blood is essential for transporting oxygen to cells and organs so it can be used in the Krebs cycle to produce energy in the form of adenine triphosphate (ATP) so the cell, tissue or organ can carry out its plethora of functions. When a cut occurs, and the body starts to lose blood, it is very important to stop this bleeding as fast as possible so that homeostasis can be restored. A very complex and sophisticated mechanism is in place to repair and fix these problems, of which NO is a major component. When damage occurs in an endothelium layer, platelet aggregation acts as a plug and stops the blood escaping from the small vessels. NO is produced by both endothelial cells and platelets along with a chemical known as the von Willebrand factor, which causes platelets to adhere to endothelial cells. Once a platelet becomes stuck, it promotes more to attach and creates a 'plug'. With this platelet plug in place, a protein present in the blood plasma called fibrinogen polymerizes into the commonly known protein, fibrin. This creates a mesh type structure, trapping blood cells and creating a gel-like complex or a clot. This process should only happen when damage has occurred to the endothelial cells but it can sometimes happen when unprovoked.

If a clot forms when bleeding has not taken place for it to be induced, this can cause serious issues, such as blocking important blood vessels, which could lead to heart attacks or strokes. NO is also key to solving this problem, not only does it promote platelet aggregation but it can also help prevent

it. Like in smooth muscle cells platelets contain guanylate cyclase (GC) which NO can readily bind to and cause a cascade of biochemical reactions.

This leads to the internal concentration of calcium ions increasing, affecting the adhesion properties of the platelets and preventing them from aggregating in the same manner thus reducing the clots size and potential for damage. [1,7]
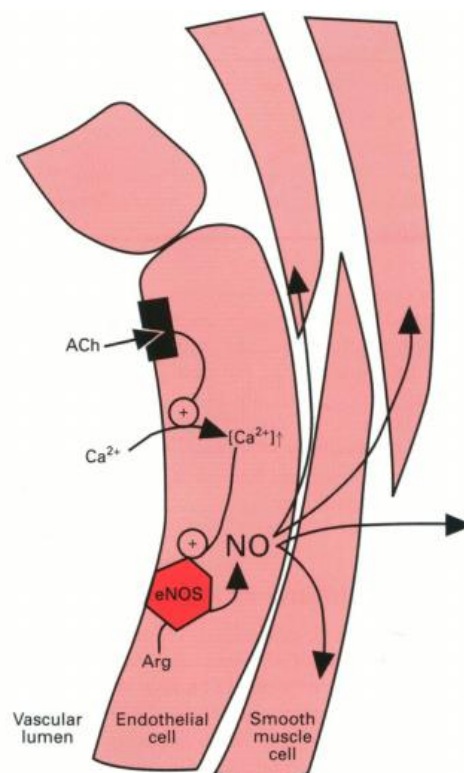
Figure 5: Schematic diagram of eNOS increasing levels of NO in smooth muscle cells which can decrease blood pressure. Taken and adapted from reference 16.

The human brain is a very complex organ with an unquantifiable amount of neurones, all working independently from each other and controlled by simple electrochemical signals being passed between synapses. For a signal to transfer across the synaptic cleft, small molecules called neurotransmitters are needed to convert the electrochemical signal to a chemical response. Due to the size of the nitric oxide molecule it can readily diffuse across membranes, makeing NO an versatile

neurotransmitter. NO is formed in the postsynaptic nerve cell following the activation of nNOS and readily diffuses outwards to act upon neighbouring cells [17].

Unlike other neurotransmitters NO is not terminated by re-uptake mechanisms and instead the concentration of NO is only terminated by its forward reactions with other substrates like guanylate cyclase or superoxide.
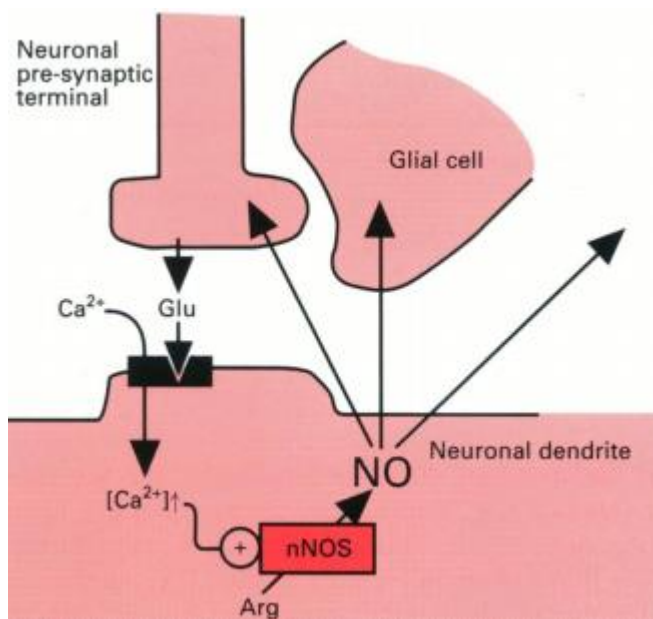
Figure 6: Schematic diagram showing NO as a neurotransmitter produced by nNOS. Taken and adapted from reference 16.

As much as NO plays a positive role within the body, causing vasodilation, nerve responses and being embroiled in long term memory development, it has also been found to be heavily involved in the regulation of foreign bodies and apoptosis. The body has two main defence cells involved in the deletion of harmful substances. Granulocytes and macrophages both of which contain digestive enzymes to dispose of their targets through a process known as *phagocytosis*. Within these cells the NO producing enzyme iNOS, the isoform known to produce highest concentrations of NO, has been found in high abundance[12] especially in cases of inflammation and infection, indicating that nitric oxide plays a role in the immune response to these stimuli. Due to the short half-life of NO it is unlikely that NO directly causes cell death and it is more apparent that it initiates a cascade of

reactions that brings about apoptosis. As already described, NO readily reacts with superoxide to form peroxynitrite (ONOO$^-$) a very powerful oxidant. It is thought that it is this reactive molecule that causes the cytotoxic effects associated with nitric oxide.[1, 13, 14]
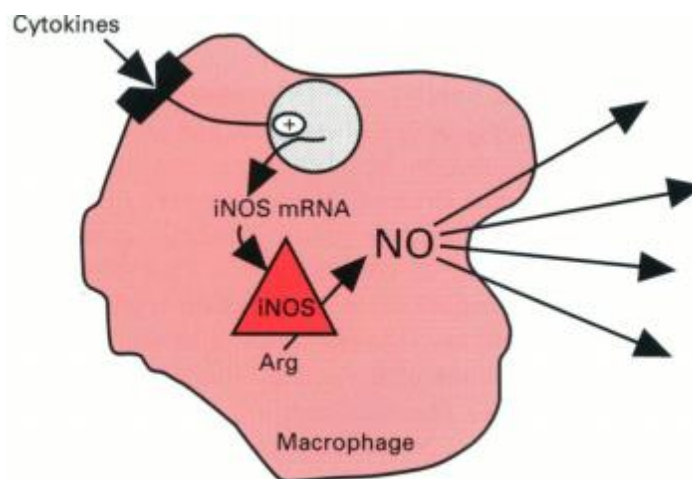
Figure 7: NO produced by iNOS is involved in immune response and is produced in much higher concentrations than that seen by the other isoforms. Taken and adapted from reference 16

The production of peroxynitrite can cause amino acid nitration, particularly to tyrosine and thus can result in enzymes being denatured.[17-21] Peroxynitrite alone may not, however give the whole picture of NO's cytotoxicity towards foreign bodies. NO binds strongly to metal ions as already seen within the ferric centre of guanylate cyclase[22] (as shown in Fig. 3 and 4). Many enzymes in mammalian cells contain metal ion centres for example the enzyme aconitase, an important enzyme used in the oxidative phosphorylation process in respiration. This enzyme is known to have a ferric core and therefore binds readily to a molecule of NO, which causes enzyme inhibition or denaturation. If this was to occur in the cells of an unwanted, foreign body, like a microbe, respiration would be disrupted leading to cell death.

The level of nitric oxide present in a cell or tissue is key to the interaction and effect that will be caused. Too little NO can cause an increase in blood pressure and the potential for clots to form as well as insufficient polarisation of neurons for the correct signals to be sent within the central nervous

system (CNS). On the other hand, if the concentration of NO is too high it can cause cytotoxic effects from DNA damage to disease progression. Although this is beneficial in terms of microbe deletion and as an anti-inflammatory agent, if the concentration remains high it can cause damage to healthy cells. Therapeutically moderating and influencing levels of NO is a useful tool for helping the body remain at a homeostatic level. This can be achieved by designing molecules that can either increase or decrease systemic levels of nitric oxide. The alteration of these levels in disease systems and states could be a successful treatment option and is a viable research area.

1.1- Enhancement of NO levels

Nitric oxide is involved in several biological processes including blood pressure regulation, platelet aggregation, microbe defence and several others as already discussed previously. Medically these processes can be affected by increasing the concentration of NO involved in these specific processes and could be used as potential therapeutic options in several conditions such as angina, arteriosclerosis, erectile dysfunction, cancer, Raynaud's syndrome and even in vascular stents and for wound healing applications.[1,7,15,17]

Other than increasing our consumption of foods containing L-arginine, which is the known substrate for NO production, there needs to be a method of sustainably increasing systemic levels of NO in a controlled way. This can be achieved using donor compounds that have been designed specifically to decompose and release a known concentration of NO at the desired site of action. Ever since the discovery of NO as a biological messenger molecule, a myriad of different NO donors have been investigated and are now grouped into various classes depending on their structures and properties. Long before the role of NO in vasodilation was discovered, clinicians have been prescribing drugs that produce nitric oxide to combat angina and heart attacks, although their mechanism of action, via the release of NO, was not known at the time. One of the oldest known NO-donors is GTN, glyceryl trinitrate, **6** or as it's more commonly recognised nitroglycerin, the explosive ingredient in dynamite. It was first discovered in 1847 by Italian chemist Ascanio Sobrero[23,24] who was experimenting with

glycerol **5** and strong acids (scheme 4). GTN, **6** is a very explosive liquid that can be detonated just by vibrations so at first Sobrero kept his discovery secret for more than a year, as he was afraid of its potential for harm and militarisation from his government.
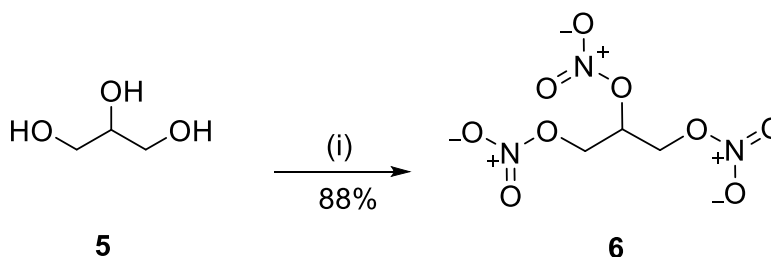
Reagents and conditions: (i) HNO_3/H_2SO_4

Scheme 4: The nitration reaction of glycerol to form the powerful explosive nitroglycerin or GTN.

Famous chemist and founder of the Nobel Prize, Alfred Nobel, a student of Sobrero's was the first person to find a commercial use for GTN **6** when he stabilized it by mixing it with silica (clay) to form what we now know as dynamite.[24] However GTN **6** is not limited to being used as an explosive. It was first used medically by the physician William Murrell in 1878 for the treatment of angina. Murrell[25] found that a 1% solution of GTN **6** in ethanol reversed the symptoms of angina. At the time this was a fantastic discovery as it was a topical treatment for quite a series illness, patients could put a patch of GTN **6** under the tongue and have the symptoms reversed within minutes. However this was not without its short comings, excessive GTN **6** use can lead to temporary tolerance of the drug. This phenomenon was described as the 'Monday morning headache'. Workers at the factory that produced GTN **6** would find that after the weekend that they would have a terrible headache on their return to work. This was attributed to the rapid onset of vasodilation when they became exposed to GTN once returning to work after a two day break.

Nitroglycerin **6** is a potent vasodilator belonging to the class of compounds called organic nitrates, due to the nitrate groups contained in its structure. Essentially it is a pro-drug, as upon absorption it is rapidly broken down to release nitric oxide which then proceeds by the mechanism highlighted

(Fig. 3 and 4) earlier to induce relaxation of smooth muscle cells. Other organic nitrates (Fig. 8) have been developed with similar effects to GTN **6** but are not as regularly prescribed[1,26]. Isosorbide dinitrate **7** (ISDN) is a more stable version than GTN[26] and therefore has a much slower release of NO. It is therefore used for long term treatment and is applied as a sublingual medicine; however the issues of tolerance still occur with this compound. Pentaerythrityl tetranitrate **8** (PETN) is also an organic nitrate, very similar to GTN in structure and has the ability to release NO rapidly, and does so without building up tolerance. Although a good NO-donor compound, due to the extra nitrate group and the ratio of nitrogen to oxygen PETN **8** is classed as being highly explosive and has been implicated in several terrorist attacks since its initial production, and so it is no longer commonly prescribed.

7
Isosorbide dinitrate (ISDN)

8
Pentaerythrityl tetranitrate (PETN)
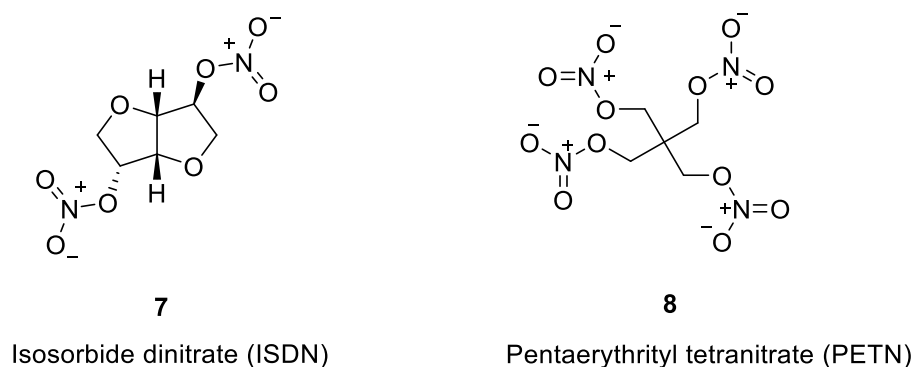
Figure 8: Modern alternatives to GTN for use as NO-donors.

Clearly having compounds that are good NO-donors but also high explosives is not very pharmaceutically viable. This major drawback led to the development of a number of different classes of NO-donors, with different structural features and stabilities either through structural design or serendipity. The vast majority of NO donors are organic based compounds, however there are a few compounds, one of which can be found in the BNF (British National Formulary[26]) that are classed as inorganic NO donors or metallic nitrosyls. The most commonly recognised compound in this class is sodium nitroprusside **9** (SNP) a bright red cyanoferric compound (Fig. 9).
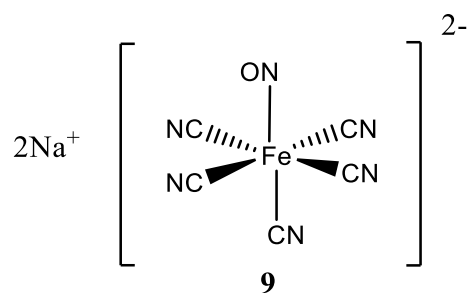
Sodium nitroprusside (SNP)

Figure 9: Sodium nitroprusside, an example of a metallic nitrosyl.

SNP **9** rapidly releases nitric oxide in the presence of both thiols and light. Several theories surround the actual mechanism of release but it is commonly reported that SNP binds to oxyhaemoglobin and in doing so produces NO, cyanide and methemoglobin. The production of the by-product hydrogen cyanide (HCN) is associated with most of SNPs side effects, from intracranial bleeds to cyanide poisoning and is one reason for its more limited use nowadays.[27] Another theory on its release is that endogenous thiols such as glutathione or cysteine react with SNP form an *S*-nitrosothiol **10** as an intermediate compound which then decomposes to release NO into the bloodstream. Studies have shown that a thiol-iron complex is detectable, using UV-Vis spectrophotometry at a wavelength of 560 nm, suggesting that SNP may release NO via this mechanism[27] shown in scheme 5.
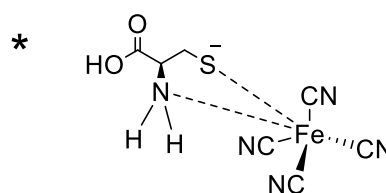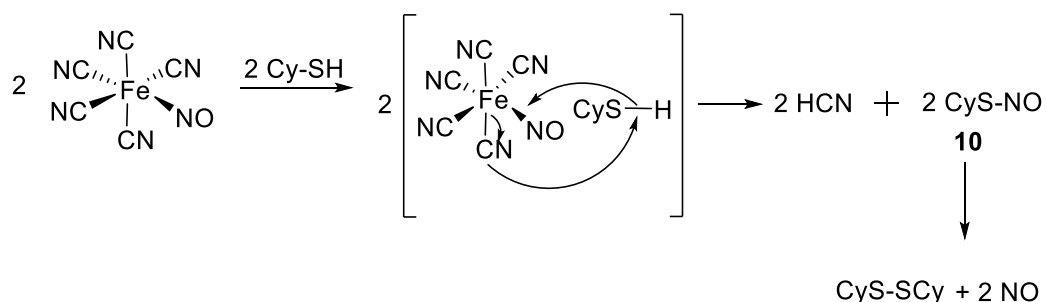
Scheme 5: Proposed[28] mechanism of SNP decomposition by cysteine resulting in the formation of an *S*-nitrosothiol and a cysteine-iron (II) complex as shown by the asterik.Another compound from the inorganic NO-donor class is an intensely black, crystalline solid first discovered by a French army scientist named Francois-Zacherie Roussin, and is aptly known as Roussin's black salt[29] **11** shown in Fig. 10.

11

Roussin's black salt
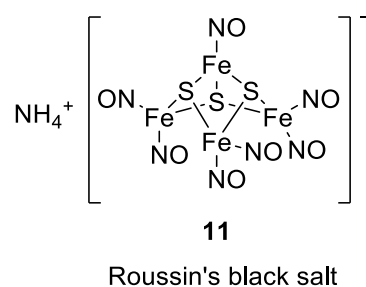
Figure 10: Roussin's black salt, a potent inorganic NO donor[29].

Produced from the reaction of nitrous acid, potassium hydroxide, potassium sulphide and iron (II) sulphate, Roussin's black salt **11** is a known NO-donor and has even been linked to having anti-bacterial effects. Roussin's discovery was made by mere accident when investigating nitrous acids ability to make azo dyes when treated with various amines. This crystalline black salt served as a novel way of 'storing' NO at the time of its discovery and could be forced to release NO readily by addition of different copper salts.[29]

1.1.1- *S*-Nitrosthiols (SNOs)

S-Nitrosothiols, also known as thionitrites, are organic compounds that have a nitroso group attached to a sulphur atom of thiol group. Their general formula is written as R-SNO. The synthesis of these compounds is relativity straightforward and was first conducted in 1909 by H.S. Tasker[30] through the reaction of nitrosyl chloride (**12**) with thiophenol (**13**) to yield a 'red-wine' coloured compound, **14** (scheme 6). Tasker reported that the new thiol compound rapidly gave off nitric oxide at room temperature, indicating how unstable these RSNOs are under mild conditions.[31]
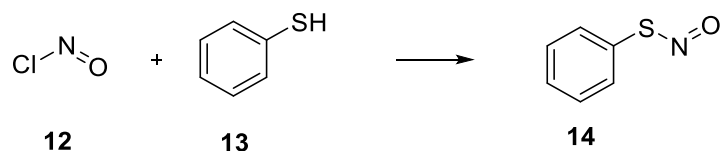
Scheme 6: First described synthesis of an *S*-nitrosothiol by Tasker in 1909[30].

The first synthesis of *S*-nitrosothiols, opened up a gateway to the production of more stable versions of the RSNO structure. Historically these compounds are brightly coloured with primary and secondary thiols, producing red or pink crystals whilst tertiary thiols yield green compounds.[32] The intensely coloured properties of these compounds can be exploited analytically, especially using UV-Vis spectrophotometry, as the evolution of NO can be monitored by the loss of colour. The current, classic way of making substituted RSNOs is to react the thiol of choice with a form of NO^+, which is usually generated as N_2O_4 under acidic conditions.[30-34]

NO has a relatively shot half-life, and measurable concentrations in tissues have been found in the nanomolar range meaning that the body has a way of chemically 'storing' it in the blood plasma. This is done *in vivo* by the nitration of endogenous thiols (shown in Fig. 11) such as cysteine (**16**) and glutathione **17** shown in the figure below and can be found in the micromolar range within tissues.[35,36]

16	17
L-Cysteine	Glutathione

18	19
S-Nitrosocysteine	*S*-Nitrosoglutathione (GSNO)
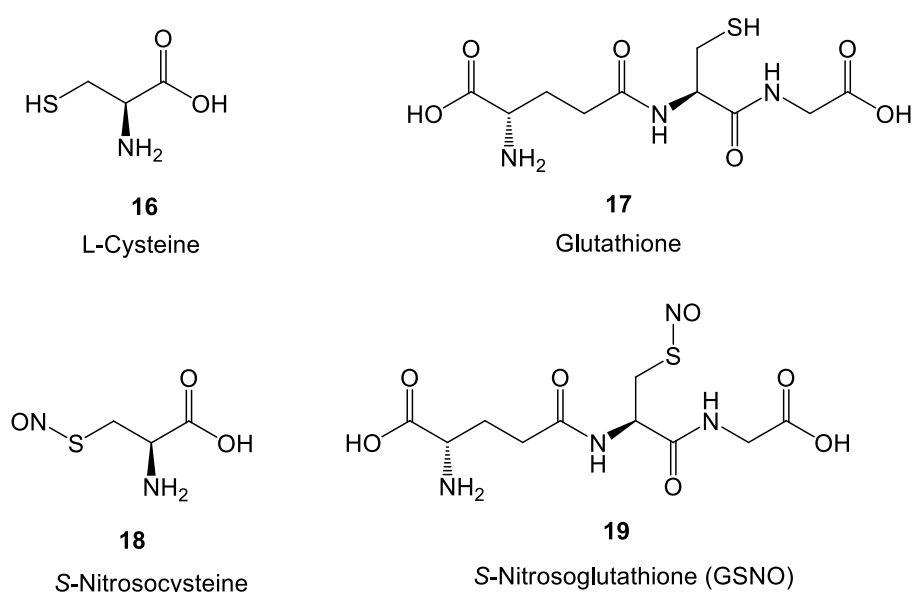
Figure 11: Two common endogenous thiol compounds **16**, **17** and their *S*-nitrosothiol counterparts.

Once an *S*-nitrosothiol has been formed *in vivo* it can readily diffuse throughout the tissue and essentially 'deliver' NO to other sites in the tissue and act as a reservoir of nitric oxide. Trans-nitrosation (scheme 7) can also occur, where nitric oxide is exchanged from one thiol compound to another.[37] This enables the nitrosation of a variety of compounds such as proteins and even serum albumin[38] and allows the body to maintain a relatively constant level of NO when not producing it through the NOS catalyzed reaction.

$$RSNO \; + \; R'S^- \; \rightleftharpoons \; R'SNO \; + \; RS^-$$
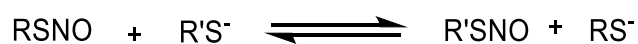
Scheme 7: General reaction of transnitrosation of an endogenous thiol *S*-nitrosothiol where R≠R'.

S-Nitrosothiols decompose readily to afford NO and the corresponding disulphide via a homolytic bond cleavage as shown in scheme 8.[39] Heterolytic cleavage can also occur but this does not produce the desired form of NO, as it instead produces either the positively or negatively charged NO ion depending on the movement of electrons.[40-41]

$$2 \; RS-NO \longrightarrow 2 \; R\dot{S} \; \; 2 \; \dot{N}O$$
$$\longrightarrow RS-RS$$
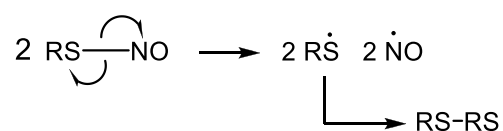
Scheme 8: General decomposition reaction of RSNOs, usually via homolytic cleavage and the formation of radicals[34].

RSNOs can undergo three different types of decomposition to produce nitric oxide.[40] Thermal decomposition, where temperatures as mild as room temperature can sometimes be sufficient, is believed to be a two-step process, which firstly involves the homolytic S-N bond cleavage to produce the two corresponding radicals and is then followed by two thionyl radical dimerizing to give the disulphide. Literature indicates that the rate of thermal decomposition depends of the stability of the

starting thiol, for instance primary and secondary thiols decompose more rapidly than tertiary ones due to stabilising steric and inductive effects[42].

A second type of NO release is photochemical decomposition. As the name suggests this is the breakdown of the RSNOs due to light, especially UV light. When a RSNO is irradiated with light, particularly at a wavelength of 340 or 545 nm, the RSNO decays to give NO.[43]

A third method of RSNO decay is via metal ion catalysed decomposition and is shown in scheme 9. The breakdown of RSNOs can be catalysed by certain d-block metals such as iron, mercury, silver and copper.[43-45] Copper, found in relatively high concentrations in the body has had the most focus in terms of research. It is thought that copper in the form of Cu^{2+} is reduced by the RSNO primarily, and initiates a chain reaction in which the Cu^+ ion reacts with another RSNO to yield the disulphide and nitric oxide.[41]

$$2RS^- + 2\,Cu^{2+} \longrightarrow RSSR + 2Cu^+$$

$$Cu^+ + RSNO \longrightarrow Cu^{2+} + RS^- + NO \xrightarrow{H^+} RSH$$

$$RSH + HNO_2 \longrightarrow RSNO + H_2O$$
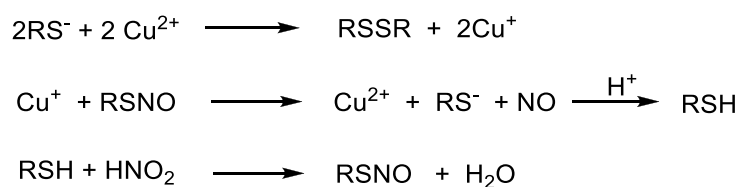
Scheme 9: Decomposition of RSNOs is catalysed by copper producing NO and free thiol.[41, 46]

An example of this type of decomposition is illustrated by *S*-nitroso-1-thio-2,3,4,6-tetra-*O*-acetyl-β-D-glucopyranose **19** (SNAG) which binds to copper ions and breaks down by the pathway shown in scheme 10. This decomposition occurs via the formation of a new seven membered intermediate, **20**, involving the copper ion and the lone pairs available on both the sulphur and oxygen atom.[41,44]
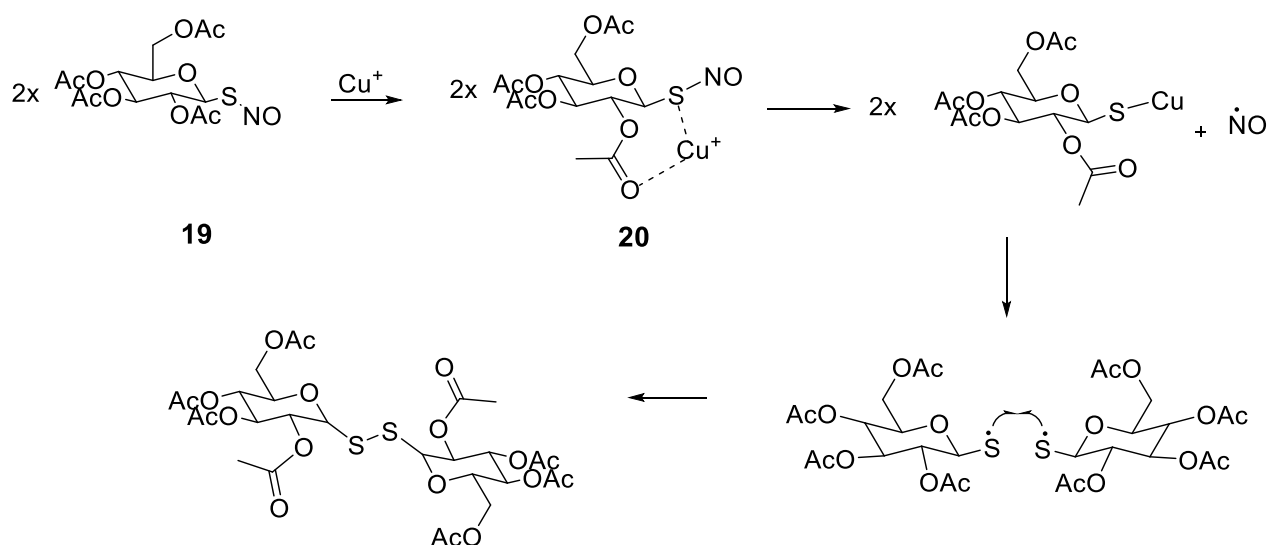
Scheme 10: Copper catalysed decomposition of SNAG **19**, a carbohydrate based *S*-nitrosothiol. The reaction proceeds via a **7** membered intermediate compound, **20**.

SNAG **19,** as well as the majority of other S-nitrosothiols, is known to cause vasodilation and relaxation of smooth muscles *in vivo* through the release of nitric oxide upon decomposition. Butler[47] and researchers found that treatment of the human forearm with SNAG **19** produced significant, dose-dependent vasodilation in a reproducible manner. Graph 1 shows a summary of their data, showing that as you increase the dose of SNAG **19** the Laser Doppler Flux increases in a positive correlation. The Laser Doppler Flux is used to measure the blood flow in the skin. This is done by scanning the surface with a laser beam (2 mW) and measuring the resulting back scattering of light from erythrocytes, whose velocity will change depending on the rate of blood flow. The faster the flow (increased vasodilation) the greater the Laser Doppler flux.[47]
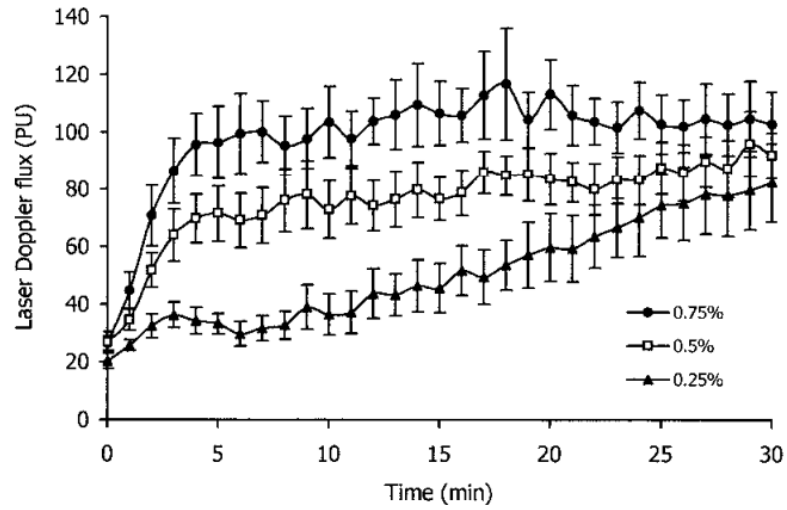
Graph 1: Vascular responses to three doses of SNAG **19** applied to the forearm skin of eight males. Taken from reference 47

1.1.2- NO-hybrids

As previously mentioned, nitric oxide plays a key role in vasodilation and immune response, but producing viable NO-donors is a relatively new research area over the past 40 years. One strategy many researchers use is to combine an already proven drug with a NO donating group, to form a NO-hybrid; such hybrids represent an expanding area in the NO-donor work. These 'dual-action' compounds can work symbiotically to either promote more than one response or reduce associated side effects. The rationale behind these compounds is to promote an existing drug compound, with a proven track record of effects, and increase its activity by having an additive effect when coupled to a NO-releasing group, as well as incorporating nitric oxide's cytoprotective nature[48]. A common series of compounds linked to NO are the non-steroidal anti-inflammatory drugs (NSAIDs) such as aspirin **21**, nicorandil **22**, naproxen **23** or ibuprofen **24** [49-53] (Fig. 12). It has been found that the introduction of NO into these existing drugs has reduced the side effects associated with them such as GI disturbances and ulcer formation. A study by Gasco[49] found that having the NO moiety present in the NSAID reduced gastric ulcerogenic properties without affecting the anti-inflammatory activity.
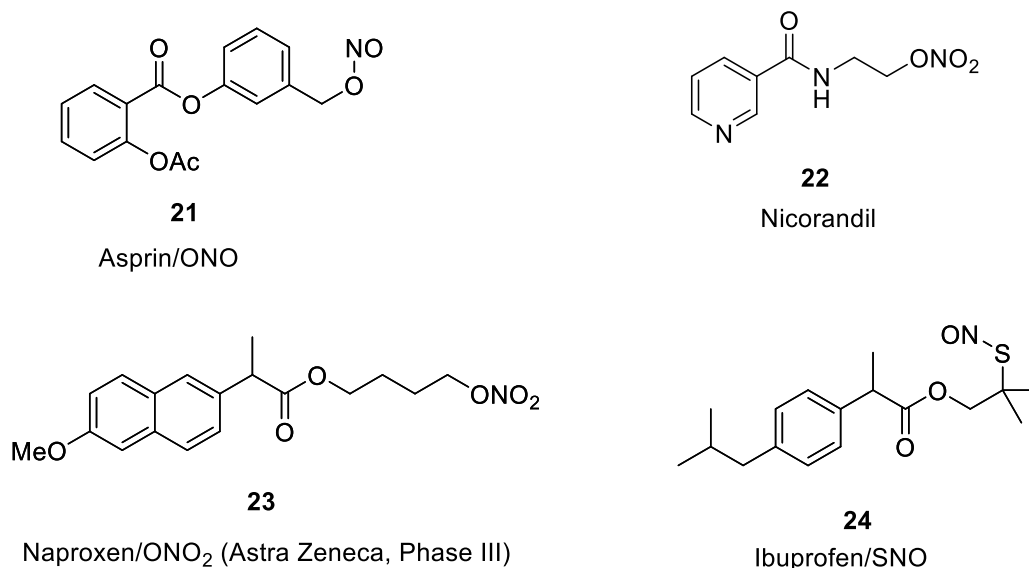
Figure 12: Commonly prescribed NSAIDs coupled with an NO donor to make novel NO-hybrids[48-52].

Nitric oxide has also been coupled to a plethora of different drug compounds, to create dual action compounds with enhanced biological profiles. Examples range from β_2-agonists **25** for treating pulmonary disease,[54] anti-malarial compounds **26**,[55] and calcium channel blockers **27**[56] to bisphosphonate drugs **28**[57] that treat osteoporosis and has even been seen to reverse multidrug resistance (Fig. 13). This wide array of examples shows the enormous potential for NO-donors in pharmaceutical research and their varied applications.

25
β_2-agonist/NO donor

27
Ca^{2+} channel blocker/ NO donor

26
Anti-malarial/ NO donor

28
Osteoporosis/ NO donor
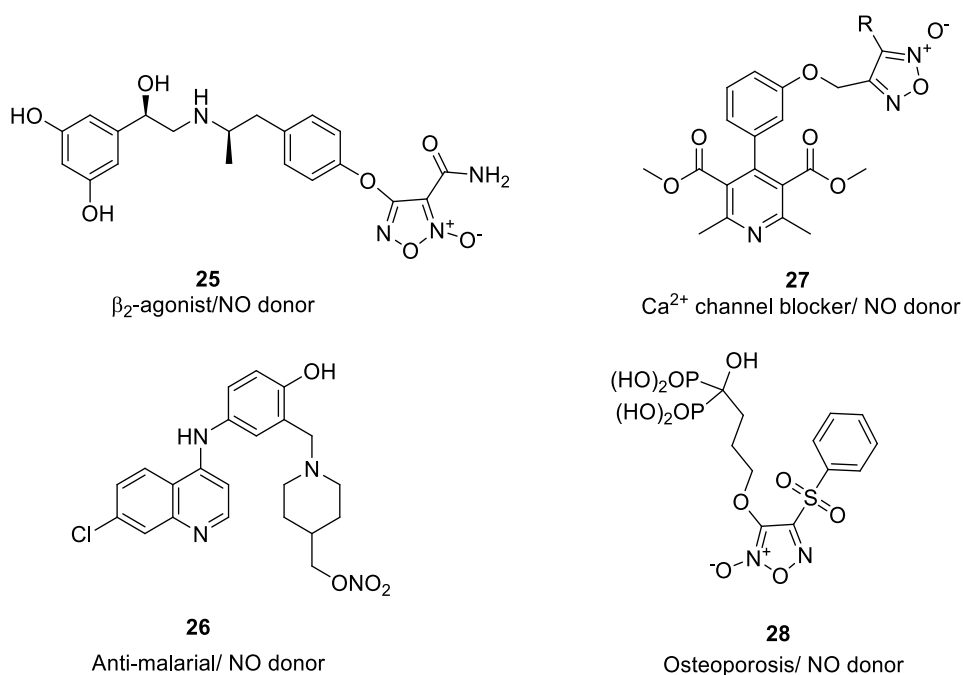
Figure 13: NO-hybrid versions of common marketable drugs used to treat various conditions.

1.1.3- Furoxans

The furoxans, also known as 1,2,5-oxadiazole-2-oxides **29** (Figure 14) have the NO moiety 'locked' in a five membered heterocyclic ring system which improves stability allowing the release of NO in a more controlled manner compared to *S*-nitrosothiols and the metallic nitrosyls.

R=R' or R≠R'
alkyl or aryl substituents
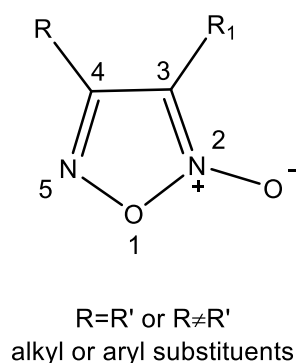
29

Figure 14: The general structure and numbering system of 1,2,5-oxadiazole-2-oxide compounds also known as furoxans.

Furoxans are known to decompose to give nitric oxide via several different mechanisms. The usual manner of decomposition (scheme 11) is via a photochemical reaction but they can also ring open in the presence of thiols. Glutathione **17** can attack the ring system at the three position, to give an alkyne and NO. Depending on the substituents, such as a carbonyl group (see scheme 12), this can cause the furoxan ring to convert into an isoxazole ring, **31**, which is brightly coloured, and releases NO_2 (a characteristic brown gas) which is then converted into water and nitric oxide.[58-60]

ᨧᨧ Denotes rest of molecule
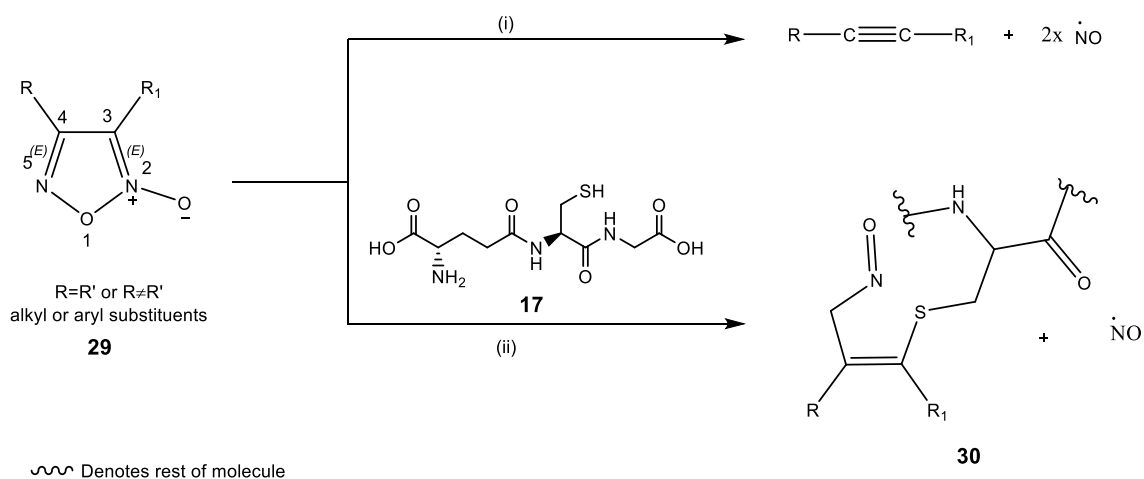
Reagents and conditions: (i) *hv* (ii) thiol/thiolate

Scheme 11: The general decomposition pathways for furoxans[58-60].

The mechanistic differences in release can be utilised when monitoring NO release from furoxan compounds and therefore the stability of the parent compound. The isoxazole, **31,** by product formed by production of NO can easily be monitored using UV-Vis spectrophotometry, yielding peaks at 254 nm (the yellow region of the electromagnetic spectrum). [61, 62]
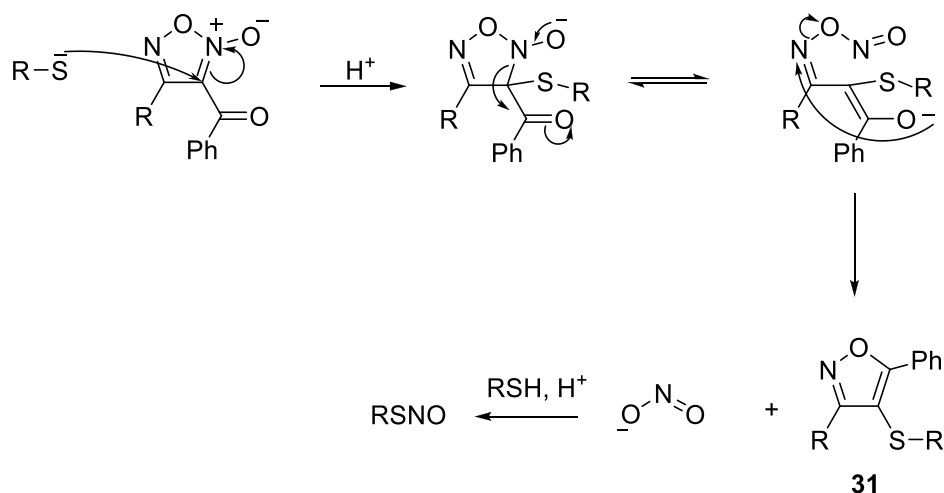
Scheme 12: Thiol induced decomposition of furoxans produces the isooxazole compound 31 and nitrite.

Furoxans were first synthesised in 1845 from the oxidation of anethole **32**, a common aromatic flavouring, by a chemist called Tonnies (scheme 13). Tonnies reported[63-64] that treatment of anethole with sodium nitrite produces 'a compound that has gained two atoms of nitrogen and oxygen'. Following this first ever production of a furoxan ring there have been several different procedures and conditions developed to produce a library of 1,2,5-oxadiazole-2-oxide compounds.
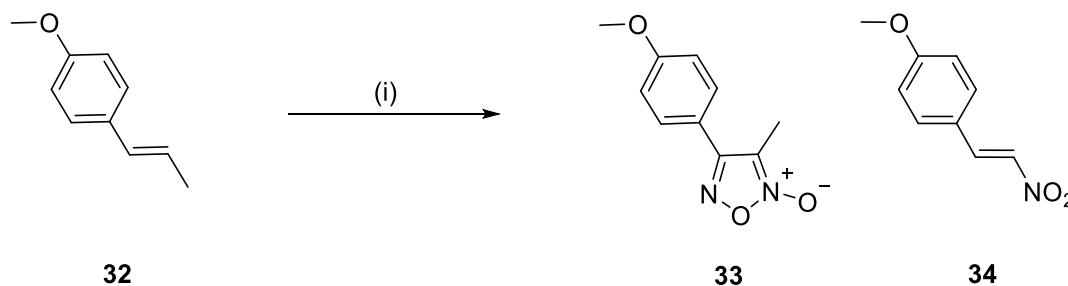
Reagents and conditions: (i) $NaNO_2$, CH_3COOH/HCl

Scheme 13: The first synthesis of a furoxan, **33**, starting from anethole, **32**, using acidic conditions.

The site of reactivity of the first synthesised furoxan is the double bond in anethole **32**, so it's not surprising that the majority of chemistry producing the desired furoxan ring involves manipulation of this double bond. In 1903, it was reported[64] that a reaction between styrene, the aromatic alkene commonly known for its polymerised form, produces a 1,2,5-oxadiazole-2-oxide upon reaction with sodium nitrite. However as well as forming the furoxan product it was noted that a side reaction was forming the nitrated styrene, instead of the desired product. [65] It was concluded that this happened due to the steric hindrance of the aromatic substituents in proximity to the double bond which in their orientation prevented the ring closure process and thus only nitrated the starting material much like **34** in scheme 13. More recently an equivalent reaction using very similar chemistry to Tonnies was performed by Italian chemist Alberto Gasco, who documented that the conversion of the alkene double bond to the 1,2,5-oxadiazole-2-oxide heterocycle occurred via a 'pseudonitrosite' intermediate **35**.[66] This intermediate compound is produced via an 'ionic' mechanism (depicted in scheme 14). When combined, acetic acid and sodium nitrite form the reactive species NO^+ and NO_2^-

, which initiates the nucleophilic addition to the alkene bond. This then causes the adjacent olefinic carbon to become positively charged, resulting then in the addition of the negatively charged nitrite ion.

$$2\ NaNO_2\ +\ 2\ CH_3COOH \longrightarrow 2\ CH_3COO^-\ Na^+ + 2\ HNO_2$$

$$H_2O\ +\ N_2O_3 \rightleftharpoons NO_2^-\ +\ NO^+$$
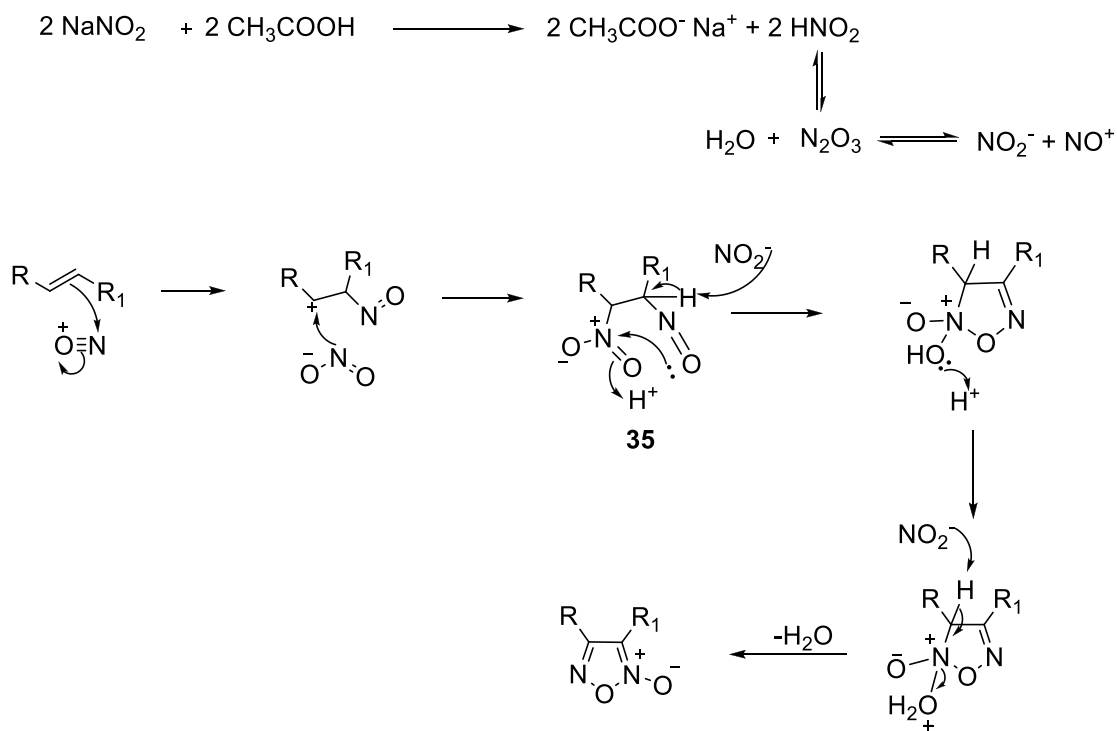
Scheme 14: Gasco's ionic mechanism for the production of the furoxan ring using the reactive species NO^{2-} and NO^+ formed from the decomposition of nitrous acid.[66]

Several reactions have been carried out using this alkene chemistry[58,66-69], most, if not all the starting materials have had an alcohol or a carbonyl group adjacent to the double bond. This suggests that an oxygen species or at least an electronegative atom is needed for the generation of the 'pseudonitrosite' intermediate **35**. It is possible that an amine or even a halogen adjacent to the alkene double bond could also generate this intermediate, but the question remains as to whether this interaction is needed for the reaction to take place. This chemistry has also been frequently used to generate the NO-hybrid compounds mentioned earlier such as compounds **25** and **28** (Fig. 13).

Furoxan compounds can also be synthesised from other simple starting materials and the acetophenone **36** is just one of the many options. The acetophenones, of which there are many, are a series of aromatic compounds that have been a widely used in furoxan research due to their relatively inexpensive nature. It has been reported that when exposed to concentrated nitric acid, acetophenones can form furoxans (scheme 15) with aromatic rings (from the starting material) flanking the carbons of the heterocycle **37**[61]. A combination of acetic acid and concentrated nitric acid has been reported to produce the reactive N_2O_3 species required for the formation of the furoxan ring as already shown in scheme 14. [70-72]
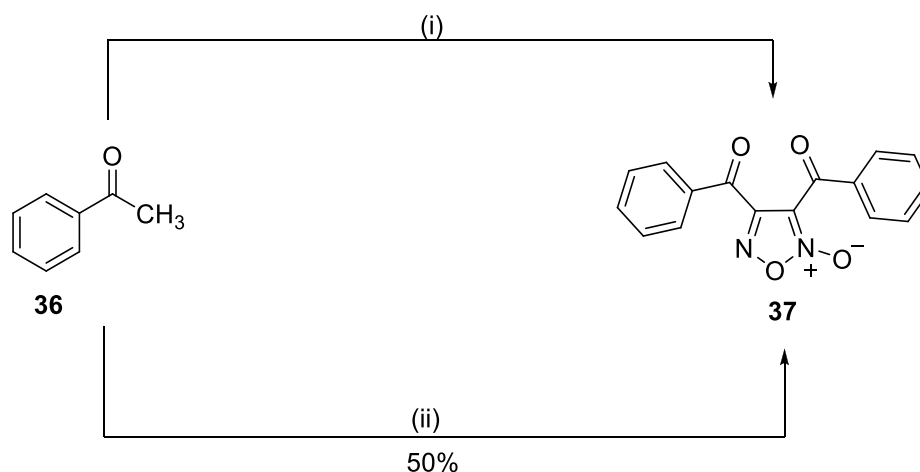
Reagents and conditions: (i) HNO_3/H_2SO_4 (ii) HNO_3/CH_3COOH, $NaNO_2$, 60°C, 1hr

Scheme 15: Two synthetic routes to the furoxan ring starting from a simple, cheap starting material **36**. Both routes require acidic conditions to generate the reactive species NO_2^- and NO^+.

A major drawback of using an acetophenone starting material and the procedure outlined in scheme 15 is the formation of unwanted by-products, shown in scheme 16. If too much water is present in the reaction, the corresponding benzoic acid **38** can form instead of the furoxan ring **37**. It has also been reported that the benzoylformic acid **39** can also be produced. Additional side products formed from nitration of the aromatic ring is also a problem with this chemistry and can produce highly coloured compounds,[73] which can be used as an identifier of by product formation.
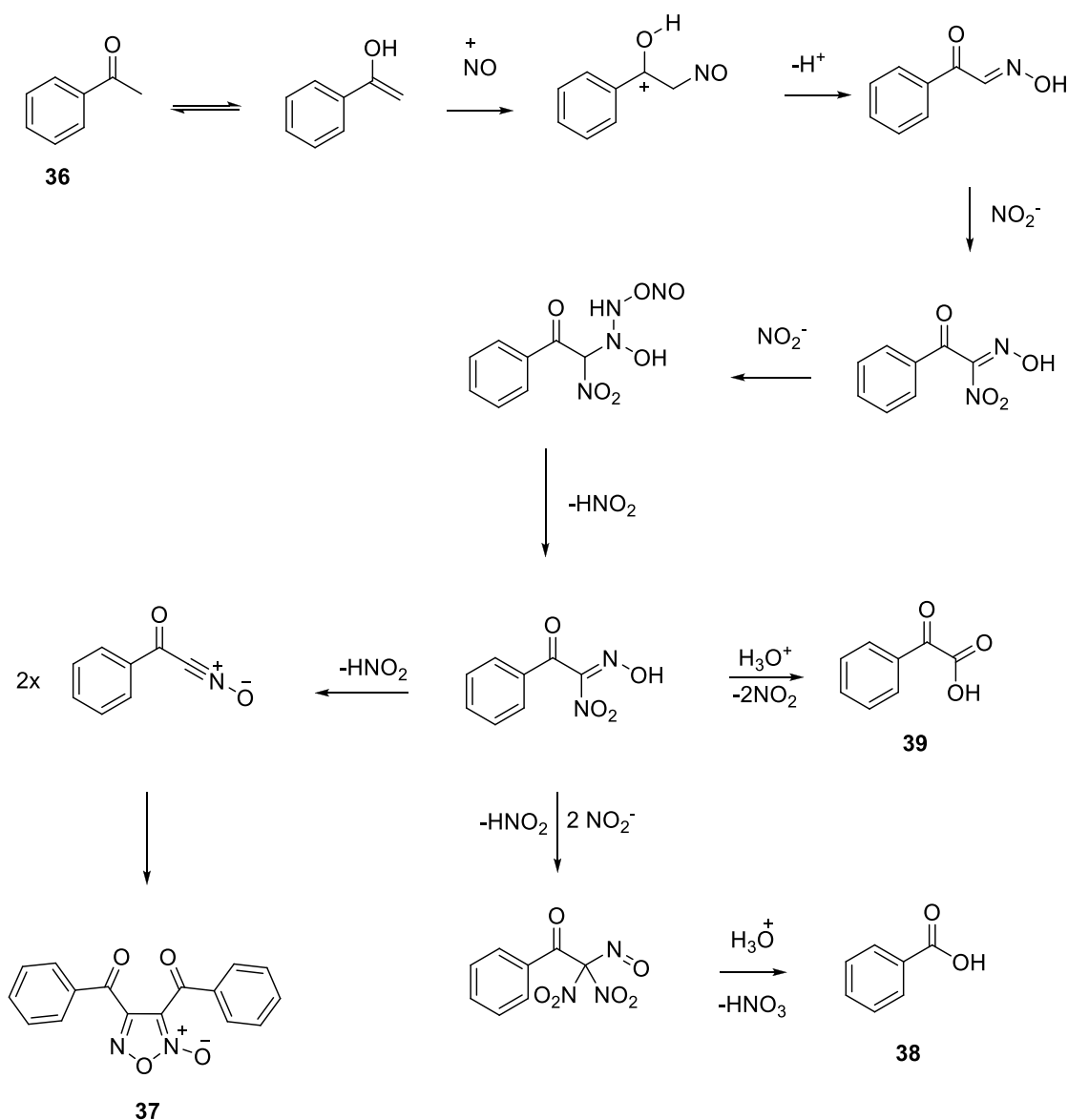
Scheme 16: Reaction to form the furoxan compound **37** from an acetophenone. Depending on the reaction conditions various by-products can form such as **38** and **39**. (Taken and adapted from reference 73)

An alternative starting material for the synthesis of the furoxan heterocycle is the oxime motif, C=N-OH. Many different derivatives of oximes have been reported for the formation of furoxans **29**.[58,59,74-76] The dioxime starting material **40** is a popular starting point in furoxan synthesis as it already contains the desired nitrogens and oxygens for the oxadiazole heterocycle, therefore a simple dehydration or oxidative reaction (scheme 17) is all that is needed to generate the product.

This conversion can be completed using a variety of strong oxidants such as potassium ferricyanide[77] and sodium hypochlorate, but these are sometimes avoided due to their handling issues. [59]
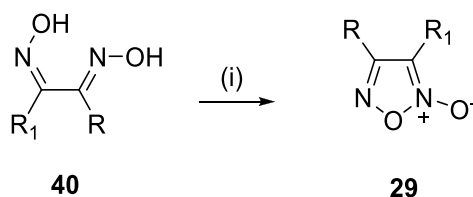
Reagents and conditions: (i) $K_4[Fe(CN)_6] \cdot 3H_2O$ or NaOCl

Scheme 17: The formation of a furoxan involving the oxidation of a dioxime 40.[77]

To avoid these more toxic reagents other methods have been developed, such as direct exposure to nitrogen tetroxide (N_2O_4), stirring in concentrated nitric acid or conversion to the oxime-chloride and then ring closure by treatment with a strong base. An interesting procedure, making use of ligand and inorganic chemistry is the treatment of a substituted dioxime compound **41** with copper (II) chloride in the presence of copper perchlorate, shown in scheme 18.[78] Unlike other oxidative reactions, this produces the furoxan compound **42** as a ligand complexed to the copper. The authors then report that by utilising simple ligand exchanged chemistry, the furoxan can then be 'freed' from the copper by treatment with ammonia.[78] Although an interesting method for the production of the desired heterocycle, the publication is contradictory, stating on numerous occasions that a strong base is required to formulate the furoxan as a ligand, but then indicate that no base is needed for the ligand formation. The lack of analytical data on the final compounds produced by this copper mediated route, bring into question how pure and repeatable the published synthesis is.
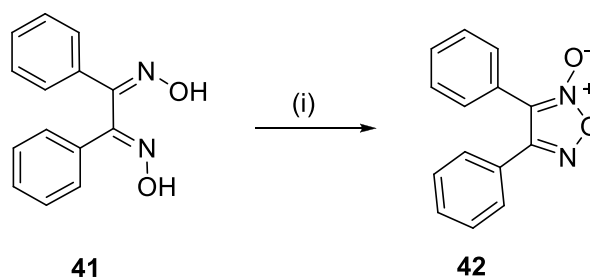
Reagents and conditions: (i) CuCl$_2$, NaClO$_4$, Et$_3$N, CH$_3$CN, RT, 12hrs (ii) NH$_3$, RT, 1hr

Scheme 18: Conversion of a dioxime to the furoxan ring in the presence of copper: The furoxan is generated as a ligand and is isolated through ligand exchange chemistry[77].

The standard way of producing the furoxan seems to be in a one pot process by reacting the oxime (**43**) or dioxime directly under oxidative conditions.[74] However a popular method found in the literature involves converting the acidic proton of the oxime compound to a halogen atom (scheme 19), to essentially produce a good leaving group for the second step of ring cyclisation.[77] Treating the oxime compound with either *N*-chlorosuccinamide or hydrochloric acid produces the chlorinated oxime (**44**) in high yield (90%). Exposure of this to a strong base leads to the ring closure and the loss of HCl and the formation of the desired furoxan product **29**.
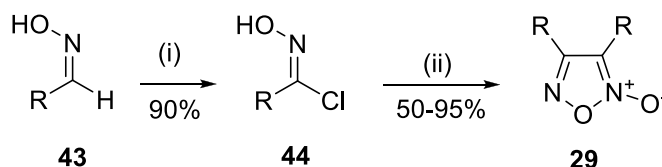
Reagent and conditions: (i) NCS or HCl, RT, 2hrs (ii) Et$_3$N, diethyl ether, 40°C, 5hrs

Scheme 19: A two-step reaction to form the furoxan ring via a chlorinated oxime **44**.

1.1.4- Diazeniumdiolates

An alternative class of NO donors that are synthetically interesting and of reasonable stability are the NONOates. Recently renamed to the diazeniumdiolates after several arguments amongst researchers, these compounds all share a common feature, the NONO moiety, shown in Fig. 15. [79] The name diazeniumdiolate can be broken down in to three parts to explain its origin. Firstly the 'diazen' part refers to the two sp^2 hybridised nitrogens and the 'ium' denotes the nitrogen's formal positive charge. Finally the 'diolate' can be attributed to the negatively charged oxygens attached to each nitrogen.
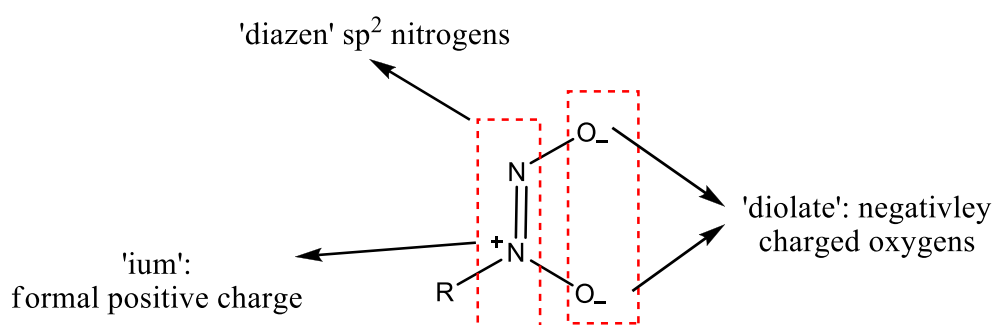
Figure 15: Schematic diagram explaining the nomenclature for these compounds.[79]

This class of NO-donors can be split again in to further subclasses depending on what the atom directly attached to the NONO moiety is. This can either be a carbon, nitrogen, oxygen or sulphur. The latter two are the most uncommon elements to be attached to the NONO structure (as shown in Fig. 16). Oxygen is more predominantly used when compared to the sulphur subclass and is formed as an inorganic salt, known as Angeli's salt **45** and is primarily used in biomedical research as a source of NO⁻, however it can also release NO under acidic conditions or in the presence of copper.[79, 80] Only one *S*-diazeniumdiolate **46** has been isolated and was prepared by passing NO gas over potassium sulphite. This compound decomposes to give nitrous oxide (N_2O) and sulphate ions so has never been of much interest as an NO-donor.

45

O-Diazeniumdiolate

46

S-Diazeniumdiolate

47

N-Diazeniumdiolate

48

C-Diazeniumdiolate
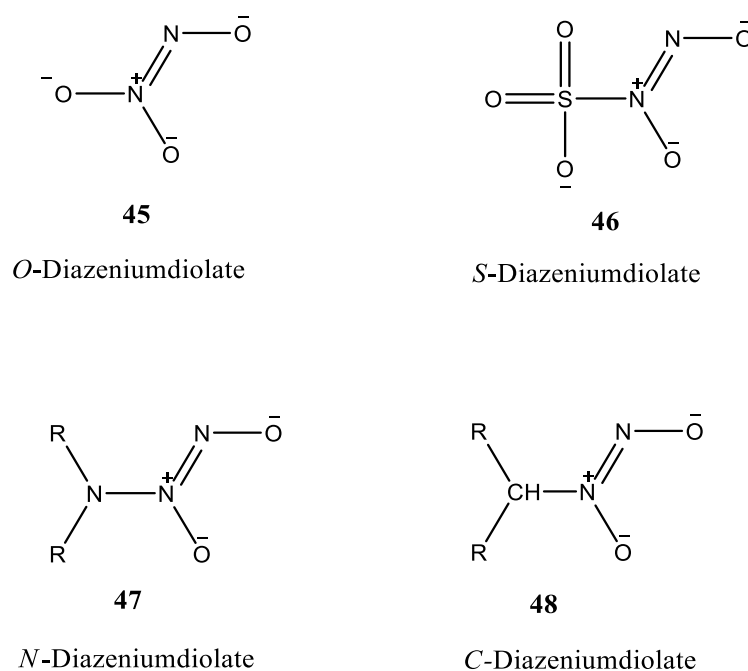
Figure 16: The four isolated derivatives of diazeniumdiolate structure. The NONO motif is either connected to an oxygen, a sulphur, a nitrogen or a carbon atom.

The nitrogen **47** and carbon **48** bound diazeniumdiolates are by far the most researched derivatives[79] in the NONO class. N-bound diazeniumdiolates (**47**) were first synthesised in the 1960s by Drago[81] by directly exposing NO to diethylamine **49** (scheme 20). Even though they were first made over 50 years ago the NO donating ability of this class of compounds has only been thoroughly investigated since the discovery of NO's biological importance.

49

50
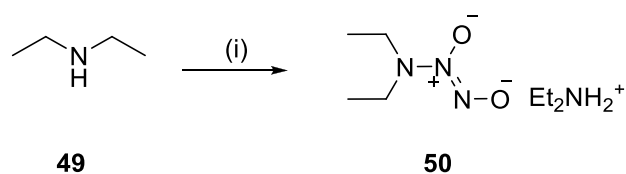
Reagents and conditions: (i) NO (g)

Scheme 20: Reaction of NO gas with diethylamine, produces the *N*-diazeniumdiolate[80]

Since the Drago work[81], several variants of *N*-bound diazeniumdiolates **47** have been synthesised for use as NO donors in the biomedical industry. Due to the stability of the compounds formed most are produced by treatment of the relevant amine with NO gas to produce the NONO functionality. However additional chemistry can be done at either end of the *N*-diazeniumdiolate **47** structure to generate an entire compound library. The amine group can be introduced into other molecules as a linker (for example as an amide) between biologically active molecules[82] and the NO-releasing unit. The oxygen on the NONO terminus can be alkylated (scheme 21) using various aromatic or alkyl halides to produce a 'protected' version of the *N*-diazeniumdiolate.
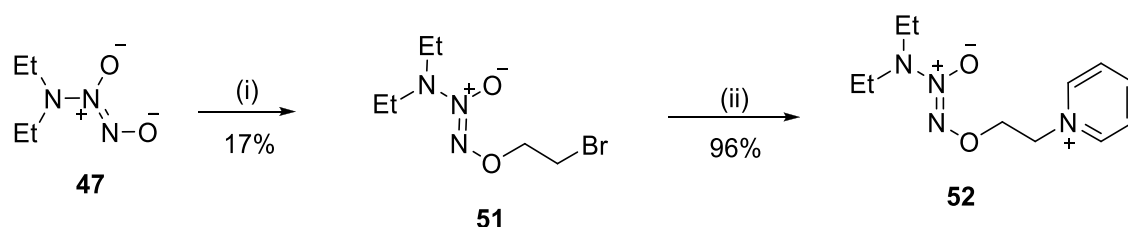
Reagents and conditions: (i) Dibromoethane, DMF, 0°C, 12 hrs (ii) pyridine, EtOH, 70°C, 20hrs

Scheme 21: Potential sites of derivatisation proposed by Keefer 2002.[79]

Although several different *N*-diazeniumdiolates have been synthesised[81,83] the mechanism of their release comes with some disadvantages that can be argued to be detrimental for their use as safe NO donors in a pharmaceutical setting. In the presence of acid or light *N*-diazeniumdiolates decompose to release nitric oxide and the free amine **53**, this amine can then react with oxygen to produce a nitrosamine **54** (scheme 22).[84] Nitrosamines are known to have carcinogenic properties and have been linked to several types of cancer when exposed to high concentrations of them.[85-87]
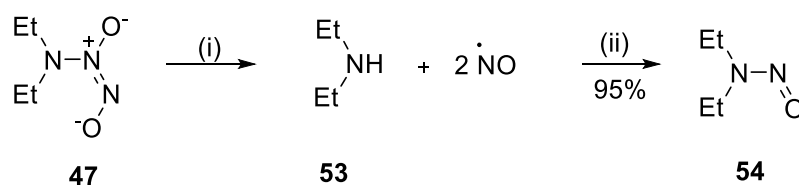
Reagents and conditions: (i) H$^+$/ hv (ii) O$_2$

Scheme 22: General decomposition route of the *N*-bound diazeniumdiolates when exposed to acid or light.

As with other diazeniumdiolates, nitrogen bound derivatives can form bi-dentate ligands with metals and therefore act as chelators of copper, iron, colbolt and zircon amongst others.[88] An example of this complexation is shown with copper **55** in Fig. 17.
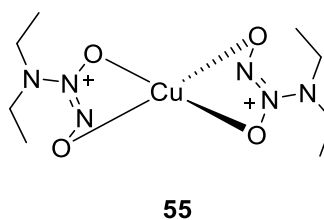
Figure 17: Diazeniumdiolates can coordinate to metal ions forming a bi-dentate ligand.

The last diazeniumdiolate subclass of the four and by far the most researched are those where the NONO moiety is directly attached to a carbon atom **48**. These were first synthesised by Traube in 1895 by the reaction of NO with a carbanion[79]. Since then several different carbon bound diazeniumdiolates **48** have been produced utilising a range of starting materials including oximes, alkenes, alcohols, nitriles and ketones.[79, 89] The wide range of possible starting materials gives this class of diazeniumdiolates **48** a lot of scope for research as there are many derivatives that can be synthesised at a later stage of a synthetic route (scheme 23).
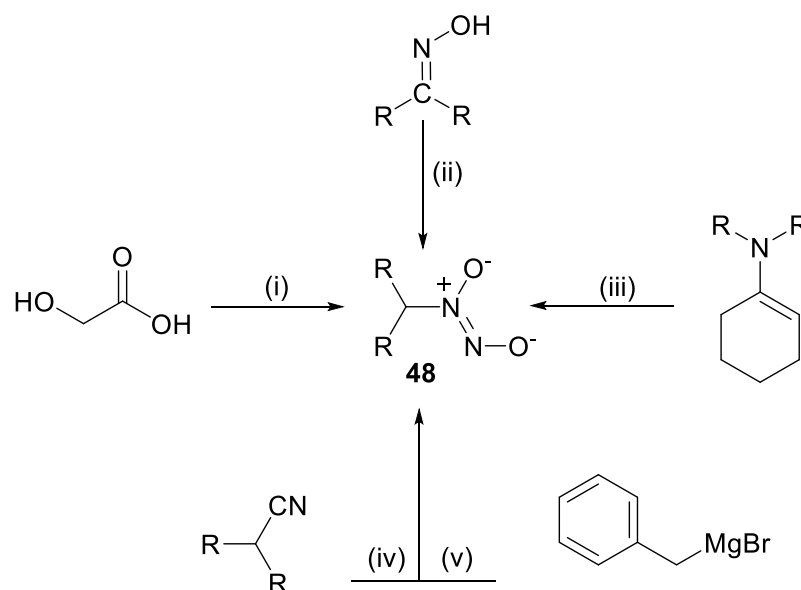
Reagents: (i) $NO_{(g)}$ NaOMe (ii) $NaNO_2$, HCl or $NO_{(g)}$, or *i*-PrONO, NaOMe, (iii) $NO_{(g)}$, Ether, (iv) $NO_{(g)}$, NaOMe, (v) $NO_{(g)}$

Scheme 23: Various synthetic routes for the production of *C*-diazeniumdiolates starting from an array of different functionalities

One compound in particular, that has seen a lot of research in terms of synthesis and derivatization, is the aromatic diazeniumdiolate called cupferron **56**. Named after its strong affinity for copper and iron, it is routinely used as an industry grade metal chelator, particularly in the purification of plutonium.[79]

Cupferron compounds are generally synthesised from the nitrosation of *N*-hydroxyamines (**58**) in the presence of ethyl nitrite and ammonia gas[89] (scheme 24). However, exposure of nitrobenzene **57** to gaseous NO will also afford the cupferron structure, but as this is a fairly expensive method due to the need for pure NO gas, the former method is more commonly seen.
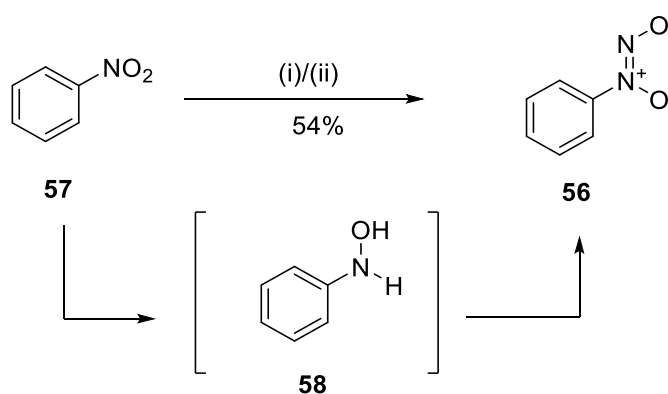
Reagents and conditions:(i) Zn, NH$_4$Cl, 0°C (ii) EtONO, NH$_3$, 0°C, 15mins

Scheme 24: Synthesis of the common metal chelator and NO-donor cupferron **56**.

As mentioned before in terms of the N-diazeniumdiolates, you can also alter the stability of the cupferron **56** compound by performing chemistry at the terminal oxygen in the NONO group. Alkylation chemistry at this terminus (shown in scheme 25) can be performed with a variety of reagents, depending on the desired final product. Alkyl halides, sulfates, acid halides and even epoxides have seen purchase in the past. However there is some argument amongst researchers as to which oxygen, out of the two available is best able to support the alkylation chemistry. After some dispute from Russian chemists,[79] who argued that the O^1 position (depicted in scheme 25) is the more nucleophilic site, it is now widely agreed[79,90,91] that any alkylation would occur preferentially at the O^2 site and any O^1 alkylation would be a side reaction producing an unstable product and isolated. Interestingly, the O^1-alkylation product was recently observed (see scheme 25) and isolated during the reaction of neocupferron, the naphthalene derivative of cupferron, with alkyl halides but was verified as a low yielding side reaction.[91]

12%
minor intermediate product

52%
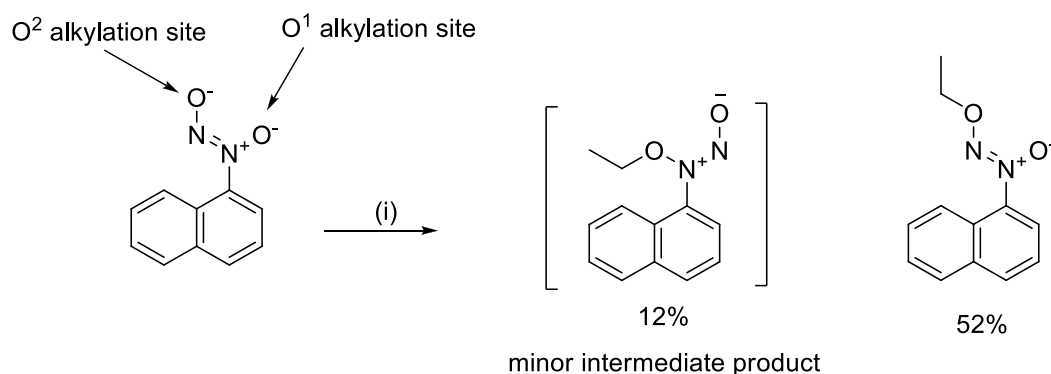
Reagents and conditions: (i) CH_2H_5I, DMF, 0°C, 24hrs

Scheme 25: Alkylation of cupferron is shown to occur favourably on the O^2 alkylation site rather than at O^1 site. [91]

Alkylation at the O^2 terminus can act like a protecting group for the diazeniumdiolate in terms of NO release and tends to increase the stability of the parent cupferron compound[89]. Compared to the cupferron derivatives where the aromatic ring had been decorated in either the *para* or *ortho* positions, the *O*-alkylated cupferrons were intrinsically more stable to decomposition and NO release.[91,92]

As a metal chelator, cupferron compounds are excellent, but the same cannot be said for its use as NO-donors. Cupferron **56** is inherently unstable at room temperature and can release NO in the presence of mild oxidants, enzymatically or in the presence of light.[11,79] It has been found that substituents placed in the *ortho* position on the aromatic ring caused the decomposition rate to increase due to the substituent position preventing the cupferron molecule **56** becoming planar.[93] Substitution in the *para* position of the ring alters the sensitivity of these compounds to oxidants and enzymatic decomposition but having an electron withdrawing group *para* to the NONO functionality appears to increase the stability of the compound.[92]

It is worth noting however that upon decomposition (scheme 26) the *C*-diazeniumdiolates produce benign compounds and are therefore more biologically appropriate compared to the *N*-diazeniumdiolates.
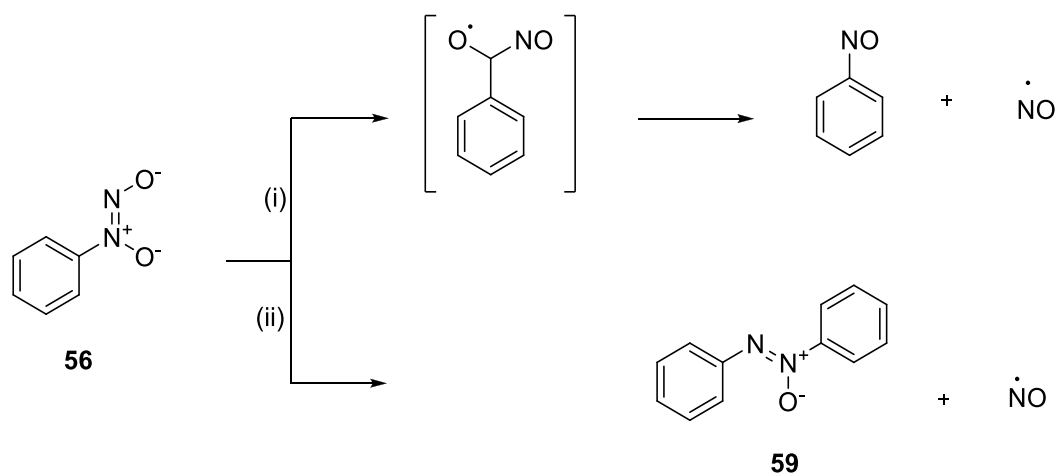
Reagents and conditions: (i) [O], or e- (ii) hv, or Δ

Scheme 26: Proposed decomposition routes for *C*-diazeniumdiolates in the presence of an oxidant, heat or light. All resulted in the production of NO.

The azoxy compound **59** produced through exposure to temperature or light can be easily detected by UV-Vis spectrophotometry and can be a used as an indicator for successful NO release[94]. Currently the measurement of the compounds produced upon NO release has been the most common method for monitoring decomposition rates, however this doesn't give any clue about relative release of NO in terms of speed of decomposition or conditions that effect release.

1.2- Reduction of NO levels

Nitric oxide is produced at the site of action, by the NOS class of enzymes. As already mentioned these can be split in to inducible and conservative NOS depending on their dependence on calcium ions (Ca^{2+}) for their activation. It has just be shown that the levels of nitric oxide can be increased by using a variety of different compounds to act as NO-donors, producing one or two equivalents of NO per mole of starting material. This is therapeutically beneficial for conditions such as arteriosclerosis where the blood vessels become thicker and drastic expansion is needed for relief, but what happens if there is too much NO within a system or tissue.

Some medical conditions such as Alzheimer's (AD), Huntington's (HD)[94]and Parkinson's (PD)[95,96] disease, are classed as neurodegenerative diseases due to the degeneration of a selected population of neurons, and this is thought to be effected by high levels of NO. It is theorised that either NO alone or in combination with superoxide and peroxynitrite ($ONOO^-$) are predominant effectors of degeneration of neuronal pathways. Figure.18 shows the relationship between peroxynitrite, NO and cytotoxicity.[98] The exact mechanism of how NO contributes to neurodegeneration is not yet fully understood but multiple theories and evidence exist, suggesting that it occurs through DNA damage and protein modification. Reactive oxygen species (ROS) react with nitric oxide to form the peroxynitrite. This oxidant has the potential to react with other compounds and produce toxic peroxide like species that can cause DNA damage.[97]
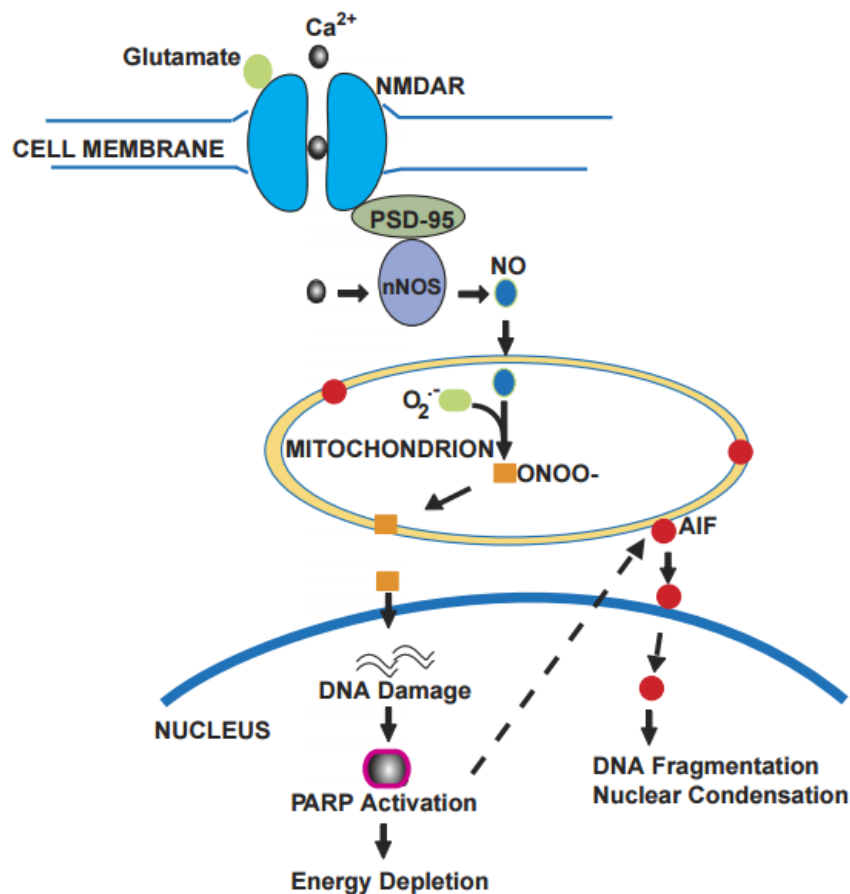
Figure 18: The production of NO can lead to oxidative damage via its metabolite peroxynitrite (ONOO⁻).[98]

NO has also been linked to neuronal damage caused by stroke, due to the high levels of NO that can build up and the oxidative damage it can propagate. A stroke occurs when a blood vessel to the brain becomes blocked, this causes oxygen starvation in the brain and increases the stimulation of the glutamate receptor, causing large amounts of calcium ions to be released which then stimulates the nNOS enzyme to produce NO and as described before in large concentrations it can be cytotoxic[1,99,100]. NO has also been implemented in cerebral ischemia, a condition where there is insufficient blood flow to the brain to meet metabolic demand.[101,102] In cases of cerebral ischemia high levels of nitrotryosine have also been detected. Nitrotyrosine is a marker for peroxynitrite metabolism, and an indicator of NO production. NO has also been linked to cases of rheumatoid arthritis, inflammation disorders and cerebral palsy.[103]

As there is now increasing evidence that nitric oxide may play a destructive role in the brain[96-100], ways of reducing *in vivo* levels of nitric oxide are needed. There are two such ways in which these high levels can be affected. One involves halting or reducing enzymatically produced NO by NOS. Nitric oxide is produced at the synapse upon stimulation of the glutamate receptor NDMA and activation of nNOS enzyme by Ca^{2+} ions. The substrate for this reaction is the common, simple amino-acid, L-arginine **1**. It is this substrate that holds one of the keys to the inhibition of the nitric oxide synthase enzyme. By mimicking the binding interactions that occur between the NOS enzyme and the substrate a potent and selective inhibitor could be produced to help alleviate the high levels of NO in the aforementioned conditions.

L-Arginine, being an essential amino acid, has a very simple structure; due to this there is a large amount of synthetic scope in terms of compounds that can mimic its binding potential. The highlighted guanidine terminus on L-arginine (Fig. 19) is the main point of interaction with the NOS enzyme and it is this motif that reoccurs in current NOS inhibitors work.
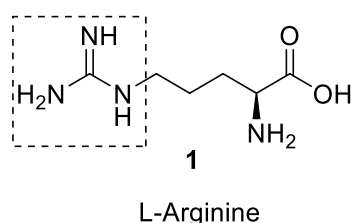
Figure 19: L-Arginine, the substrate for each isoform of NOS. Highlighted is its guanidine terminus, the used to design active NOS inhibitors.

Several quantitative structural activity relationship (QSAR)[104,105] studies have explored the structural and docking profiles and identified the optimal requirements for the binding of inhibitor molecules to the NOS enzyme. They found that although active sites of each NOS enzyme are practically identical they differ in a single amino acid between the nNOS and eNOS protein structures. As each isoform's active site catalyses the same reaction a key feature must be the involvement of a guanidinium biostere to mimic the terminus of L-arginine **1** as highlighted in red in Fig. 19. This

interaction is key as docking relationships show the guanidine group in L-arginine hydrogen bonds to a Glu592 residue in NOS, shown in Fig. 20[104].

The difference in the single amino acid plays a large part in selectivity as the alpha amino nitrogen of L-arginine interacts with both Glu-592 and Asp-597 in nNOS and Glu-592 and Asn-368 in eNOS (Fig. 20). This difference in amino acid interactions causes compounds docked in nNOS to adopt a curled conformation within the active site and thus increases the electronic stabilisation of the compound, while in eNOS it remains flatter.[104]
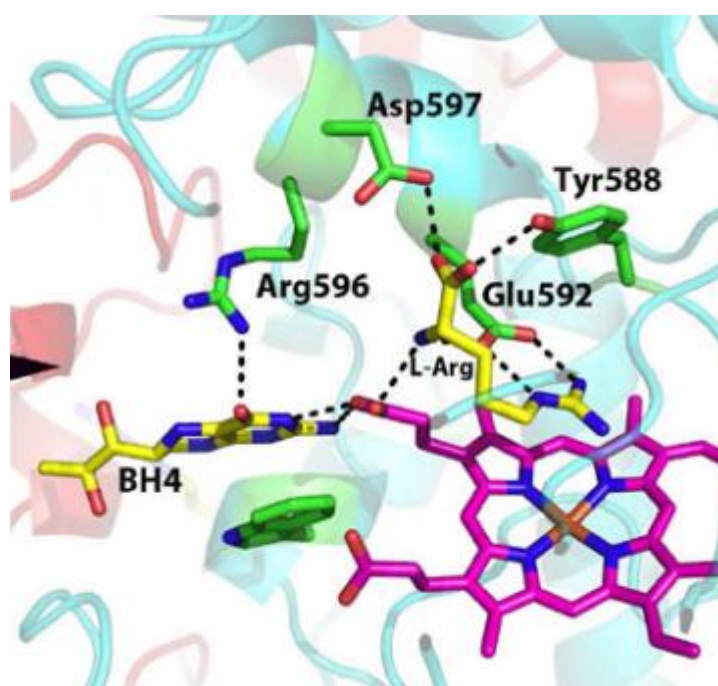
Figure 20: NOS substrate L-arginine (shown in yellow and labelled L-Arg) docked into the NOS active site. Key interactions from the haem group and Glu-592 account for L-Arginine's binding ability. The structure highlighted in magenta represents the haem centre of NOS. Taken from reference 104.

The main problem with this method of inhibition is that each NOS enzyme has the same substrate and therefore drug compounds that mimic *L*-arginine **1** too closely will not be selective for a particular enzyme. Selectivity is key if a viable therapeutic treatment is going to be produced from the inhibition of NOS, as all three isoforms are found throughout the body, especially in the brain. Cerebral tissue contains eNOS for essential cranial blood flow, glial cells are known to produce iNOS

for immune responses and nNOS is present for neuronal function. Without selectivity there is a high probability that the wrong NOS enzyme will be inhibited which could cause more drastic problems, especially if occurring in the brain. For example if nNOS is over producing NO in the brain and a non-selective inhibitor is applied, eNOS may halt production of NO in cerebral tissue, which may lead to a stroke or cerebral ischemia. This is a current challenge and concern as without potent selectivity no inhibitor will be pharmaceutically viable.[106, 107]

Several nNOS inhibitors have been synthesised as arginine analogues, the most noteworthy are L-nitroarginine methyl ester (L-NAME **60**) and asymmetric dimethyl arginine (ADMA **61**) which have chemical structures that are almost identical when compared to the original substrate[108] (Fig.21). Other inhibitors that are commercially available are Spermidine **62** and Melatonin **63**. All are potent and selective inhibitors of nNOS.[109]

60

L-NAME
(L-Nitro Arginine Methyl Ester)

IC_{50} = 500 nM K_i = 15 nM

61

ADMA
(Asymmetric Dimethyl Arginine)

IC_{50} = 2.21 μM K_i = 0.4 μM

62
Spermidine

IC_{50} = 100 μM K_i = 1.1 μM

63
Melatonin

IC_{50} = 0.02 nM K_i = 0.08 μM
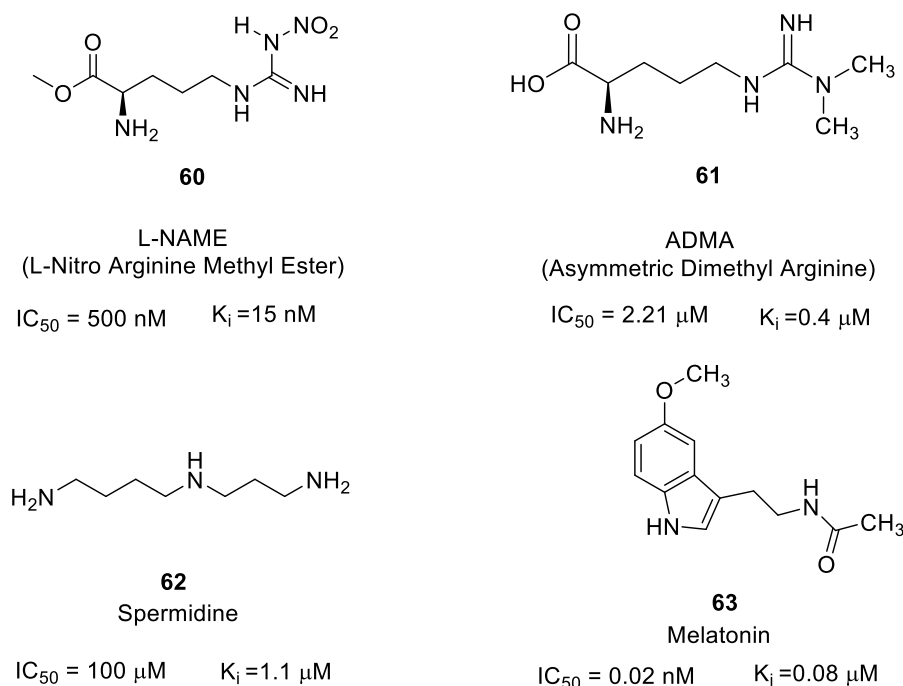
Figure 21: L-NAME, **60**, ADMA, **61**, Spermidine **62** and Melatonin **63**. Four marketable NOS inhibitors with various selectivity's for nNOS. The potency (IC_{50}) and inhibition constant (K_i) for nNOS is stated below the chemical structure.

Once L-arginine has docked within the NOS active site, it is converted to *L*-citrulline through the five electron transfer mechanism previously depicted in scheme 3. *L*-Citrulline is then reused in the catalytic cycle to generate more L-arginine. Due to the production of NO being a catalytic procedure, interfering with the concentrations of L-citrulline could also affect the levels of nitric oxide produced. Analogues, **64** and **65** of L-citrulline (Fig. 22) have been found to be potent inhibitors of NOS activity.[104]

64

65
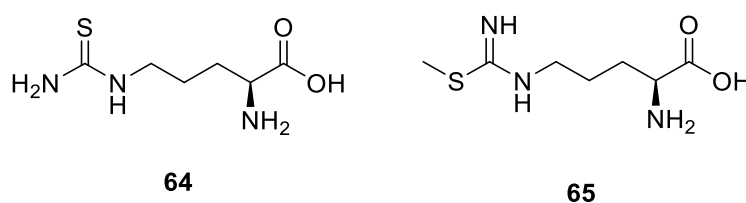
Figure 22: Two potent NOS inhibitors that are both derived of *L*-citrulline. Thiocitrulline, **64**, and *S*-methyl-*L*-thiocitruline, **65**.[103]

Professor Silverman from Northwesten University has performed an extensive research on nNOS inhibition.[110,111] Initial work in the area allowed him to conclude that the poor selectivity of some NOS inhibitors was because the same reaction is occurring at the active site of each isoform of NOS and therefore to obtain selectivity a compound needed to extend further from the active site into the second sphere of amino acids within the binding site. By focusing on one isoform of NOS his research group managed to find the one amino acid difference in the second sphere of amino acids between nNOS and eNOS.[110] Silverman developed a lead compound **66** (Fig.23), through exploration of evidence from Glaxo-Smith-Klein that *L*-nitroarginine was a selective inhibitor of nNOS and eNOS. Additional amino acid chains were coupled to *L*-nitroarginine to extend the 'reach' out of the active site. This process lead to the development of the lead compound shown in Figure 23.
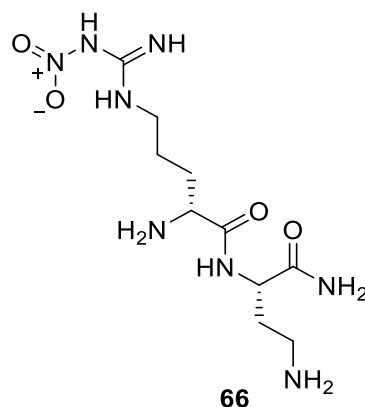
Figure 23: Silverman's lead compound for inhibition of NOS, derived from L-Nitroarginine.

The development of this lead compound **66** and the corresponding computer modelling promoted a new type of approach dubbed 'fragment hopping'. This new approach applied small changes in the pharmacophoric element of the molecule to create a new library of compounds based on fragment binding and bioisosters that kept to the pharmacophore's rules. This *de novo* method of lead compound formation enabled the synthesis of a new non-peptide based compound **67** and with further optimisation produced the lead compound **68**, which was potent in the nanomolar (nM) region and is shown in Figure 24.
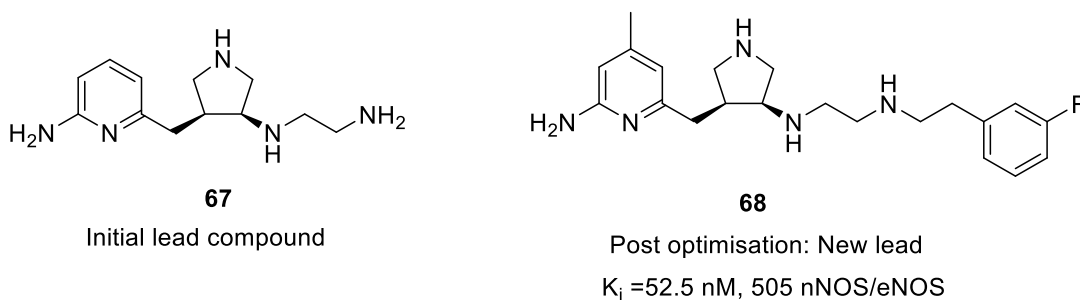
Figure 24: After fragment hopping, a new lead compound was found, **67**. The aminopyridine ring showed enhanced binding in the active site. Compound **68** is post optimisation to make it more lipophilic.

Problems still arose with the new lead compound **68** in the fact it had poor blood brain barrier diffusion. This issue was solved by crystal structure docking (Fig.25) of lead compound (**68**) into the

nNOS active site. The aminopyridine ring was concluded to interact with the haem section in nNOS through π-π stacking interactions, while the pyridinium nitrogen interacts through hydrogen bonding with Asp-597 in the amino acid sequence of the enzyme. It is this particular interaction that induces the selectivity for nNOS, as eNOS has a different amino acid residue at that part of the sequence[111] and therefore doesn't have the same binding interaction at that point. For a successful inhibitor of nNOS, a molecule needs to adhere to the pharmacophoric rules seen by Silverman; it must contain a guanidinium type group for selectivity and also be large enough to 'reach' out of the active site and interact with neighbouring amino acid side chains.
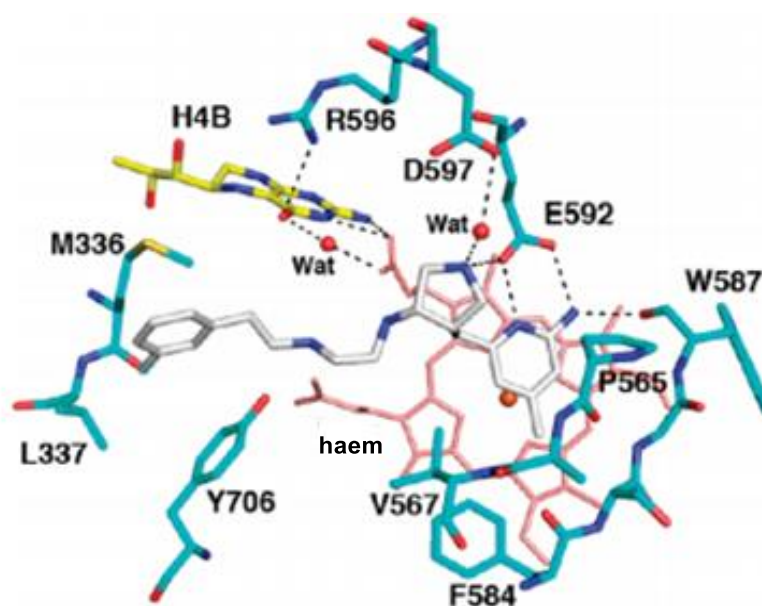
Figure 25: Lead compound **68** (shown in grey) docked within the active site for nNOS. The aminopyridine ring interacts with the glutamate group of the haem centre (shown in pink) of NOS and the haem centre itself through π-π interactions and hydrogen bonding.[110]

Inhibiting the enzyme that produces NO is only one way to reduce the *in vivo* levels. An alternative method is employing scavenger molecules to essentially 'mop' up excess nitric oxide. A scavenger

molecule is one that can be added to a reaction or system to remove or deactivate unwanted compounds before they cause damage or side reactions. The ability of a molecule to be an effective radical scavenger comes from the compounds capability to rapidly donate a hydrogen atom and the possibility of radical stabilisation, usually due to conjugate electronic effects. The compound class known as the flavonoids are well-known anti-oxidant scavengers and are constantly mentioned by the world media as the new 'holy grail' in diet management.

Flavonoids **69** are essentially 'built' to be radical scavengers[112-114] and are successful due to the high amount of phenolic hydrogens coupled with the large amount of conjugation that exists in their structures. The general mechanism for action is proposed as follows: A hydrogen atom from the hydroxyl group (*19*) is donated to the radical, producing in the process a phenoxyl radical at positon *19*. This is then stabilised by the adjacent α,β-unsaturated ketone, which moves the radical to carbon *9* (Fig. 26). Movement of the radical to the *9* position creates a tertiary radical and therefore creates a more stable compound, due to the fact that tertiary radicals are inherently more stable than primary and secondary ones. The other hydroxyl groups positions around the A and C rings have been highlighted (Fig. 26) by researchers to be essential for effective radical scavenging due to electron donating ability and their 'attractiveness' to radical compounds, in particular the OH groups on the C ring at *C14* and *C15*.[114]
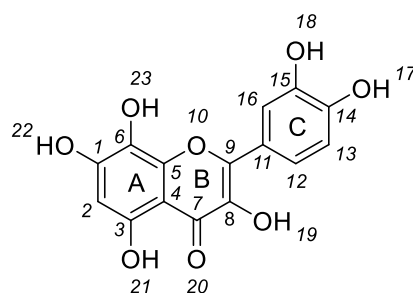
69

Figure 26: General structure **69** for the flavonoid class of compounds.

Curcumin **70** is the main compound found in the spice turmeric (Fig.27) and has recently been linked to having medical potential against a variety of conditions, from cystic fibrosis[115] to cancer[116-118] and Alzheimer's disease[119]. Although not a true flavonoid, curcumin, **70** contains most of the same key structural motifs, and therefore it is no surprise that it acts as a successful radical scavenger.[115]
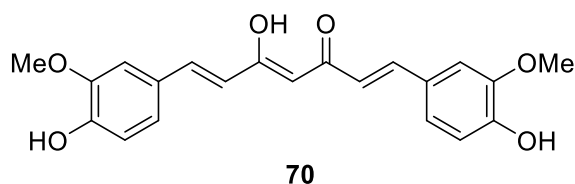
Figure 27: Curcumin **70**, the biologically active compound found in turmeric. Shown existing in its enolated form but can also be found as the diketal tautomer under some conditions.

Due to the high amount of conjugation present in the curcumin **70** structure it can stabilise radicals fairly well, producing many resonance structures and therefore acting as a successful scavenger[115] as shown below in scheme 27 with its reaction with a DPPH radical, a common scavenger testing compound. Once in its reduced form it (DPPH-H) it changes colour from purple to orange.
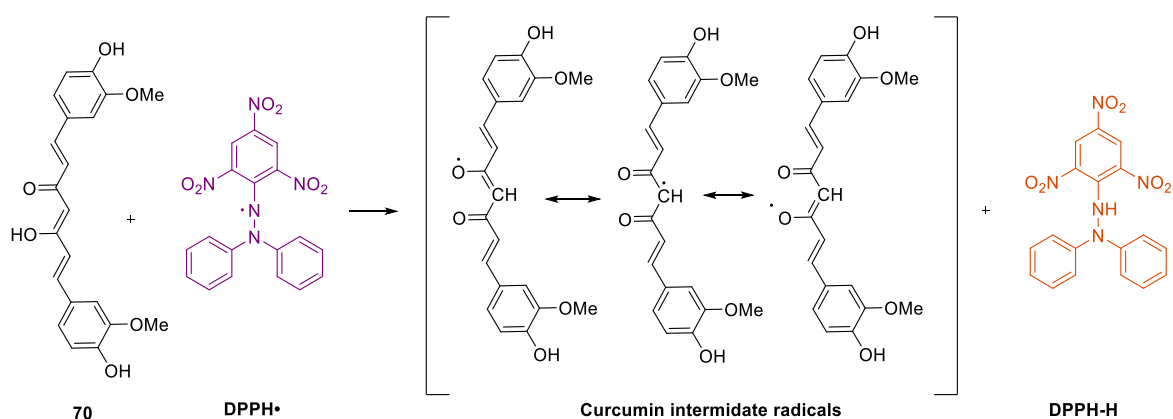
Scheme 27: Curcumin **70**, acting as a radical scavenger with DPPH, a radical tester compound. Curcumin easily stabilises the radical through three resonance forms shown in the square brackets. Adapted from reference [115]

1.3- Rationale and Target Compounds

As described previously there are numerous medical conditions that involve nitric oxide in one way or another. Conditions that need an increase in the systemic levels of NO such as angina have a limited arsenal of compounds that can be used to treat them, as many of the currently prescribed options could be considered to be outdated due the timeline of their discovery coupled with the adverse effects they cause, notably the potential cyanotoxicty from SNP.[27] It is quite apparent that there is a need for a compound or class of compounds that can act as nitric oxide donors in a conservative and predictable manner and whose metabolites or mechanism does not lead to toxic or damaging consequences. Producing a compound that can provide a known amount of NO could be greatly beneficial for the pharmaceutical industry let alone have a huge impact on patients living with one of the aforementioned conditions. On the other hand, there are also several conditions, Huntington's, stroke and Alzheimer's to name but a few that could be benefited from the reduction in nitric oxide levels through the use of NOS inhibitors or radical scavengers. Developing and synthesising compounds that can reduce the amount of NO being produced at the site of these diseases could go a long way to treat the symptoms if not help underpin the mechanism behind their causation. To address the need for the moderation of NO levels within the body a series of compounds will be designed and synthesised to separately enhance or reduce levels of nitric oxide.

Combretastatin is a small natural product isolated from the bark of the Africa bush willow tree, the *Combretum caffrum*.[120] Whilst being one of the smallest natural products of interest to researchers, it has also been used for many years by the San people of Africa as a 'well-being' tonic in addition to being used as a coating for their spear tips.[119] When isolated from the bush willow bark it was found to be a mixture of compounds, three of which are noteworthy (Fig. 28) with combretastatin A-4, **73**, being the most potent against cancer cell lines. [121-123]
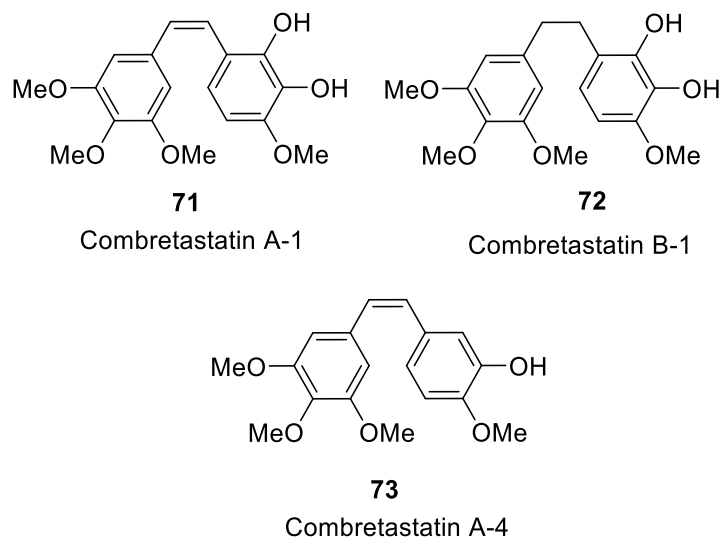
Figure 28: The three isolated compounds from African bush willow. Combretastatin A-4 (73) is the most biologically active.[120-122]

It was concluded that combretastatin A-4 **73** was potent due to its pharmacophoric similarity to another natural product, colchicine **74**[124] which is known to have a specific binding site in tubulin and is routinely used to treat gout. Figure 29 shows the similarities[125] between the two natural products, with the trimethoxy unit on both benzene rings as well as the two aromatic rings being bridged by an aliphatic bond (shown as a bold outline in Figure. 29).
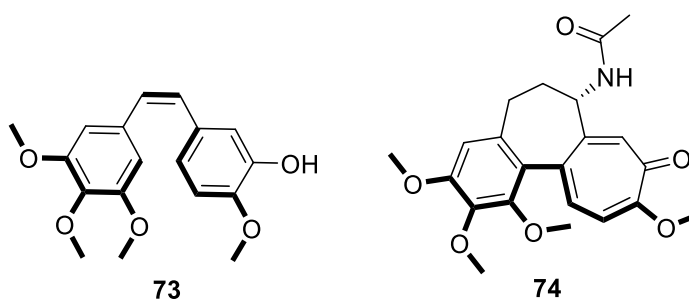
Figure 29: Colchicine, **64**, and combretastatin, **63**, have many key structural similarities explains why combretastatin binds to the colchicine site in tubulin.

Cancerous growths[125] are caused by uncontrollable division of cells and can be classified as being blood or organ cancers. Organ cancers are found between the endothelial cells of an organ and are usually solid structures. One such structure prone to over polymerization is the protein tubulin, the precursor to the microtubule structures found throughout the body. Combretastatin **73** has been found to be potent against cancer cell lines and in particular as a vascular disrupting agent (VDA).

Combretastatin has shown to be quite prevalent against solid tumours, as for a tumour to survive it needs a strong vascular structure and blood flow supporting it. Combretastatin **73** works by attacking the immature endothelial cells in tumours and forcing the shape of the cell to change to a more spherical one, this then acts as a 'plug' and prevents blood flowing through the capillary bed thus causing oxygen deprivation inside the tumour, leading to apoptosis and tumour death.[126-127] Combretastatin **73** binds within the colchicine **74** binding site[124,128] and halts replication as shown in Fig. 30, slowing down the process enough so that polymerisation does not occur.
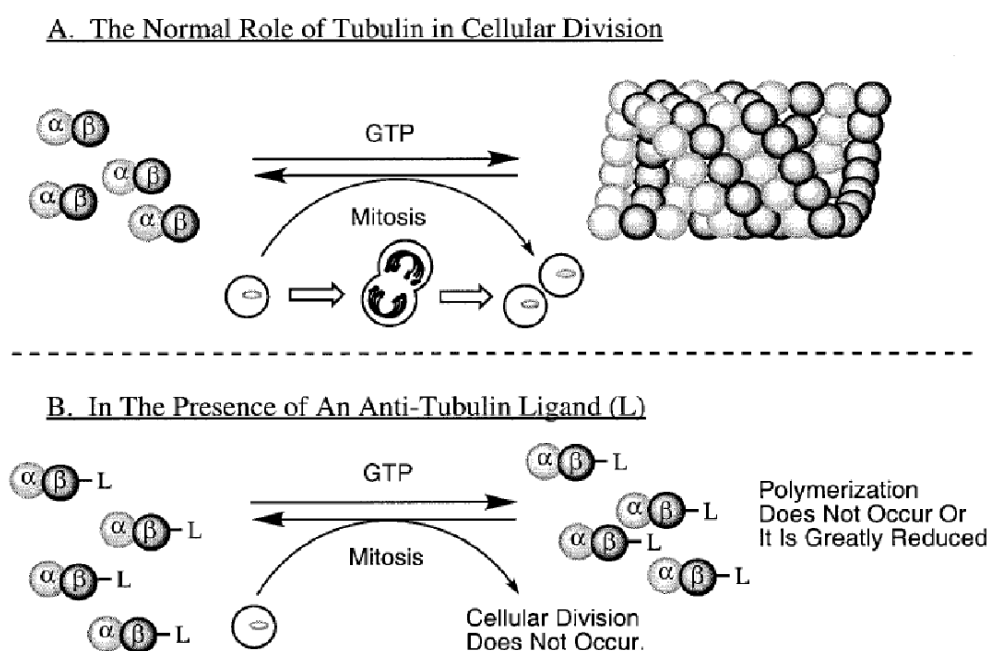
Figure 30: How combretastatin (shown here as an anti-tubulin ligand) disrupts cellular division preventing tumour growth. Taken from reference 129

You might be thinking where does nitric oxide fit into all of this? Due to its simplicity, combretastatin (**73**) has had several QSAR studies conducted on its structure to determine any key interactions taking place that would account for its potency. It was revealed that the trimethoxy motif on the A ring and the *cis* orientation were essential for combretastatins binding potency, as shown in Fig.31.[124, 130, 131]
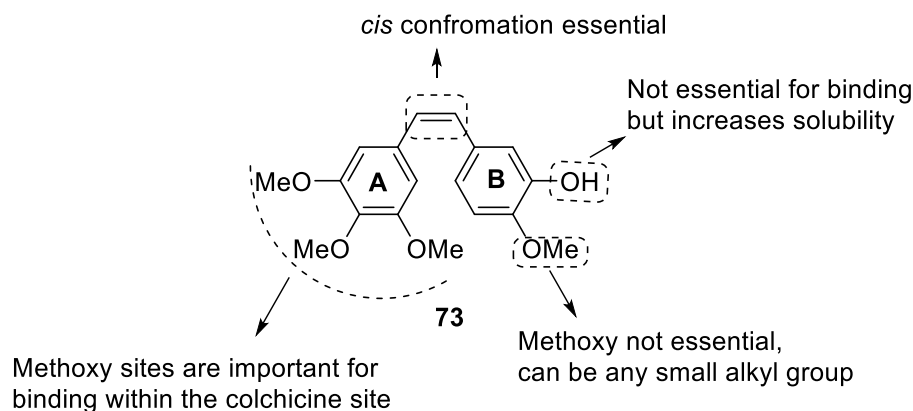
Figure 31: Combretastatin A-4's, **73**, key structural features for anti-tubulin activity.[124,130,131]

The *cis* conformation has also been shown to be essential for binding due to its resemblance to key portions of colchicine (Fig. 29 and 31), but it is prone to isomerisation *in vivo*, therefore there needs to be a way to maintain this orientation so that activity doesn't diminish. The way we are proposing to solve this is by implementing the furoxan ring, mentioned earlier, into the structure by replacement of the olefinic bond. This will essentially 'lock' the structure in the *cis* orientation and keep the rigidity needed for activity. Another reason for the employment of the five membered heterocycle, is that clinical trials have shown that combretastatin **73** is not very water soluble due to the high amount of hydrophobicity present in the structure, therefore causing it to have poor bioavailability. By introducing the 1,2,5-oxadiazole-2-oxide **29** structure it should increases the potential for hydrogen bonds due to the electronegative nature of the heterocycle and the presence of both nitrogen and oxygen as hydrogen bond acceptors.

Two different analogues of combretastatin (shown in Figure 32) fused with a furoxan ring (from herein known as combretafuroxan compounds) will be synthesised by adapting synthetic routes already mentioned in section 1.1.3.1. The first class ('Series 1', **75**) will resemble the parent combretastatin by having two decorated aryl rings directly attached to the furoxan, this will enable direct comparison with the parent compound (due to similar tether lengths) in terms of anti-cancer activity and water solubility. The second class ('Series 2', **76**) of combretafuroxans will by synthesised with a ketal unit effectively bridging the aryl rings and the furoxan ring. The addition of two extra oxygen atoms may help to increase hydrophilicity further by increasing the number of potential hydrogen bonds that can be formed.
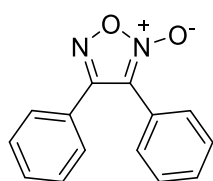
75

Combretafuroxan Series 1

76
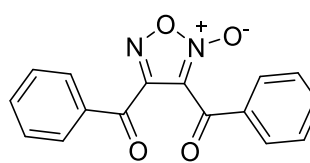
Combretafuroxan Series 2

Figure 32: Planned combretafuroxan compounds to assess the ability substituents positioned around the aromatic rings have on the effect of NO release and anti-cancer activity.

An additional reason for using the furoxan structure is that within NO donor research, stability is a key issue. Furoxans tend to be the more stable of the NO-donor classes, compared with the *S*-Nitrosothiols and metallic nitrosyls, as the NO portion of the molecule is trapped within a five membered ring. By incorporating the furoxan within an already stable natural product (effectively producing a fused NO-hybrid) it may produce a symbiotic relationship between NO and combretastatin in a way that stabilises the furoxan and also combretastatin. The release of nitric oxide from the combretafuroxan (**75** or **76**) can also act as way to alleviate the cardiotonic side effects experienced with combretastatin.

The 3,4,5-trimethoxy substituents located on the 'A' ring of combretastatin are thought to be essential for binding[130] within the tubulin structures (Fig. 29) and this motif was incorporated into the early

work of combretafuroxans from our own research group[132]. Combretafuroxan compounds, symmetrically substituted with a tri-methoxy group on both the A and the B rings, were found to be highly potent against a variety of ovarian cancer cell lines with IC_{50} values ranging from 3.64 μM to 8.04 μM for the A2780 cell line and 4.64 μM to 10.19 μM for the cisA27 cell line.[132] The difference in these values can be attributed to the different positions that the methoxy compound was substituted in, the most potent compound was a 2,4,6-trimethoxy substituted combretafuroxan (adhering to series 2 motif in Fig. 32) producing a low μM range across the eight cell lines it was tested on. Changing the substitution pattern to 3,4,6-trimethoxy arrangement led to a slight loss in activity in all cell lines suggesting that the relative position of substitution on the A and B rings are key to its activity.

Combretafuroxans that adhere to the series 1 motif in Fig.32 and are decorated with a tri-methoxy units will be synthesised (their structures can be seen in Fig. 33) by exploiting the alkene double bond chemistry developed by Gasco (as shown in section 1.1.3.1). The 3,4,5 the 2,4,6 and the 2,4,5-trimethoxy combretafuroxans compounds have previously been synthesised[131] and their anticancer properties tested against ovarian cancer cell lines with interesting results (sub 20 μM activity).
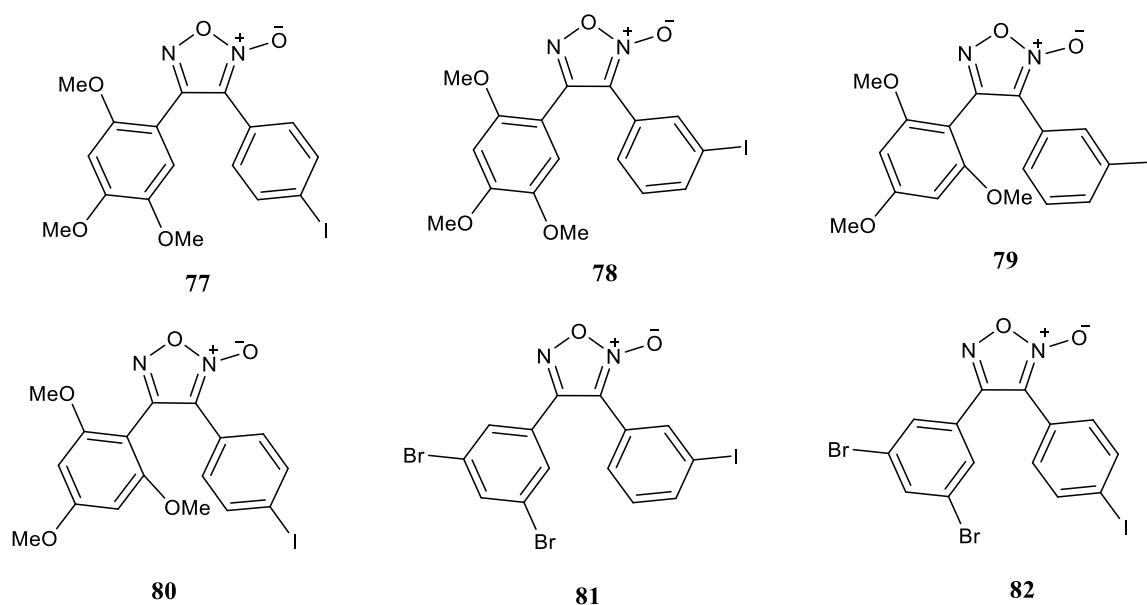
NB: Compounds **79** and **80** 6-OMe bond is exaggerated due to its 2D positioning

Figure 33: Planned combretafuroxan compounds within in the series 1 model. To be synthesised from simple stilbene starting materials.

Interestingly at the same time as this work, a publication arose in the literature from Steve Ley's research group.[133] This publication stated that halogenation of the 'A' ring in replacement of two of the methoxy groups, increased the activity of their tetrazole combretastatin (**83-85**) analogues fivefold in comparison to the trimethoxy version as it induced 'optimal packing' in the colchicine binding site.An abstract of their findings is shown in Figure. 34. The findings by the Ley group (Fig. 34), interested us and partially influenced the substituents we chose to decorate our A and B rings with in the combretafuroxan model.
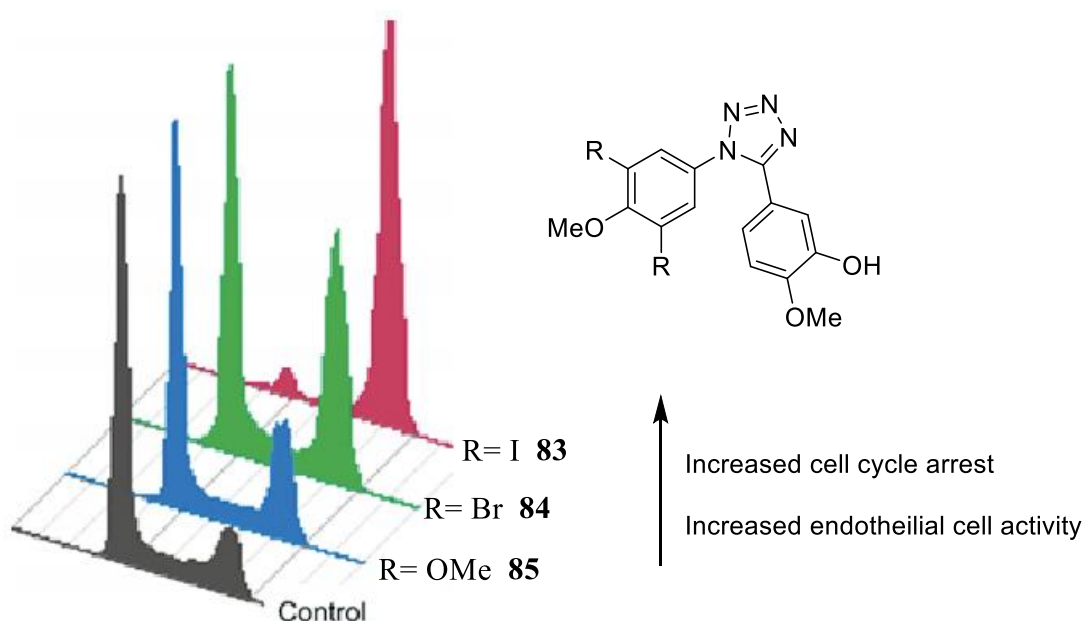
Figure 34: Graph showing the increase in cell apoptosis on human umbilical vein endothelial cells (HUVECs) when OMe is exchanged for a halogen atom. (Adapted from reference 133)

A plan of symmetrically *para* substituted combretafuroxans was devised, to find a correlation between substituents and anti-cancer activity through small subtle structural changes to the A and B rings. These structural modifications should also have an effect of on the relative nitric oxide release from the furoxan ring due to the different electronic effects atoned to each group as mentioned before in section 1.1.3 (page 28) on furoxan decomposition. Fig. 35 shows the twelve compounds (**86-97**) that will be synthesised based on the series 2 motif shown in Fig.32.
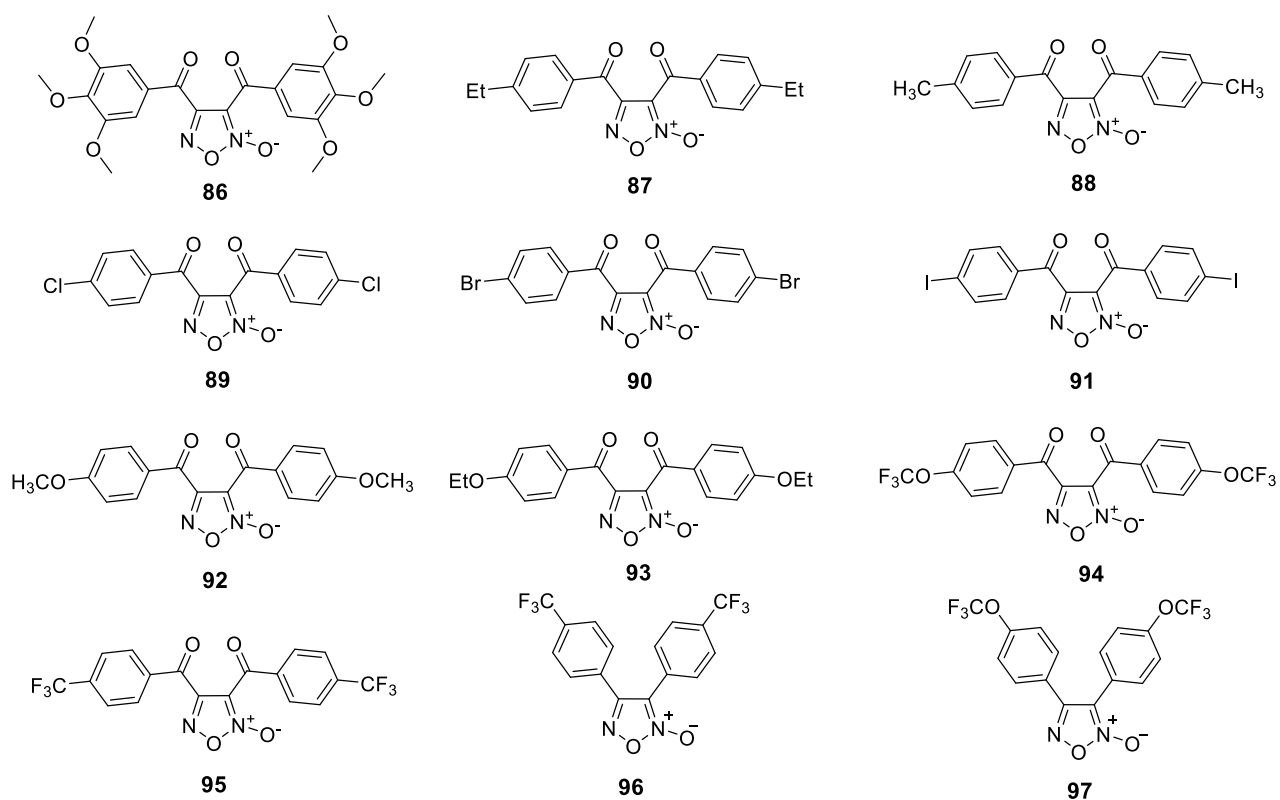
Figure 35: Planed combretafuroxan compounds **86-97** with varying substituents in the para position as well as a trimethoxy substituted analogue.

The mechanism of NO release from furoxan compounds is well established (scheme 11 and 12) and researched especially by Gasco.[66] Furoxan compounds can be fairly dependable that they will release nitric oxide when exposed to thiol or thiolate compounds, however, there isn't always a viable source of these inductors for NO release. Therefore alternative compounds that produce NO via a different mechanism, but at the same time are stable compounds, unlike some *S*-nitrosothiols, is a desirable goal. One such class of compounds, stable under these conditions and whose mechanism of NO release is not fully understood, are the diazeniumdiolates and in particular, the carbon based diazeniumdiolate, cupferron **56**.

Cupferron **56** is described as being able to release NO under numerous conditions such as light and temperature but at a rate far too unpredictable for therapeutic application. Therefore the stabilisation of this compound could produce a range of potentially tuneable NO-donors, which can release nitric oxide in a more conservative controlled fashion. Research has already been carried out on whether

substituents on the aromatic ring of cupferron alter stability,[79, 91] however alkylation of the terminal oxygens is a relatively untouched area. We aim to systematically alkylate (Fig. 36) at the terminal oxygen (O^2 site) increasing by two carbon units **98-101** each time to assess whether chain length of the 'protecting' group effects the rate of NO release and if there is a trend amongst this. Along with mono alkylated cupferron derivatives, a series of compounds that contain two cupferron molecules **102-105** will also be synthesised using the same chemistry and assessed to see if using an alkyl chain as a synthetic 'bridge' effects the rate of NO release.
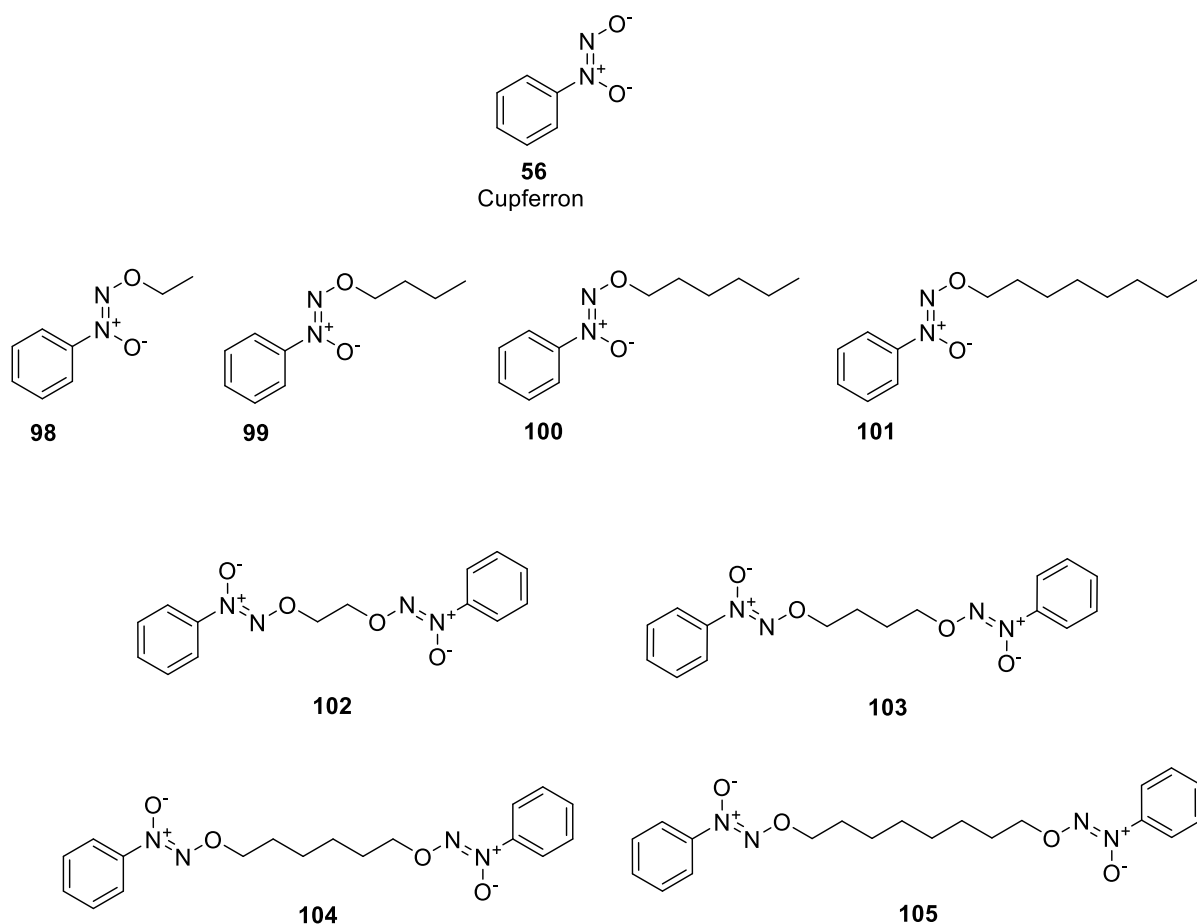
Figure 36: Planned cupferron derivatives synthesised by alkylation chemistry at the O^2 site. Both mono and di cupferron compounds will be synthesised.

The compounds **98-105** produced from within the cupferron series (Fig. 36) will be tested for their nitric oxide releasing capabilities under physiological conditions as well as irradiation with ultraviolet light. It is the hope with this type of chemistry the stability of the parent compound will be increased and therefore produce a series of more effective NO-donors.

As aforementioned, nitric oxide levels are finely balanced by homeostasis. We have hypothesised methods to increase the level of NO if it should be required to treat various vascular-related diseases, however when levels of nitric oxide are too high and at risk of becoming toxic we need an alternative approach. We therefore aim to design and synthesise a class of novel and selective neuronal nitric oxide synthase (nNOS) inhibitors for potential therapeutic relief of these severe conditions. Our rationale is to expand on the work conducted by Silverman,[103, 110-111, 134-136] by using the 4-aminopyridine unit to mimic the guandinium group of L-arginine **1** and build upon key observations had while studying their current research.

106

Silverman's potent nNOS inhibitor
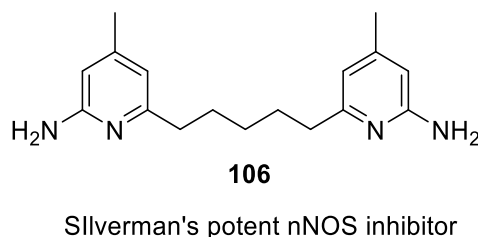
Figure 37: The most potent compound post optimisation for the Silverman group. The crystal structure for this compound docked in nNOS was obtained and used for computational studies.

Whilst looking at the most potent compound **106** studied by Silverman during docking studies (Fig. 38) using the Keele Active Virtual Environment (KAVE) and Pymol software an interesting observation was found. Looking at the 3D profile of the docked molecule it appears that the back bone of **106** and other analogues 'over hang' several amino acid residues within the active site of nNOS. This provided an area that could potentially be exploited to increase the binding potential of the inhibitor in the active site of the nNOS isoform.
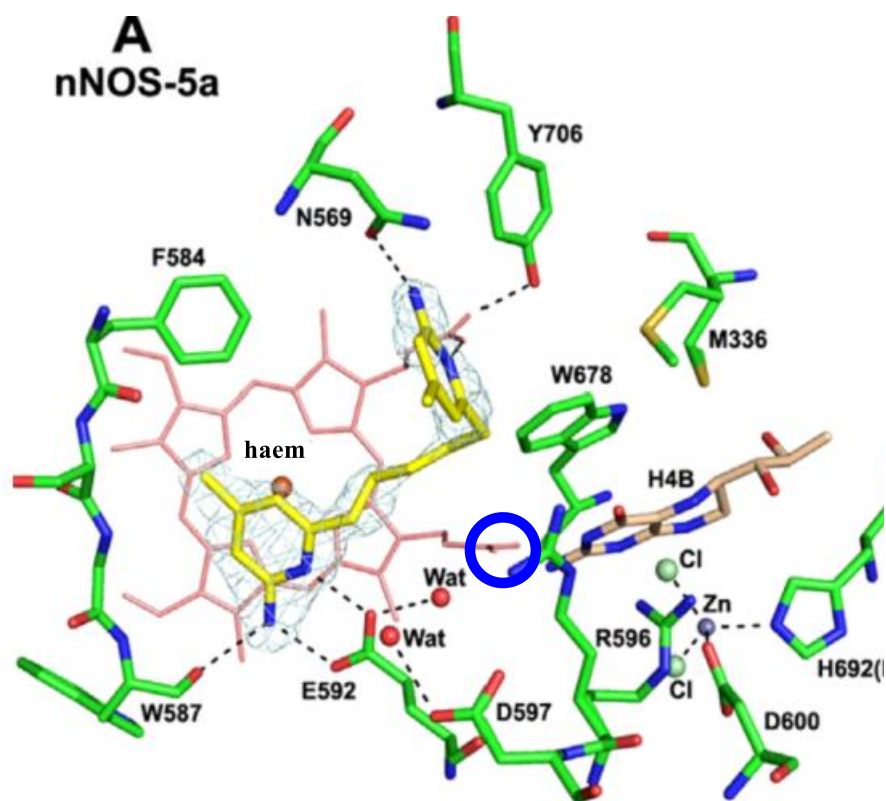
Figure 38: Compound **106** (shown in yellow), Silverman's potent inhibitor, docked within the active site of nNOS showing interaction between the haem groups of nNOS with the aminopyridine ring. Circled in blue is a propionic acid group identified as a possible unexplored interaction. NB: Three aminopyridine rings are shown due to the crystal structure being unresolved. The two aminopyridine rings on top of each other show two possible conformations they can adopt.

The yellow structure shown here is the crystal structure for compound **106** (Fig. 38). The aminopyridine ring is interacting with the haem portion of nNOS through π-π stacking. This interaction forces the alkane linker out of the plane and contorts it slightly. It is the twisting of the structure that highlighted the propionic acid (circled in blue in Fig. 38) group of the haem residue positioned directly above the centre of the 5 carbon chain linking the two aminopyridine rings. The propionic acid group, existing as the carboxylate (COO⁻) could potentially become a strong hydrogen bond acceptor (HBA) as well as offering potential ion-dipole interactions with appropriate groups. Fig. 39 part A, again shows compound **106** docked in nNOS, with the propionic acid group 'hanging' over the second carbon in the linker chain.

The distance from the carboxylate group to the hydrogen of the inhibiter was measured to be 2.6 Å, suggesting that with the correct hydrogen bond donor in place a viable and successful hydrogen bond interaction could take place and therefore increase the binding interaction of the nNOS inhibitor.
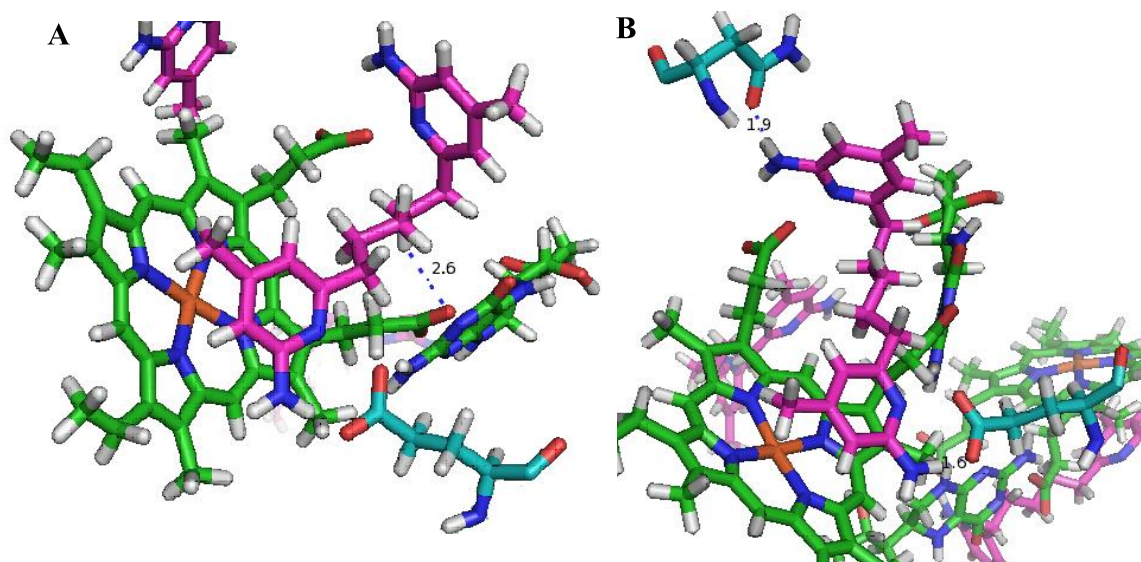
Figure 39: Part 'A' shows compound **106** (shown in magenta) docked in the nNOS active site. The distance between the carboxylate on the haem group (shown in green) and the hydrogen on the inhibitor (magenta) was found to be 2.6 Å suggesting that a hydrogen bond interaction could be exploited at this site. 'B' shows compound **106** can interact with two amino acid residues present in the nNOS structure. The amino group on the aminopyridine ring can hydrogen bond with both asparagine (1.9Å) and glutamic acid (1.6Å).

Fig. 39 part B shows the interaction of compound **106** with two amino acid residues present within the backbone of the nNOS enzyme. The hydrogen bonding interactions with asparagine (top left of Fig 39-B) and a glutamic acid residue (bottom right) validate the need for the aminopyridine moiety and the terminus of the inhibitor. The π-π interaction of the pyridine ring with the pyrrole rings that make up the haem group of nNOS can also be seen in part A and B of figure 39.

This observation suggested that there was a site of unexplored derivatisation that could be taken advantage of if the correct substituents could be placed along the alkane chain. Computational studies has led to the design of five new linkers (Fig. 40) to replace the pentane chain separating the aminopyridine rings as seen in compound **106** and produce five novel nNOS inhibitors (Fig. 40)
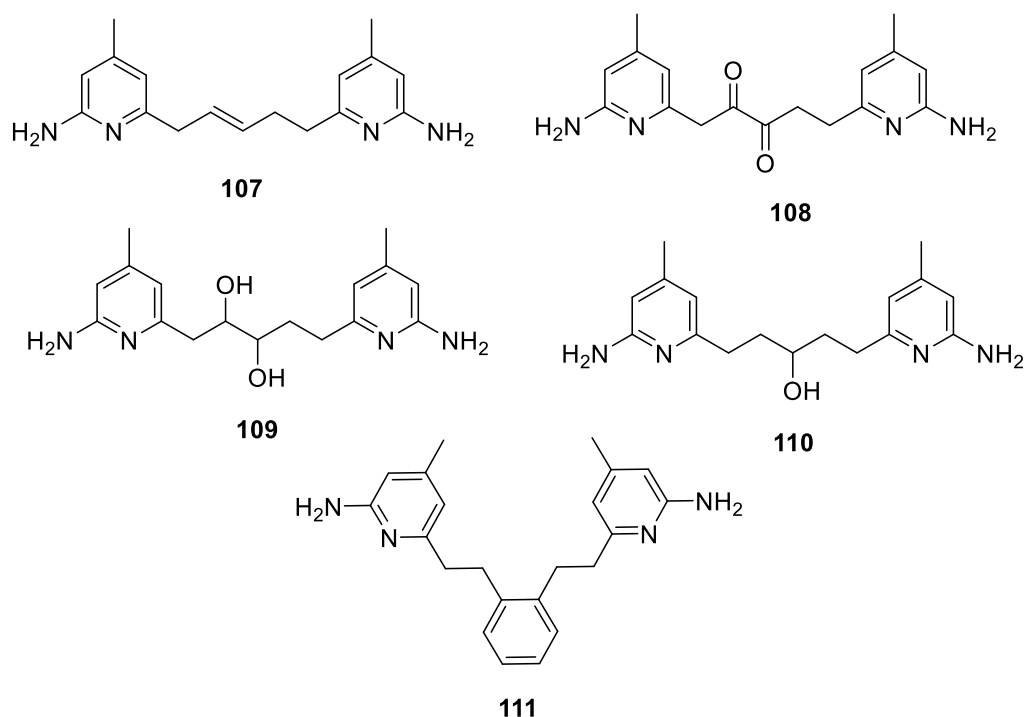
Figure 40: Proposed linker compounds to synthetically implement between two aminopyridine rings. Linkers offer difference in HBD ability and allow for further chemistry at a later date.

The diol **109** and the propanol **110** linkers can act as hydrogen bond acceptors and donators Linker B **108** is a diketone linker and has the potential to form ion dipole interactions with the negatively charged oxygen present when the propionic acid group is existing as the carboxylate. The alkene **107** and the xylene **111** linkers can be utilised as synthetic building blocks, which can be reacted with further once in place to add additional functionality. Inhibitors **107** and **111** also have the potential to provide hydrophobic interactions, similar to the one the parent molecule had using the pentane chain.

A further goal in the NO reduction work and also related to the NOS work and increasing the HBD potential is making use of the radical scavenger curcumin **70** as a potential inhibitor of NOS. Curcumin already has the HBA and HBD motifs situated within the molecule and therefore is a great candidate as a NOS analogue **112** under our current proposed hypothesis (see Fig. 38/39) Not only can curcumin act as a radical scavenger, by implementing an L-arginine **1** motif into its structure it has the potential to have dual functionality of acting as a NOS inhibitor and a scavenger.
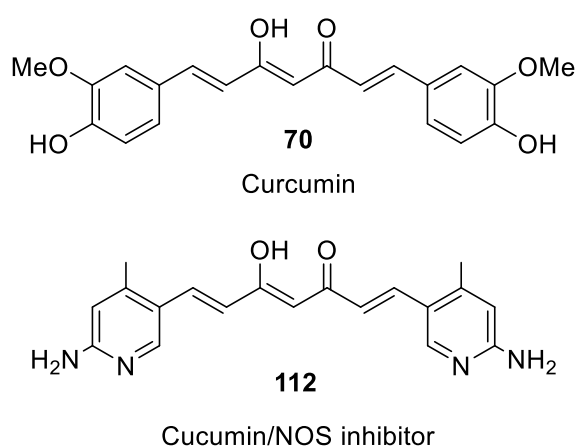
Figure 40: Natural product curcumin, **70,** and the objective dual function inhibitor **112.**

1.4-   Overall objectives

Due to the plethora of applications nitric oxide has within the body, both beneficial and detrimental there is a real need for compounds that can potentially aid in these processes, by either increasing or decreasing levels of nitric oxide *in vivo*. My research aims to synthesise two separate types of NO compounds, ones that can enhance levels of nitric oxide and ones that can work on reducing levels of NO.

To enhance the levels of NO, two types of NO-donor compounds that can release nitric oxide under differing conditions and thus can be made tailorable to specific disorders will be synthesised. Furoxan compounds (**77-82** and **86-97**) will be synthesised in a systematic way, by varying the para substituent attached to the phenyl ring or manipulating the trimethoxy units positioning around the

aromatic ring. Their relative NO release will be monitored using a NO analyser in the presence of thiol/thiolate. Cupferron analogues (**98-105**) will also be synthesised through a series of systematic alkylations at the preferential O^2 site. The stabilisation effect of these alkyl chains on the parent compound will be assessed under various conditions including light and heat. To further test furoxan compounds **77**-**82** and **86**-**97**'s ability to release nitric oxide, vasodilatory tests will be performed by collaborators at Kingston University (UK). The vasodilatory work will establish how effective each furoxan is at releasing NO and its ability to bring about relaxation of smooth muscle cells.

The reduction of NO levels requires a different approach and therefore a series of novel NOS inhibitors will be synthesised, building on the work of Silverman. Various linkers, exploiting the potential HBD/HBA and electronic interactions, will be implemented between two aminopyridine rings, which will be mimicking the guanidinium terminus of L-arginine **1**.

References

1. A. Butler and R. Nicholson, "Life, Death and Nitric Oxide", RSC paperbacks, The Royal Society of Chemistry, Cambridge UK, 2003.

2. F. Guthrie, *J. Chem. Soc.*, 1859, **11**, 245-252

3. http://nobelprize.org/nobel_prizes/medicine/laureates/1998/illpres/index.html

4. R. F. Furchgott, *Angew. Chem. Int. Ed*. 1999, **38** (13-14), 1870-1880

5. L. J. Ignarro, *Angew Chem. Int. Ed.* 1999, **38** (13-14), 1882-1892

6. F. Murad, *Angew. Chem. Int. Ed.* 1999, **38** (13-14), 1857-1868

7. S. Moncada, M. Randomski, and R. M. J. Palmer, *Trends in Pharm. Sci*, 1991, **12**, 87

8. R. M. J. Palmer, A. G. Ferrige and S. Moncada, *Letters to Nature*, 1987, **327**, 524-526

9. A. R. Butler, F. W. Filtney, D. Lyn. Wiliams, *Trends in Pharm. Sci*, 1995, **16**, 1, 18-22

10. T. S. Hakim, K. Sugimori, E.M. Camporesi, and G Anderson, *Physiol. Meas*, 1996, **17**, 267–277

11. Y. C. Hou, A. Janczuk and P. G. Wang, *Curr. Pharm. Des*., 1999, **5**, 417-441

12. P. Tripathi, *Indian J. Biochem. Biophys.*, 2007, **44**, 310-319

13. W. K. Alderton, C. E. Cooper, and R.G. Knowles, *J. Biochem*, 2001, **357**, 593-615

14. D. Stuehr, S. Pou, and G. Rosen*, J. Biol. Chem*, 2001, **276**, 14533-14536

15. C. Napoli, and L. J. Ignarro, *Nitric Oxide*, 2001, **5**, 88-97

16. R. G. Knowles and S. Moncada, *J. Biochem.,* 1994, **298**, 249-258

17. A. R. Butler, D. L. H. Williams, *Chem. Soc. Rev.* , 1993, 233- 241

18. F. Y. Liew, and F. Cox, *Immunol Today*, 1991, **12**, 17-18

19. S. L James, *Microbiol. Rev*., 1995, *59*, 533-547

20. V. L. Dawson and T. M. Dawson, *J. Chem. Neuroanat.*,1996, **10**, 179-190

21. S. Moncada and J. O. Bolanos, *J. Neurochem.*, 2006, **97**, 1676-1689

22. J. Kerwin, J. Lancaster, and P. Feldman, *J. Med. Chem. Perspective*., 1995, **38**, 22, 4343-4362

23. A. Sobrero, *Liebigs Annalen der Chemie*, 1847, **64**, 398

24. N. Marsh and A. Marsh, *Clin. Exp. Pharmacol. Physiol*, 2000, **27**, 313-319

25. W. Murrell, Lancet, 1879, 80

26. Joint Formulary Committee. British National Formulary. 64 ed. London: BMJ Group and Pharmaceutical Press; 2012

27. J. A. Friederich and J. F. Butterworth IV, *Anesthesia and Analgesia*, 1995, **81**, 152-162

28. L. Grossi and S. D'Angelo, *J. Med. Chem.*, 2005, **48**, 2622-2626

29. F. W. Flitney, I. L. Megson, D. E. Flitney and A. R. Butler, *Brit. J. Pharmacol.*, 1992, **107**, 842

30. H. S. Tasker, and H. O. Jones, *J. Chem. Soc. Trans*, 1909, 1910-1918

31. N. Hogg*, Annu. Rev. Pharmacol. Toxicol*., 2002, **42**, 585-600

32. D. L. Williams, *Acc. Chem. Res.*, 1999, **32**, 869-876

33. V. G. Kharitonov, A. R. Sundquist, and V. S. Sharma, *J. Biol. Chem*, 1995, **270**, 28158

34. P. Wang, M. Xian, X. Tang, X. Wu, Z. Wen, T. Cai, and A. Janczuk, *Chem. Rev*, 2002, **102**, 1091-1134

35. B. Gaston, *Biochimica et Biophysica Acta*, 1999, **1411**, 323-333

36. I. Kluge, U. Gutteck-Amsler, M. Zollinger and K. Quang Do, *J. Neurochem.*, 1997, **69**, 6, 2599-2607

37. Y. Zhang and N. Hogg, *Free Radical Biol. Med*, 2005, **38**, 831-838

38. J. S. Stamler, O. Jaraki, J. Osborne, D. I. Simon, J. Keaney, J. Vita, D. Singel, C. R. Valeri and J. Loscalzo, *Proc. Nat. Acad. Sci*, 1992, **89**, 7674, 7677

39. S. C. Askew, D. J. Barnett, J. McAninly, D. L. H. Williams, *J. Chem. Soc, Perkin Trans 2*, 1995, **4**, 741-745

40. R. J. Singh, N. Hogg, J. Joseph and B. Kalyanaraman, *J. Biol. Chem.*, 1996, **271**, 31, 18596-18603

41. D. L. Williams, *Chem. Commun.*, 1996, 1085-1091

42. H. M. S. Patel and D. L. H. Williams, *J. Chem. Soc. Perkin Trans 2,* 1990, 37-42

43. H. Al-Sa'doni and A. Ferro, *Clin. Sci.*, 2000, **98**, 507–520

44. A. Butler, J. McAninly, L.H. Williams, S. Askew, and C. Russell, *J. Chem. Soc., Chem. Commun*, 1993

45. Q. Timerghazin, G.H. Peslherbe, and A.M. English, *Org. Lett*, 2007, **9**, 16, 3049-3052

46. D. R. Noble and D. L. H. Williams, *Nitric oxide*, 2000, **4**, 392-398

47. F. Kahn, R. J. Pearson, D. J. Newton, J. J. F. Belch, and A. R. Butler, *Clin. Sci.*, 2003, **105**, 577-584

48. C. M. Turnbull, P. Marcario, T. A. Sheldrake, L. Lazzarato, C. Cena, R. Fruttero, A, Gasco, S. Fox, I. L. Megson and A. G. Rossi, *J. Inflammation*, 2008, **5**, 1-10

49. A. Gasco, and P. Tosco, *Pure Appl. Chem.*, 2008, 80, **8**, 1693-1701

50. A. Gasco, and A. Rossi, *J. Inflammation*, 2008, **12**, 1-10

51. L. Megson, and A. Gasco, *Br. J. Phamracol.*, 2006, **148**, 517-526

52. D. Ding, and L. Fang, *Bioorg. Med. Chem. Lett.*, 2007, 1062-1066

53. A. Gasco, *J. Med. Chem.*, 2001, **44**, 3463-3486

54. M.L. Lolli, B. Rolando, P. Tosco, S. Chaurasia, A. Di. Stilo, L. Lazzarato, E. Gorassini, R. Ferracini, S. Oliaro-Bosso, R. Fruttero and A. Gasco, 2010, *Bioorg. Med. Chem.*, **18**, 2428-2438

55. M. Bertinaria, S. Guglielmo, B. Rolando, M. Giorgis, C. Aragno, R. Fruttero, A. Gasco, S. Parapini, D. Taramelli and Y. C. Martins, *Eur. J. Med. Chem.*, 2011, 1-11

56. A. Di Stilo, S. Visentin, C. Cena, A. M. Gasco, G. Ermondi and A. Gasco, *J. Med. Chem.*, 1998, **41**, 5393-5401

57. R. Fruttero, M. Crosetti, K. Chegaev, S. Guglielmo, A. Gasco, F. Berardi, M. Niso, R. Perrone, M. A. Panaro, N. and A. Colabufo, *J. Med. Chem.*, 2010, **53**, 5467-5475

58. R. M. Paton, *Comprehensive Heterocyclic Chemistry I*, 1984, 393-426

59. R. M Paton, *Comprehensive Heterocyclic Chemistry II*, 1995, 229-265

60. G. N. Nikonov, and S. Bobrov, *Comprehensive Heterocyclic Chemistry* III, 2008, Vol.5, 315-394

61. W. F. Nirode, J. M. Luis, J. F. Wicker and N. M. Wachter, *Bioorg. Med. Chem. Lett.*, 2006, **16**, 2299-2301

62. P. G. Wang, T. B. Cai, N. Taniguchi, Nirtic oxide donors: For Pharmaceutical and Biological Applications, Science, John Wiley and Sons, 2005

63. P. Tonnies, *Chem. Ber*, 1903, *13*, 1845-1880

64. H. Wieland, *ANN.*, 1903, **329**, 225-268

65. H. Takayama, S. Shirakawa, M. Kitajima, N. Amimi, K. Yamaguchi, Y. Hanasaki, T. Ide, K. Katsuura, M. Fujiwara, K. Ikichi, K. Konno, S. Sigeta, T. Yokota and M. Baba, Bioorg. *Med. Chem. Lett*, 1996, **16**, 1993-1996

66. A. Gasco, R. Fruttero, B. Ferrarotti, A. Serafino, and A. Di Stilo, *J. Heterocyclic. Chem.*, 1989, **26**, 1345

67. H. Takayama, *Bioorg. Med. Chem. Lett.*, 1996, 1993- 1996

68. A. Gasco, *ANN*, 1991, 1211-1213

69. X. Dong, and Y. Hu, *Eur. J. Med. Chem.*, 2010, **40**, 3986-3992

70. E.R. Alexander, M. R. Kinter and J. D. McCollum, *J. Am. Chem. Soc*, 1950, **72**, 2, 801-803

71. H.R.Snyder and N. E. Boyer, *J. Am. Chem. Soc*, 1955, **77**, 16, 4233-4237

72. D. A. Shirley, B. H. Gross and M. J. Danzig, 1958, *J. Org. Chem.*, **23**, 7, 1024-1026

73. H. Tezuka, M. Kato and Y. Sonehara, *J. Chem. Soc. Perkin. Trans. 2*, 1985, 1643-1647

74. V. N. Yarovenko, S. A. Kosarev, I. V. Zavarzin and M. M Krayushkin, *Russ. Chem. Int. Ed.*, 2002, **51**, 8, 1504-1509

75. M. Curini, *Tet. Lett*, 2000, 8817-8820

76. Kwang-Jin Hwang ,Y. C. Park, H. Jin Kim, J. H. Lee, *J. Biochem*, 1998, **62**, 9, 1693-1697

77. R. L. Willer, *J. Org. Chem.*, 1985, **50**, 5123-5127

78. J. V. Burakevich , *J. Org. Chem.*, 1971, **36**, 1, 5-7

79. J. A. Hrabie and L. K. Keefer, *Chem. Rev*, 2002, **102**, 1135-1154

80. A. Angeli, *Samml. Chem. Chem-Tech. Vortr*, 1908, **13**, 1-50

81. R. S. Drago, E. F. Paulik, *J. Am. Chem. Soc*, 1960, **82**, 96-98

82. J. E. Saavedra, M. N. Booth, J. A. Hrabie, K. M. Davies and L. K. Keefer, *J. Med. Chem.*, 1999, **64**, 5124-5131

83. R.S. Nyholm and L. Rannitt, *J. Inorg. Syn.*, 1957, **5**, 117-118

84. P. G. Parzuchowski, M. C. Frost and M. E. Meyerhoff, *J. Am. Chem. Soc*, 2002, **124**, 12182-12191

85. M. J. Hill, G. Hawkswort and G. Tattersall, *Br. J. Cancer*, 1973, **28**, 562-567

86. K. Straif, S. K. Wieland, M. Bungers, D. Holthenrich, D. Taeger, S. Yi and U. Keil, *Brit. Med. J.*, 2000, **57**, 180-187

87. E. V. Arnold, B. G. Doleski and R. E. Raulli, *United States Patent*. Patent No: US 7,569,559 B2, 2009

88. J. Brown, *J. Am. Chem. Soc.*, 1917, 2358-2366

89. T.A. Balaban, E. R. Garfield, M. J. Lesko and A. W. Seitz, *Org. Prep. Pro. Int*., 1998, **30**, 439-446

90. Y. Hou, W. Xie, N. Ramachandran, B. Mutus, A. J. Janczuk and P. G. Wang, *Tet. Lett*, 2000, **41**, 451-456

91. Y. Hou, W. Xie, A. J. Janczuk and P. G. Wang, *J. Org. Chem.*, 2000, **65**, 4333-4337

92. A. D. McGill, W. Zhang, J. Wittbrodt, J. Wang, H. Bernhard Schlegal and P. G. Wang, *Bioorg. Med. Chem. Lett.*, 2000, **8**, 405-412

93. E. R. Garfield, T. A. Bablaban, A. W. Seitz, J. D. Klein and M. Lesko, *International Patent*, WO: 96/36326, 1996

94. J. R. Hwu, C. S. Yau, S-C Tsay and T-I Ho, *Tet Lett.* 1997, **38**, 52, 9001-9004

95. A. W. Deckel, *J. Neurosci. Res.*, 2001, **64**, 99-107

96. S. Hunot, F. Boissiere, B. Faucheux, B. Brugg, A. Mouatt-Prigent, Y. Agid and E. C. Hirsch, *Neuroscience*, 1996, **72**, 2, 355-363

97. L. Zhang, V. L. Dawson and T.M. Dawson, *Pharmacol. Ther.*, 2006, **109**, 33-41

98. J. B. Schulz, R. T. Matthews and M. F. Beal, *Curr. Opin. Neurol.*, 1995, **8**, 480-486

99. V. L. Dawson and T. M. Dawson, *Prog. Brain Res.*, 1998, **118**, 215-29

100. R. Shukla, *Ann. Neurosci.*, 2007, **14**, 1-14

101. http://dictionary.reference.com/medical. Date accsessed 18/06/2015

102. P.E. Chabrier, C. Demerle-Pallardy and M. Auguet, *Cell. Mol. Life Sci.*, 1999, **55**, 1029-1035

103. H. Ji, S. Tan, J. Igarashi, H. Li, M. Derrick, P. Martasek, L. J. Roman, J. Vasquez-Vivar, T. L. Poulos and R. B. Silverman, *Ann Neurol.*, 2009, **65**, 2, 209-217

104. H. Matter, P. Kotsonis, O. Klingler, H. Strobel, L. G. Frohlch, A. Frey, W. Pfleiderer and H. H. H. W. Schmidt, *J. Med. Chem*, 2002, 2923-2941

105. J. Vitecek, A. Lojeck, G. Valacchi and L. Kubala, *Mediators of Inflam. Rev.*, 2012, 1-22

106. http://www.rcsb.org/pdb/101/motm.do?momID=133. D. Goodsell: Molecule of the Month review 2011. Date accssesed 18/06/2015

107. T. Fischmann, A. Hruza, X. D. Niu, J. D. Fossetta, C. A. Lunn, E. Dolphin, A. J. Prongay, P. Reichert, D. J. Lundell, S. K. Narula and P.C. Weber, *Nat. Strut. and Bio.*, 1999, **6**, 233-242

108. S. Pfeiffer, E. Leopold, K. Schmidt, F. Brunner and B. Mayer, *Br. J. Pharmacol.*, 1996, **118**, 1433-1440

109. www.scbt.com Date accessed 18/06/2015

110. R. B. Silverman, *Acc. Chem. Res.*, 2008, **42**, 439-451

111. F. Xue, J. Fang, S. L. Delker, H. Li, P. Martasek, L. J Roman, T. L. Polous and R. B. Silverman, *J. Med. Chem.*, 2011, **54**, 2039-2048

112. K. E. Heim, A. R. Tagloaferro and D. J. Bobilya, *J. Nutr. Biochem.*, 2002, **13**, 572-584

113. C. A. Rice-Evans, N. J. Miller and G. Paganga, *Free Radical Bio. Med.*, 1996, **20**, 933-956

114. D. Amic, D. Davidovic-Amic, D. Belso and N. Trinajstic, *Croatica Chemia Acta.*, 2003, **76**, 55-61

115. T. Ak, I. Gulcin, *Chemico-Biologcal Interactions*, 2008, **174**, 27-37

116. H. Tezuka, M. Kato and Y. Sonehara, *J. Chem. Soc. Perkin Trans 2*, 1985, 1643-1647

117. D. I. Batovska and I.T. Todorova, *Curr. Clin. Pharmacol.*, 2010, **1**, 1-4

118. W. V. Farrar, *J. Chem. Soc*, 1964, 904-906

119. Y. Hou, W. Xic, A. Janczuk and P.G. Wang, *J. Org. Chem.*, 2000, **65**, 4333-4337

120. D. Thompson, Molecule of the month, http://www.chm.bris.ac.uk/motm/combretastatin/combv.htm

121. R. G. Pettit, M. G. Cragg, L. D. Herald and M. J. Schmidt, *Can. J. Chem*, 1982, **60**, 1374-1376

122. R. G. Pettit and B. S. Singh, *Can. J. Chem.*, 1987, **65**, 2390-2396

123. R. G. Pettit, C. Temple (Jnr), L.V. Narayanan, R. Varma, K. M. Simpson, *Anti-Cancer Drug Des.*, 1995, **10,** 299-309

124. G.C Tron, F. Paglial, E. Del Grosso, A. A. Genazzani and G. Sorba, *J. Med. Chem.*, 2005, **48**, 3260-3268

125. World Health Organisation, http://www.who.int/topics/cancer/en/

126. G. Nagaiah and S.C. Remick, *Future Oncol.*, 2010, **6**, 8, 1219-1228

127. Oxigene pipeline drugs- How combretastatin works. - http://www.oxigene.com/our_science/how_our_drugs_work/

128. E. Hamel, *Pharmac. Ther.*, 1991, **51**, 377-401

129. K. G. Pinney, M. P. Mejia, V. M. Villabos and G. R, Pettit, *Bioorg. Med. Chem.*,2000, **8**, 2417-2425

130. S. Ducki, G. Mackenzie, N. J. Lawrence and J. P. Snyder, *J. Med. Chem*, 2005, **48**, 457-465

131. T. McGown, *J. Org. Biomol. Chem.*, 2003, **1**, 3033-3037

132. M. E. Richardson, PhD thesis, Keele University, 2012

133. T. M. Beale, D. M. Allwood, A. Bender, P. J. Bond, J. D. Brenton, D. S. Charnock-Jones, S. Ley, R. M. Myers, J. W. Shearman, J. Temple, J. Unger, C. A. Watts and J. Xian, *Med. Chem. Lett.*, 2012, **3**, 177-181

134. P. Mukherjee, M. A. Cinelli, S. Kang and R. B. Silverman, *Chem. Soc. Rev.*, 2013

135. H. Huang, H. Li, P. Martasek, L. J. Roman, T. L. Poulous and R. B. Silverman, *J. Med. Chem*, 2013, 56, 3024-3032

136. Q. Jing, H. Li, J. Fang, L. J. Roman, P. Martasek, T. L. Poulos and R. B. Silverman, *Bioorg. Med. Chem.*, 2013, **21**, 5323-5331

Chapter 2.0- Results and Discussion

The results and discussion chapter will be split into three sections. The first comprising the synthetic routes used in the generation of NO-donors and inhibitors. The second will contain details concerning the measurement of NO release including background and. The final section will contain the biological results generated by collaborators at Kingston University (UK).

2.1 Synthesis

2.1.1- Combretafuroxan compounds

The rationale for developing a series of substituted combretafuroxan compounds within either series 1 or 2, allows for a large amount of research scope. For each combretafuroxan series to have any potency against cancer cell lines, better or comparable to the parent compound, combretastatin A-4, it will need to have key structural similarities, notably the *cis* conformation. The structural back bone of the parent compound combretastatin is essentially a Z-stilbene[1] which makes synthetic analogues relatively straight forward to make. Petitt[2], who first isolated combretastatin from the bark of the African willow, used standard Wittig chemistry to synthesise the substituted stilbene. The rationale for the inclusion of a furoxan ring within the combretastatin structure is an easy one and it is all down to orientation, sterics and solubility. The *cis* orientation that combretastatin A-4 adopts is one of the reasons for its high potency.[3] The double bond forces the two phenyl rings to be an optimal distance apart for binding with in the tubulin site[4,5]. However *in vivo*, the parent compound is prone to isomerisation and readily converts to the less active *trans* conformer. The furoxan ring forces the combretastatin to remain in the most optimal orientation while also having the dual action of improving water solubility.

72 | P a g e

2.1.1.1- Synthesis of Stilbene compounds

The general reaction scheme for the production of the substituted stilbene compounds (**120-125**) is shown in scheme 1. Classic Witting chemistry[6] was utilised in the production of the stilbene compounds **120-125** (shown in scheme 28), these were then treated with sodium nitrite under acidic conditions, comparable to those used by Gasco[7,8], to generate the combretafuroxans **77-82**.
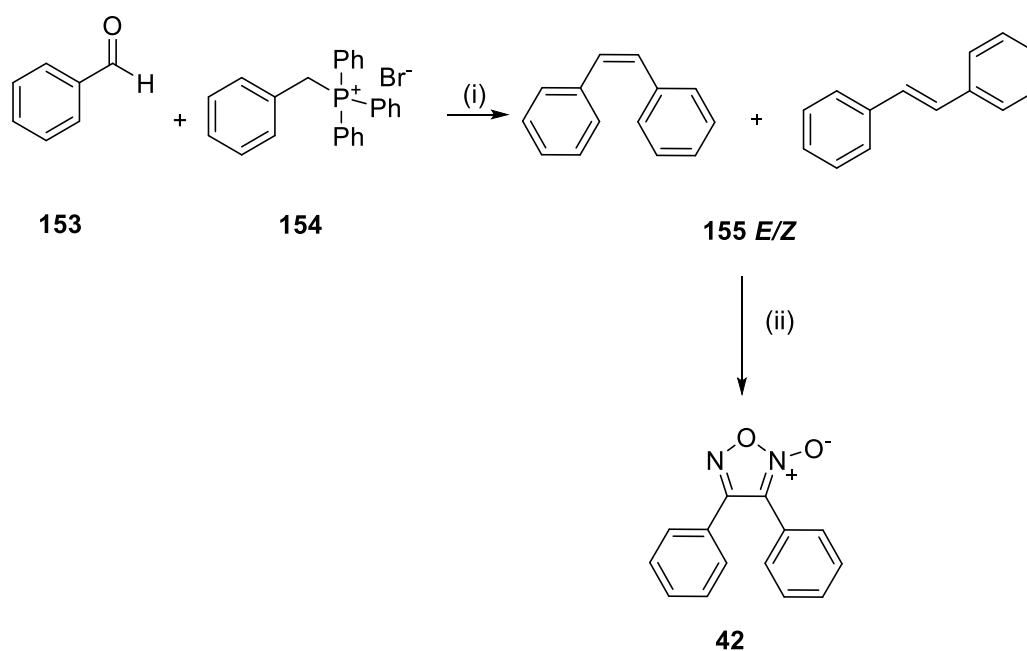
Reagents and conditions: (i) *n*-BuLi, dry THF, -78°C, 2hrs (ii) NaNO$_2$, CH$_3$COOH, 60°C, 2hrs

Scheme 28: Standard Witting reaction[6] to produce a mixture of *E/Z* stilbene compounds. These can then be reacted on to generate the desired combretafuroxan compound, **42**.

Adapting a method found in the literature[9] mono-substituted iodo phosphonium bromides, in the *meta* and *para* positions **117** & **118** and *para*-bromo phosphonium bromide **119** were synthesised from their corresponding benzyl bromides and triphenylphosphine (scheme 29). These were synthesised in high yields (86-88%) for use in the later Wittig reaction and creation of the required stilbene compounds **120-125** *E/Z* as shown in scheme 30.
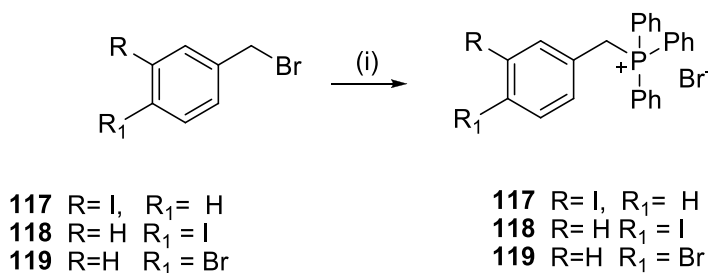
Reagents and conditions: (i) PPh$_3$, 55°C, 24 hours

Scheme 29: Reaction of bromobenzyl compounds with triphenylphosphine to produce the phosphobium bromide compounds **117**-**119** for scheme 28.

The synthesis of the stilbene compounds was initially straight forward route using standard Witting chemistry by reacting substituted aldehydes with phosphonium bromides to create the desired olefinic bond in a mixture of *E* and *Z* isomers which could then be separated using flash column chromatography.

E stilbene   *Z* stilbene

117 R$_5$= I, R$_6$= H   R=R$_2$=R$_3$= OMe, R$_1$=R$_4$=H   **156**
118 R$_5$= H R$_6$ = I   R=R$_2$=R$_4$= OMe, R$_1$=R$_3$=H   **157**
119 R$_5$=H R$_6$ = Br   R$_1$=R$_3$=Br R=R$_2$=R$_4$=H   **158**
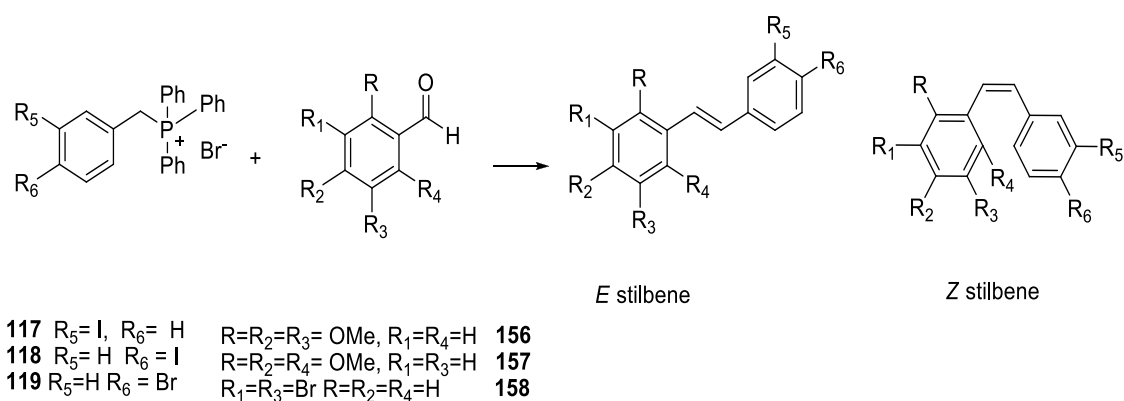
Compound Number	R	R$_1$	R$_2$	R$_3$	R$_4$	R$_5$	R$_6$
120 *E/Z*	OMe	H	OMe	OMe	H	I	H
121 *E/Z*	OMe	H	OMe	OMe	H	H	I
122 *E/Z*	OMe	H	OMe	H	OMe	H	I
123 *E/Z*	H	Br	H	Br	H	I	H
124 *E/Z*	H	Br	H	Br	H	H	I
125 *Z*	H	H	Br	H	H	H	Br

Scheme 30: Reaction of substituted phosphonium bromides with benzaldehydes to produce a mixture of *E* and *Z* stilbenes **120**-**125**.

Diagnostically, ^{1}H NMR spectroscopy and specifically *J* couplings were used to determine if the production of the stilbene compounds were successful. Literature[9] indicates that the *E* isomers have a *J* coupling of 16 Hz compared to 12 Hz for the *Z* isomers, although due to the mixture of isomers not all *J* couplings were isolated.

The appropriate halogenated phosphonium bromide **117-119** was sparingly dissolved in dry THF and deprotonated using *n*-Buli at -78^{0}C, creating the reactive ylide species that are famous to the Wittig reaction. To this solution trimethoxy substituted aldehydes **156-158** (scheme 30) were added and left to stir at room temperature for 1 hour before being worked up, by the addition of water, to yield the *E/Z* stilbene analogues in various yields (2.3% to 22%). Of the isolated *E/Z* stilbenes, ratios of *cis*:*trans* isomers were found at 1:4 *E/Z*. The production of phosphonium oxide **160** is the driving force for this reaction as production of the oxygen-phosphorous bond is highly energetically favourable and its formation is shown in scheme 31.
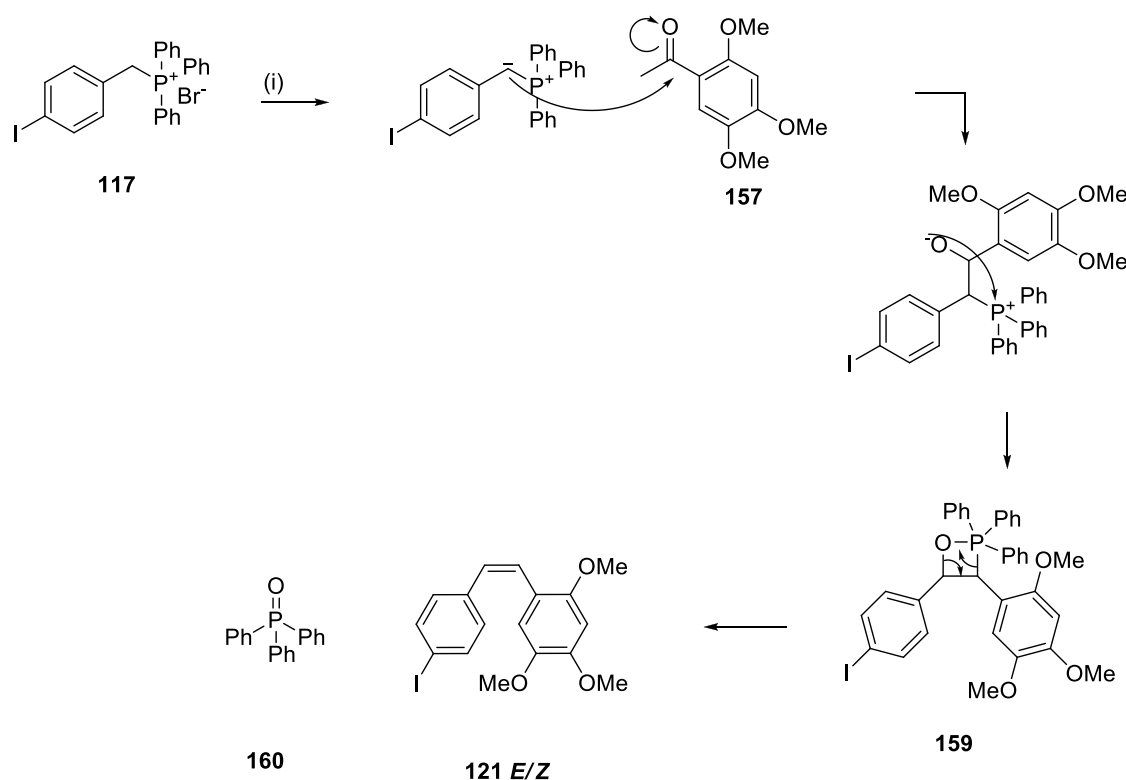
Reagents and conditions: (i) *n*-BuLi, dry THF **-20°C**

Scheme 31: Mechanism for the Wittig reaction between the phosphonium bromide **117** and trimethoxybenzaldehyde **157**. The driving force for this reaction is the formation of the very strong P-O bond and generation of phosphonium oxide **160** and the alkene.

The purification of these compounds proved to be a very challenging. Both *E* and *Z* isomers were almost inseparable using thin layer chromatography (TLC) and column chromatography. Several solvent systems were tried, ranging from 1:1 to 100:1 petroleum ether:ethyl acetate, none of which managed to produce a successful separation of the isomers, expect for one compound (**122**).. During the synthesis and purification of these stilbene compounds (**120-125 *E/Z***), it was discovered that isomerisation was occurring rapidly and the ratio of E/Z (1:4) was changing. Compound **122**, the stilbene that was successfully separated, was used to test this change in olefinic bond orientation. A ^{1}H NMR study was conducted were a sample of compound **122 *E*** and **122 *Z*** (*cis* and *trans* stilbene) were either exposed to light or kept under dark conditions. Using diagnostic olefinic ^{1}H peaks between 6 and 7 ppm the ratio of *cis* to *trans* was determined and showed that over time there was a slow conversion to the *trans* conformation as the preferred isomer. This phenomenon only occurred

when compound **122 *E/Z*** was kept under dark conditions. In the presence of ambient light compound **122 *E/Z*** began to isomerise but then rapidly degraded and decomposed. These findings led to all compounds being protected from light and stored at a low temperature to slow down the isomerisation process. Graph 2 showing the isomerisation that occurred under dark conditions is shown below.
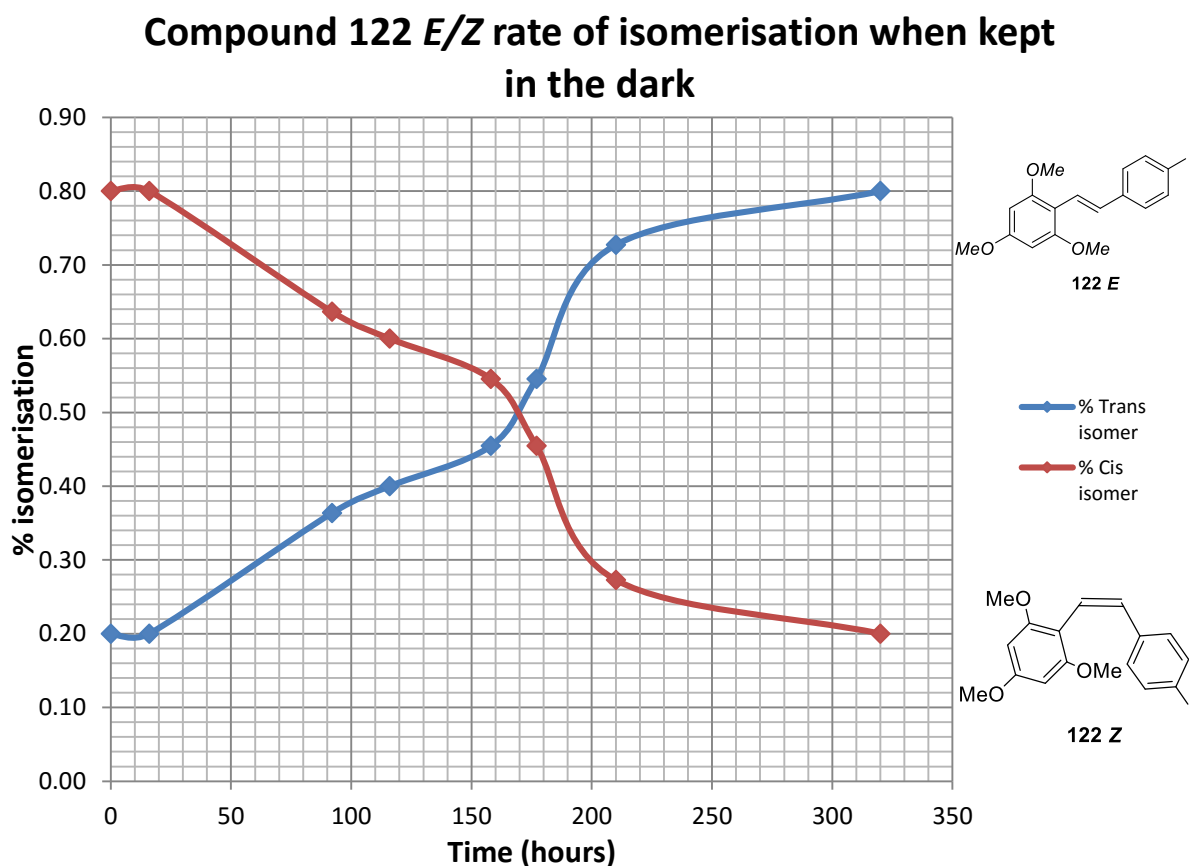
Graph 2: Isomerisation graph showing the change in conformation over time for compound **122 *E/Z***.

Although stilbenes **120-125 *E/Z*** could not be separated by conventional chromatography techniques, this didn't affect the forward synthesis and the reaction to generate the furoxan ring. This is due to the 'ionic' mechanism[7] that is undergone to form the 1,2,5-oxadiazole-2-oxide ring previously shown in scheme 14 (chapter 1, page 30). The orientation of the double of bond should not alter the reaction of the NO^+ ion being attacked and therefore the forward synthesis towards furoxan compounds **77**-

82 was preceded without further purification. Stilbene's **120-125 *E/Z*** were dissolved in acetic acid, to which dilute HNO_3 was added in a dropwise fashion. To this solution a catalytic amount of solid sodium nitrite ($NaNO_2$) was added causing the evolution of a brown gas, noted as being nitrogen dioxide (NO_2) gas. However the synthesis of furoxans from the substituted stilbenes proved to be unsuccessful on several attempts. High purity sodium nitrite was also used (99.9995%) but this yielded no desired product. The number of equivalents of sodium nitrite was also changed in relation to what is reported in the literature.[7,9-11] Sodium nitrite was used in both three and seven fold excess to that of the stilbene staring materials (**120-125 *E/Z***), however all reactions returned unreacted starting material, with no isolation of the desired furoxan product. When several attempts at converting the substituted stilbene compounds to their corresponding furoxan derivatives **77-82** appeared not to be giving the desired product and only produced unreacted starting material, the validity of the procedures being adapted were discusssed[7,10]. Various theories about temperature control were considered, as Gasco states[7] that addition of sodium nitrite should be done at exactly 14°C, which appeared to be quite a strange option. To understand Gasco's procedure in a more in-depth way, so any further alterations to his method could be done logically and through direct observations, it was decided that the synthesis of furoxans from alkenes reported in the literature[7, 12] should be repeated using the identical starting materials and conditions quoted in the publication, as this should give an indication of the validity of the procedure and provide key experimental observations that could be applied to our stilbene compounds. The two most common starting materials for the majority of Gasco's furoxan work used were but-2-enal **161** and cinnamyl alcohol **162**. Reactions of these compounds with sodium nitrite have been reported to successfully produce the furoxan ring **126** from the alkene double bond, as shown in scheme 32.

161 →(i) 25%→ **126**

162 →(ii) 42%→ **127**
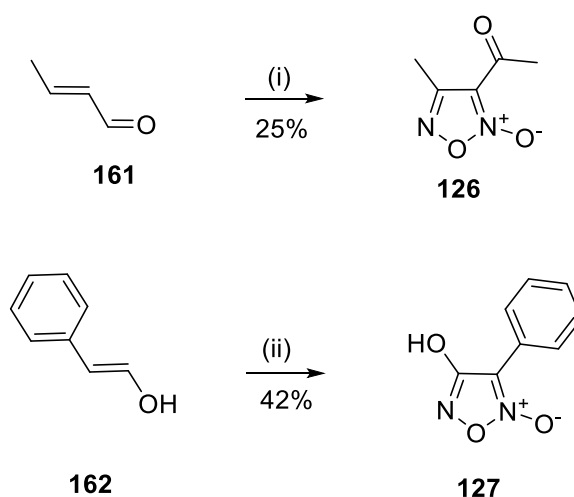
Reagents and conditions: (i) AcOH, HNO_3, $NaNO_2$, 14°C (ii) AcOH, HNO_3, $NaNO_2$, RT

Scheme 32: Two historic reactions from the literature converting an alkene double bond to the furoxan ring[7]

1,2-Diphenylethene, **155**, the unsubstituted stilbene compound most directly linked to the work with the combretastatins, was converted to the furoxan ring by Vellaquez[10] using the a similar procedure to Gasco[7] ($NaNO_2$ and acetic acid) but with the addition of the solvent 1,4-dioxane, this was probably to increase the solubility of the reagents and to ensure all reaction intermediates stayed within solution.

155 →(i) 26%→ **128**
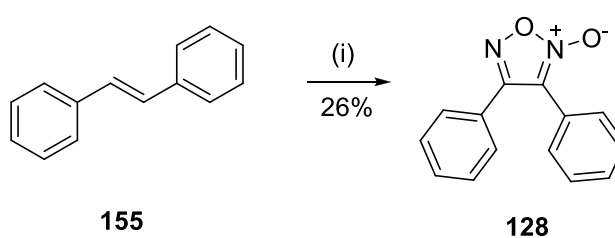
Reagents and conditions: (i) AcOH, HNO_3, $NaNO_2$, 1,4-dioxane

Scheme 33: Reaction of *trans* stilbene with NaNO2 to produce the furoxan ring in the place of the double bond. Both Gasco and Vellaquez successfully completed this reaction.[7, 10]

Using the historic synthesises found in the literature[7,10,12], compounds 3-acetyl-4-methyl-1,2,5-oxadiazole 2-oxide **126** and 1,2-Diphenyl furoxan **128**, were successfully synthesised. Crotonaldehyde, or but-2-enal **161**, was dissolved in acetic acid and cooled to 14°C while aqueous $NaNO_2$ was added dropwise. After an hour, an aqueous work up was completed and after purification through flash column chromatography the desired furoxan was recovered in 23%. Diagnostic peaks for the imine (C=N) and the *N*-oxide bond were sought out in carbon NMR spectroscopy and were found respectively at 154.3 and 110.3 ppm indicating the successful conversion of the double bond to the furoxan ring, **126**.

The *trans* stilbene compound, (1,2-diphenylethene, **155**) was dissolved in a combination of 1,4-dioxane and acetic acid. In contrast to the Gasco method[7], this reaction[10] was then heated to between 50 and 60°C before solid sodium nitrite was added. This reaction was successful in producing the desired furoxan compound, but also produced with it an inseparable by-product which was found to be the nitrated starting material, **129** as shown in scheme 34. Diagnostic peaks for the furoxan ring **128** were found at 156.2 and 114.3ppm by ^{13}C NMR spectroscopy for the new imine bond (C=N) and the *N*-oxide (C=N[+]-O[-]) respectively. The by-product was confirmed as the nitrated stilbene through mass spectroscopy, yielding a peak of 226.0862 m/z, corresponding to compound **129**. Repeating the literature reaction of cinnamyl alcohol **162** with sodium nitrite in acidic conditions, performed by Gasco[12] and researchers, failed to produce any desired furoxan compound **127** and only starting material was recovered upon multiple attempts.
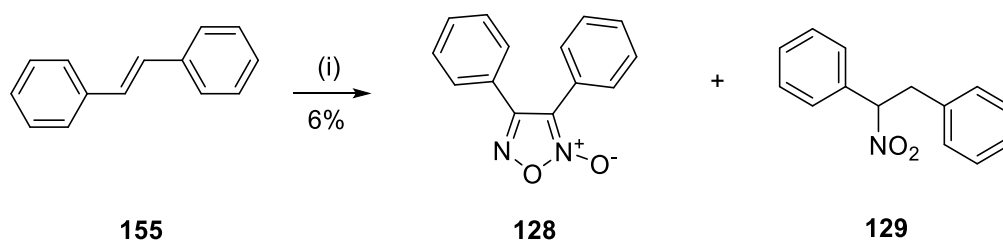
Reagents and conditions: (i) AcOH, HNO_3, $NaNO_2$, 1,4-Dioxane, 55°C, 6.5hrs

Scheme 34: Reaction of *trans* stilbene with $NaNO_2$ following a procedure highlighted in the literature, successfully producing the desired furoxan compound as well as the nitrated by-product.

With viable conditions in place for the formation of the furoxan ring, these were applied to the substituted stilbene compounds **120-*E/Z* 125-*E/Z***. Vellaquez's procedure[10], of seven equivalents of sodium nitrite and a temperature of 60°C was used but again to ill effect, as no reaction appeared to have occurred. Steric hindrance was thought to play a factor in why the furoxan ring is failing to form, especially for the 2,4,6-trimethoxy compounds (**121 *E/Z*** and **122 *E/Z***),. Due to the position of the 2 and 6-methoxy group on the aryl rings, they may be large enough to prevent the alkene initiating a nucleophilic attack with the nitrosonium ion, by blocking one face of the alkene bond. A representation of compounds **122 *E/Z*'s** three-dimensional orientation is shown in Fig. 41. The 2-methoxy group appears to sit directly above the alkene bond's hydrogen atom at C7 and C45 (*cis* and *trans* respectively) and may be close enough to cause steric hindrance and prevent the initial reaction with the NO$^+$ ion. The *trans* stilbene's three-dimensional structure **122 *E*** indicates a that there isn't a lot of 'space' for the alkene bond to orientate itself to behave as a nucleophile as the stilbene exists as a much more planar structure. This may explain why the methoxy substituted stilbene compounds **121 *E/Z*** and **122 *E/Z*** were unsuccessful in the forward synthesis and didn't produce the desired furoxan ring.
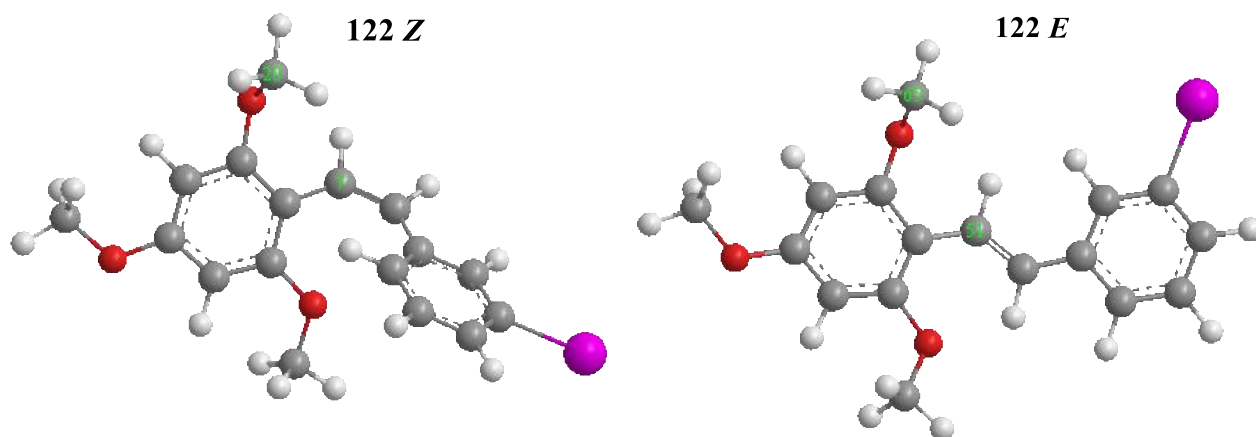
Figure 41: 3D representation of compound **121 *E/Z*** showing the steric hindrance caused by the 2-methoxy group adjacent to the double bond. Three-dimensional model created using Chembio3D Ultra 13.0.

With the trimethoxy compounds not producing the desired furoxan product (**121-122**), it was thought that the position *ortho* to the double bond was causing the reaction to fail due to steric hindrance coupled with the ring activation and possible loss of aromaticity induced by the methoxy groups; as the oxygen of the methoxy group (in the *ortho* position) donates its lone pair into the ring, movement of electrons towards the olefinic bond would cause a loss in aromaticity and is therefore energetically un-favoured, a paradigm which would cause a high barrier to overcome. These electronic effects prompted the synthesis of another stilbene compound **123 *E/Z***. Starting from 3,5-dibromobenzaldehyde, with the rationale that replacing the 2-methoxy group with the much smaller hydrogen atom should remove the steric hindrance issue as shown in Fig.42. As bromine is much less electronegative than oxygen, the aromatic ring should be less activated and therefore enable the double bond to engage in nucleophilic attack with the NO$^+$ species produced in the furoxan reaction.

123 *Z*   **123 *E***
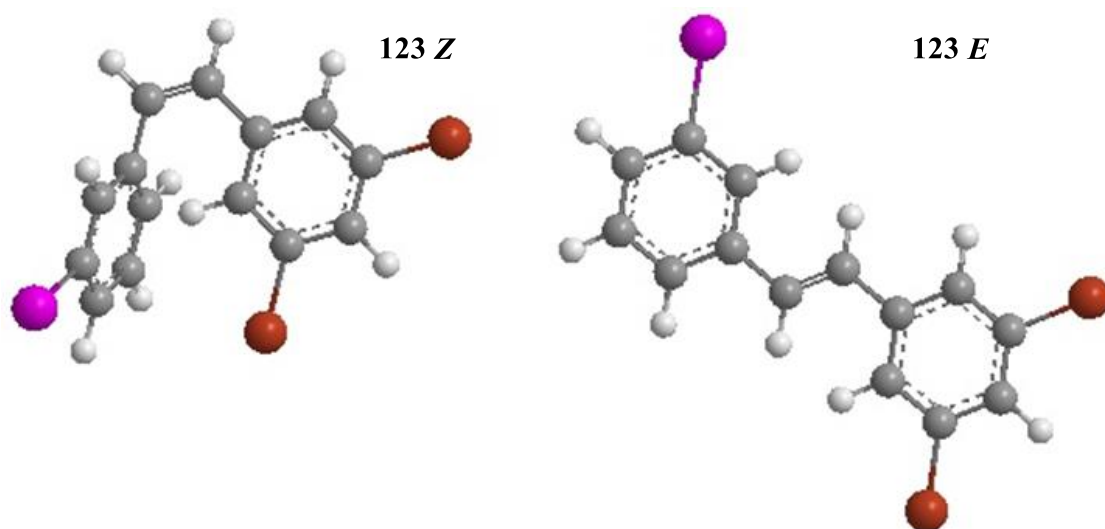
Figure 42: 3D representation of compound **123 *E/Z*** without a substituent in the 2 position reducing the steric effects over the double bond. Three-dimensional model created using Chembio3D Ultra 13.0.

Our theory of enhanced reactivity towards heterocylic ring formation with the 3,5-dibromo stilbene, also failed to produce the desired combretafuroxan compound. Reacting the (*Z/E*)-3,5-dibromo-5-(3-iodostyryl)benzene **123** with sodium nitrite in the presence of acetic acid only returned starting material after several attempts. Increasing the number of equivalents of sodium

nitrite towards an excess (1 equivalents to 7 equivalents) also had no effect on the success of the reaction and continued to yield only starting material. This suggests that steric hindrance was not the only issue. It is possible that the electronic effects of the chosen substituents are making the addition of the NO^+ electrophile unfavoured.

Returning to the literature procedures[11,12] highlighted the need for an oxygen atom in the starting material to be adjacent to the double bond. This prompted the inclusion of an oxygen atom within our structures to study their ability to produce the desired furoxan ring. Literature indicates[13] that caffeic acid, a cheap and relatively available starting material, had been successfully converted to a furoxan derivative in 50% yield (scheme 35) from the reaction with acidified nitrite.

However further reading[14] indicated that the conversion was not a clean one, producing multiple by-products. To test this reaction and minimise the amount of by-products formed, caffeic acid phenyl ester (CAPE, **158**), a derivative of caffeic acid was instead reacted in the presence of acetic acid and NaNO$_2$ in an attempt to yield the furoxan (scheme 35). Several attempts at this reaction failed to produce the desired product, returning unreacted starting material each time.
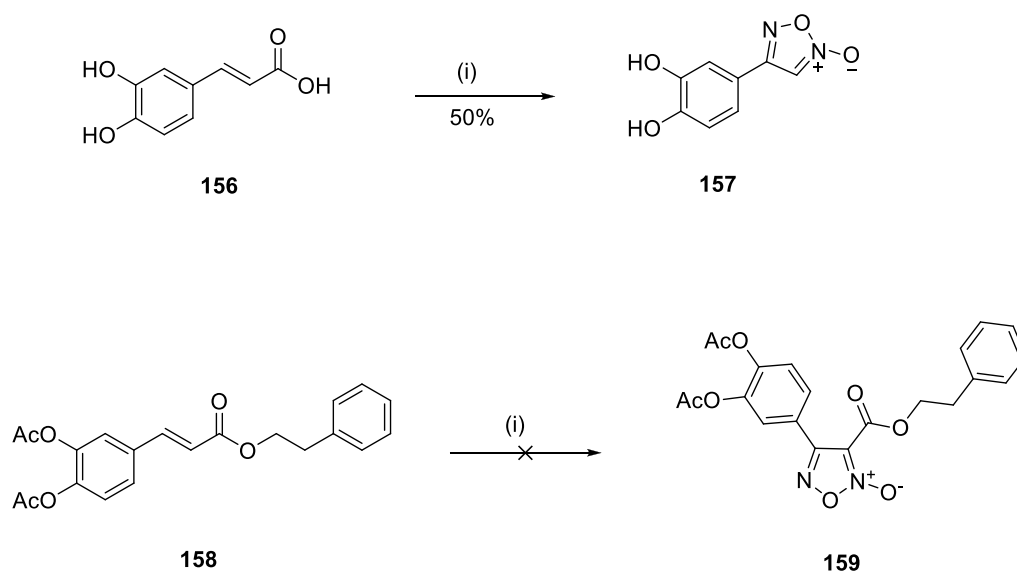
Reagents and conditions: (i): NaNO$_2$, AcOH, HNO$_3$

Scheme 35: Caffeic acid **156** reaction from the literature producing the furoxan ring[13] and the reaction of CAPE **158** with acidic nitrite.

Due to caffeic acid **156**, and CAPE **158**, not yielding the desired products, attention turned to the chalcones. These are common organic compounds consisting of a α,β-unsaturated ketone, whose synthesis[15] is relatively straight forward. The reaction of two readily available starting materials, a benzaldehyde and a acetophenone, in the presence of a base affords the chalcone motif. Due to the presence of an oxygen atom, in the form of a ketone group, adjacent to the double bond we theorised that it may be possible to generate the furoxan ring from the α,β-unsaturated ketone **130** (shown in scheme 36). If successful, the chalcone derived furoxan would be able to act as a synthetic scaffold for combretafuroxan series with the addition of an unsymmetrical ketone group between the furoxan ring and the A and B ring.
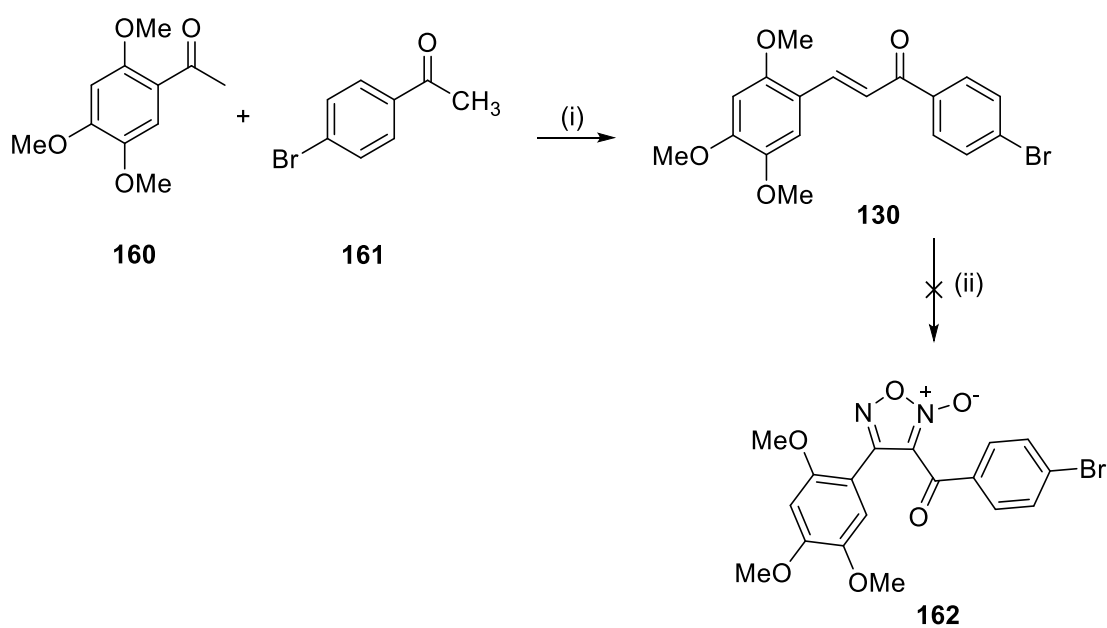
Reagents and conditions: (i) MeOH, 5% NaOH, 25°C,24hrs (ii) NaNO$_2$, AcOH, 1,4-Dioxane, 60°C, 24hrs

Scheme 36: Reaction of 2,4,5-trimethoxybenzaldyde, **160**, with 4-bromoacetophenone, **161**, to produce compound **130**, a chalcone[15]. The second step to produce the furoxan ring failed under the conditions used.

2,4,5-Trimethoxybenzaldeyde **160** and 4-bromoacetophenone **161** were dissolved in methanol and stirred with 5% sodium hydroxide for 24 hours. Addition of water led to a yellow precipitate to form which was then recrystallized from hot ethanol to give a luminous yellow powder of **130**. The next reaction to generate the furoxan compound **162** followed the Velaquez procedure,[10] using NaNO$_2$ (99.999%) in acetic acid and dioxane at 60°C. However the desired reaction did not occur and only starting material **130** was recovered.

Direct furoxan synthesis from substituted stilbene compounds using the double bond chemistry by Gasco[7,12] and Velaquez[1o] was not producing the desired product and therefore a different approach was sought out. After scouring the literature for a different methodology, it was decided that two different procedures[4,16] should be combined in the hope that a viable route for successful production of the combretafuroxan compounds**77-82** would be developed. An interesting publication[4] that could be applied to our work on both combretastatin analogues and furoxan synthesis provided a possible synthetic route to explore. The authors converted a stilbene compound to a dioxime derivative which was then cyclised to form the furazan ring. A furazan ring is very similar to the furoxan ring as both are oxadiazoles but the former lacks the ability to release nitric oxide as it does not possess the *N*-oxide bond. Adapting the procedure[4] to produce the furoxan ring **80** from the oxime starting material **132** can be done using coordination chemistry found in the literature.[16]
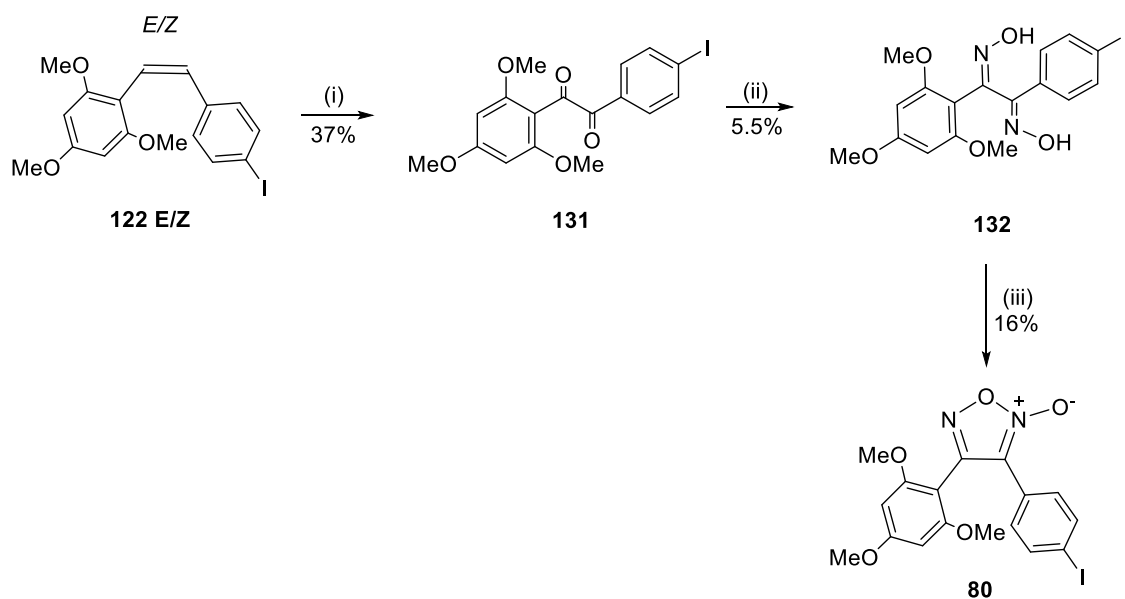
Reagents and conditions: (i) $KMnO_4$, Ac_2O, 0°C, 1hr (ii) $NH_2OH.HCl$, pyridine, EtOH, 90°C, 72hrs
(iii) $CuCl_2$, $NaClO_4$, Et_3N, CH_3CN, NH_3, 25°C, 12hrs

Scheme 37: Reaction of stilbene **122 *E/Z*** to the furoxan **80** via a diketone **131** and dioxime **132** intermediate[4,16]. NB: Compounds **122 *E/Z*, 132** and **80**'s 6-OMe bond is distorted due to its positioning in the 2D plane.

A test reaction was implemented on compound **122- *E/Z*** to see how viable this new proposed route was. Compound **122-*E/Z*** was successfully treated with potassium permanganate to yield the diketone compound **131** in 37% yield as shown in scheme 10. The diketone **131** was then converted, without any further purification to the dioxime **132** by reacting it with hydroxylamine hydrochloride producing a 5.5% yield. Following the second publication[16] the dioxime compound **132** was dissolved in acetonitrile and treated with copper (II) chloride and sodium perchlorate causing an intense green solution to form, indicative of ligand formation. After 12 hours a green oil was separated from the reaction mixture and immediately treated with aqueous ammonia. A further colour change was noted at this point, changing the green oil to a deep blue solution, this was also an indication that ligand exchange had occurred forming the copper-ammonia complex which is historically known to be a deep blue coloured compound. Liquid-liquid extraction of the furoxan complex was completed using chloroform and gave the desired furoxan **80** compound in a 16% yield. Although this reaction did produce the desired furoxan compound **80,** it was decided that due to the

number of steps and low yield (0.3% overall) that it wasn't a feasible option for progression with the stilbene compounds.

2.1.1.2 -Synthesis from oxime starting materials

A positive result from the stilbene work was that successful conversion to the furoxan was possible, but it wasn't until the double bond had been converted to the dioxime moiety that the furoxan formed. As aforementioned (chapter 1.1.3, page 40), the oxime moiety already has the correct stoichiometric amount of nitrogen and oxygen present and therefore is a much simpler, easier route for ring closure and production of the oxadiazole-2-oxide ring. Building on the use of oximes as a starting material, a convenient procedure was found that produced the desired furoxan ring in a one-pot synthesis (scheme 38). A Russian group,[17] led by Krayushkin, reacted substituted amino-oximes with sodium nitrite in the presence of sulphuric acid and produced the furoxan ring in high yield (60-91%) and as a collectable precipitate. Giving that the yield for our dioxime work only gave a 16% yield and involved a three step process, this alternative synthetic route was a very attractive option.
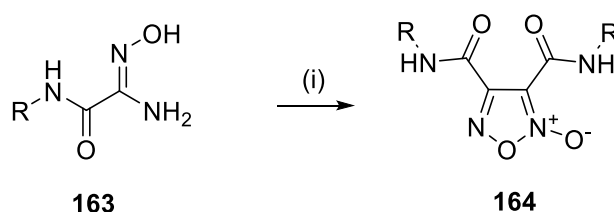
Reagents and conditions: (i) $NaNO_2$, H_2SO_4, -20°C, 15mins

Scheme 38: Reaction of aminooxime compounds with sodium nitrite yields the furoxan ring. Taken from reference 17.

Adapting Krayushkin's procedure[17] to use benzoximes as our starting material, to synthesise symmetrical combretafuroxans that adhere to the 'series 1' model (chapter 1.3, page 61), trifluromethyl and trifluromethoxy benzyl oximes were purchased. The CF_3 group strongly deactivates aromatic rings and therefore may amend some of the possible electronic interactions that may have been occurring with the stilbene to the furoxan synthesis. The starting material was

suspended in 20% sulphuric acid, to which sodium nitrite was added while the temperature was maintained between -5 and -15°C. After several attempts at this reaction, no furoxan product was isolated either as a precipitate as stated in the literature or when an organic extraction was carried out.

R= CF$_3$ **165**   R= CF$_3$ **96**
R = OCF$_3$ **166**   R= OCF$_3$ **97**
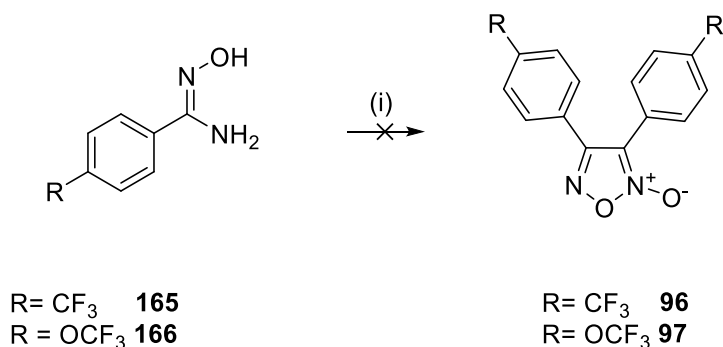
Reagents and conditions: (i) NaNO$_2$, H$_2$SO$_4$, -20°C, 12 hours

Scheme 39: Reaction of benzoaminoximes with acidic NaNO$_2$ produced the desired combrefuroxans **96-97**.

The main problem with this reaction is that, two molecules of oxime starting material are needed to combine and expel NH$_2$ as a leaving group. Here is where it was theorised the problem might lie. Strong bases are notoriously bad leaving groups and therefore the amino (NH$_2$) group isn't going to want to be removed from the oxime molecule and hence ring closure and the formation of the oxadiazole-2-oxide isn't going to occur. To overcome this, we aimed to convert the amino group into a better, less basic leaving group such as a halogen atom. It would seem that the Russian researchers also explored this[17] and again provided a straight forward method to the synthesis of the desired furoxan ring, this time in a two-step method, first converting the carbamoylformamide oximes **165/166** to their corresponding carbamoylformamide oxime-chloride **135** and then treating the new improved leaving group with a base to generate the furoxan ring with expulsion of the chlorine group as the salt as depicted in scheme 40.

R= CF$_3$ **165**   R= CF$_3$ **135**   R= CF$_3$ **96**
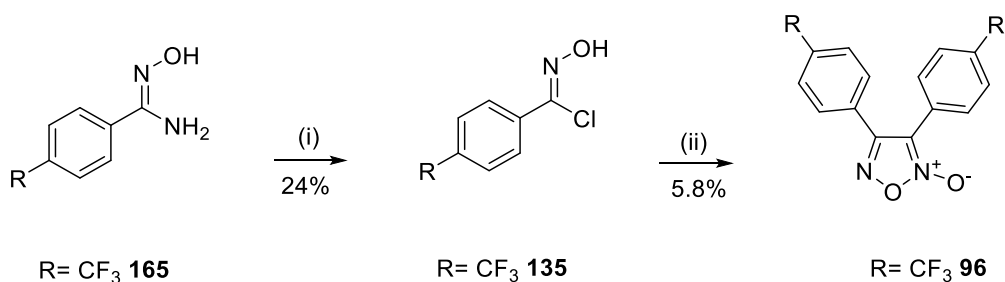
Reagents and conditions: (i) NaNO$_2$, HCl, -20°C, 2hrs (ii) Et$_3$N, Et$_2$O, 12hrs

Scheme 40: Two step synthesis of furoxan compound **96**. Reaction of aminooxime with HCl and NaNO$_2$ provides a suitable leaving group for the second step.

Reaction of **165** with 18% hydrochloric acid and sodium nitrite successfully produced the desired chlorinated oxime in a 24% yield. Column chromatography was used to purify this intermediate (7:3 petroleum ether:ethyl acetate) and was notably easier than the stilbene columns due to the very decent separation on TLC. The next step of the forward synthesis was to react the chlorinated oxime **135** in the presence of a base to initiate the ring closure mechanism. The first attempt of this reaction used trimethylamine as a base and caused no reaction, it was thought the reaction failed due to trimethylamine not being a strong enough base. The second attempt at this reaction proved to be fruitful, this time using pyridine as a base. Pyridine has a pK_b of 5.2 compared to 11.1 of trimethylamine and hence is a stronger base. Using pyridine afforded the desired substituted furoxan compound **96** as a precipitate (5.8%) with no further purification needed.

With the successful generation of the furoxan ring **96** from the chlorinated oxime intermediate **135**, all be it in relatively low yield (24%), attention was turned to the oxime starting material, which was fairly expensive, to be producing a 5% yield of furoxan. This led to a literature search being conducted for an alternative synthetic route to the required oxime starting material, from chemicals that were more readily available to us, such as benzaldehydes. A 2006 publication by a group of Serbian chemists[18] stated that the desired oxime compounds could be produced in very high yields (72-100%) in a solvent-less reaction solid with hydroxylamime hydrochloride and sodium hydroxide by grinding the starting materials together in a pestle and mortar as depicted in scheme 41.
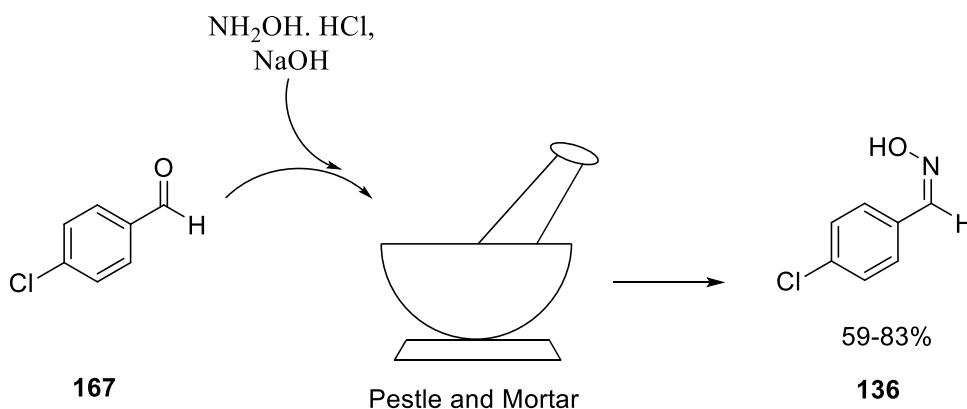
Scheme 41: A unique procedure for the production of benzoxime compounds **136** in a solventless reaction using just a pestle and mortar.

4-Chlorobenzyaldehyde **167** was chosen due to its inexpensive nature and relative abundance within our laboratories and the added advantage that it was a solid starting material. The benzaldehyde **167**, hydroxylamine hydrochloride and sodium hydroxide pellets were added in a 1:1.2:1.2 ratio. To this powdered mixture, silica was added to act as a 'binding' agent while the four ingredients were ground together intermittently using a pestle and mortar for 120 minutes before being washed with water to remove any inorganic salts remaining. Although initially sceptical about this method, the oxime compound **136** was isolated in an 83% yield. The authors[18] stated that the silica was present due to the 'unreactive' nature of aromatic ketones to this kind of chemistry. This led us to repeat the reaction, to test this statement without the addition of silica. The same reactants were used in the same 1:1.2:1.2 ratio and ground in the usual manner for the same duration as outlined above. The consistency of this mixture was notably different to the first attempt; it produced a dough like consistency and was much harder to efficiently grind. However in contrast to the literature, the desired oxime compound was isolated but in a lower yield of 59% suggesting that the silica perhaps plays a role in providing a surface on which the reaction occurs, much like an inorganic catalyst would.[18] As a comparative procedure[19] the same reaction was carried out, but this time introducing a solvent. 4-Chlorobenzyaldehyde **167** was dissolved in diethyl ether and to it aqueous $NH_2OH.HCl$ and NaOH were added at room temperature before being left to stir vigorously for 2 hours. After an

aqueous work up and the removal of the ether, a white solid corresponding to the 4-chlorobenzaldehyde oxime **136** was recovered in 87% yield (scheme 42). The addition of a solvent seems to only offer a slight improvement of yield compared with the solvent-less reaction and therefore both routes appear to offer viable options to the synthesis of the desired oxime **136**.
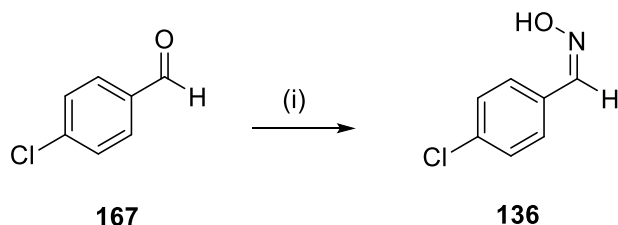
Reagents and conditions: (i) $NH_2OH.HCl$, NaOH, diethyl ether, 25°C, 2hrs

Scheme 42: Alternative route for the generation of benzooximes, used as a comparative tool to the solventless reaction.

The next step for this oxime route is the generation of a good leaving group by replacing the acidic hydrogen of the oxime with a chloride. In contrast to the first step of the two step synthesis used earlier[17] (scheme 40) the oxime compound (derived from the solventless procedure[18] scheme 41) was dissolved in THF and introduced to *N*-chlorosuccinimide at room temperature.[20] This product was isolated in a 88% yield, as pale yellow flakes and was determined to be the desired chloro-oxime compound **137** as shown in scheme 43.

To compare the products from two synthetic routes used to produce the oxime moiety the oxime **136** isolated from the aqueous procedure[19] (scheme 42) was reacted with *N*-chlorosuccinimide under the same conditions resulting in the isolation of a yellow solid in 96% yield. This suggests that both routes to the formation of the oxime-chloride compound (**137**) work effectively and give comparable results and therefore either route is a viable option.
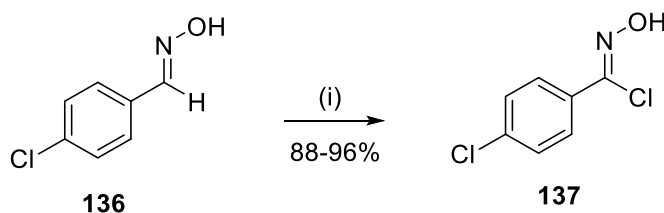
Reagents and condtions: NCS, THF, 25°C, 2hrs

Scheme 43: The chlorination reaction using *N*-chlorosuccinimide to produce the oxime-chloride compound **137**, which is the intermediate compound in the generation of the furoxan ring.

Unfortunately the forward synthesis from the *p*-chlorobenzooxime chloride **137** failed to produce the furoxan ring under the basic conditions quoted in the literature[17]. Krayushkin reported a 50% recovery of furoxan compound using this procedure, however when *p*-chlorobenzooxime chloride **137** was refluxed in the presence of an equimolar amount of trimethylamine, no furoxan product was isolated. Increasing the equivalents of trimethylamine to two and four returned unreacted starting material. Theoretically with the better leaving group in place like the chloride in **137**, the simple ring closure reaction should be successful, however this was not the case. The fact that Krayushkin only isolated a 50% yield suggests that the production of the furoxan ring is not very favoured.

2.1.1.3- Synthesis from an acetophenone

The second series (Fig. 43) of combretafuroxans contains a two ketone groups acting as a bridge between the aromatic rings and the oxadiazole-2-oxide centre ring while still maintaining symmetry.

76
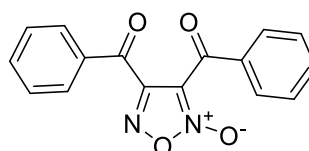
Combretafuroxan series 2

Figure 43: Combretastatin analogue.

The starting material for this series is the relatively inexpensive acetophenones. Two acetophenone molecules combine under acidic conditions and in the presence of sodium nitrite to produce the furoxan ring at the heart of the structure. The reason for this second series (Fig. 43) is to increase the number of hydrogen bond acceptors and therefore to improve solubility[1,2] since this is an issue with the parent compound combretastatin A-4. This series allows comparison of the NO releasing abilities and anti-cancer properties when two ketones are inserted, causing the structure to 'bend' slightly in comparison to the combretastatin's predominantly *cis* orientation. This increase in tether length between the A and the B ring may also cause 'series 2' to dock differently within the colchicine binding site and therefore potentially improve its binding potential.

73
Combretastatin A-4

76
Combretafuroxan Series
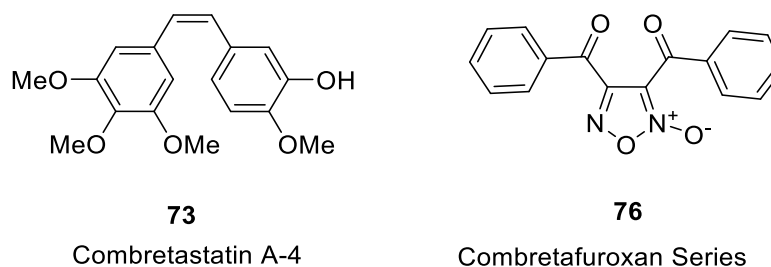
Figure 44: Combretastatin A-4 and series 2. Both contain two A and B aryl rings. Series 2 contains a carbon linker bridging the two rings in addition to the furoxan ring for increased rigidity.

As aforementioned (chapter 1.3, page 63) the Ley group[21, 22] found that halogenation of one of the aromatic rings increased anti-tumour activity five-fold of compounds similar to combretastatin A-4 **73** and this observation influenced the initial work. Preparations to modify our acetophenone starting materials to include a halide on the aromatic ring were sought out from the literature. The trimethoxy substituents are known to be of fundamental importance for a potent binding activity of combretastatin[4,5,23], therefore starting with substituted methoxy acetophenones, it was planned to halogenate in the 3 and the 5 positon on the acetophenone ring as shown in scheme 44)
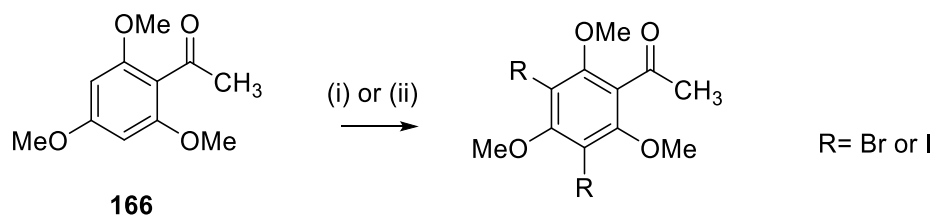
Reagents and conditions:(i) Br$_2$, DCM, 25°C 1hrs (ii) NaI, NaOCl, EtOH, 0°C, 1hr

Scheme 44: Halogenation of trimethoxyacetophenones under various conditions.

Bromination of 2,4,6- trimethoxyacetophenone **166** was attempted by exposing the acetophenone to a solution of bromine. The reaction was carefully monitored using TLC in a 4:1 petroleum ether: ethyl acetate eluent and then was purified using column chromatography. ^{1}H NMR analysis showed that no reaction had occurred, so a sample of **166** was analysed using GC-MS to exploit the unique isotopic properties of bromine. It was discovered that bromination at the 3 or the 5 position on the acetophenone ring had in fact occurred but on a very small scale and (shown as compound **167** in Fig.45) providing a mass peak of 353 m/z. This mass peak corresponds to the dibromonated version of **166** but with the loss the aceto group.
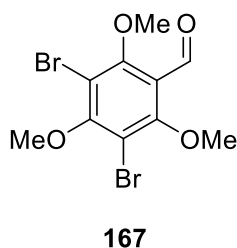
Figure 45: Isolated product from failed bromination reaction of trimethoxyacetophenone.

Iodination of 2,4,6-trimethoxyacetophenone was also attempted using sodium iodide in the presence of sodium hypochlorate (NaOCl) at 0°C. Addition of sodium thiosulphate and acidification with HCl during the work up procedure produced a brown solid which was recrystallized from boiling water. The resulting chocolate brown solid was analysed and found to be unreacted starting material. Additional attempts at this reaction were attempted by increasing the volume of sodium hypochlorate but no desired iodinated acetophenone was isolated from either reaction. A different approach to

generate the halogenate acetophenone compounds was to start from the triol compound (**168**) and halogenated the ring under the same conditions to give the 3,5-subsituted iodo/bromoacetophenone. Introducing the methoxy group can then be done once halogenation has been completed, as a second step using methyl iodide in the presence of potassium carbonate[24] with a reported literature yield of 98%. However this alternative route to halogenated trimethoxy acetophenones was not successful, as the first step would not produce the desired product and gave either no reaction or a degraded version of the starting material on multiple attempts.
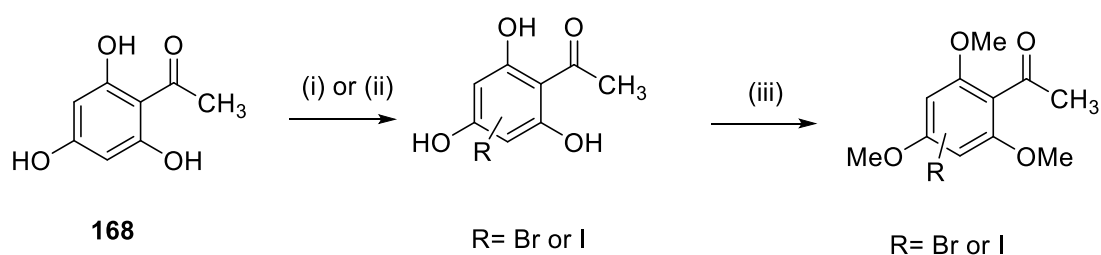
Reagents and conditions: (i) Br$_2$, DCM (ii) NaI, NaOCl, EtOH (iii) MeI, K$_2$CO$_3$, Acetone

Figure 46: Planned two step synthesis of halogenated acetophenones building on the work by the Ley group[21,22] where halogenated combretastatin has heightened activity compared to the parent compound.

After unsuccessful attempts at iodinating and brominating in the *meta* position of the acetophenone, attention turned to synthesising combretafuroxan compounds with varying substituents in the *para* position. The position of the substituents in this series was partly chosen as Nirode[25] had made some successful headway in synthesising para-substituted furoxans by reacting acetophenoens with acetic acid and sodium nitrite. The literature provides two different routes to the production of combretafuroxan compounds from the acetophenone starting material. One method developed by Nirode and co-workers[25] uses the combination of acetic acid and sodium nitrite to form the oxadiazole ring, by producing the reactive NO$^+$ and NO$_2^-$ species *in situ* from of nitrous acid. The second route[26,27] involves using concentrated nitric acid, usually at around 50°C and sodium nitrite to produce the desired heterocycle. To give the best success rate for the production of a series of *para* substituted combretafuroxan compounds both procedures were attempted in tandem, each of which had varying success.
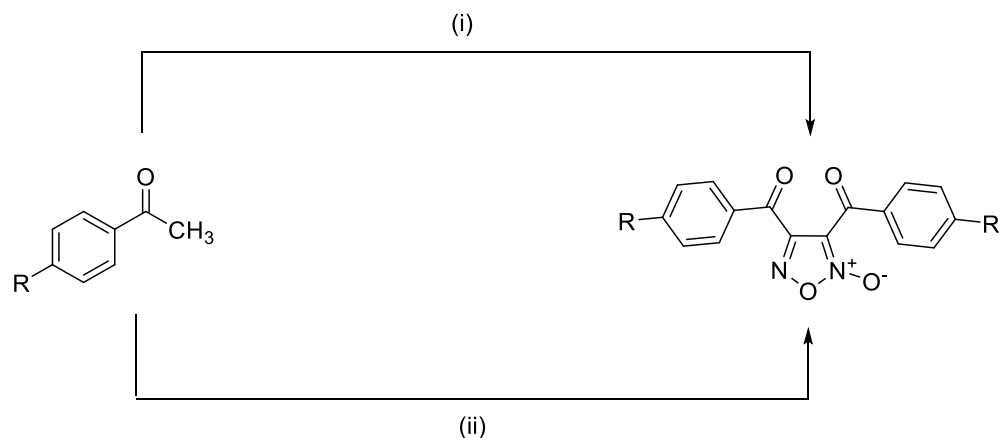
Reagents and conditions: (i) AcOH, HNO$_3$, NaNO$_2$, 60°C, 2hrs (ii) HNO$_3$, NaNO$_2$, 80°C, 2 hrs

Scheme 45: Two alternative routes to the production of the furoxan ring starting from the readily available acetophenone starting material.

It was found that the concentrated nitric acid procedure[26, 27](route (ii) in scheme 45) which was conducted at 50, 60 and 80^{0}C often produced no desired product, and was a very violent reaction producing plumes of NO$_2$ gas upon addition of sodium nitrite. It is likely that this very rapid evolution of NO$_2$ caused the reaction to fail or produce the un-wanted by products, possibly due to the energetics of the reaction and that nitration of the ring is more favourable than addition to the carbonyl carbon. Using and adapting Nirode's procedure[25], several combretafuroxan compounds were successfully synthesised in varying yields (2-29%). Reaction of the *para* substituted acetophenone with combination of acetic acid and nitric acid and a catalytic amount of NaNO$_2$ produced a range of products (as seen in scheme 46), as shown by TLC and crude NMR analysis. Notably the nitrated product (scheme 46), where a NO$_2$ group has replaced the aceto portion of the acetyl group, was produced as a highly coloured compound and was successfully isolated from any furoxan product through column chromatography. The corresponding benzoic acid by-product was also isolated from several of the reactions as a precipitate upon dilution of the reaction with ice-cold water.
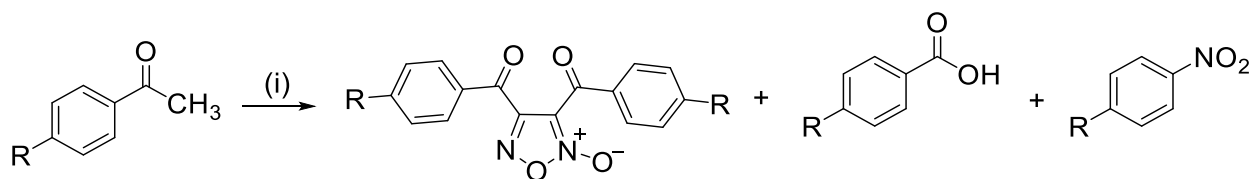
Reagents and conditions: (i) AcOH, HNO₃, NaNO₂

Scheme 46: Reaction of acetophenone produces the furoxan ring and two by-products, the corresponding benzoic acid and a nitrobenzene compound.

Tezuka et al[28] reported that the formation of by-products, such as benzoic acid, are produced due to too much water in the reaction, which as the formation of the oxadiazole ring requires aqueous acid is a challenging hurdle to overcome. The carbonyl peak (C=O) and the missing C=N and C=N⁺O⁻ peaks at 154 and 112 ppm respectively, from the ^{13}C NMR spectrum were key indicators of side product formation (Fig. 47).The ability to form the furoxan ring seemed to be heavily dependent on
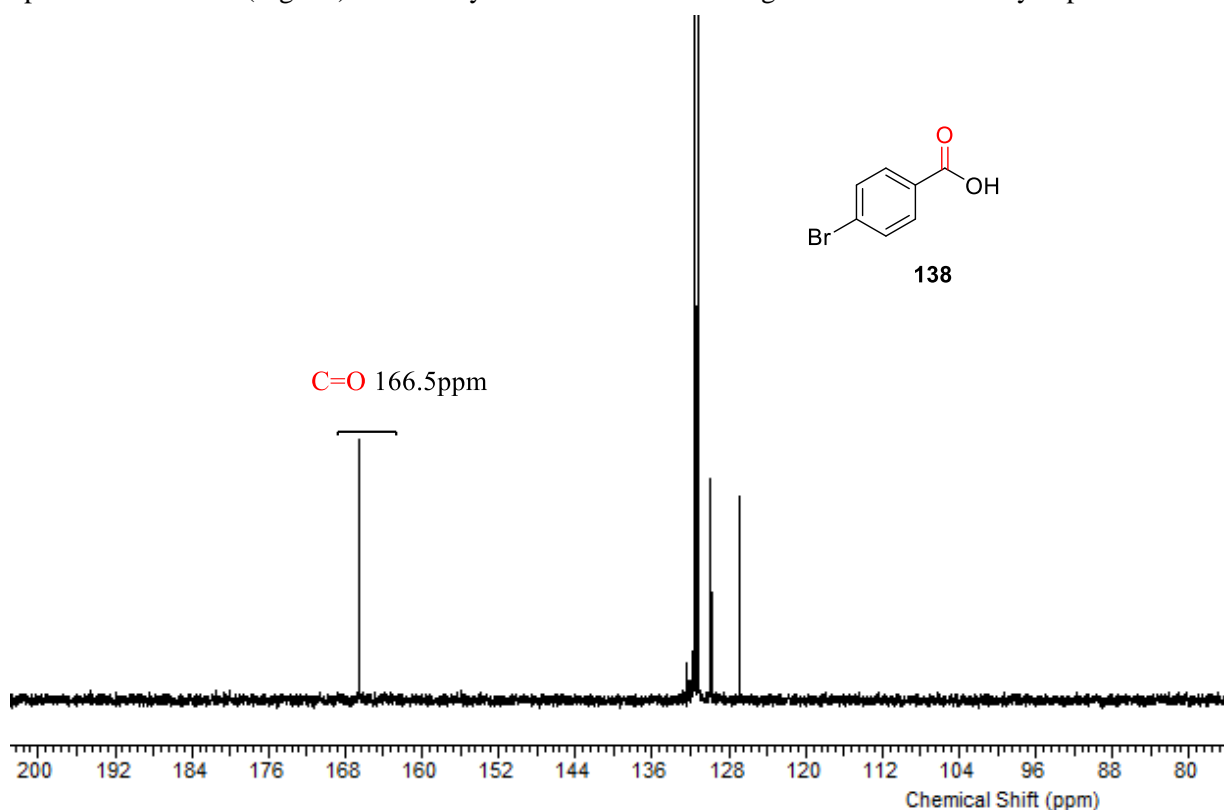
the substituent(s) on the benzene ring. Functional groups that encouraged crystallisation from the

Figure 47:^{13}C NMR spectrum showing a carbonyl peak at 166.5 ppm, a peak this low is diagnostic for the formation of the benzoic acid by-product.

reaction, seemed to be more preferential at forming the furoxan ring compared to either their corresponding benzoic acid or nitro by-products. In particular the halogen series and the more lipophilic substituents were better at precipitating out of the reaction and yielding the correct product. Substituents that were more water soluble failed to precipitate on the addition of ice water and therefore required an aqueous work up to obtain the furoxan. The various conditions used and the relative by -products and furoxan rings formed are summarised in table 2. Using the combination of acetic acid and nitric acid (route (i) in scheme 18) was by far the preferred route for producing furoxans in addition to by-products. The use of neat concentrated nitric acid gave no furoxan ring instead only by-products were isolated.
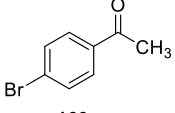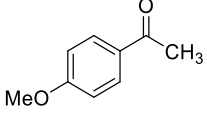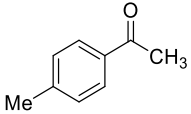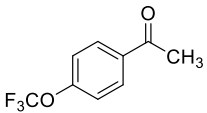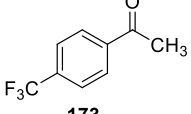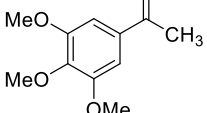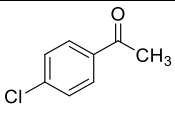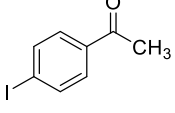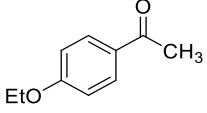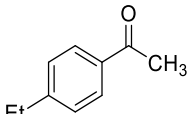
Starting Material	Reagents	Temp of reaction (°C)	Duration (hours)	Yield of Furoxan (%)	Yield of Benzoic Acid (%)	Yield of Nitro product (%)
4-bromoacetophenone **169**	Acetic acid/ HNO$_3$	80	2	12	9.8	0
4-methoxyacetophenone **170**	Acetic acid/ HNO$_3$	60	2	21	25.3	0
4-methylacetophenone **171**	Acetic acid/ HNO$_3$	60	2	2	N/A*	0
4-(trifluoromethoxy)acetophenone **172**	Acetic acid/ HNO$_3$	60	4	23	3.6	N/A*
4-(trifluoromethyl)acetophenone **173**	Acetic acid/ HNO$_3$	60	4	20	0	0
3,4,5-trimethoxyacetophenone **174**	Acetic acid/ HNO$_3$	60	4	9	0	0
4-chloroacetophenone **175**	Acetic acid/ HNO$_3$	55	2	20	0	0
4-iodoacetophenone **176**	Acetic acid/ HNO$_3$	55	2	15	20.5	0
4-ethoxyacetophenone **177**	Acetic acid/ HNO$_3$	55	2	2	N/A*	N/A*
4-ethylacetophenone **178**	Acetic acid/ HNO$_3$	55	2	29	21	0

Table 2: Table comparing both routes to the furoxan ring, the conditions used and by-products formed. * Trace evidence from LRMS found evidence of nitro and benzoic acid by-products after initial ^{1}H and ^{13}C NMR spectroscopy was inconclusive of their formation.

From the variety of starting materials used and the differing conditions utilised to generate the series of combretafuroxan compounds **86-95**, the key factor on whether the desired product forms appears to be substituent dependent. Functional groups that either promote crystallisation, or precipitate from the reaction solution, notably the halogenated compounds, tend to produce the furoxan product in a higher yield and in a much cleaner process due to the ease of isolation. This is perhaps due to the compounds precipitation from the reaction mixture; no work up procedure is required and therefore may prevent some by-products, such as the benzoic acid, from forming as there is less chance of exposure to an aqueous environment. The alkyl substituted acetophenones all required an aqueous work-up, extraction with organic solvents (DCM) and vacuum distillation. This exposure to excess solvents and steps may have contributed to the presence of the benzoic acid by-product[27]. Purification by column chromatography and recrystallization was also needed for all furoxan compounds before any pure furoxan product was obtained.

The mechanism (scheme 47) for the generation of the furoxan ring from the acetophenone starting material is fairly straight forward and utilises the reactive species NO^+ and NO_2^- that are generated *in situ* by the action of sodium nitrite on acetic acid as aforementioned in chapter 1 (page 37). The acidic medium of the reaction provides optimal conditions to initiate the reaction by protonating the acetophenone. This allows the enolate resonance structure to form and promotes the coupling of the enolate and the nitrosonium ion (NO^+). Proton transfer forms the oxime moiety which is then attacked by the nitrite anion (NO_2^-). The nitrite ion has an unpaired electron so can be considered a radical, which then attacks the oxime carbon-nitrogen double bond. Movement of electrons causes the oxime nitrogen to become a radical. This can then attacks another nitrite ion to generate structure **179** in scheme 20. Two simultaneous reorganisations leads to the loss of two molecules of nitrous acid (HNO_2) to form the nitrile oxide, which then combines with another nitrile oxide in solution to ring close and form the furoxan ring **37**.[26-28] The product determining step of this reaction is generation of the nitrile oxide form **179**, as reaction of H_3O^+ with compound **179** produces the benzoyl acid and reaction with another nitrite ion leads to the assembly of the benzoic acid by-product. Once the nitrile oxide is formed, ring closure and generation of the desired furoxan ring **37** is more likely.
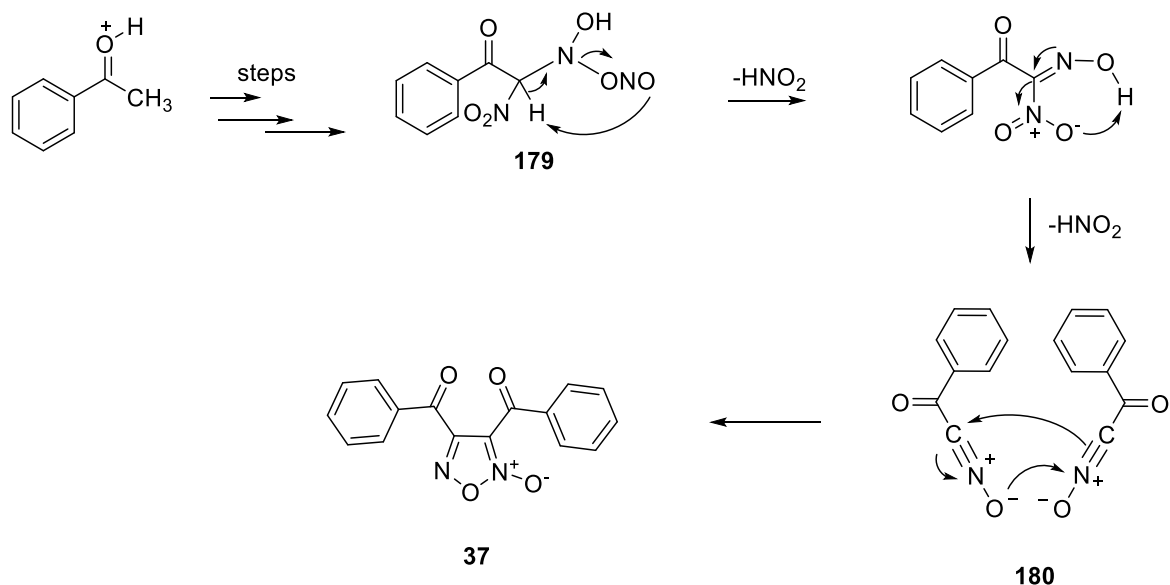
Scheme 47: Mechanism proposed by Tezuka[28,] for the generation of a furoxan ring from an acetophenone starting material.

Looking at the mechanism (scheme 47) involving the acetophenone starting material, generation of the desired product appears to be in a delicate balance with the production of by-products such as benzoic acids. The more water present in the system the more the reaction is pushed in the direction of the acid by-product as described by Tezuka[28], who found that with 50% water content in the solution the yield of corresponding benzoic acids was close to 50%. Removal or reduction of the water drives the yield of furoxan compounds back towards the 60% mark.

With generation of by-products a likely outcome from this reaction, distinguishing the success of the reaction became of paramount importance and was helped greatly by ^{1}H and ^{13}C NMR analysis coupled with high resolution mass spectroscopy (HRMS).

2.1.1.4- Analysis of furoxan formation

The beauty of synthesising furoxans from acetophenones is the ability to distinguish at an early stage if the reaction has been successful. Due to the loss of methyl group on the acetyl part of the molecule, integration in ^{1}H NMR spectroscopy can be utilised to determine the reduction or loss of any methyl character, however the crude mixture is often very complex and direct conclusions from this evidence tend not to be made. Instead a crude ^{13}C NMR spectrum can usually indicate the production of the

furoxan, due to the appearance of four diagnostic peaks (depicted in Fig. 48). If we look at the general structure of the series 2 combretafuroxan (Fig. 48) compounds, four diagnostic peaks can be recognised for the easy identification of the desired product.
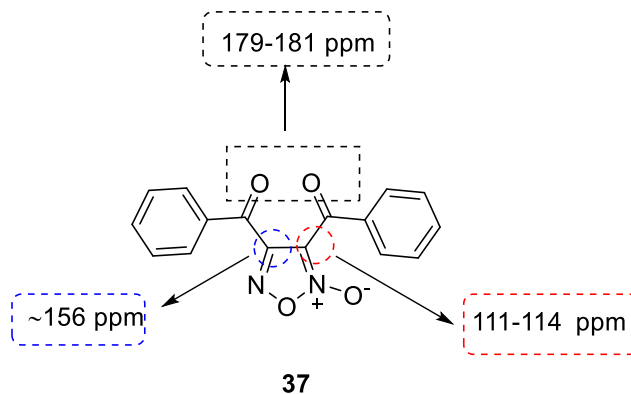
Figure 48: Diagnostic peaks for the successful synthesis of furoxan compounds. Peaks present in ^{13}C NMR spectroscopy in these regions provide good evidence of furoxan production.

The two carbonyls produce two separate peaks between 179 and 180 ppm and lie very close together. If the benzoic acid by product has been produced its carbonyl bond is found slightly further upfield between 166-175 ppm (as already seen in Fig.47). Arguably the most important diagnostic peaks in furoxan formation come from the two sp^2 hybridised carbons of the oxadiazole heterocycle. The imine type carbon (C=N) is shifted downfield towards a chemical shift value of around 156 ppm, one side of the aromatic carbons peaks. The C-N-oxide (C=N$^+$-O$^-$) bond is pushed further upfield due to the electronic effects from the formal charges present on the heteroatoms. This *N*-oxide bond usually appears around 111-114 ppm, meaning essentially the oxadiazole's carbon atoms lie either side of the aromatic carbons from the acetophenone rings. This distinct separation pattern in ^{13}C NMR spectroscopy is characteristic of all furoxan compounds synthesised from acetophenone starting materials and is a very useful diagnostic tool. [29-31]
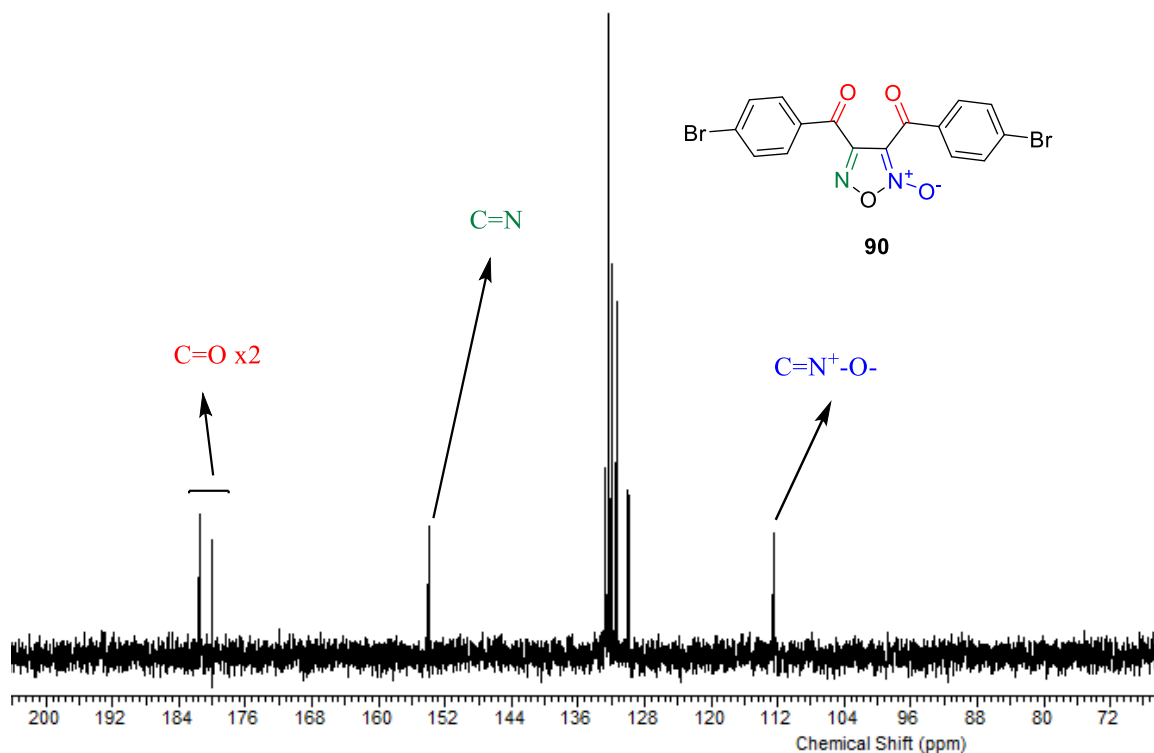
Figure 49: ^{13}C NMR of combretafuroxan compound **90**. Diagnostic peaks are the imine bond (green), the *N*-oxide bond (blue) and the two carbonyl peaks (red).

Formation of the nitro by-product could also be obtained using ^{13}C NMR spectroscopy. Synthesis of this by-product removes the carbonyl group and replaces it with a NO$_2$ substituent, this causes the loss of the diagnostic C=O peaks as seen in Fig. 50. The absent peaks, combined with the addition of a C-NO$_2$ peak at 129 ppm confirms the presence of the unwanted by-product as shown in Fig. 51.
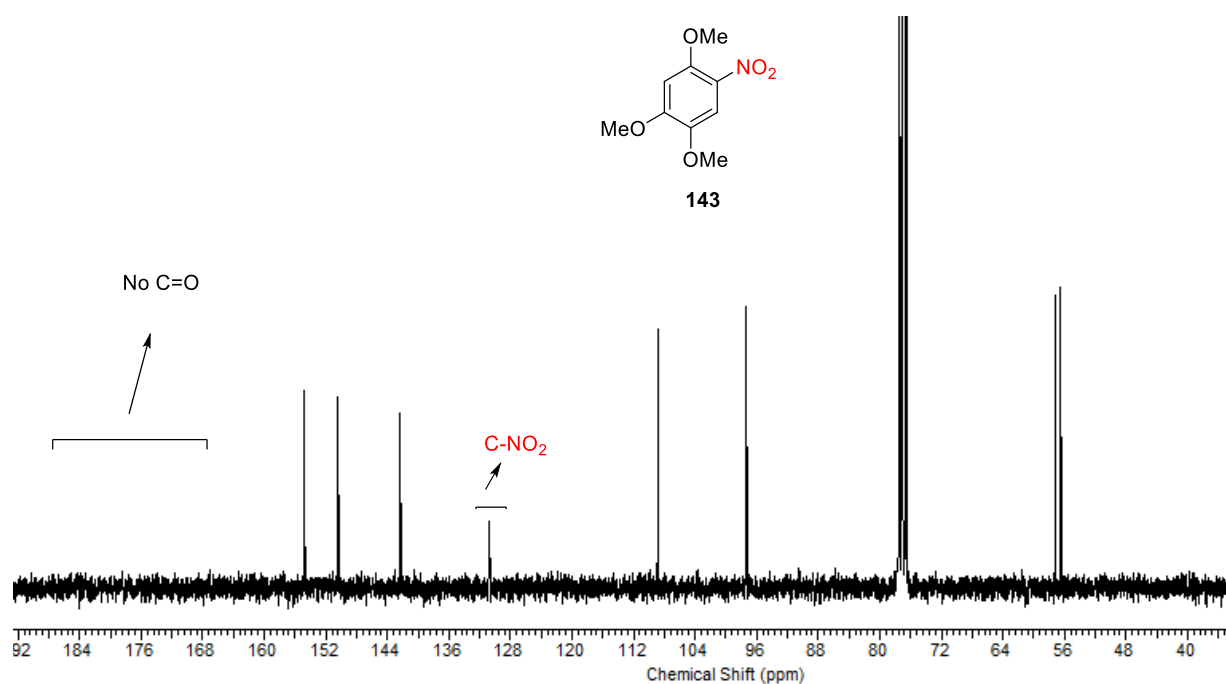
Figure 50: ^{13}C NMR of nitro by-product **143**. The diagnostic peaks for the characterisation of these compounds is the missing carbonyl peaks and the new C-NO$_2$ bond

In summary, synthesising 1,2,5-oxadiazole-2-oxide compounds can be a synthetic challenge but as shown in section 2.1.1.3 it is possible to isolate the furoxan ring. Synthesis from an acetophenone starting material was by far the most lucrative method for generating the desired products and afforded compounds **86-95**. Of the two synthetic routes explored, it was found that the use of a combination of acetic acid and dilute nitric acid with the addition of a catalytic amount of solid sodium nitrite was the preferred route in the production and isolation of combretafuroxan compounds **86**-**95**. The main issue with furoxan production using this style of chemistry is controlling the formation of by-products that are readily produced. The more likely a substituted acetophenone (**169-178**) is to precipitate from the aqueous media, the easier isolation of furoxan product. This is representative in the relative yields obtained from these reactions. Compounds with lipophilic groups such as halogens produced the highest yields of furoxan (20-23%). Almost every reaction led to the recovery of benzoic acid by-products (10-25%) confirming what is found in the literature[28], that the formation of the 1,2,5-oxadiazole-2-oxides is not a clean one. Minimising the amount of water in the reaction appears to be key in avoiding the benzoic acid by-products forming as shown in scheme 47.

Generation of combretafuroxan compounds from an alkene bond provided the largest synthetic hurdle. Stilbene precursors, both *cis* and *trans* isomers, **120 *Z/E*-125 *Z/E*** were synthesised using classic Wittig chemistry in varying yields (2.3-22%) and although the isolation of each single isomer was not possible, the forward synthesis to the furoxan ring should not of been affected by this. Steric hindrance appeared to play a key role in the initial experiments as outlined in Fig. 41 and 42 in section 2.1.1, with the face of the alkene bond blocked from any forward reaction with a nitrosonium ion. Removal of the steric hindrance caused by the *ortho* positioned methoxy group in compound **121 *E/Z*** and replacing it with two bromine substituents in the *meta* positions of the benzene ring still did not elude the desired furoxan ring. This suggests that factors other than steric hindrance are involved. It has been previously observed[32] that the nitrosonium ion generated from the use of $NaNO_2$ can cause inefficient conversion to the furoxan ring. The use of a much more electrophilic source of NO may increase the likelihood of a successful reaction.

2.1.1.5- References

1. G. R. Pettit and M. R. Rhodes, *Anti-Cancer Drug Des.*, 1998, **13**, 183-191

2. G. R. Pettit, S. B. Singh, E. Hamel, C. M. Lin, D. S. Alberts and D. Garcia-Kendall, *Experientia*, 1989 **45**, 209-210

3. J. A. Woods, J. A. Hadfield, G. R. Pettit, B. W. Fox and A. T. McGown, *Br. J. Cancer*, 1995, **71**, 705-711

4. G. C. Tron, F. Paglial, E. Del Grosso, A. A. Genazzani and G. Sorba, *J. Med. Chem.*, 2005, **48**, 3260-3268

5. G. C. Tron, T. Pirali, G. Sorba, F. Pagliai, S. Busacca and A. A. Genazzani, *J. Med. Chem.*, 2006, **49**, 3034-3044

6. G. Wittig, W. Haag, *Chem. Ber.*, **88**, 11, 1654-1666

7. A. Gasco, R. Fruttero, B. Ferrarotti, A. Serafino, and A. Di Stilo, *J. Heterocyclic. Chem.*, 1989, **26**, 1345

8. H. Takayama, S. Shirakawa, M. Kitajima, N. Aimi, K. Yamaguchi, Y. Hanasaki, T. Ide, K. Katsuura, M. Fujiwara, K. Ijichi, K. Konno, S. Sigeta, T. Yokota and M. Baba, *Bioorg. Med. Chem. Lett.*, 1996, 1993- 1996

9. K. Gaukroger, J. A. Hadfield, N. J. Lawrence, S. Nolan and T. McGown, *Org. Biomol. Chem.*, 2003, **1**, 3033-3037

10. C. Velazquez, P. N. Praveen Roa, R. McDonald and E. E. Knaus, *Bioorg. Med. Chem.*, 2005, **13**, 2749-2757

11. X. Dong, L. Du, Z. Pan, T. Lin, B. Yang and Y. Hu, *Eur. J. Med. Chem*, 2010, 3986-3992

12. A. Gasco, *Ann.*, 1991, 1211-1213

13. G. N. Nikonov and S. Bobrov, *Comprehensive Heterocyclic Chemistry III.*, 2008, Vol. 5, 315-394

14. P. Cotelle and H. Vezin, *Tet. Lett.*, 2001, **42**, 2202-3306

15. D. I. Batovska and I.T. Todorova, *Curr. Clin. Pharmacol.*, 2010, **1**, 1-4.

16. O. Das, S. Paria and T. K. Paine, *Tet. Lett.*, 2008, **49**, 5924-5927

17. V. N. Yarovenko, S. A. Kosarev, I. V. Zavarzin and M. M Krayushkin, *Russ. Chem. Int. Ed.*, 2002, **51**, 8, 1504-1509

18. Damljanovic, M. Vukicevic and R. D. Vukicevic, *Monatshefte für Chemie*, 2006, **137**, 301-305

19. K.C. Liu, B.R. Shelton and R. K. Howe, *J. Org. Chem.*, 1980, **45**, 3916-3918

20. K. J. Hwang, Y. C. Park, H. Jin Kim and J. H. Lee, *J. Biochem.*, 1998, **62**, 9, 1693-1697.

21. T. M. Beale, D. M. Allwood, A. Bender, P. J. Bond, J. D. Brenton, D. S. Charnock-Jones, S. Ley, R. M. Myers, J. W. Shearman, J. Temple, J. Unger, C. A. Watts and J. Xian, *Med. Chem. Lett.*, 2012, **3**, 177-181

22. T. M. Beale, R. M. Myers, J. W. Shearman, D. S. Charnock-Jones, J. D. Brenton, F. V. Gergely and S. V. Ley, *Med. Chem. Comm.*, 2010, **1**, 202-208

23. R. G. Pettit, C. Temple (Jnr), L.V. Narayanan, R. Varma and K. M. Simpson, *Anti-Cancer Drug Des.*, 1995, **10**, 299-309

24. P. Gopalan, H. E. Katz, D. J. McGee, C. Erben, T. Zielinski, D. Bousquet, D. Muller, J. Grazul and Y. Olsson, *J. Am. Chem. Soc.*, 2004, **126**, 6, 1741-1747

25. W. F. Nirode, J. M. Luis, J. F. Wicker and N. M. Wachter, *Bioorg. Med. Chem. Lett.*, 2006, **16**, 2299-2301

26. E.R. Alexander, M. R. Kinter and J. D. McCollum, *J. Am. Chem. Soc.*, 1950, **72**, 2, 801-803

27. H.R.Snyder and N. E. Boyer, *J. Am. Chem. Soc.*, 1955, **77**, 16, 4233-4237

28. H. Tezuka, M. Kato and Y. Sonehara, *J. Chem. Soc. Perkin. Trans. 2*, 1985, 1643-1647

29. P. Cmoch, B. Kamienski, K. Kamiensk-Trela, L. Stefaniak and G. A. Webb, *J. Phys. Org. Chem.*, 2000, **13**, 480-488

30. G. Sorba, C. Medana, R. Fruttero, C. Cena, A. Di Stilo, U. Galli and A. Gasco, *J. Med. Chem.*, 1997, **40**, 463-469

31. R. Calvino, R. Fruttero, A. Gasco and V. Mortarini, *J. Heterocyclic. Chem.*, 1982, **19**, 427-431

32. R. Matsubara, Y. Saeki, J. Li and K. Eda, *Synthesis*, 2013, **45**, 1421-1568

2.1.2- Cupferron compounds

The diazeniumdiolates are the second class of nitric oxide donor compounds that were synthesised. Attempts were made to improve the stability of the parent compound, cupferron **56** (Fig.51) so that the release of NO could be better regulated. Cupferron **56**, is a cheaply available, industrial chelator.

56
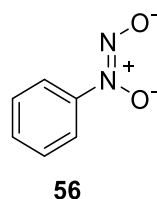
Figure 51: Parent compound cupferron, which is inherently unstable and releases NO

Synthetically the diazeniumdiolate analogues were much easier to produce compared to the furoxans due to the more simplistic alkylation chemistry involved rather than the ring closure reaction described previously. Cupferron **56** was dissolved in dry DMF under anhydrous conditions; the turbid solution was then cooled to 0^0C before 3 equivalents of alkyl bromide were added as shown in scheme 21.
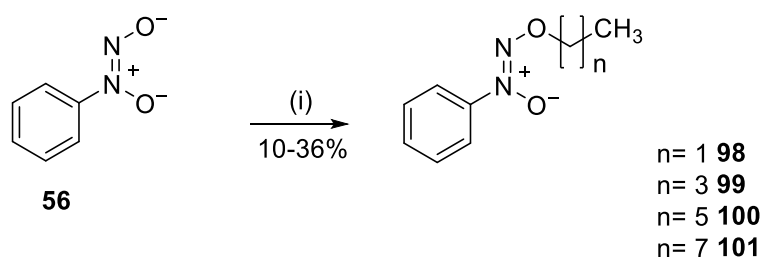
Reagents and conditions: DMF, 0°C, 2-4 days

n= 1 **98**
n= 3 **99**
n= 5 **100**
n= 7 **101**

Scheme 48: Alkylation of cupferron using bromoalkanes under mild conditions.

Upon removal of the DMF, using a cold finger apparatus, each reaction produced a black tar substance; the intense black colour could be due to some mild decomposition of the parent compound and its possible complexation with DMF. The crude gum was absorbed on to silica and purified using flash column chromatography using a 4:1 petroleum ether: ethyl acetate eluent to give the desired mono alkylated cupferrons **98-101** in reasonable yield (10-36%). Confirmation that the alkylation chemistry had been successful was straight forward. ^{1}H NMR spectroscopy showed the introduction of alkyl chains in the aliphatic region of chemical shifts between 1-4 ppm as expected, but it was ^{13}C NMR analysis that provided the diagnostic peaks. The methylene carbon that is directly attached to the terminal oxygen (labelled 'a' in Fig. 52) in cupferron is shifted considerably downfield compared to the rest of the alkane chain. Typically the O-CH$_2$ group was found between 69 and 75 ppm. The rest of the alkyl chain remained upfield between 10 and 40 ppm. The synthesis of compounds **98-101** was also confirmed using high resolution mass spectroscopy (HRMS) and all mass peaks were found within a precision of ±1.0 ppm.
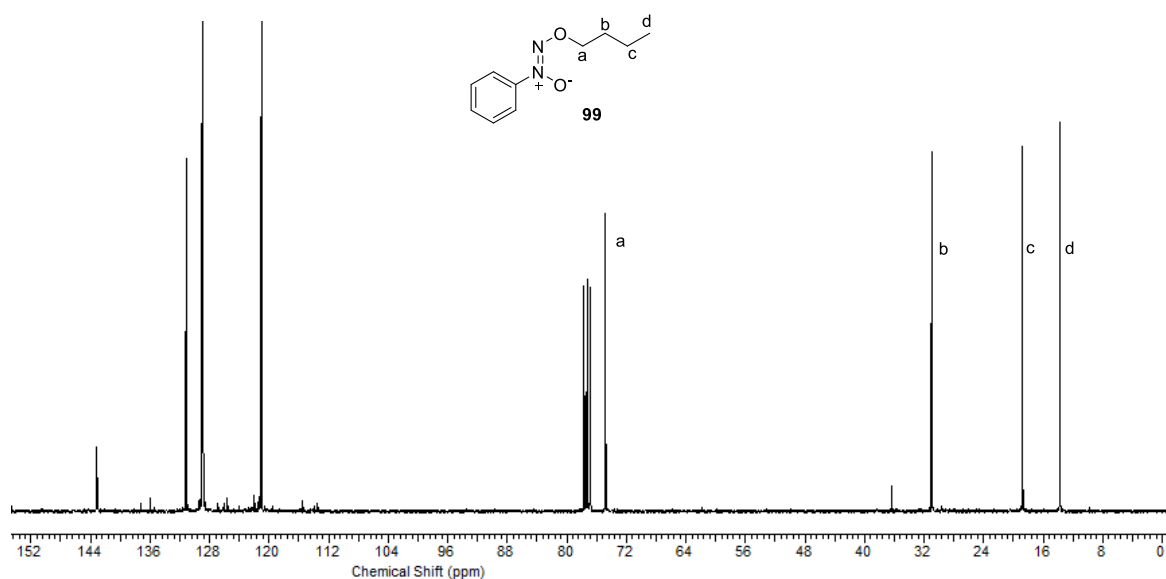
Figure 52: ^{13}C NMR spectra of compound **99** showing the separation of peak 'a' due to the electronegativity and subsequent deshielding effect of oxygen.

To produce the series of compounds where the alkane chain acts as a linker between the two cupferron molecules (depicted in scheme 49), the same chemistry[1] was exploited. Dibromoalkyl compounds (2, 4, 6, and 8 carbons long) were reacted in the same manner as the mono alkyl bromides, except this time in a 3:1 ratio of cupferron to alkyl bromide.
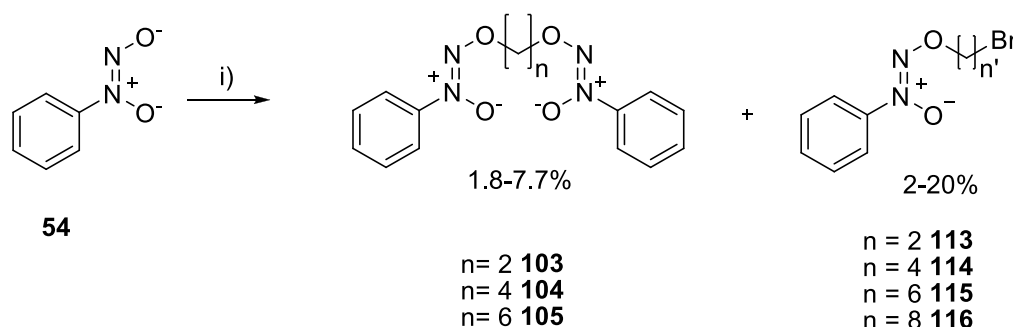
Reagents and conditions: DMF, 0°C, Br(CH$_2$)nBr, 2-4 days

Scheme 49: *O*-alkylation of cupferron with dibromo alkanes to produce the di-cupferron compounds **103-105** and the monoalkylated by-products **113-116**.

Much like the mono alkyl series, once the DMF had been removed a dark black tar was left at the bottom of the flask. Upon purification with column chromatography, using 8:1 petroleum ether: ethyl acetate as an eluent, the desired di cupferron compounds **103-105** were isolated in varying yields (1.8-7.7%). The low yield of this reaction, 1.8-7.7%, could be attributed to the by-product that was isolated during column chromatography. During the reaction, upon initial alkylation of one molecule of cupferron, the second cupferron molecule failed to displace the second bromide and resulted in mono alkylation. This resulted in the mono alkylated-bromo products **113-116** shown in scheme 49. These compounds **113-116** were confirmed through ^{1}H NMR spectroscopy as the methylene group bonded directly to the bromide appears at around 3.2 ppm as shown in Fig. 53. When compared with the di-cupferron product from the same reaction, the ^{1}H NMR spectra looks completely different with the loss of the peak at 3.2 ppm and the change of integration for the peak labelled 'b´' at 2 ppm. These half alkylated products **113-116** were also confirmed using high resolution mass spectroscopy (HRMS), taking advantage of bromine's unique isomeric characteristics..
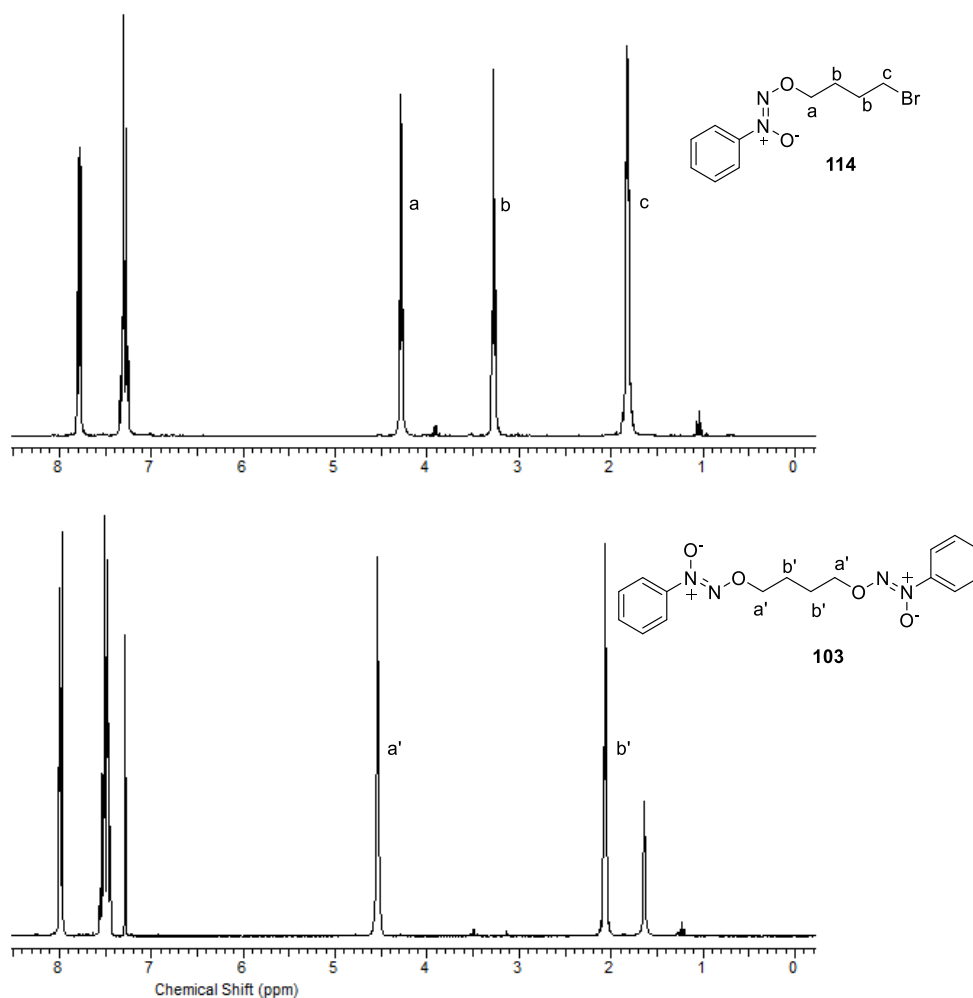
Figure 53: ^{1}H NMR spectra comparing the by-product **114** and the desired di-cupferron **103**.

Apart from producing the initially undesired half alkylated products **113-116**, the synthesis of the of di cupferron compounds produced some other interesting results. The reaction of cupferron with dibromoethane did not produce the desired di-cupferron compound **102** but instead produced the mono-bromo alkylated compound **113**. It was thought that this could be due to the alkyl chain bridging the two cupferron molecules not being long enough for the second cupferron to orientate itself in such a way to displace the second bromide. Electronic repulsion may also play a role in the reaction failure, as the formal charges surrounding the cupferron molecule may repel another cupferron if it is sitting in the wrong orientation for the S_N^2 reaction to take place.
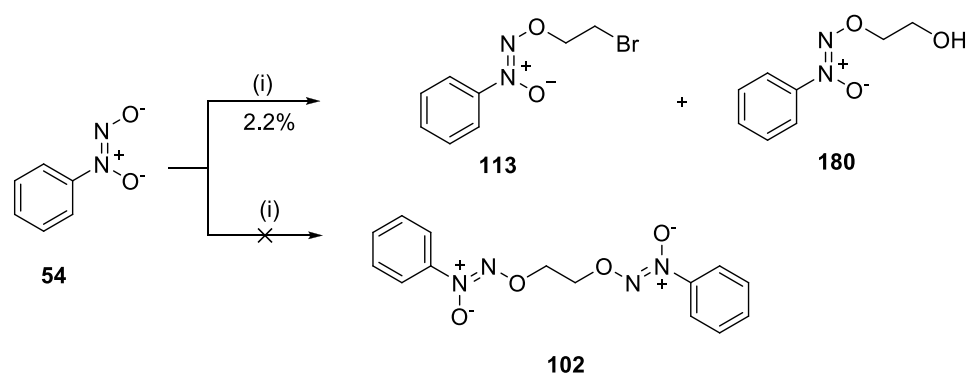
Reagents and conditions: DMF, 0°C, Br(CH$_2$)Br, 2-4 days

Scheme 50: Reaction of cupferron with dibromoethane did not produce the desired product, **102**, instead produced two interesting by-products **113** and **180**.

As well as the mono-bromo alkylated compound **113**, an additional compound was also isolated from the reaction of cupferron with dibromoethane. Compound **180** was isolated post column chromatography and its structure confirmed by HRMS. This is thought to have formed from the initial *O*-alkylation of cupferron, generating compound **113**. Upon work-up, the reaction is exposed to moisture, by the removal of DMF, this may enable a free bromide ion present in the solution to attack an available water molecule forming hydrogen bromide. The formation of hydrogen bromide, leads to the production of hydroxide, which can then attack compound **113** as shown in scheme 51 to produce the cupferron-ethylol **180**.
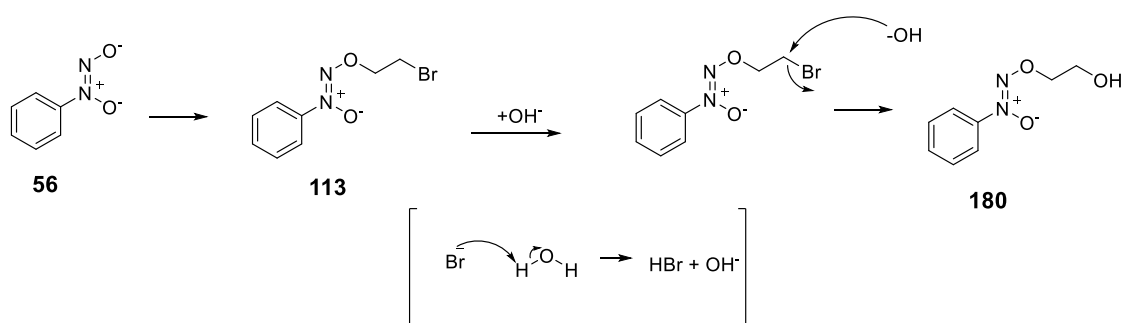
Scheme 51: Possible mechanism for the generation of compound **180** as a by-product of the reaction of cupferron with dibromoethane.

2.1.2.1- Determining of alkylating position

Within cupferrons structure there are two available sites that any alkylation chemistry could occur at. There is the terminal oxygen attached to the non-charged nitrogen and the oxygen directly attached to the nitrogen with a formal positive charge.

There has been some argument from researchers[2,3] as to what oxygen any alkylation would occur at. Only one compound in the cupferron series produced a solid product and was formed upon standing at room temperature over two days. The di-cupferron compound **103** produced large needle like crystals which enabled single crystal analysis. This single crystal structure determination (Fig. 54) gives strong evidence that it is the terminal oxygen (labelled O8 in Fig.54) that the alkylation chemistry occurs at. The single crystal study of compound **103** matched a primitive triclinic cell with the following cell parameters: a = 7.23 Å, b = 7.83 Å and c= 8.46 Å with corresponding angles of α=64.6°, β= 66.84° and γ= 73.147. The full crystallography data can be found in appendix AP01.
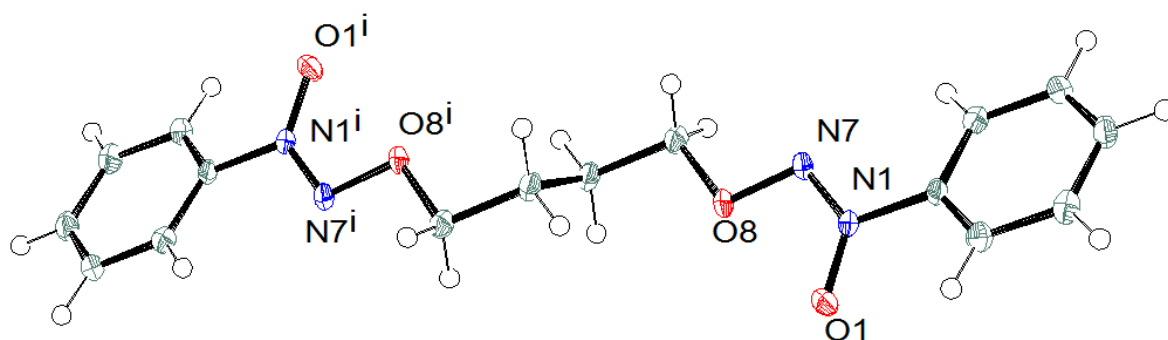
Figure 54: The single crystal structure of compound **103**, showing that *O*-alkylation occurs at the terminal O8 and O8[i] position.

The crystal structure of compound **103**, shown in Fig. 54 confirms that the *O*-alkylation occurs on the O8 terminal oxygen and it therefore can be assumed that this is the case for the non-crystalline produced compounds **98-101** and **104-105**. The two aryl rings sit in an offset planner relationship allowing for π-π stacking, and alignment of charges within the packing structure (Fig. 55). Literature[4,5] has indicated that it is possible to form the O1 alkylated derivative but they tend to be an unstable

by-product and do not affect the formation of the O8 alkylated product seen in Fig. 54. ^{15}N NMR spectroscopy was also performed on compound **103**, confirming the structure presented in Fig.54 through correlation of proton to nitrogen environments (see experimental section 4.0 for full data).
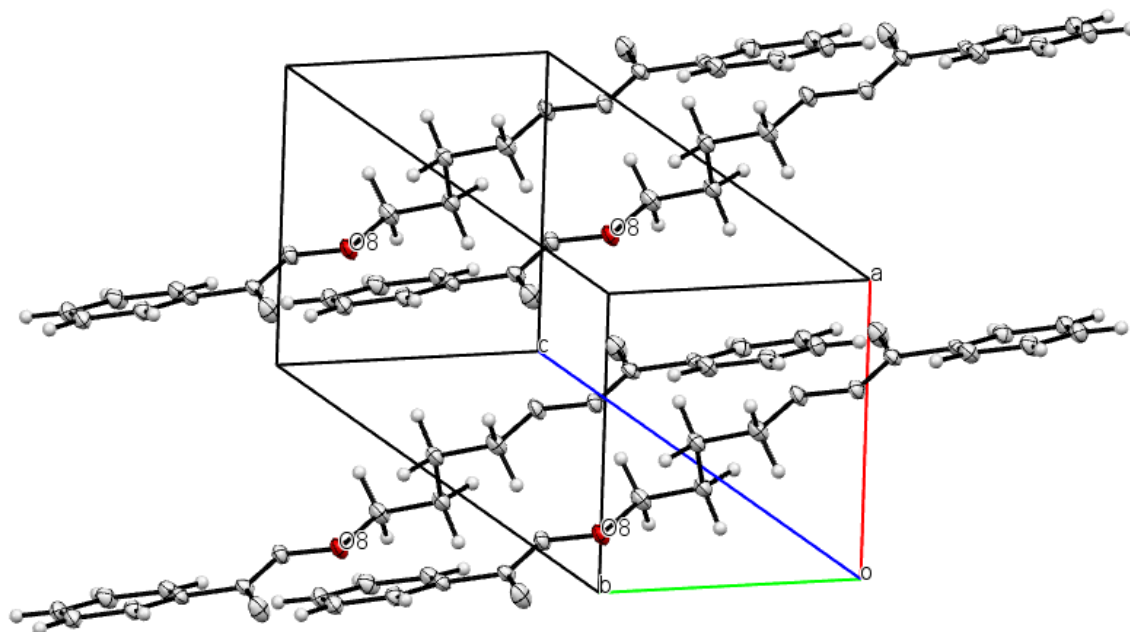
Figure 55: The crystal packing of compound **103** showing that a **103** stacks using hydrophobic interactions and π-π stacking.

However some minor evidence was found that the intramolecular cyclisation reaction to produce the 8 membered ring (Fig. 57) had also occurred during the reaction. ^{13}C NMR spectroscopy highlighted a compound with very different peaks to the previously observed mono-bromo alkylated cupferrons **113-116** and the di-cupferron compounds **103-106**. A new peak occurring at 73 ppm alongside the usual peak at 75 ppm was isolated indicating that a different compound had been synthesised as shown in Fig. 56. This was thought to be the intramolecular cyclised product where instead of another cupferron molecule's terminal oxygen displacing the second bromide on the alky chain, the oxygen attached to the positive nitrogen (labelled O1[i] in Fig. 54) attacks the methylene group (depicted as 'd' in Fig. 56) and displaces the bromine to form a 8 membered ring **181**.
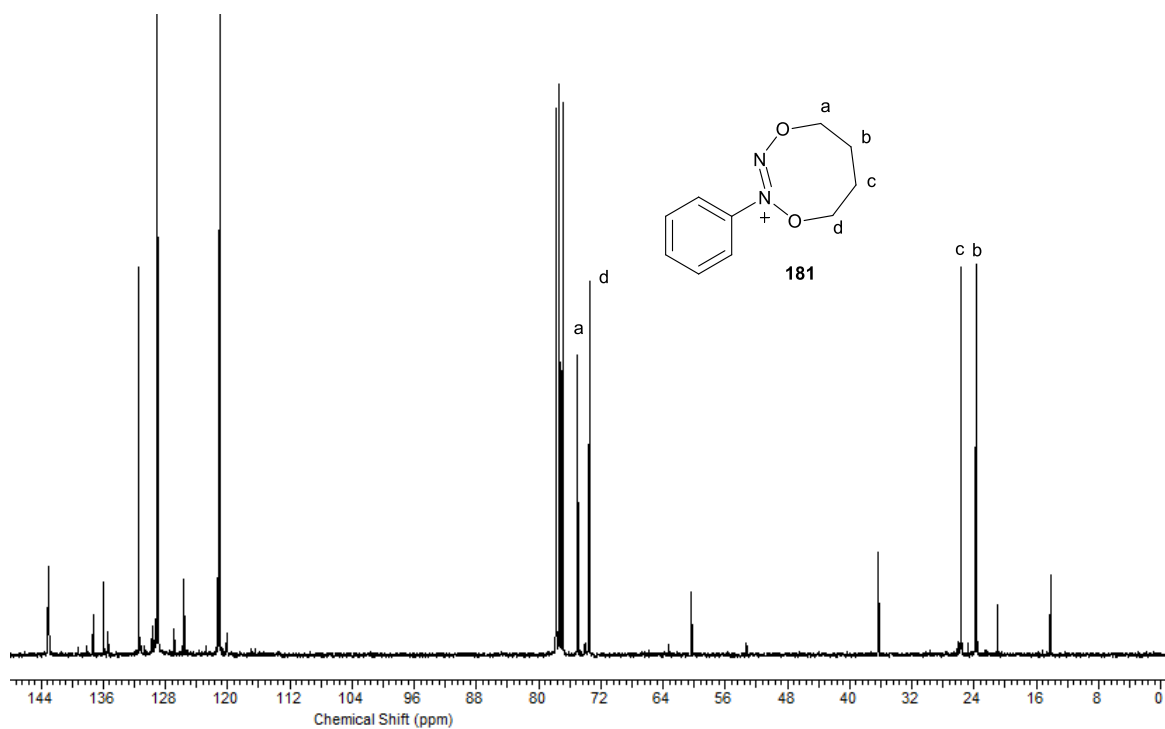
Figure 56: The ^{13}C NMR spectrum of compound **181**, presenting a new peak at 73ppm, labelled d, indicating that the intramolecular reaction has occurred.

The formation of the (Z)-2-phenyl-5,6,7,8-tetrahydro-1,4,2,3-dioxadiazocin-2-ium, compound **181** was further confirmed by mass spectroscopy, however only low resolution was obtainable, possibly due to the instability of the compound. A mass of 193 m/z corresponding to the formula $C_{10}H_{13}N_2O_2$ was isolated and the corresponding spectrum is shown in Fig 57.
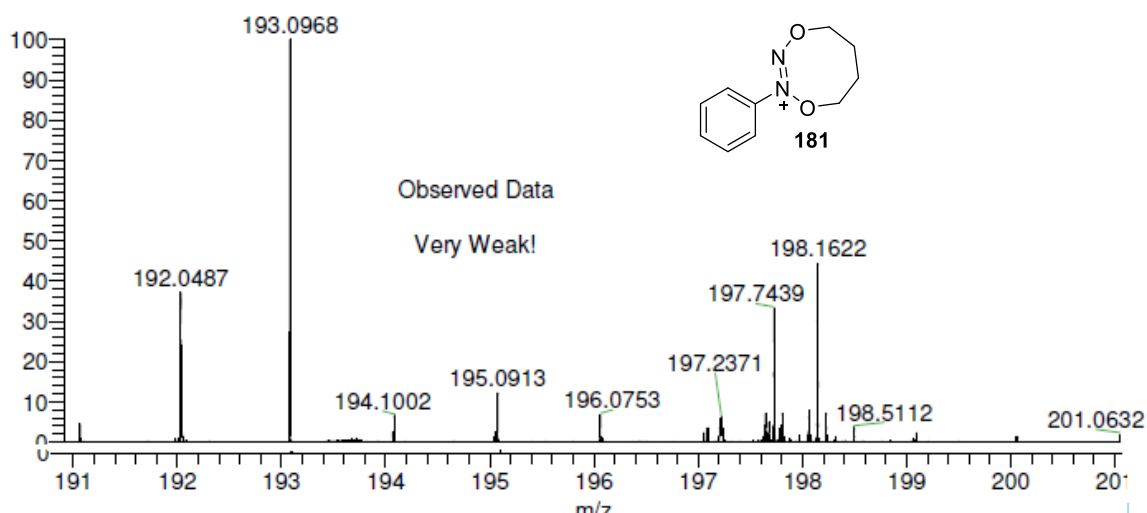
Figure 57: LRMS of a compound confirming the formation of the intramolecular ring product **181**. Spectrum produced by the NMSF.

Interestingly when analysing the HRMS for both the hexyl and octyl compounds, **104** and **105**, evidence was also found corresponding to the intramolecular ring formation in these reactions as well, although not in an isolatable yield but enough to provide accurate mass information. Compound **104**, synthesised with the hexyl linker produced a 10 membered ring **182** (Fig. 58) with a m/z of 221.1287 and compound **105** with the octyl chain produced a 12 membered ring **183** with a m/z of 251.1757. This appears to be the first isolation of any data consistent with the formation of these cupferron based large heterocycles or dioxadiazocinium-type rings.

182

10 membered intra product

183

12 membered intra product
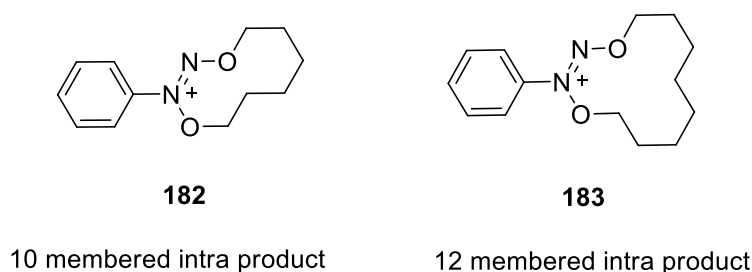
Figure 58: The two intramolecular products isolated from the HRMS generated from the reaction of cupferron with dibromohexane and dibromooctane respectively.

Mass spectroscopy also isolated another interesting compound from the reaction of cupferron with dibromobutane. A mass of 496.2141 m/z, which did not correspond to any before isolated compound, was discovered. After contemplating different structures that would fit the newly found mass peak, compound **184** (Fig. 59) was highlighted as a suitable structure, existing as a trimer type molecule. There is a possibility that if the alkylation reaction depicted in scheme 49 is left for long enough that a polymeric form of cupferron could be isolated, however this does appear to involve alkylation on both the O1 and O8 oxygen's and therefore the isolation of this compound may be impossible due to the stability of O1 alkylated cupferron compounds.[4]

184
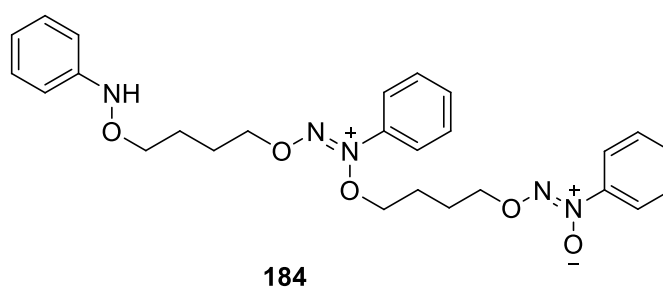
Figure 59: Compound 184, isolated from the mass spectrum of compound **181**.

In summary, the *O*-alkylation of cupferron was both successful and interesting, producing compounds **98**-**101** and **103**-**105** in varying yields, 1.8-36%. This reaction appears to be quite low yielding and can possibly be attributed to the production of the mono-bromo alkylated by-products **113-116**. The low yield may also be contributed to by the stability of the parent compound within the reaction; if decomposition of the starting material is occurring at the same time as the alkylation then the resulting yield of the desired compounds is going to be the lower than expected.

From this series of reactions, the positon of alkylation has been successfully determined; the X-ray crystal structure (Fig. 54) clearly indicates that the O8, terminal oxygen on the cupferron molecule is the preferred site of alkylation and not on the O1 oxygen. It can be assumed that the non-crystalline compounds 98-101 **and** 104-105 **are also alkylated at the O8 oxygen due to the evidence seen for the crystalline compound** 103**. However, a small amount of evidence depicted in Fig. 56, 57 and 58 suggests that the intramolecular reaction can occur, forming the 8, 10 and 12 membered dioxadiazocinium rings but not in a progressively yielding way and possibly only as a side reaction.2.1.2.2- References**

1. Y. Hou, W. Xie, A. J. Janczuk and P. G. Wang, *J. Org. Chem.*, 2000, **65**, 4333-4337

2. J. A. Hrabie and L. K. Keefer, *Chem. Rev*, 2002, **102**, 1135-1154

3. J. E. Saavedra, D. Scott Bohle, K. N. Smith, C. George, J. R. Deschamps, D. Parrish, J. Ivanic, Yan-Ni. Wang, M. L. Citro and L. K. Keefer, *J. Am. Chem. Soc.*, 2004, **126**, 12880-12887

4. Y. Hou, W. Xie, N. Ramachandran, B. Mutus, A. J. Janczuk and P. G. Wang, *Tet. Lett.*, 2000, **41**, 451-456

5. O. A. Luk'yanov, G. A. Smirnov and S. V. Nikitin, *Russ. Chem. Bull.*, 1998, **47**, 10, 1940-1946

2.1.3- NOS inhibitors

The synthesis of neuronal nitric oxide synthase (nNOS) inhibitors was planned as a three step synthetic pathway, consisting of a protection step, a deprotonation and alkylation step and then finally a de-protection step to yield a series of novel diaminopyridine based NOS inhibitors. These potential nNOS inhibitors consist of two amino-pyridine rings, which will bind strongly within the active site for nNOS due to their strong similarity to the natural substrate L-arginine.[1,2] It has been found through docking studies that the 2-aminopyridine moiety can bind into separate binding sites within nNOS, thus having two aminopyridine groups will enable the optimisation of both these sites[3].
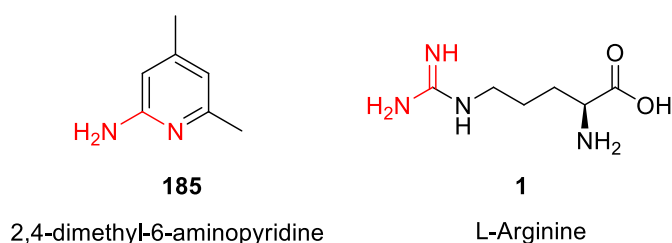
Figure 60: Natural substrate of nNOS with part of its guanidine group highlighted and its corresponding isostere in 2,4-dimethyl-6-aminopyridine.

The pi system present in the pyridine rings can also have pi- (π-π) interactions with the pyrrole rings of the haem in the active site of neuronal NOS (nNOS) as shown in Fig.61.
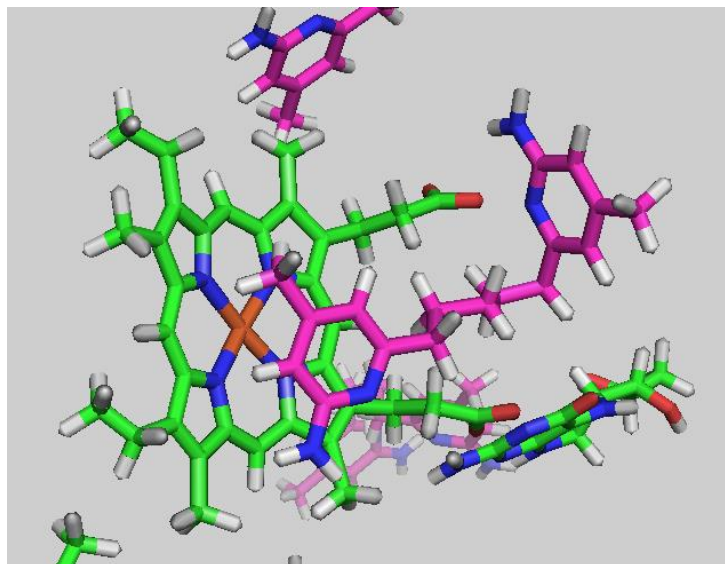
Figure 61: 3D representation of Silverman's most potent compound docked in the nNOS active site, showing the π-π interactions between the haem group, shown in green, of NOS and the aminopyridine ring, shown in magenta.

The first step of the synthesis was to protect the free amine in the 6-postion on the pyridine ring (scheme 52). This was conducted using a Paal-Knorr pyrrole synthesis[4-6] to generate a bulky pyrrole ring which would be stable to any future chemistry .To generate the pyrrole ring, 2,4-dimethyl-6-aminopyridine was refluxed with hexane-2,5-dione in the presence of *p*-TsOH acid for 24 hours under Dean-Stark conditions to generate the desired pyrrole ring **147** in 35% yield. Dean-Stark conditions are utilised to collect and isolate the water formed from the cyclisation of the pyrrole ring and to prevent any consequential ring opening and reversal of the forward reaction.
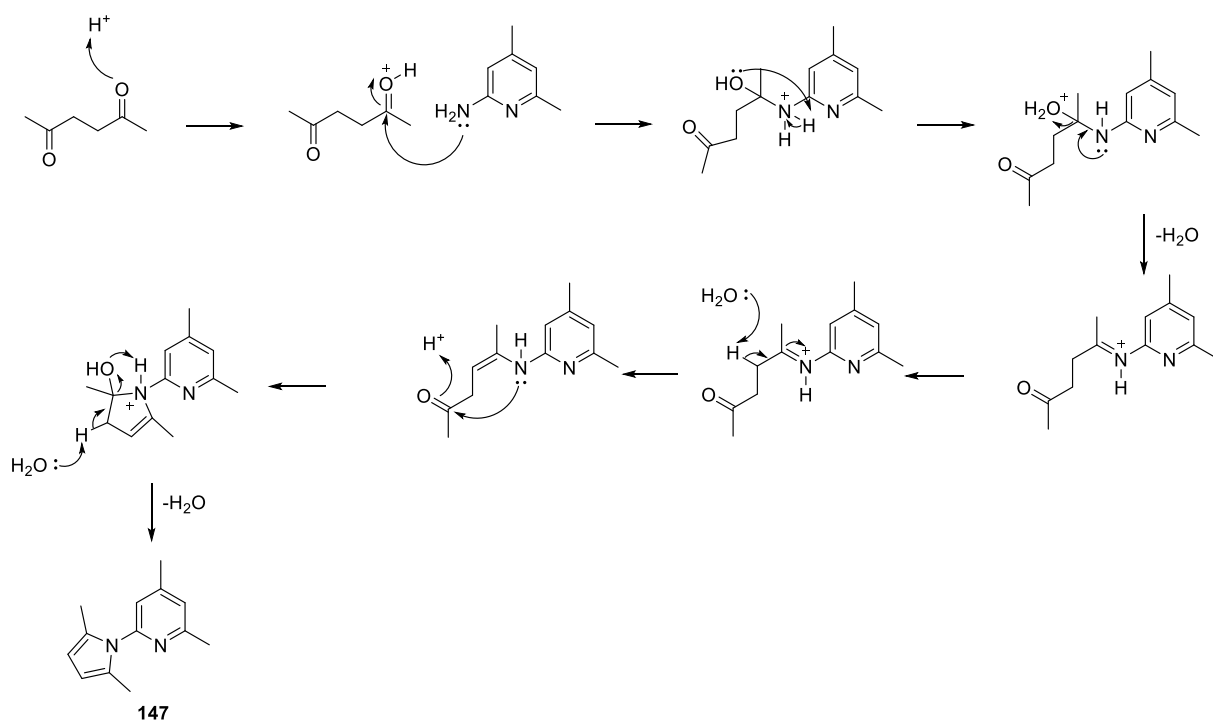
Scheme 52: Mechanism of pyrrole ring formation from the reaction of a dicarbonyl species with the free amine group of the aminopyridine ring[4]

The pyrrole ring **147** is formed through a condensation reaction between a dicarbonyl species and an amine. The lone pair of the amine attacks the carbonyl group to generate an enamine intermediate with the loss of one molecule of water. This enamine species then attacks the second carbonyl group to form a semi-pyrrolidine ring, which then rapidly loses water to yield the desired pyrrole ring, serving in this instance as a protecting group for the forward deprotonation step.[4] A small amount of acid is known to accelerate this reaction, and therefore hence the addition of *p*-TsOH as a catalyst.

The second step in this pathway is the deprotonation of the methyl group in the *ortho* position so that addition of an alkyl bromide can take place[7]. Although seemingly straightforward, the deprotonation step provided quite a few hurdles to overcome. Following Silverman's procedures[7, 8] from the literature; initial experiments were conducting with 2.5 equivalents of *n*-butyl lithium. Under anhydrous conditions the protected dimethyl pyridine compound **147** was dissolved in dry THF and cooled to -78°C before the addition of *n*-BuLi was added turning the solution into a characteristic

red colour, denoting the coordination of the lithium atom with the lone pairs of nitrogen and the stabilisation of the forming methylene anion (CH_2^-). Dibromo alkanes were then injected into the reaction to form the new carbon-carbon bond as depicted in scheme 53.
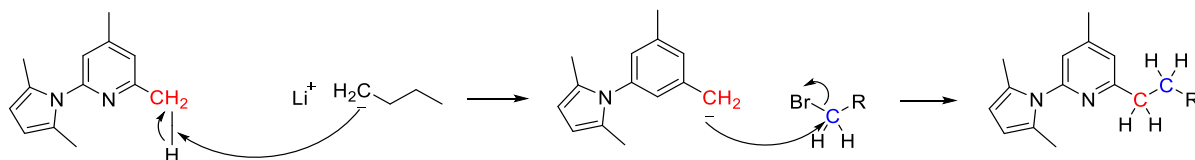
Scheme 53: General mechanism of the formation of a new C-C bond, using butyl lithium and bromoalkanes.

Initially dibromopropanol was attempted as the linker compound, injected in a 2:1 protected starting material **147** to linker **186** ratio (scheme 54). After completion of the work up procedure it was found that no reaction had occurred and the starting material was recovered in almost quantitative yield. It was thought that maybe the free hydroxyl group present in the linker could be interfering with the reaction by reacting with the *n*-BuLi or that the dibromopropanol **186** was perhaps too wet, as it is sold at 95% purity and therefore may contain a small amount of moisture that could be detrimental to the reaction. The failure of this reaction was confirmed through ^{1}H NMR analysis, as the ratio of hydrogens in the methyl region had not changed and there was no additional peak representing the newly formed methylene group. The number of equivalents of *n*-BuLi were increased from 2.5 to 5 but this still failed to return the desired product.
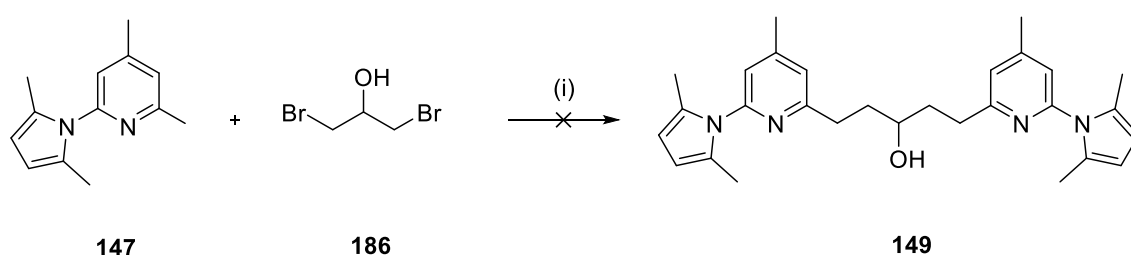
Reagents and condtions: *n*-BuLi (2.5eq), THF, -78°C, 2hrs

Scheme 54: Reaction of the pyrrole protected starting material **147** with dibromopropanol **186**.

To try and avoid any extra acidic protons and moisture in the reaction possibly being caused by a free hydroxyl group, a different linker (scheme 55) was utilised. 1,4-Dibromobut-2-ene **187** was injected in the same manner as the previous linker with 5 equivalents of *n*-BuLi but also came to no fruition.
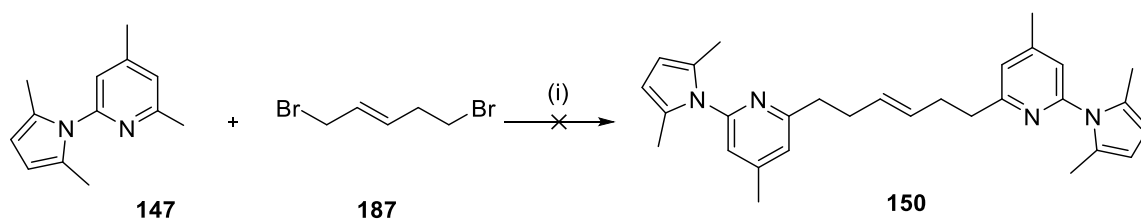
Reagents and condtions: *n*-BuLi (2.5eq), THF, -78°C, 2hrs

Scheme 55: Reaction of the pyrrole protected starting material with dibromobut-2-ene **187**.

A closer inspection of the procedure used by Silverman[7-9] highlighted that too much water was being used during the work up procedure and that this may have contributed to the lack of product. Instead of pouring the reaction onto ice, an molar equivalent (~110 μL) of water was added to minimise the amount of water present in the system in an attempt to isolate the desired product. This was conducted over several attempts, to which no product was obtained. The equivalents of *n*-BuLi were also increased from 2.5 to 6 in an attempt to cause efficient deprotonation of the starting material **147**. All the attempts to deprotonate and sequentially alkylate the pyrrole protected starting material **147** were unsuccessful.

It was theorised that deprotonation just wasn't occurring with *n*-BuLi. One explanation could be that there are four similar sites (4 methyl groups with the potential to become deprotonated as highlighted in Fig. 62) that the base could act on.

This may suggest that more base is required than first thought as any excess base is being used to deprotonate in the wrong position. However this theory can be discounted with ¹H and ¹³C NMR analysis of the reaction mixture and even post column chromatography, as unchanged starting material and the unreacted linker compound are being isolated in clean fractions. This therefore suggests that no deprotonation is occurring at all.

147
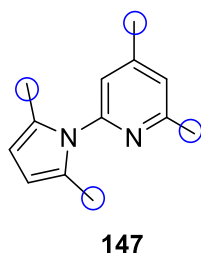
Figure 62: Pyrrole protected 2,4-dimethylaminopyridine starting material. The four methyl groups, or potential deprotonation sites, are highlighted by a blue circle.

To test if any deprotonation was occurring with *n*-BuLi, deuterium oxide (D_2O) was used instead of water in the work up procedure. Deuterium has a magnetic spin of 1, instead of spin ½ like that of hydrogen and therefore will not be seen in ^{1}H NMR spectrum. This should indicate if deprotonation has occurred, as one of the hydrogens on the methyl group will be replaced with a deuterium and therefore not be visible in the ^{1}H NMR spectrum. The ^{1}H spectrum show in Fig. 63 is a computer simulated spectra of the deprotonated and deuterated starting material **188**. The hydrogen that has been replaced with a deuterium atom has been shifted downfield towards 3 ppm from around 2 ppm. Its integration also changes from being equivalent to 3 hydrogens to being equivalent to 2 hydrogens.
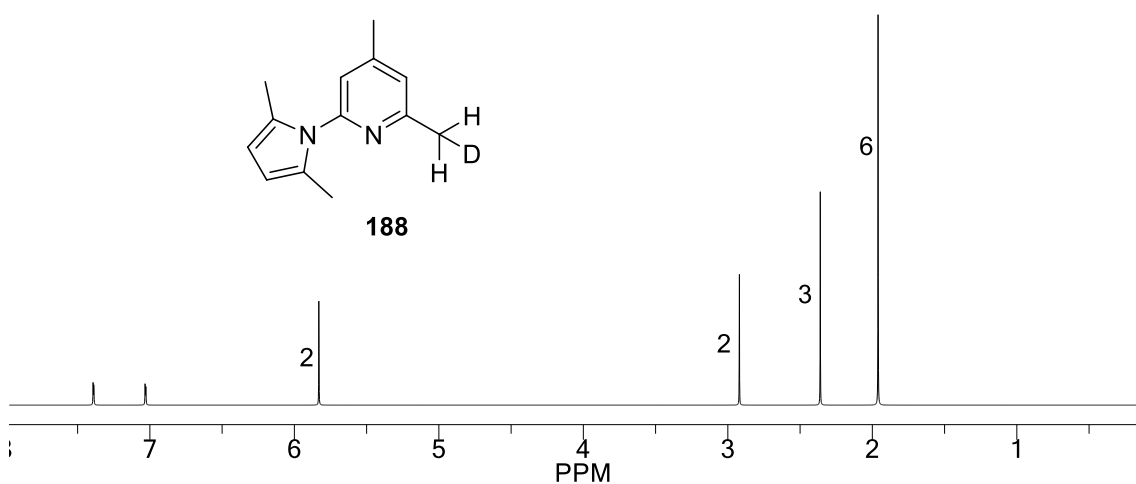
Figure 63: The computer simulated ^{1}H spectra of deuterated 2-(2,5-dimethyl-1H-pyrrol-1-yl)-4,6-dimethylpyridine, **188**, showing the shifting of the metheleyne hydrogens towards 3 ppm.

The reaction shown in scheme 54 and 55 was performed in the same method as before; protected starting material was dissolved in dry THF and cooled to -78°C before *n*-BuLi (5 equivalents) was added. Instead of introducing the dibromoalkane linker, the reaction was quenched with D_2O and extracted with diethyl ether. Upon analysis of the reaction the ^1H spectrum (Fig. 64) showed that deprotonation was unsuccessful. This can be seen through the integration of the methyl groups still representing three (3) hydrogens each, when compared with the other methyl group in the *para* positon on the pyridine ring and the two on the pyrrole ring. There should be a change in integration due to the loss of one proton and a change in chemical shift towards that of 3 ppm. This confirms that no deprotonation has occurred during the reaction.
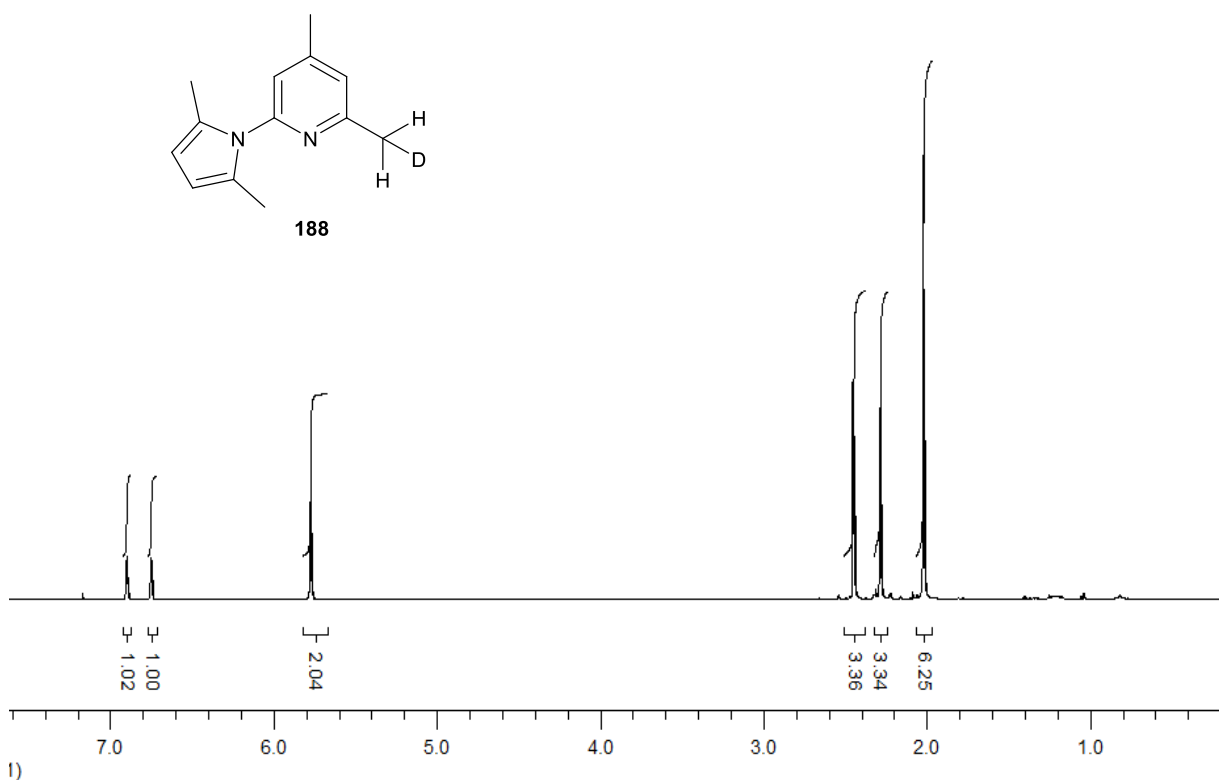
Figure 64: ^1H spectrm of the attempted deuteration of 2-(2,5-dimethyl-1*H*-pyrrol-1-yl)-4,6-dimethylpyridine, **188**, there is no shift of the methylene protons towards 3 ppm indicating that deuteration was unsuccsessful.

It was concluded that deprotonation was simply not occurring or not enough to cause the forward reaction to go to completion. The pK_a of 2-methylpyridine, a compound closely related to our starting material, is approximately 34 and n-BuLi has a pK_a of around 50. This difference in pK_a value could explain why n-BuLi failed to deprotonate the methyl group as it may not be basic enough to remove the required proton. Butyl lithium exists as a hexamer when in solution; each lithium atom of the butylithium coordinates to 2 other carbons creating a cluster of 6 lithium atoms with a triangular face[10,11]. This cluster formation (Fig. 65) can sometimes hinder the reactivity of the base. Lewis bases such as diethyl ether and THF are often used as the solvent for the reaction as they tend to disaggregate the cluster[10]. Nitrogen ligands[10,12], such as tetramethylethylenediamine (TMEDA) or sparteine (Fig. 66) can also induce deaggregation and increases the solubility of the butyl lithium reagent therefore make it more reactive.[13]
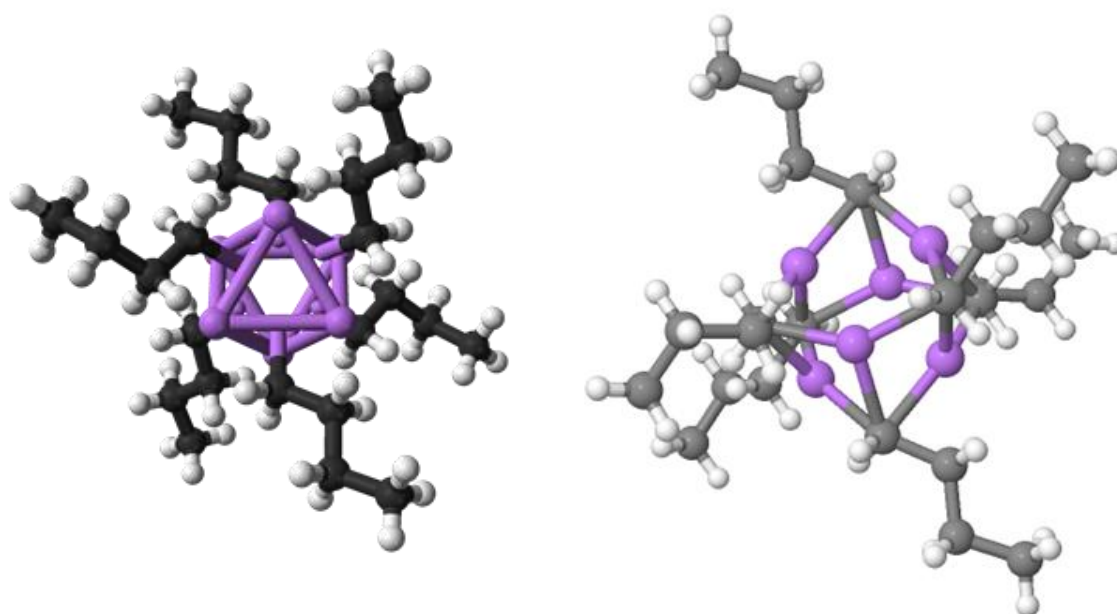
Figure 65: Crystal structures showing butyl lithium existing in its hexamer form. The lithium atoms (shown in purple) form a triangular face and coordinate with 3 butyl chains each. Taken from reference 14.

TMEDA (Fig. 66) has a high affinity for lithium ions and acts as a metal ligand causing disruption to the hexamer that *n*-BuLi adopts when solvated in hexane, it instead forces it to exist as a solvated tetramer[10,13,15] or a dimer. By decreasing the aggregation[16] of the *n*-BuLi it increases the reactivity of the base and therefore may solve the problem in our reaction.
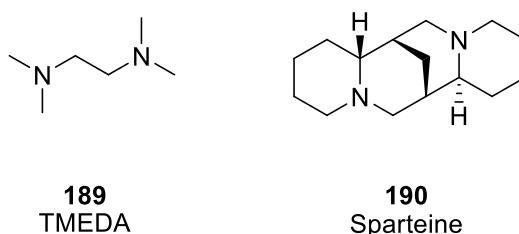
Figure 66: Two nitrogen ligands, TMEDA **189** and Sparteine **190**, known to decrease the aggregation of *n*-BuLi.

To test if this increase in basicity would cause the reaction to go to completion a model reaction was created. Due to the expensive nature of the dimethyl aminopyridine starting material **185** and the laborious purification needed to obtain pure protected starting material **147**, it was decided that 2,4,6-trimethylpyridine **191** would be used in the deprotonation experiments. The reason for this is clear, as it still contains the methyl protons required for deprotonation in our own reaction (Fig. 67) but at a much cheaper price. The linker was also changed to bromoethane for the same reasons. An initial test reaction of *n*-BuLi and 2,4,6-trimethylpyridine **191** and bromoethane as a linker also failed to give the desired product, giving validation for their use as model reactants for hypothesis testing.
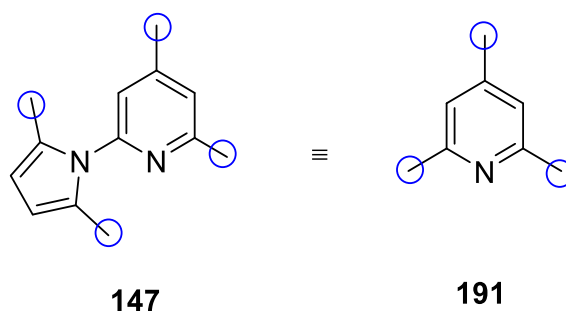
Figure 67: 2-(2,5-dimethyl-1*H*-pyrrol-1-yl)-4,6-dimethylpyridine has very similar deprotonation sites to 2,4,6-trimethylpyrdine and therefore can be used as a model reagent to test different reaction conditions.

1.1 equivalents of freshly distilled TMEDA, was added to *n*-BuLi and 2,4,6-trimethylpyridine at -78°C (scheme 56). The resulting orange solution was allowed to reach 0°C over the course of an hour before bromoethane was added causing the solution to turn pink. The reaction was allowed to progress for 30 minutes, before the resulting colourless solution was worked up by addition of a molar equivalent of ammonium chloride (NH₄Cl), and an aqueous extraction. Analysis of the resulting ^{1}H and ^{13}C NMR data showed that the reaction had not worked and unreacted starting material was recovered once again.

191   **148**
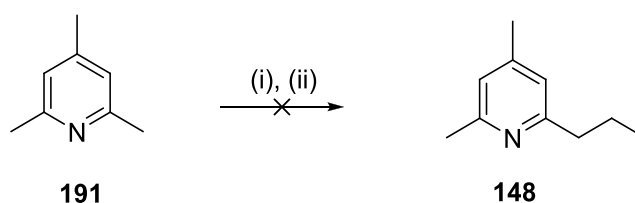
Reagents and condtions: *n*-BuLi, THF, -78°C, TMEDA, CH₃CH₂Br, 1hr (ii) NH₄Cl

Scheme 56: Reaction of 2,4,6-trimethylpyridine **191** with bromoethane. TMEDA **189** was added in an attempt to increase the reactivity of *n*-BuLi.

It was decided that perhaps *n*-BuLi was not a strong enough base, and the pK_a was not high enough for sufficient removal of the methyl proton. Comparing *n*-BuLi to other alkyl bases (Fig. 68) it can be seen that there are plenty of other options to turn to. *t*-BuLi, is known to be a very good base but has various safety issues which makes it less appealing to work with compared to the other options. *s*-BuLi has enhanced basicity, with a greater pK_a value when compared to *n*-BuLi and also has less severe handling issues compared with that of *t*-BuLi. Phenyl lithium is a slightly weaker base compared to *n*-BuLi but is a bulkier group than the butyl chain so should be less prone to nucleophilic reactions and more selective towards deprotonation.
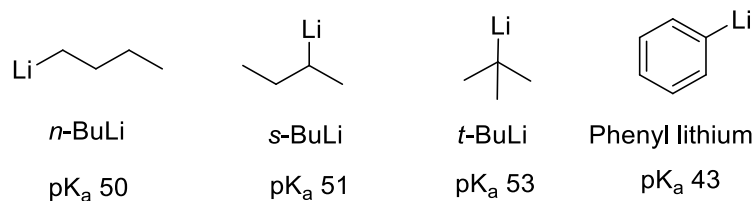
Figure 68: Various alkyl lithium bases and their relative basicity quoted in terms of pK_a.

While researching the most effective bases, an interesting publication[17] was discovered performing very similar chemistry to our own. The authors alkylated 4 and 2-picoline using phenyl lithium in a 1.1 ratio as shown in scheme 29. In contrast to many other reactions which are conducted at sub - 20°C temperatures, this reaction was refluxed for half an hour to give their desired alkylated products in 55-92% yields.
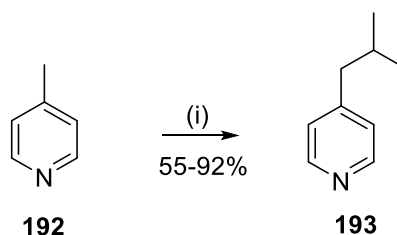
Reagents and conditions: PhLi, isopropyl bromide, diethyl ether, 40°C

Scheme 57: Reaction of 4-piccoline, 4-methylpyridine **192**, with phenyl lithium under reflux conditions.

The discovery of this work[17] coincided with a personal communication[18] from Professor Silverman. After consulting his research group, as to why the outcomes of our reactions were so different to those reported, Silverman stated that at temperatures closer to 0°C, the site of deprotonation favoured the *ortho* position. The solvent for the reaction also played a role in Silverman's reported chemistry, with THF favouring the *ortho* position while diethyl ether moved the reaction towards the *para* position deprotonation, but *n*-BuLi should still be added at -78°C.

Applying the newly found experimental procedures[17] and Silverman's suggestions to our model reaction (scheme 58), resulted in 2,4,5-trimethylpyridine **191** being dissolved in dry diethyl ether and one equivalent of phenyl lithium being introduced at -78°C, causing the solution to turn a deep red colour. After an hour the reaction was brought to room temperature before one equivalent of bromoethane was injected into the anhydrous environment, which was then refluxed at 40°C for 4 hours.
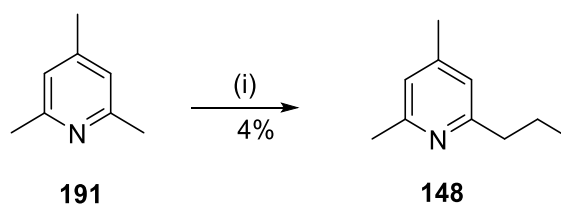
Reagents and conditions: PhLi, diethyl ether, bromoethane, 40°C, reflux, 4hrs

Scheme 58: Reaction of 2,4,6-trimethylpyridine **191** with phenyl lithium under reflux conditions to successfully produce the alkylated product.[17]

Upon work up, crude ^{1}H NMR analysis was undertaken to assess the situation as TLC analysis proved to be inconclusive to whether a reaction had occurred or not. The crude NMR data spectra (Fig. 69) didn't look very promising and just appeared to be a mixture of bromoethane and unreacted starting material. However when studied more closely (highlighted by the red arrows in Fig. 69), there was a small amount of evidence to suggest that a reaction had in fact occurred. This coupled with a faint spot on TLC, led to the crude mixture being purified by flash column chromatography in a 10:1 petroleum ether:ethyl acetate solvent system to yield 4% of desired product **148**. The post column ^{1}H NMR spectra, now clearly shows the desired product **148** with the highlighted portions being the small peaks from the crude spectrum (Fig.69). Trimethylpyridine is a symmetrical molecule and therefore with successful addition of an ethyl substituent, an unsymmetrical molecule has been formed resulting in more ^{1}H signals in both the crude and pure ^{1}H NMR spectra. The peaks highlighted can be attributed to the addition of the ethyl chain with peak at 2.6 ppm being the methylene hydrogens in the *ortho* position of the pyridine ring. Their shift downfield from 2.4 ppm in the starting material confirmed that successful deprotonation had occurred.

Crude ^{1}H NMR

CH$_2$Br

Post column chromotography

148
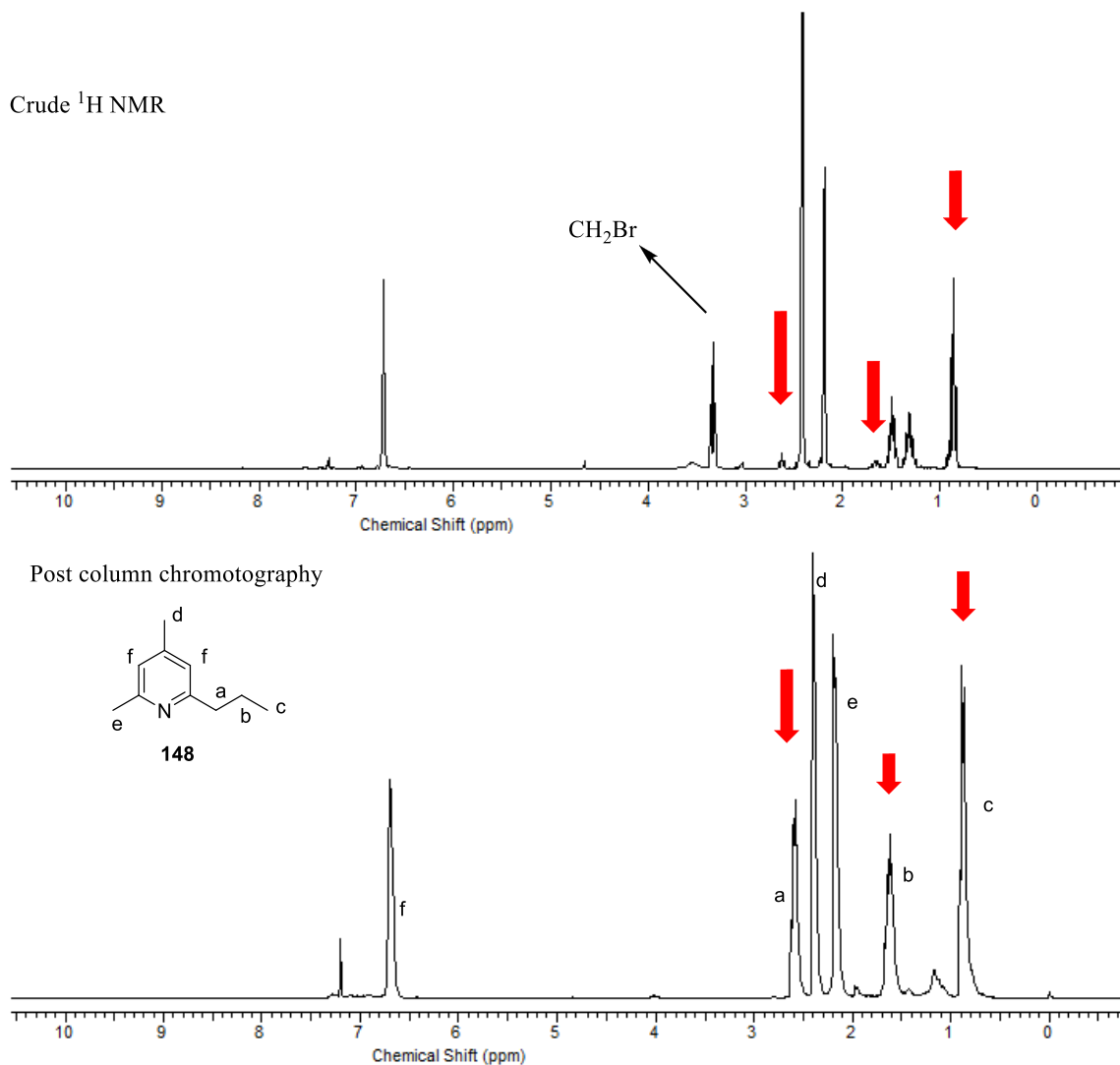
Figure 69: ^{1}H spectra of the crude and purified reaction shown in scheme 58. The red arrows indicate the diagnostic product peaks and their isolation from the crude material. ^{1}H NMR analysis conducted with at 300 MHz in CDCl$_3$.

Observations[18] found by the Silverman group concluded that a temperature closer to 0°C favours deprotonation at the *ortho* position but the use of diethyl ether as a solvent pushes the reaction more towards deprotonation at the *para* position. The ^{1}H NMR spectra shown in Fig. 69 indicates that deprotonation and alkylation has in fact occurred at the *ortho* position (labelled 'a' in Fig. 69), due

to the unsymmetrical nature of the peaks seen. The integration is 2:3:3:2:3, suggesting the presence of three separate methyl environments all integrating for 3 protons (peaks 'c', 'd' and 'e' in Fig.69) and two methylene protons integrating for 2 protons each, indicated by 'a' and 'b' in Fig. 69.

This evidence therefore slightly contradicts what Prof. Silverman saw during his experiments and perhaps the solvent has less of an effect in this procedure than first thought. The only other compound isolated from the column was unreacted 2,4,6-trimethylpyridine, **191**.

To test Silverman's observations further the same reaction was repeated but this time using THF as the solvent, in the hope that if diethyl ether was interacting with the reaction this would be quashed by the use of THF. Using the same experimental set up, and a 1.1 ratio of phenyl lithium to 2,4,6-trimethylpyridine **191**, the desired product **148** was isolated in a 2% yield. Comparing the two reactions, it appears that diethyl ether is a marginally better solvent for this type of alkylation, however, the poor isolated yield, 2 and 4% also suggests that deprotonation is still not a highly favoured process under these reaction conditions. With deprotonation and alkylation at the *ortho* proving successful, the new procedure[17] involving phenyl lithium and refluxing for 4 hours was then applied to the problematic reaction with the pyrrole protected aminopyridine starting material **147**. The protected starting material was dissolved in diethyl ether, as this gave us the best yield in the model reaction, and 1.1 equivalents of phenyl lithium were injected at -78°C to yield a bright red solution. The reaction (scheme 59) was allowed to come to room temperature over the course of 1 hour before dibromoxylene **192** was injected in in a 1.1 equivalent ratio. Dibromoxylene **192** was used as the linker in this case to try and minimise any interactions between linker and the base. The resulting solution was heated at reflux for 4 hours before being worked-up and the crude mixture purified by column chromatography.
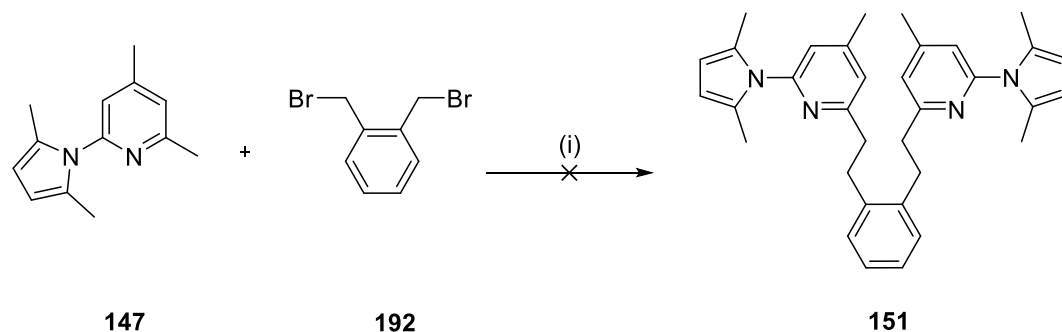
Reagents and conditions: PhLi, diethyl ether, 40°C, reflux, 4hrs

Scheme 59: Reaction of 2-(2,5-dimethyl-1*H*-pyrrol-1-yl)-4,6-dimethylpyridine with dibromoxylene under the newly discovered conditons using phenyl lithium. This reaction was unsuccsessful at producing the desired product in an isolatable yield.

Upon analysis of the reaction with both ^{1}H and ^{13}C NMR spectroscopy (Fig.70), the reaction showed a mixture of unreacted starting materials. Column chromatography produced a set of clean fractions but separation of the two spots was not possible. A GC-MS was conducted on the sample in an attempt to discover what the inseparable compounds were. It was found that the majority of product was unreacted starting material **147**. However an interesting peak was isolated from the GC column, albeit in a very small proportion compared to the starting material peak. This peak was found (Fig.71) to be for the desired product **151** with a mass peak of 502.23 m/z, and although this was proof that a successful reaction had taken place using phenyl lithium as a base, the material was inaccessible by column chromatography.
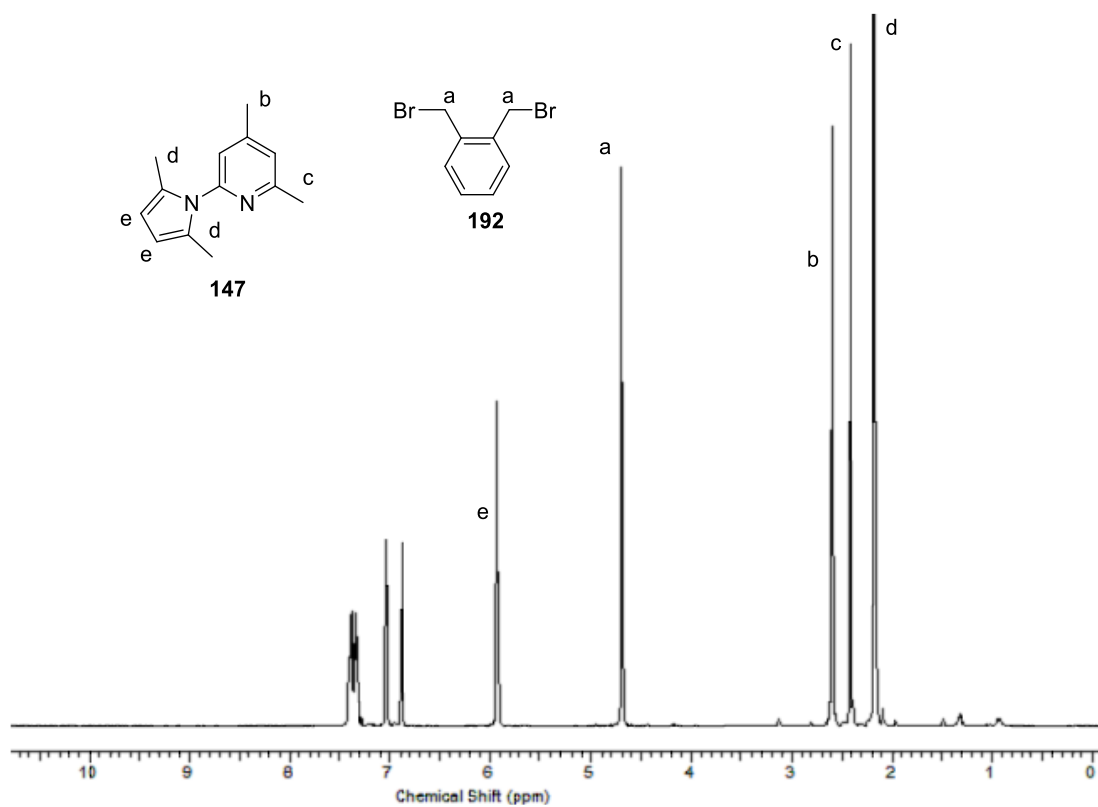
Figure 70: ¹H NMR spectrum of reaction shown in scheme 8, which appears to show a mixture of starting materials **147** and **192**.
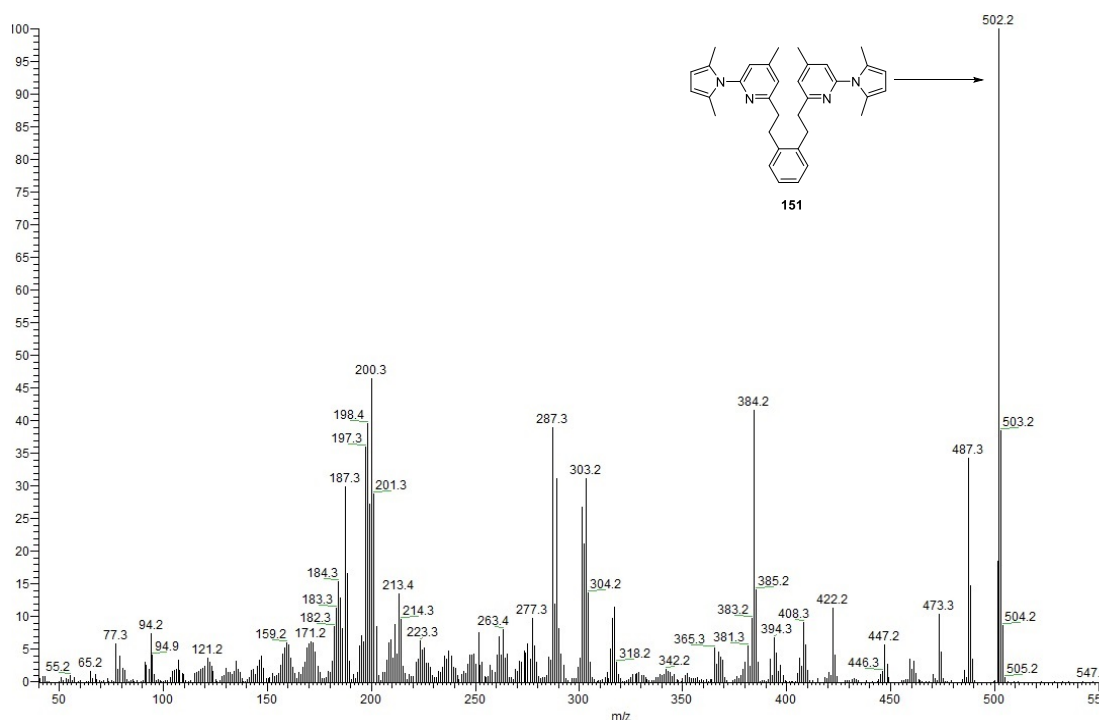
Figure 71: Low resolution mass spectrum of compound **151**, confirming the successful synthesis of the desired product.

Table 3 is a summary of the different bases, solvents and number of equivalents used in the attempt to make the protected nNOS inhibitors **149-151**. Out of the reactions that were attempted, three were successful in producing the desired products, however in either a very low yield or an unattainable one post column chromatography. Changing the base used from *n*-BuLi to phenyl lithium appeared to solve the initial deprotonation problems but failed to give a reproducible yield.

Base	Number of equivalents	Solvent	Starting Material	Successful Reaction?
n- BuLi	2.5	THF	**147**	NO
n- BuLi	5	THF	**147**	NO
n-BuLi	1.1	Diethyl Ether	**191**	NO
n-BuLi and TMEDA	1.1	Diethyl Ether	**191**	NO
Phenyl Li**	1.1	Diethyl Ether	**191**	Yes, 4%
Phenyl Li**	1.1	THF	**191**	Yes, 2%
Phenyl Li	1.1	Diethyl Ether	**147**	Yes N/A

Table 3: Summary table, showing the different bases and solvents used in the attempt to isolate desired products. ** Reactions were done at -78°C for 1.5 hours before reflux at 40°C for 4 hours.

The objective for this section of research was to synthetically produce a series of nNOS inhibitors based on the amino-pyridine ring and to expand on the work by Silverman after key interactions were highlighted in his lead compounds structure that remained unexploited. The first stage of pyrrole protecting the free amine functional group on the starting material was successful producing 30% of the product. The next step of deprotonating the *ortho* position on the pyridine ring proved to be a bigger challenge than first thought. After several reactions and adjustment of conditions (table 3), successful deprotonation occurred, however only for the model reaction. The removal of a hydrogen atom from the methyl group appears to need a strong base and the addition of a stoichiometric amount of water to quench the reaction. Although phenyl lithium is a weaker base than *n*-BuLi, it successfully deprotonated 2,4,6-trimethylpyridine **191**, where *n*-BuLi failed to do so. Comparing the pK_a values of the two bases (43 and 50 respectively) the successful deprotonation with phenyl lithium appears to go against what is expected. This may be due to the degree of aggregation seen with organolithium reagents. As aforementioned, *n*-BuLi can form hexamers in solution whereas phenyl lithium is prone to form dimers[11, 14]. This may mean that the lithium counter ion is more available to coordinate with the nitrogen lone pair of the pyridine and initiate the deprotonation.

In contrast to Silverman's observations, the use of diethyl ether as solvent saw deprotonation at the *ortho* position preferential to the *para* position. Although deprotonation was made possible with the use of phenyl lithium, a much stronger alternative may be needed to afford a higher yield of the desired compounds. A variant of a Schlosser's base or another suitable 'superbase' may be required to produce a more workable yield for the deprotonation step in this synthesis. The rationale of optimising the hydrogen bond interaction with the propionic acid group within the haem group of nNOS is still a good one, and now that successful deprotonation has occurred, with optimisation compounds **149-151** can by synthesised and eventually tested for their inhibitory potential.

2.1.3.1- References

1. H. Matter, P. Kotsonis, O. Klingler, H. Strobel, L. G. Frohlch, A. Frey, W. Pfleiderer and H. H. H. W. Schmidt, *J. Med. Chem.*, 2002, 2923-2941

2. J. Vitecek, A. Lojeck, G. Valacchi and L. Kubala, *Mediators of Inflammation Review*, 2012, 1-22

3. F. Xue, J. Fang, S. L. Delker, H. Li, P. Martasek, L. J Roman, T. L. Polous and R. B. Silverman, *J. Med. Chem.*, 2011, **54**, 2039-2048

4. V. Amarnath, D. C. Anthony, K. Amarnath, W. M. Valentine, L. A. Wetterau and D. G. Graham, *J. Org. Chem*, 1991, **56**, 6924-6931

5. L. Knorr, *Chem. Ber.*, 1884, **17**, 2, 2863-2870

6. C. Paal, *Chem. Ber.*, 1884, **17**, 2, 2756-2767

7. Q. Jing, H. Li, J. Fang, L. J. Roman, P. Martasek, T. L. Poulos, and R. B. Silverman, *Bioorg. Med. Chem.*, 2013, **21**, 5323-5331

8. H. Huang, H. Li, P. Martasek, L. J. Roman, T. L. Poulous and R. B. Silverman, *J. Med. Chem.*, 2013, **56**, 3024-3032

9. F. Xue, J. Fang, S. L. Delker, H. Li, P. Martasek, L. J Roman, T. L. Polous and R. B. Silverman, *J. Med. Chem.*, 2011, **54**, 2039-2048

10. V. H. Gessner, C. Daschlein, and C. Strohmann, *J. Chem. Eur.* 2009, **15**, 3332-3334

11. M. Schlosser, L. S. Hegedue, B. H. Lipshutz, J. A. Marshall, E. Nakamura, E. Negishi, M. T. Reetz, M. F. Semmelhack, K. Smith and H. Yamamoto, *Organometallics in Synthesis: A Manual*, 2004, John Wiley and Sons Ltd

12. M. A. Nichols and P. G. Williard, *J. Am. Chem. Soc.* 1993, **115**, 1568

13. H. L Lewis and T. L. Brown, *J. Am. Chem. Soc.*, 1970, **92**, 4664

14. T. Kottke and D. Stalke, *Angew. Chem. Int. Ed. Engl.*, 1993, **32**, 580-582

15. E. W. Abel, F. G. A. Stone and G. Wilkinson, *Comprehensive Organometallic Chemistry Two*, 1995, Elsevier

16. S. T. Chadwick, A. Ramirez, L. Gupta and D. B. Cikkum, *J. Am. Chem. Soc.*, **207**, 129, 2259-2268

17. C. Osuch and R. Levine, *J. Org. Chem.*, 1956, 1723-1725

18. R. B. Silverman and Q. Jing, Personal communication, 23.02.2015

2.2- NO release methodology and results

As nitric oxide has an extremely short half-life (approximately 5 seconds in solution[1]) measurement of any donated NO needs to occur either *in situ* or as direct reaction of NO with something that is more stable and therefore quantifiable. Ozone based chemiluminescence (Fig. 73) was the method used to test if the synthesised compounds (described in section 2.1.1 and 2.1.2) were capable of releasing NO and in addition identify the experimental conditions by which release could be best supported.

In the presence of ozone, nitric oxide produces nitrogen dioxide in an excited state, NO_2*. Upon relaxation of this excited species back towards its ground state, a photon is emitted and amplified by a photo-multiplier tube (PMT) which produces a readable signal. Typically this signal is measured in millivolts and the relative information is obtained through manipulation of the area under the curve (AUC), although it has been quoted that 1mV is approximately equal to a 1nM concentration of NO.[2]

$$\dot{N}O + O_3 \longrightarrow NO_2^* + O_2$$

PMT

Analyser

NO_2

Key

∿∿∿ = photon

PMT = photo multiplier tube
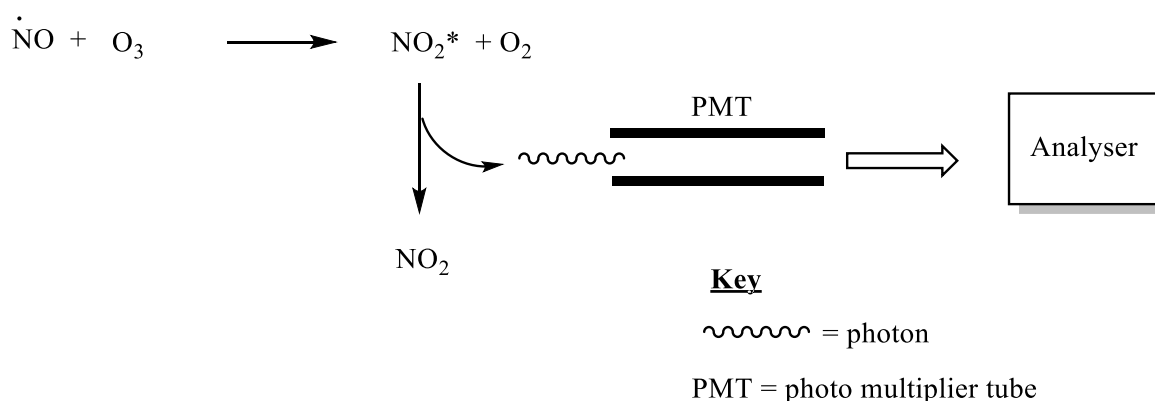
Figure 72: Basic schematic showing how NO measurement is possible using ozone chemiluminescence.

Due to the reactive nature of nitric oxide, side reactions can readily occur producing nitrite (NO_2) or nitrate (NO_3^-) products which would alter the total reading of nitric oxide being produced as it is NO's reaction with ozone which creates the readable signal. To account for any side reactions, and to make sure all NO produced by the compounds being tested was being recorded, we needed a way

to convert the nitrite and nitrate back into 'free' measureable NO. The oxidation of nitrite using acidified potassium tri-iodide solution was utilised to convert any nitrite formed in the chamber back into NO (as shown in scheme 60).

$$I_3^- \longrightarrow I_2 + I^- \quad (1)$$

$$KI \longrightarrow K^+ I^- \quad (2)$$

$$2NO_2^- + 2I^- + 4H^+ \longrightarrow 2NO + I_2 + 2H_2O \quad (3)$$
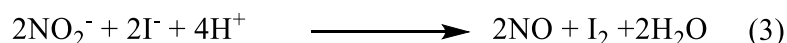
Scheme 60: Reactions required for measurement of NO levels from nitrite (NO_2^-) ions.[2]

Potassium tri-iodide disassociates in solution to form iodine and free iodide ions as shown by equation 1 (scheme 60). These iodide ions can then oxidise any nitrite (NO_2^-) ions present back into nitric oxide which can then go on to react with ozone and produce a measureable photon as already shown in Fig. 73. This redox reaction works best at 40°C and can be used to convert other NO metabolites produced, such as RSNOs.[2]

Nitrate ions (NO_3^-) can also be converted back into NO following a redox reaction using acidic vanadium trichloride (VCl_3 in 1M HCl) but a much higher temperature, 95°C, is needed for this oxidation to take place (scheme 61). Nitrate ions react with free V^{3+} ions in solution to form a stoichiometric amount of nitric oxide and vanadium oxide.

$$2NO_3^- + 3V^{3+} + 2H_2O \xrightarrow{95°C} 2NO + 3VO_2 + 4H^+$$
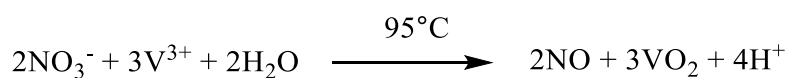
Scheme 61: Reaction of nitrate (NO_3^-) ions with vanadium (III) chloride for the measurement of NO. [2]

The main problem with measuring nitrate levels with this nitric oxide analyser (NOA) apparatus is the risk of contamination. When measuring low levels of nitrate, anything over a concentration of 1μM can be considered a contamination and will affect the baseline and interpretation of results. The main source of contamination is the water used to produce standard samples. During the initial experiments it was found that the water source had a high concentration of nitrate present and therefore any measurement of nitrate from our samples was impossible.
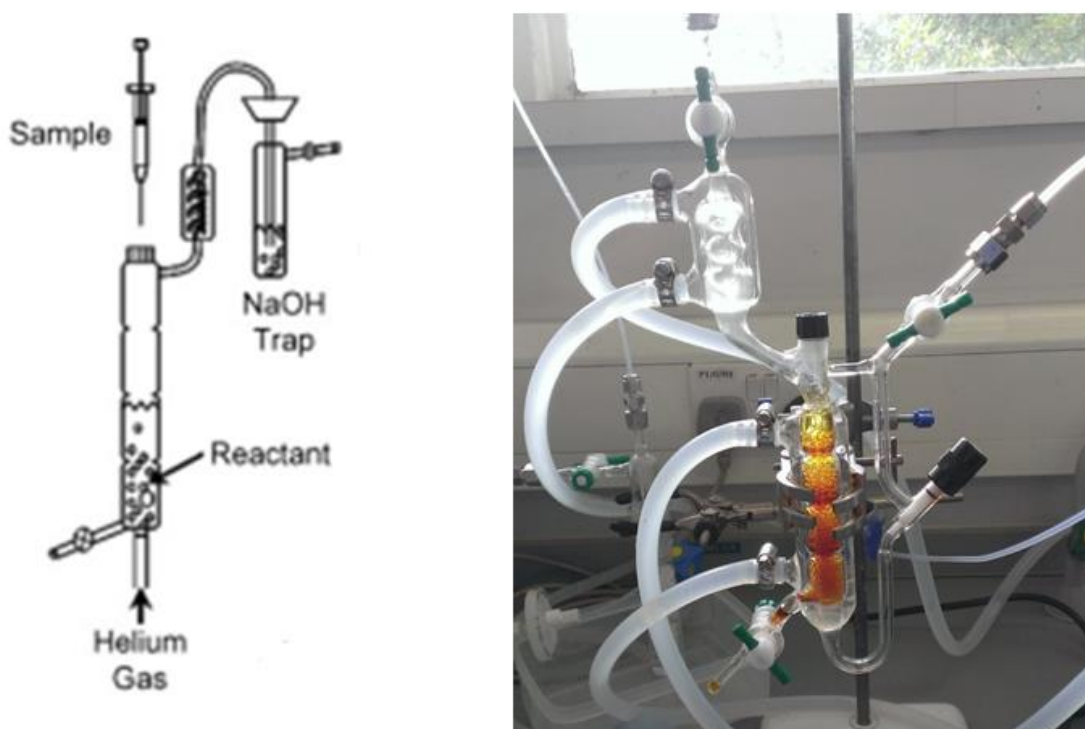
Figure 73: Schematic drawing[2] of the reaction chamber alongside a photo of the actual apparatus.

To determine the concentration of nitric oxide released from our compounds, a calibration curve was needed.[2] This was created by injecting known quantities (100 μL) of varying concentrations of sodium nitrite into the reaction chamber (Fig. 73) which contained a reservoir of tri-iodide solution. This data was then plotted to generate a standard straight line graph as shown by graph 2. The area under each NO peak is typically measured as it provides the total NO release/detected rather than a time course for NO release which can be affected by other factors.[3] Fig. 73 shows the experimental

set up for analysing nitric oxide levels, the reaction chamber is surrounded by a water jacket to maintain a constant temperature within the cell. Pure inert gas such as helium or nitrogen gas flows continuously throughout the apparatus to ensure any NO generated goes to the detector as well as providing an inert environment to limit the amount of oxidative reactions that can occur. Analytes, once produced are forced through a glass chamber containing sodium hydroxide solution, this ensures that none of the reaction medium travels through to the detector and etches the sensitive photo-multiplier tube (PMT).

Calibration Curve for NO release derived from NaNO$_2$

$y = 6E+08x + 58.307$
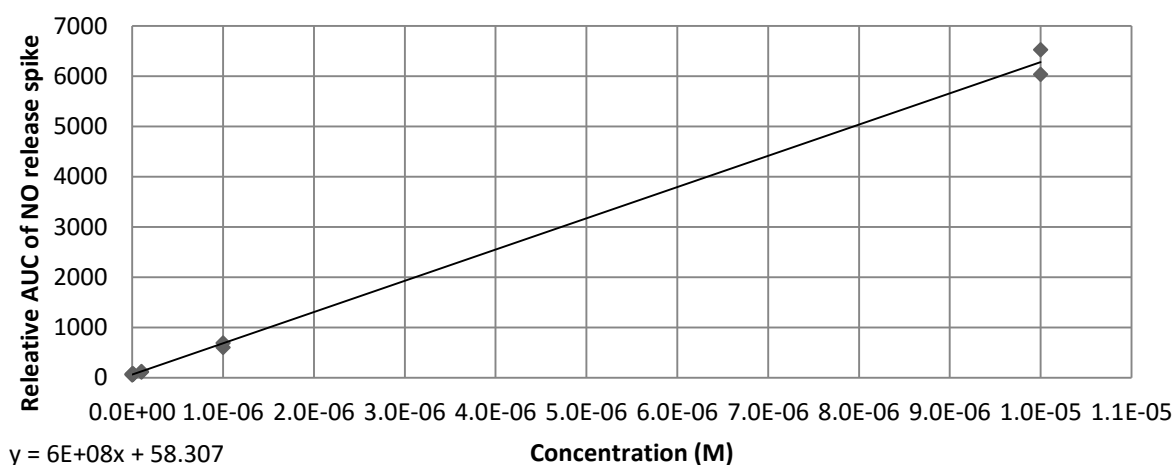
Graph 2: Calibration curve for NO release. Obtained by injecting known quantities (100 μL) of varying concentrations (six in total) of sodium nitrite solutions.

Using the formula generated from the calibration curve, this indicates that if the NO release from a compound produces an area under the curve (AUC) of 3500 it would correspond to 5.73 μM of nitric oxide being released. The parameters generated from this calibration graph were used for all the concentration calculations relating to this NO release work.

2.2.1- NO release from a known NO-donor

After successfully producing a calibration curve (graph 2) using sodium nitrite, it was decided that the capabilities of the NOA should first be tested using a compound know to release 'pure NO' rather than being converted from nitrite to NO. To do this, a known NO-donor was chosen so that any observations seen could be compared to what is found within the literature.

SNAG **19,** an *S*-nitrosothiol, is known to decompose to release nitric oxide under three main conditions as already mentioned in chapter one. Both light and temperature can bring about the evolution of NO from SNAG, but in the presence of copper this effect is reported to be accelerated.[4-8].
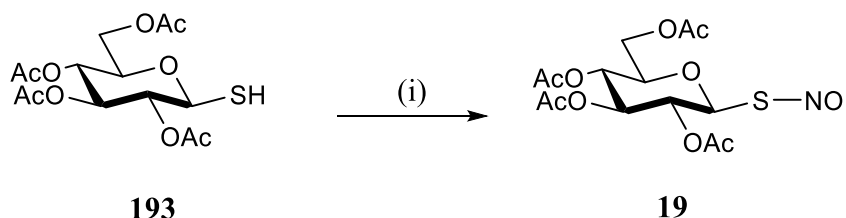
Reagents and conditions: (i) N_2O_4, EtOH, 5 minutes, $N_{2(g)}$, in dark

Scheme 62: Reaction of Pre-SNAG **193** with nitrite fumes to produce SNAG **19**.

SNAG, **19**, was synthesised[5] by nitrosating 1-thio-2,3,4,6-tetra-*O*-acetyl-β-D-glucopyranose, **193**, with a continuous stream of N_2O_4 fumes. These fumes were generated *in situ* from the action of concentrated hydrochloric acid on ground sodium nitrite of high purity. The volume of ethanol in the final solution was corrected back to 5ml to account for any evaporation during the reaction since the thiol containing vessel was flushed with nitrogen for 3 minutes once the nitrosation was complete. This was done to remove any excess fumes and any nitrosated ethanol produced in the reaction. SNAG, **19**, was used directly from the EtOH solution, which was a bright orange solution, without any further purification. The crude experimental set up for this reaction is shown in Fig. 74.
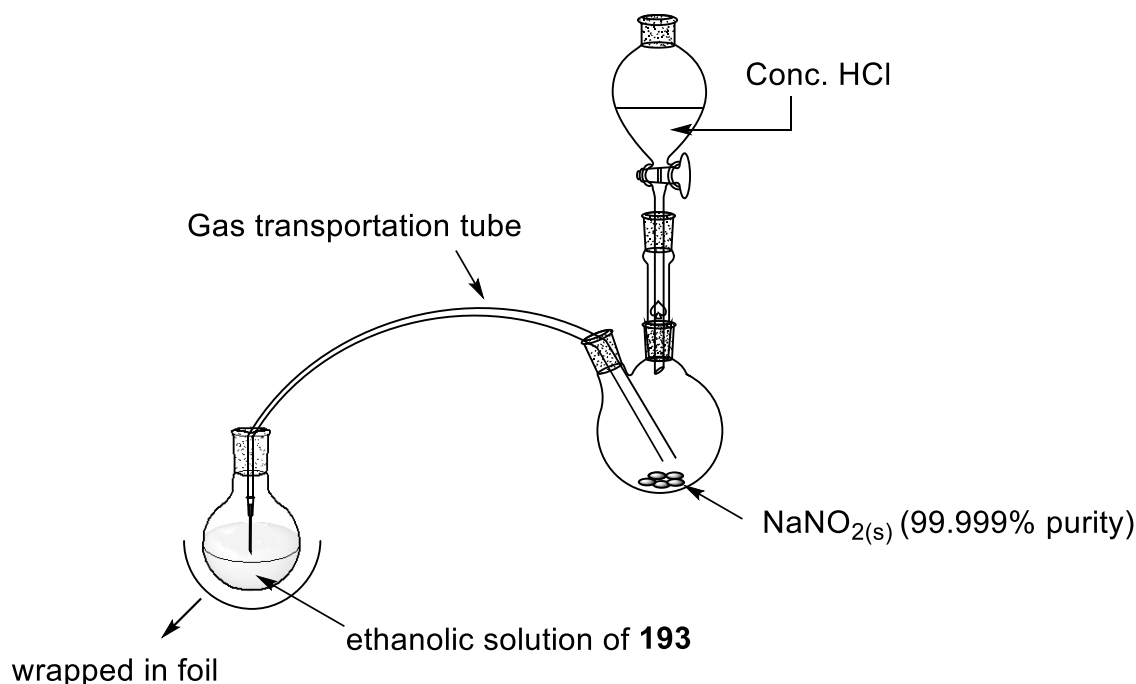
Figure 74: The reaction set up for the nitrosation of SNAG **19**.

The NOA reaction chamber shown in Fig. 73 was incubated at 37°C before a 10μM solution of SNAG **19** was injected and monitored for NO release over 1 minute. Initial screening showed that all measureable NO was released within 1 minute and hence this time frame was used for the collection of data. The same initial set up was used for the photochemical test however, before and during addition of the 10 μM solution of SNAG, **19**, the reaction chamber was irradiated with 254 nm of light within a foil casing.

The copper catalysed reaction was observed at 37°C but SNAG **19** was injected into the reaction chamber containing a reservoir of copper sulphate ($CuSO_4$). A concentration of 2 μM of $CuSO_4$ was used, to ensure that the copper was in an excess and that any results observed were due to the catalytic effects of copper and not any other effect. The results from each NO release study are shown in graph 3.

NO release from SNAG ,19, at 37°C under different conditons
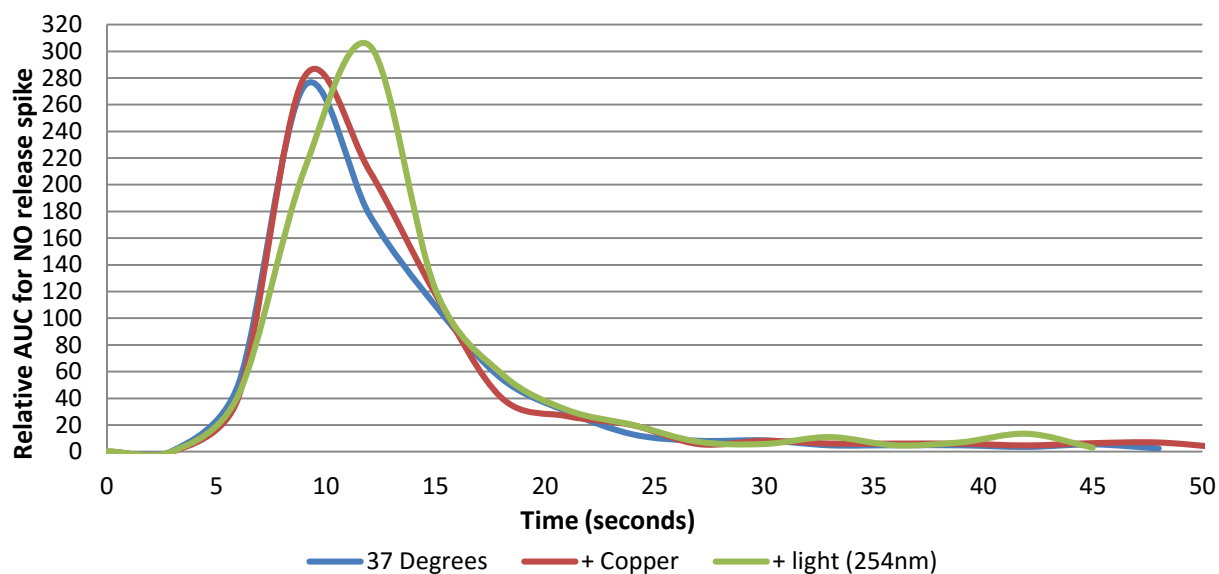
Graph 3: NO release from SNAG **19** under different conditions analysed for 60 seconds.

In a consistent fashion with what is reported in the literature[4-6] the copper catalysed reaction does produce the fastest release of NO with the majority being produced in the first 10 seconds. With the chamber incubated at 37°C SNAG **19**, also produced the majority of NO before 10 seconds but failed to produce as much in terms of arbitrary units (AUC). Under photochemical conditions, after irradiation with 254 nm light, SNAG **19** produced the most NO but taking a slightly longer time to do so, around 12 seconds. This is perhaps due to the induction of radicals upon decomposition with light.[9] Under photolysis conditions, homolytic cleavage occurs producing the NO radical and a sulphide radical which then rapidly forms the corresponding disulphide, although this should be a rapid process it may explain why more NO is measured under photochemical conditions as formation of the disulphide is energetically favourable due to the strength of the S-S bond.[10] With the NOA able to detect the levels of 'pure' NO released from SNAG **19**, attention was turned to monitoring the NO release of the novel NO-donors

The combretafuroxan compounds (**86-95, 126/128**) and the cupferron compounds (**96-105**) have very different mechanisms of release and therefore required different approaches to experimentally obtain NO release data. Each set of compounds were analysed in a different way and the methodology and

results will be outlined in this section. However within each compound set the conditions of the experiments were kept absolutely constant to allow for direct comparisons in NO release behaviour to be observed.

2.2.2- NO release from cupferron compounds

Cupferron compounds **98**-**105** in addition to the furoxan compounds mentioned earlier were analysed for their NO releasing capabilities using photochemical decomposition, to test the claims for NO release as described in the literature[1]. The reaction chamber was irradiated with UV light (experimental setup is shown in Fig. 75) at a wave length of 254 nm, to this chamber 3 mL of 7 mM cupferron compound (dissolved in diethyl ether) were injected and a NO signal was seen almost instantly.

The parent compound, cupferron **56**, when tested under these conditions rapidly produced NO to a scale the instrument could not interpret suggesting just how unstable cupferron is as a NO-donor. Because of this unquantifiable result the photochemical release of compounds **98**-**105** could not be compared directly to the parent compound.
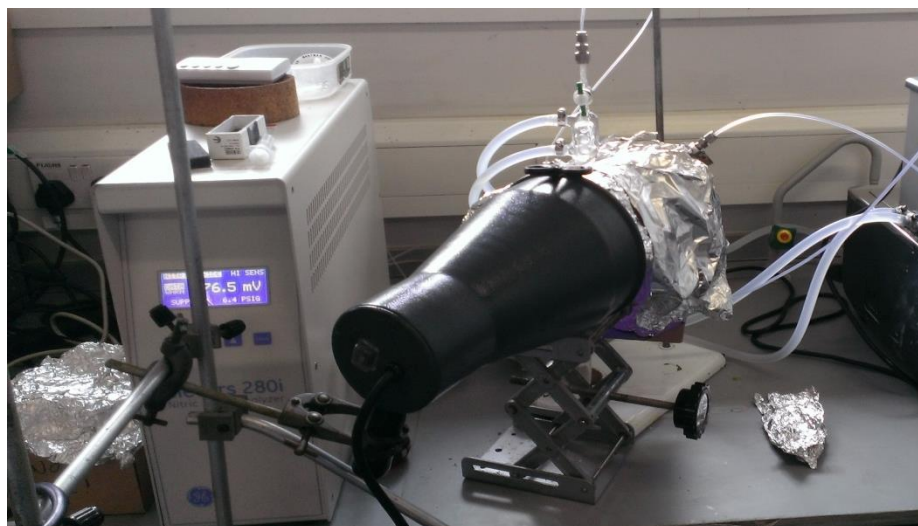
Figure 75: Picture of the experimental set-up for photochemical release studies using the nitric oxide analyser (NOA) on the cupferron series of compounds.

Cupferron derivatives were monitored for their NO releasing capabilities over 15 minutes. Mono alkylated cupferron compounds **98-101** varied in their ability to release NO when exposed to a wavelength of 254nm. Each compound tested had heightened stability in comparison to cupferron with all compounds releasing the majority of NO in the first three minutes and gradually reducing the amount of NO production over the next 12 minutes. The most stable compound was found to be the mono butyl derivative **99** producing 16 times less nitric oxide than the mono hexyl derivative **100**. Mono hexyl cupferron **100** also managed to produce 11 times more NO than the mono ethyl derivative **98**. This can be seen in graph 4. Similarly to cupferron, compound **101** alkylated with an octyl chain, produced unquantifiably high levels of NO and were unmeasurable under the experimental conditions used. It may be said that alkylation with an eight carbon chain length on the terminal oxygen of cupferron decreases its stability, however this may have also decreased its solubility and therefore measurement of NO release. Comparatively two, four and six carbon alkylations greatly increase the stability of cupferron and its release of NO under photochemical conditions.

NO release of mono alkylated cupferron compounds at 254 nm
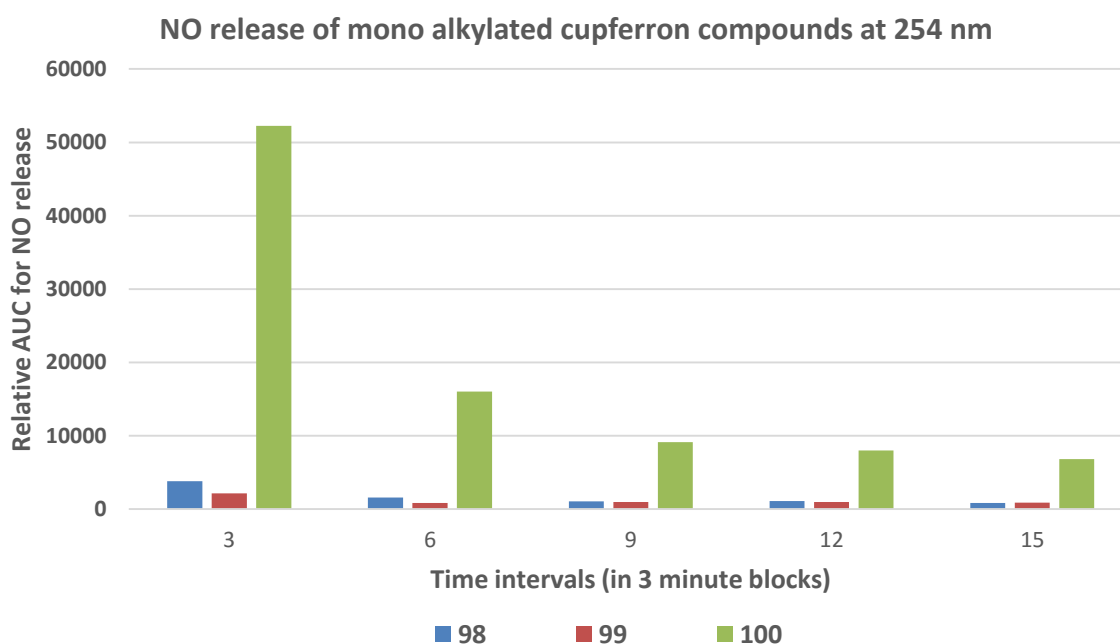
Graph 4: Analysis of NO release from compounds **98-100** over 15 minutes. Measurements were conducted using NOA in the presence of UV light (254 nm).

Under the same experimental conditions compounds **103-105**, with two cupferrons linked by a four, six or an eight carbon chain were also tested for their NO releasing capabilities in the presence of 254 nm light (graph 5). In comparison to cupferron all dicupferron compounds **103-105** were more stable than the parent compound, with the butyl linked cupferron **103** being the most stable over 15 minutes producing around eight times less NO than the hexyl linked compound **104**. Unlike its mono-substituted counterpart **101**, compound **105** with an octyl linker was successfully measurable under the reaction conditions producing slightly more NO (1.7 times more) than the butyl linked compound **103**. In comparison to the hexyl linker **104**, the eight carbon chain **105** produced 4.8 times less NO making the di hexyl **104** the least stable compound of the di-cupferron series.

NO release from allklylated di-cupferron derivatives at 254 nm
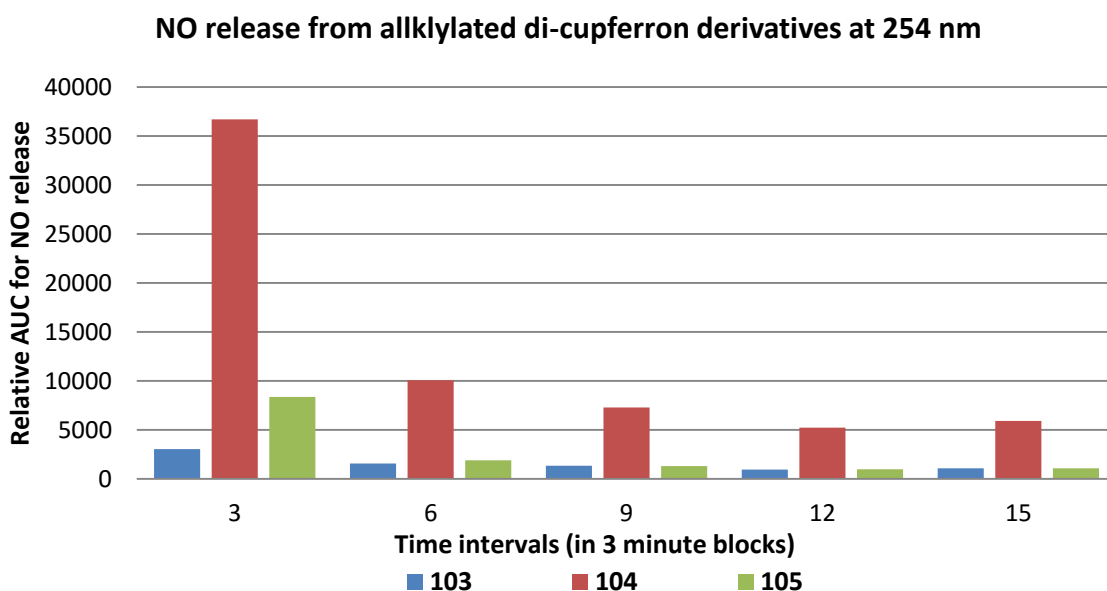
Graph 5: Analysis of NO release from compounds **103-105** over 15 minutes. Measurements were conducted using NOA in the presence of UV light (254 nm).

As the mono octyl compound **101** produced unquantifiable results we cannot compare mono and di alkylations for that chain length. However the hexyl and butyl compounds **99/100** and **103/104** all produced NO at a level that was readable on the equipment. Comparing the compounds that contain a butyl chain (**99** and **103**) length, under the same experimental conditions (graph 6) shows that the mono butyl **99** is more stable than its di cupferron counterpart **103** producing less NO over 15 minutes. The di cupferron **103** compound produces 1.4 times more nitric oxide upon exposure to UV light at 254 nm.

Comparing NO release from butyl cupferron derivatives 99 & 103 in the presence of UV light
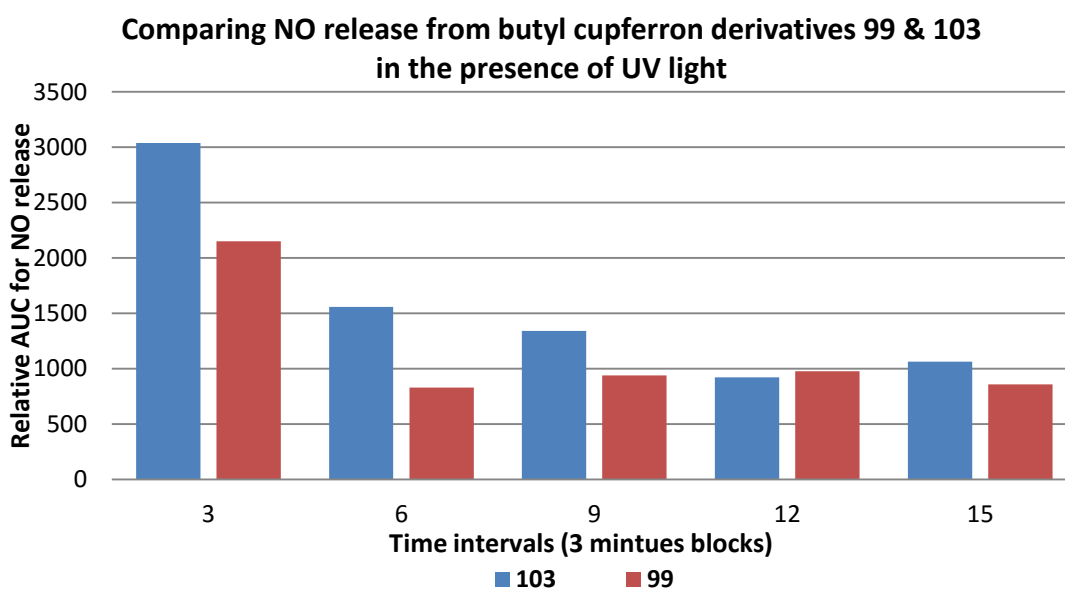
Graph 6: Comparing the NO release from compounds **99** and 103, mono and di cupferron compounds in the presence of UV light (254 nm).

Interestingly comparing the hexyl derivatives **100** and **104**, (graph 7) the opposite trend to graph 6 is seen. In this case compound **104** was more stable than its mono cupferron counterpart **100** and therefore released less NO over 15 minutes.

Comparing the NO release from hexyl cupferron derivatives 100 and 104 in the presence of UV light (254 nm)
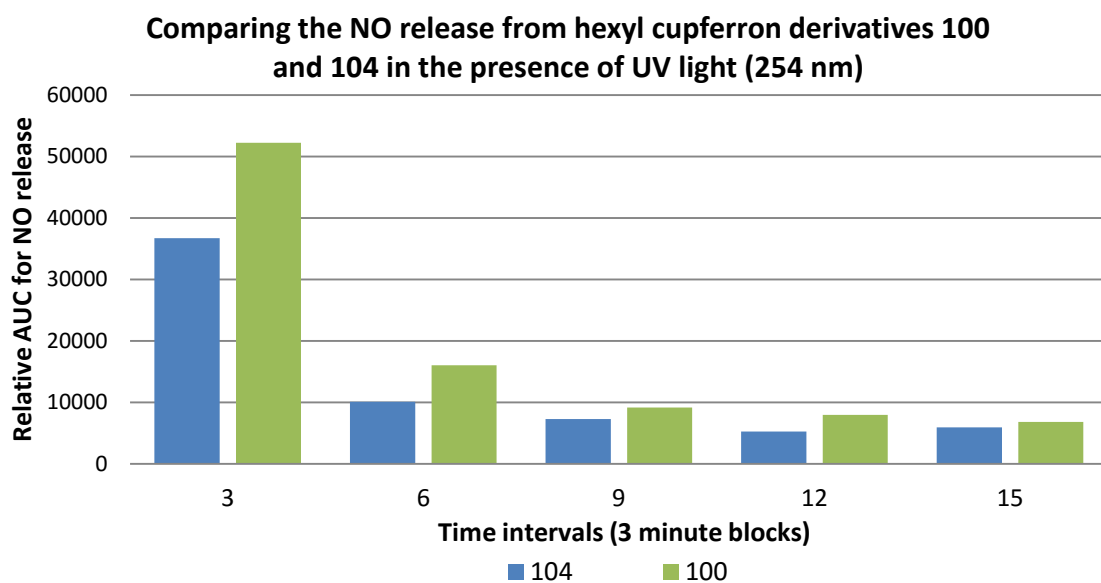
Graph 7: Comparison of compounds **100** and **104**, mono and di cupferron compounds in the presence of UV light (254 nm).

The di cupferron series **103-105** appears to have a unique mechanism of NO release, by first expelling the alkyl linker through a homolytic bond cleavage. This creates a di-radical alkyl chain, which then quickly cyclises to form a cycloalkane (scheme 63) due to it being more energetically favourable to exist as a ring structure than as the di-radical. This leaves the cupferron molecule with an *O*-radical in the terminal position. Movement of electrons causes the expulsion of NO and the formation of a nitrosobenzene molecule **195** and the nitric oxide is detected by the NOA. High resolution mass spectroscopy (HRMS) confirmed the formation of cyclohexane and cyclooctane from the di cupferron compounds **104** and **105** (full HRMS for each cycloalkane can be found in appendices AP02 and AP03 respectively). Compound **103** with the butyl linker showed no evidence of any cyclobutane product; this is possibly due to cyclobutane being a strained ring and not the most energetically favourable conformation for a butane chain. This may also explain why **103** was the

most stable compound, since the expulsion of nitric oxide may therefore be energetically less favourable.
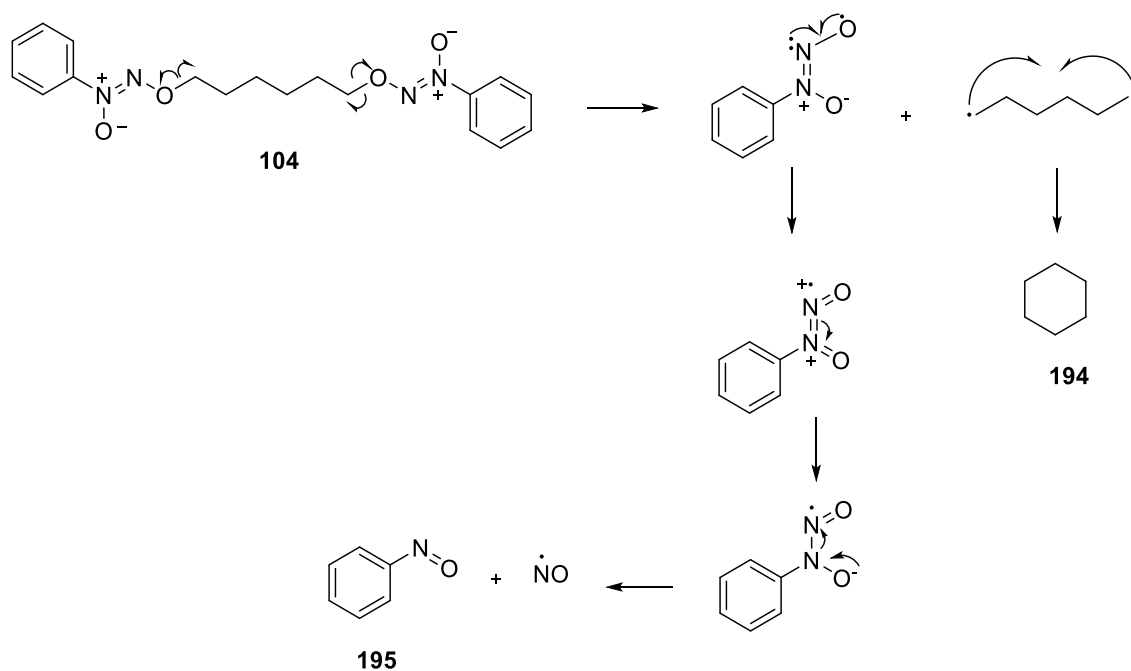
Scheme 63: Proposed mechanism of photochemical induced NO release from cupferron compounds.

Literature indicates that when cupferrons decompose under thermal or photochemical conditions that along with nitric oxide being produced, an azoxy compound (scheme 64) is also generated.[12, 13] No evidence of the azoxy compound **196** was isolated from our experiments, however this indicates a possible mechanism for NO release for the mono alkylated compounds **98-101**.
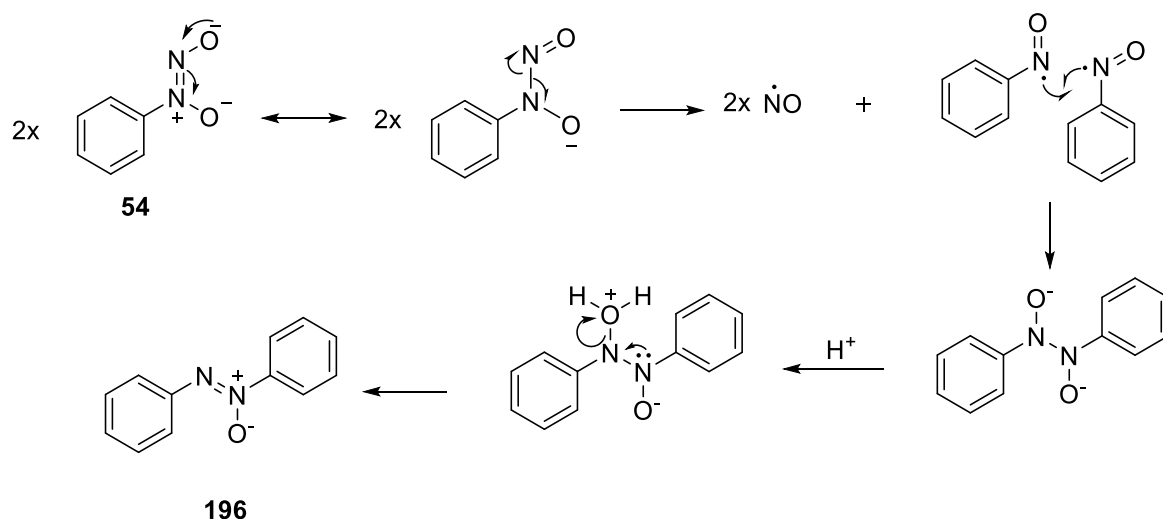
Scheme 64: Cupferron's decompostion in the presence of light can yield nitric oxide along with an azoxy compound, **201**.

The cupferron compounds were also tested for their thermal stability at 25°C and 37°C and compared to the parent compound cupferron (graph 8). Cupferron's NO release over 15 minutes was set as 100% release and each derivative was then related back to the parent compound.

%NO release compared to Cupferron
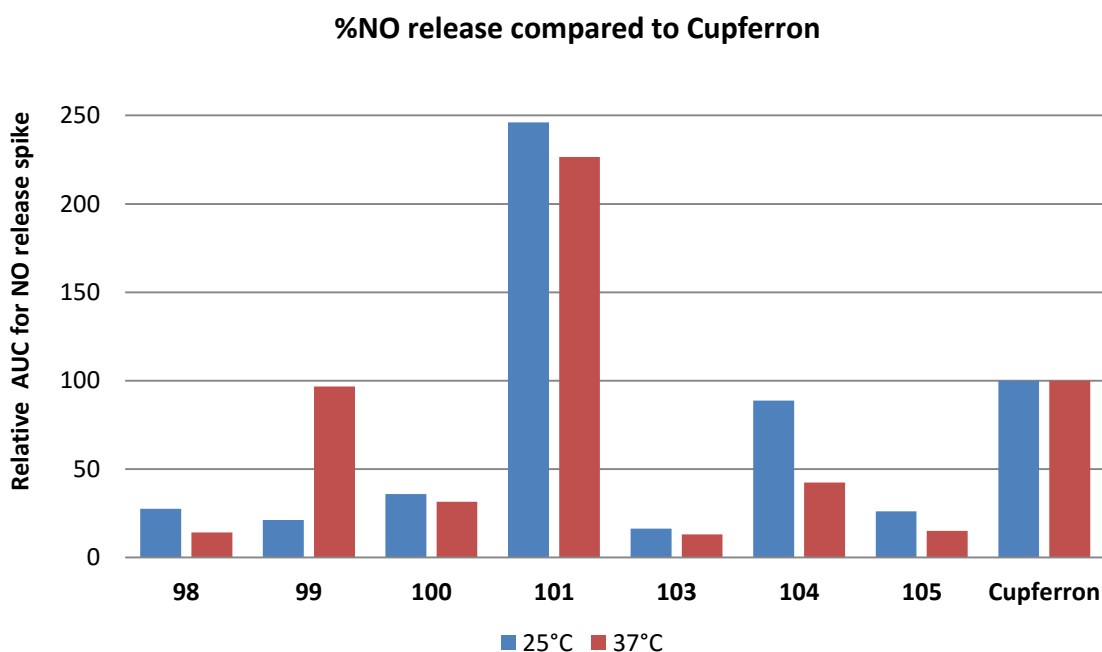
Graph 8: Comparison of cupferron derivatives **98-105** with the parent compound **54**. Compound **101** alkylated with an octyl chain produced more NO than cupferron at both 25 and 37°C.

When compared directly to cupferron both the di-cupferron and the mono-cupferron derivatives were more stable at both 25°C and 37°C with the exception of the mono-octyl compound (**101**). Mono-octyl cupferron (**101**) produced 40% more NO than cupferron at 25°C and 44% more NO at 37°C. This suggests that the mon-ooctyl compound **101** is inherently less stable than cupferron under both thermal and photochemical conditions. As you increase the chain length of the cupferron derivatives from two carbons to eight carbons the solubility will obviously change. Mono-octyl cupferron, having the longest chain and only two electrostatic atoms present (the N^+ and O^- from the diazeniundiolate) is likely to be the least soluble in an aqueous solution and as a result is not solvated to the same degree as the other compounds in the series and can therefore release more NO as shown in graph 8.

The general trend with the cupferron derivatives appears to be that as you increase the temperature from 25°C to 37°C, the compounds release less nitric oxide. The exception to the trend is compound **99**, cupferron alkylated with a butane chain, this produces an almost directly comparable amount of nitric oxide to that of cupferron.

In terms of the stability of the cupferron derivatives **98-105** shown in graph 8 a stability factor was generated by directly comparing the compounds with cupferron once cupferron was set at 100% release. This allowed the direct comparison of each compound with its un-alkylated parent compound at both 25°C and 37°C.

Compound Number	Linker chain	Stability factor in reference to cupferron at 25°C	Stability factor in reference to cupferron 37°C
98	Ethyl	4	7
99	n-Butyl	5	1
100	n-Hexyl	3	3
101	n-Octyl	0	0
103	n-Butyl (Dicupferron)	6	8
104	n-Hexyl (Dicupferron)	1	2
105	n-Octyl (Dicupferron)	4	7

Table 4: Stability of cupferron derivatives compared to cupferron at both 25°C and 37°C. Stability factors were calculated by comparing % NO release per compound to cupferron, where cupferron was set at 100% release. . **98-101** are mono alkylated cupferron and **103-105** are dicupferron derivatives.

The most stable compound at 25°C was compound **103**, with a stability factor of 6. This means that in comparison to cupferron, compound **103** (dicupferron bridged by a butyl chain) is 6 times more stable releasing 84% less NO over 15 minutes compared to cupferron. The least stable compound at 25°C was found to be compound **104** which had a stability of 1, meaning that it is as stable as the parent compound producing just 12% less NO than cupferron. At 37°C, representative of body temperature, compound **103** was again the most stable compound with a stability factor of 8. This means that **103** is 8 times more stable than the parent compound at 37°C, releasing 87% less NO over 15 minutes. Interestingly at 37°C the mono ethyl cupferron **98** and the di-octyl compound **105** had a comparable stability to that of **103** with a stability factor of 7 each releasing 86% and 85% less NO respectively over 15 minutes than the parent compound **54**. A general trend that can be obtained from this NO release work is that as the alkyl chain increases by 2 carbons both mono alkylated and dicupferron compounds become more thermally stable with increasing temperature from 25°C to 37°C. The exception to this rule appears to be the monobutyl cupferron **99** which released comparable levels of NO to the parent compound cupferron at 37°C.

Cupferron derivatives **98**-**105** are capable of releasing NO in the presence of both light and heat (37°C) with varying levels of stability. SNAG **19**, the known NO-donor mentioned previously in chapter 2.2.1 was also capable of releasing nitric oxide under these conditions and therefore can be compared to the cupferron compounds **98**-**105**. In terms of NO released per millimole (mM) of compound, cupferron derivatives produce significantly more NO under both photochemical (254 nm light) and thermal (37°C) conditions. This suggests that in terms of NO donor capabilities that cupferron derivatives **98**-**105** are considerably better at releasing NO compared to SNAG **19** with compounds **99** and **101** producing 36 and 85 times more NO per mM of compound respectively. This data can found in appendix AP04.

2.2.3-NO release from combretafuroxan compounds

As aforementioned (chapter 1.1.3) furoxan compounds can release nitric oxide in a variety of ways including thermally, photochemically or by oxidation. Initial tests on compounds **86**-**128** found they were all thermally stable at 37°C. This led to oxidative and photochemical release being explored.

Furoxan compounds **86**-**128** were analysed for their NO release under photochemical conditions, irradiating the reaction chamber (shown in Fig. 73 and 75) with light at a wavelength of 254 nm. To this chamber, 1 mM solutions of furoxan were injected and their relative NO release analysed using the nitric oxide analyser (NOA). Each furoxan compound successfully released NO in the presence of ultra-violet light confirming reports in the literature that describe this type of release.[14, 15] Graph 9 shows the relative release of NO per furoxan compound in terms of the area under the curve (AUC) for the NO spike that was obtained following the injection of the furoxan derivative into the reaction chamber.

Photochemical release of furoxan compounds at 254 nm
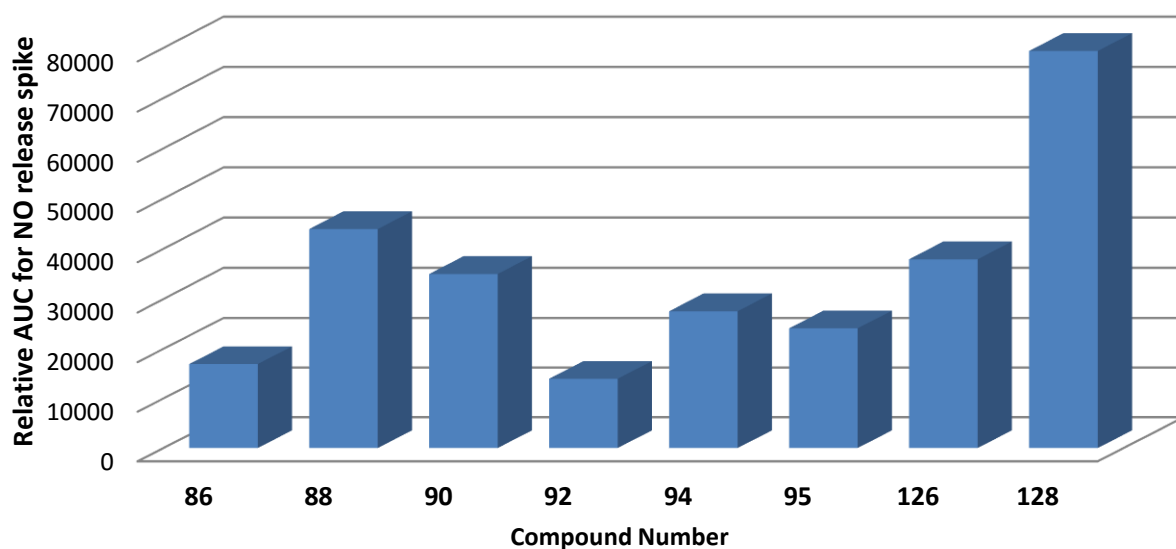
Compound Number:
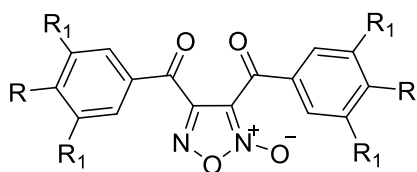
R₁= OMe R=Ome **86**
R₁ = H   R= Me   **88**
R₁=H   R= Br   **90**
R₁= H   R= OMe **92**
R₁=H   R= OCF₃ **94**
R₁= H   R= CF₃   **95**
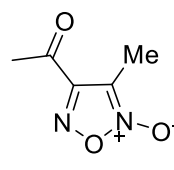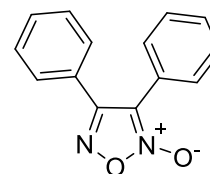
Graph 9: Photochemical release of NO from furoxan compounds **86**, **88**, **90**, **92**, **94**, **95**, **126** and **128** at 254 nm.

Graph 9 shows that each furoxan compound tested, released nitric oxide at 254 nm to some degree. Compound **128** produced by far the most nitric oxide with around 5 times more NO released than compound **92** which was the *para* substituted methoxy derivative. A general trend appears to be that an electron donating substituent provides a stabilising effect towards NO release compared to those compounds **94** and **95** with an electron withdrawing functionality such as the trifluromethyl (CF_3) or trifluromethoxy (OCF_3) group.

Mechanistically it has been stated[16] that aryl substituted furoxan compounds decompose in the presence of light to yield nitric oxide and a corresponding alkyne compound, however these alkynes are rarely isolated due to their rapid decomposition under the reaction conditions. Auricchio[16] and researchers managed to 'trap' the forming alkyne **197** compound using a 2+2 cycloaddition with various alkenes to generate the phenanthrene type structure **198**, as shown in scheme 65.
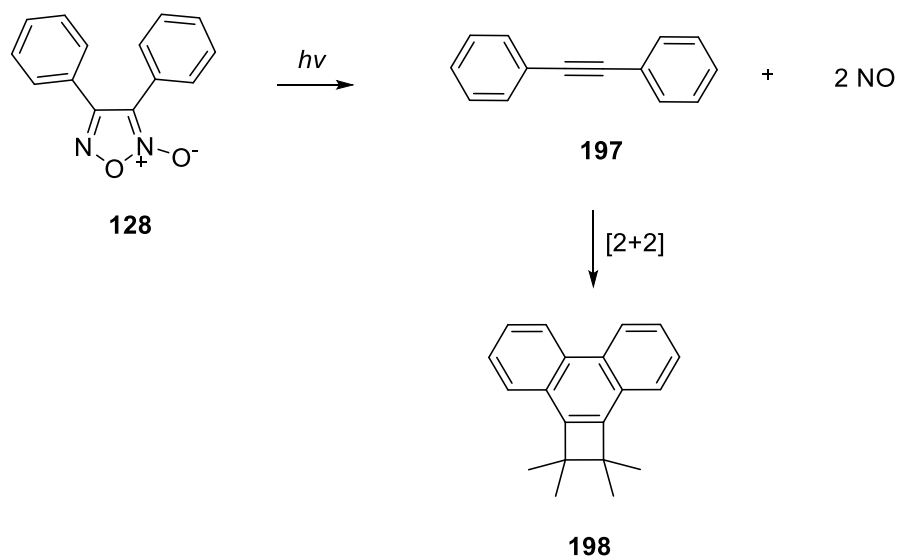
Scheme 65: Photochemical release of NO from furoxan compounds can yield an alkyne. Auricchio[16] isolated these by trapping the alkyne with a [2+2] cycloaddition.

The authors found that furoxans substituted with two phenyl rings produced the largest proportion of corresponding alkyne, this correlates with the results from graph 9 as compound **128** released the most NO and therefore would have produced the corresponding alkyne. Interestingly evidence of the alkyne formation, and production of 1,2-diphenylethyne was found in the sample of **128** that HRMS was performed on (shown in Fig.76). This suggests that ambient light conditions (such as those seen during sample preparation for HRMS) are enough to induce the release of nitric oxide for the furoxan compounds.
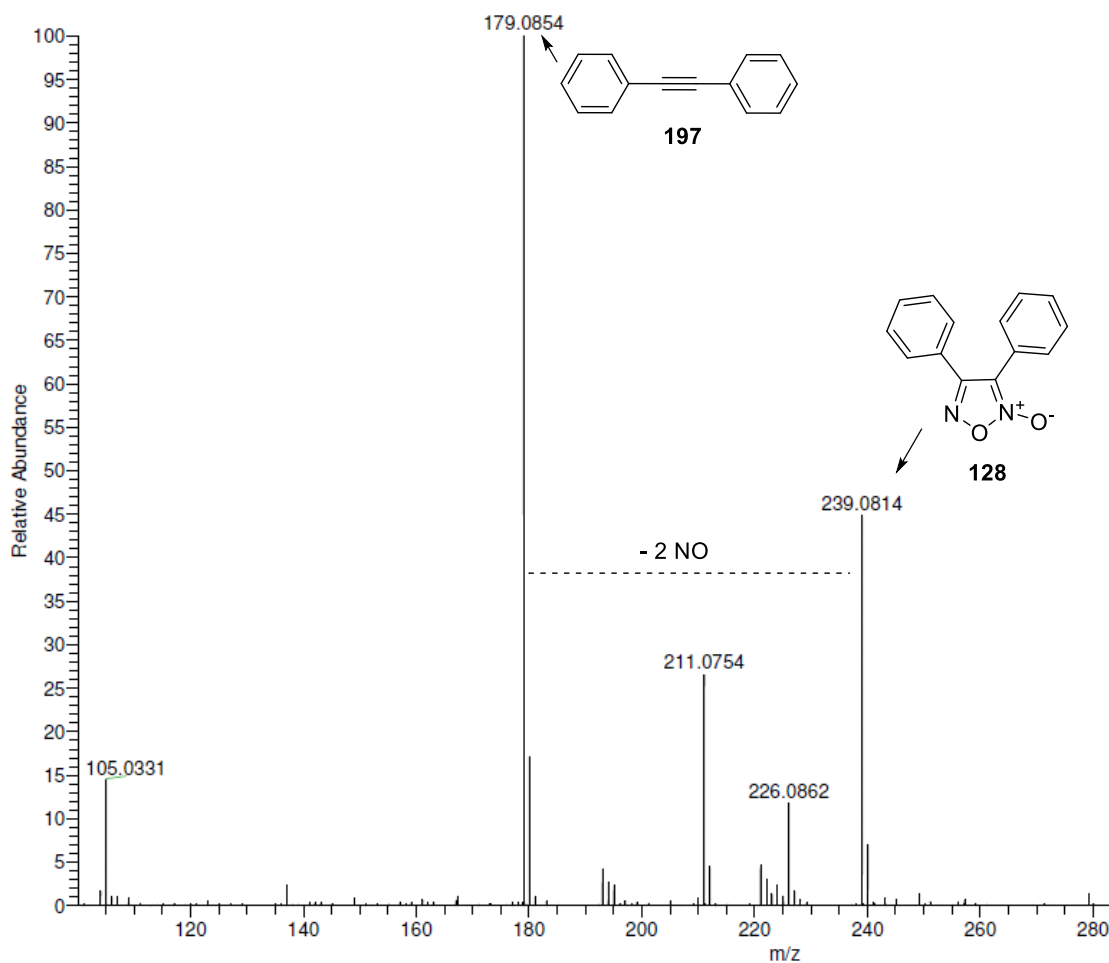
Figure 76: HRMS data for compound **128**, showing the isolation of 1,2-diphenylethyne and thus confirming the mechanism of NO release.

As seen by Auricchio,[16] no other alkyne compounds (such as that of **199** shown in scheme 66) were isolated, suggesting their rapid decomposition upon formation or an alternative mechanism of NO release.
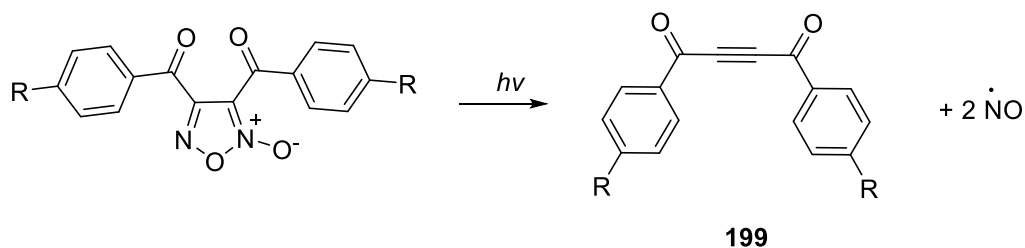
Scheme 66: Acetophenone produced furoxan compounds, when exposed to light would release NO to yield a diketo-alkyne type compound **195**. These compounds could not be isolated from the reaction chamber of the NOA.

With confirmation that the combretafuroxan series of compounds (**86-128**) were capable of releasing nitric oxide under photochemical conditions, it was sought to see if they were also capable of releasing nitric oxide under oxidative conditions as often seen in the literature. [15,17-21] Initial experiments involved the oxidative release of NO in the presence of different concentrations of thiolate in the form of potassium thioacetate. Ratios ranging from 0.5- 4 and an excess of thiol with respect to furoxan compound were tested with varying results. It was found that it took an excess, 10:1 ratio of thiolate:furoxan, to promote release of NO from the furoxan compounds. As aforementioned (scheme 60) an acidified tri-iodide solution was used to obtain nitric oxide from nitrite, however it also appeared to cause NO to be released from the furoxan compounds directly. Due to the oxidative nature of triiodide, it was theorised that I_3^- was decomposing the furoxan compounds and producing a NO signal, without providing information on the relative NO release from that compound in the presence of thiolate. The initial injection of furoxan compounds into the reaction chamber containing an acidic tri-iodide solution at 40°C gave an intense peak, however the volume of NO released using the tri-iodide method cannot be quantified as this is due to the decomposition of the entire furoxan ring and is not indicative of their relative NO release. To produce accurate results that would provide information on each compounds relative NO release potential, experimental procedures were altered to account for this observation. Furoxans were instead injected (shown schematically in Fig.77) into a solution of excess potassium thioacetate which produced an initial signal, then acidified triiodide solution was introduced into the reaction chamber to convert any nitrite by-product that formed back into NO for detection. A combination of these two peaks would then equate to the total NO release for that compound.
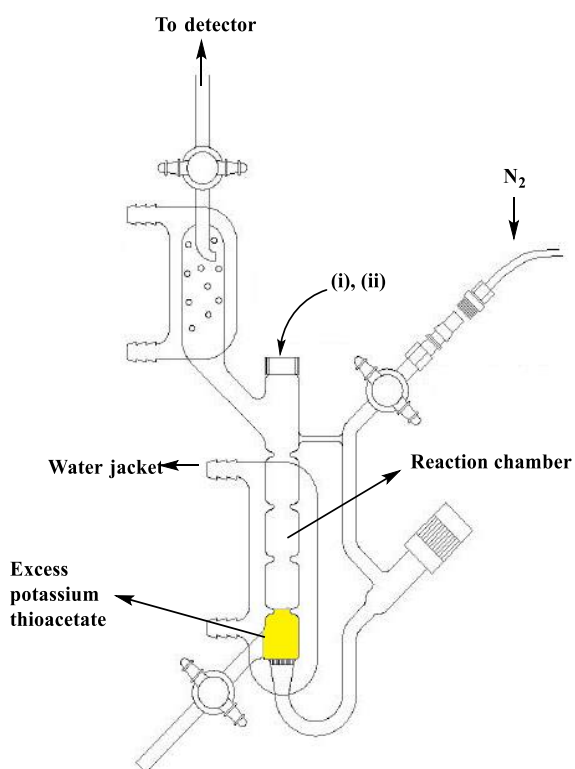
(i) 100 μL of 1mM furoxan (ii) 1.0ml of triiodide

Figure 77: Schematic diagram of reaction vessel used to obtain NO release data from furoxan compounds using oxidative conditions. Taken and adapted from reference 2.

The reaction chamber (Fig. 77) was filled with excess potassium thioacetate solution. To this 100uL of 1mM furoxan was added into the chamber resulting in an initial peak on the analysis window. This was determined to be 'free' NO released by the thiolate attacking the ring and being detected before it is converted to nitrite (NO_2). Excess (1ml) of acidic tri-iodide solution was then injected into the chamber, oxidising any nitrite that had formed back into NO for detection. The results of this experiment are shown in graph 10. Each combretafuroxan compound (**86-128**) was tested for their NO release under these oxidative conditions.

Free NO, nitrite and total NO release from furoxan compounds 86-128
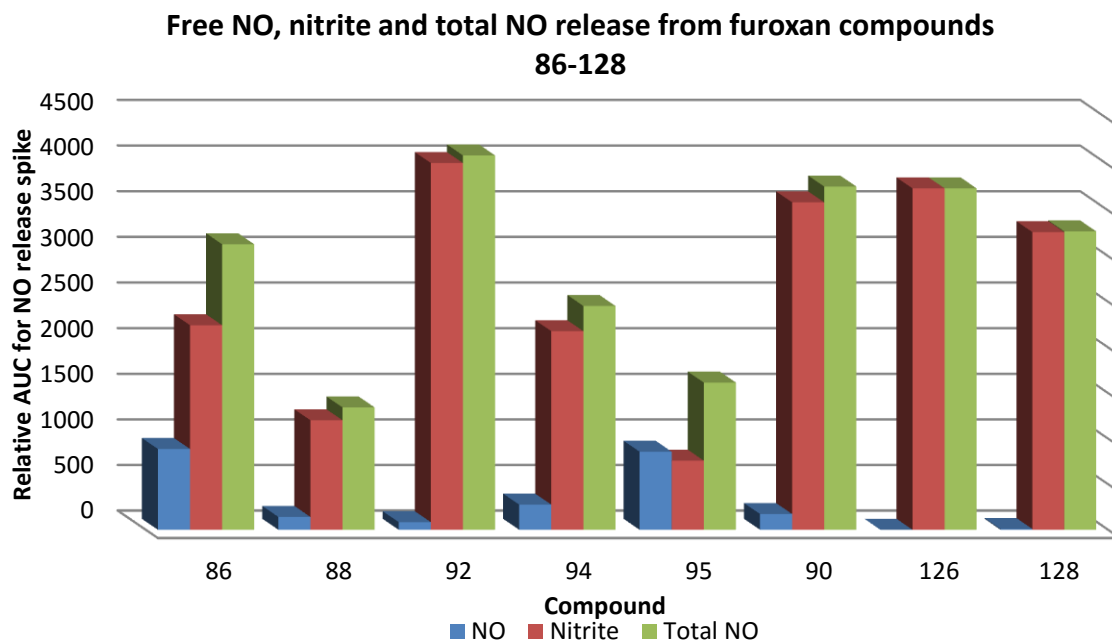
Graph 10: Oxidative release of NO from furoxan compounds, showing the amount of NO obtained as the 'free' form, nitrite and a combination of the two. Relative NO release is measured as the area under the curve (AUC) of each spike produced from the release of NO.

Splitting the data into three distinct sets helps show the complete story. In terms of 'free NO' (shown as the blue bars in graph 10) compounds **86** and **95** produced around 6 times more NO than the next compound, **88**. This appears to follow the trend as seen with the photochemical release (graph 9) as **95** has an electron withdrawing group, CF_3, in the *para* position and **86** has 6 electron donating methoxy groups decorating its structure, indicating that an electron withdrawing substituents release more NO in comparison to electron donating substituents. However this is not a consistent trend as **86** releases more NO than **94** which is substituted with the electron withdrawing group, OCF_3. This paradigm suggests that electronics have little effect on the release of nitric oxide under oxidative conditions and photochemical conditions (graph 9) and supports the idea that as the compounds tested do not behave exactly the same, the substituents themselves, must play a role in the release of nitric oxide other than in terms of electronics.

In terms of the total NO (green bars in graph 10) released at 40°C, a trend can be identified. It can be said that the alkyl substituents are more stable towards the release of nitric oxide compared to

their *O*-alkyated counterparts. This suggests that *O*-alkylated compounds (**92** and **94**) are less stable producing 3 and 1.5 times more NO than their respective alkyl compounds **88** and **95**. This trend is confirmed by the trimethoxy substituted furoxan **86**, which also produces more NO than the methyl substituted furoxan **88** and suggests that the introduction of an electronegative atom such as oxygen destabilises the furoxan in terms of its NO release.

To convert the data produced in graph 10, into a more useable form such as the actual concentration of NO released, the calibration curve depicted in graph 2 needs to be used. The concentration of nitric oxide release per furoxan compound can be calculated using the parameters from the calibration graph. The data presented in table 5 correlates to the total NO release produced for each compound under oxidative conditions.

Compound number	Total NO (AUC)	Concentration of NO $x10^{-6}$ (mol/dm^{-3})
88	1342.5	2.14
92	4102.7	6.74
95	1615.0	2.59
94	2453.9	3.99
90	3761.7	6.17
86	3129.8	5.11
128	3271.0	5.24
126	3741.4	6.13

Table 5: The actual concentration of NO released from furoxan compounds under oxidative conditions. Results were obtained using the calibration curve in graph 2.

In the presence of thiolate, compound **92** produced the highest concentration of NO at 6.74 µM. Following the trend mentioned earlier, as the substituents positioned around the aryl ring become more electron withdrawing, the combretafuroxan compound becomes more stable with respect to the release of nitric oxide. This is consistent with what is presented in the literature, as Nirode observed that electron-withdrawing substituents present on the aryl rings resulted in a lower NO yield.[17] Compound **95** produced around 2.6 times less NO with a concentration of 2.59 µM. From the data generated, the most stable combretafuroxan appears to be compound **88** which contains a methyl

group in the *para* position of each aryl ring producing only 2.14 µM of nitric oxide under the conditions studied.

Although each furoxan compound successfully produced nitric oxide upon exposure to thiolate, the concentration produced per furoxan compound does not correlate to the initial concentration injected into the reaction vessel. As outlined in Fig. 77, 1 mM of each furoxan (**86, 88, 90, 92, 94, 95, 126, and 128**) was injected into the chamber containing and excess of thiolate. This in turn released micromolar (µM) levels of NO. This equates to a 1000 fold difference in concentration unaccounted for from each furoxan compound. There are two possible explanations as to where the missing NO has gone. It is thought that during the decomposition of the furoxan to produce nitrite that a significant proportion of nitrate may have also formed. Due to experimental limitations with the nitric oxide analyser (NOA), nitrate levels could not be measured and therefore the remaining concentration may be existing as unquantifiable nitrate. Another explanation for the missing concentration could be that the furoxan compounds are photosensitive. As seen in graph 9 in the presence of light, furoxan compounds (**86, 88, 90, 92, 94, 95, 126, 128**) can release substantially more nitric oxide, around a 10x enhancement in release profile for **128** compound, than they do under oxidative conditions. The experimental preparation for oxidative release is quite laborious in preparing the conditions required for analysis and it is therefore possible that photochemical induced NO release occurred before the furoxan compounds were exposed to thiolate producing the observed lower concentrations. The furoxan compounds appear to release less nitric oxide than anticipated under oxidative conditions, this paradigm was confirmed by our collaborators who found that compounds **86, 88, 90, 92, 94, 95, 126,** and **128** released less than 5% nitric oxide in total when analysed using the Greiss test, a classic method for the analysis of nitric oxide.

Despite a lower concentration of nitric oxide being recovered than expected, the production of NO from the oxidation of nitrite does confirm findings from the literature in terms of the mechanism of release. Upon release of NO from the furoxan compounds, literature[14,17] indicates that a new heterocycle is formed known as an isoxazole **200** along with a molecule of nitrite as before depicted

in scheme 12 (chapter 1.1.3, page 35). Evidence of this formation was found using compound **94** as a test sample (scheme 67).

Isolated from HRMS: 448.9783 ppm
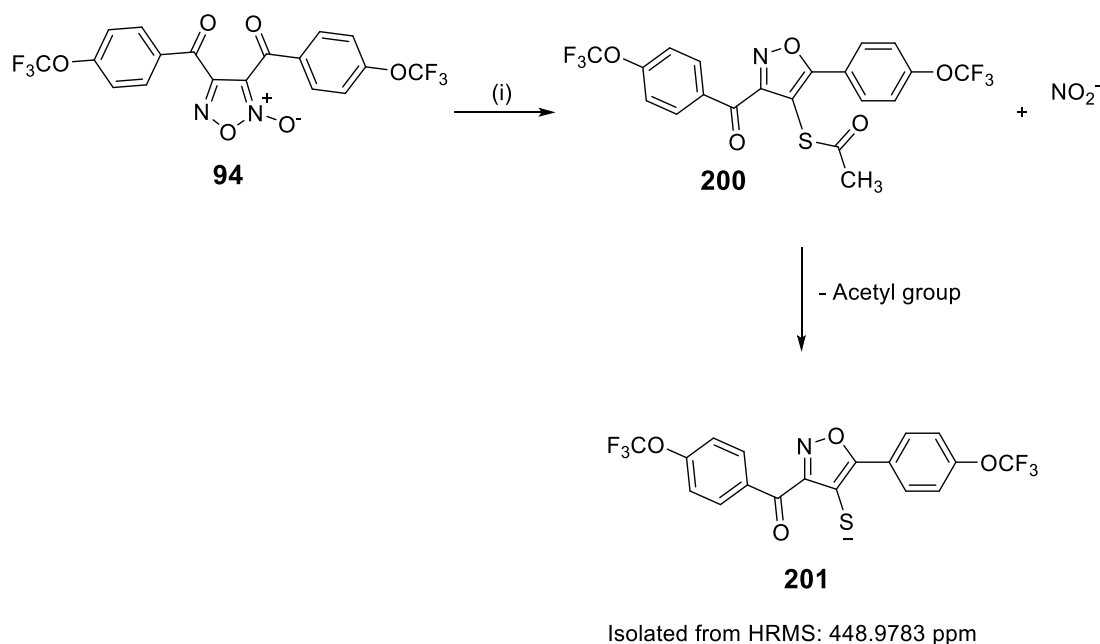
Reagents and conditons: Potssium thioacetate 10mM, diethyl ether

Scheme 67: Thiol induced release of NO leads to the formation of a new heterocycle, the isoxazole ring **200**. Its partially decomposed form **201** was found for compound **94** using HRMS.

HRMS data confirmed the presence of the isoxazole ring with a mass of 448.9783 ppm, however this corresponds to the free thiolate having lost the acetyl group from the original potassium thioacetate starting material shown in scheme 64. The presence of the isoxazole ring **201** in the reaction vessel confirms the mechanism of NO release as aforementioned in chapter 1.1.3 (scheme 12, page 35) and reinforces the mechanism of which nitrite (NO_2^-) is produced.[14,17] Interestingly the isoxazole ring has recently been published[22] as a combretastatin analogue, for increasing rigidity of the *cis* double bond and showed promising anti-tubulin functions. This could suggest that there may be a limited loss of anti-tubulin activity in the combretafuroxan compounds upon initial decomposition as the isoxazole-combretastatin is also active towards tumour reduction. There is also potential that the combretafuroxan could act as a novel prodrug formulation, and convert to the active isoxazole-

combretastatin *in situ* with release of nitric oxide and have synergistic effects as the release of NO can relieve the cardiotonic side effects often seen with anti-tubulin compounds.

Ozone-based chemiluminescence was a useful technique for measuring NO-release and allowed the successful measurement of the nitric oxide releasing capabilities of synthetically novel NO-donors spanning two classes. However, the sensitivity issues, such as the background atmosphere affecting baseline readings, meant that certain experiments and conditions were not viable. Problems with the levels of nitrate in standard samples meant that the levels of nitrate produced from our compounds could not be measured and therefore the full picture and profile for the furoxan compounds could not be established. Although there were experimental constraints, the NO-release methodology used, successfully showed that all furoxan based NO-donors were able to release NO under both photochemical and oxidative conditions. It appears that the substituents decorating the aryl rings in compounds **86, 88, 90, 92, 94, 95, 126, 128** have little effect on the relative NO release under these conditions other than that electron withdrawing groups appear to produce a lower amount of NO compared to those compounds with a more electron donating group attached to the aryl ring. This may be due to the positon that the thiolate attacks the furoxan being affected by the electronics of the compound, electron withdrawing groups are known to increase the electrophilicity of the benzoyl carbon[16] may cause the thiol to attack the carbonyl carbon preferentially to the imino carbon of the furoxan and thus affect the level of NO release. However photochemical decomposition produces a higher amount of NO per compound compared to oxidative induced release suggesting that **86-128** have a high degree of photosensitivity to both natural light and 254 nm light.

The cupferron derivatives **98**-**105** tested were all capable of releasing nitric oxide in the presence of light (254 nm). The alkylation chemistry performed on the terminal oxygen appears to have a stabilising effect on the parent compound for the majority of the NO-donors. All compounds except **101** evolved less nitric oxide than non-alkylated cupferron, **56**. The most stable compound appears to be **103**, where a butyl chain links two molecules of cupferron, this stability may be due to the mechanism of release and that the formation of a butyl di-radical and the subsequent ring closure to

form the cyclobutane ring is energetically unfavourable compared to the cyclohexane and cyclooctane rings formed from decomposition of compounds **104** and **105** respectively.

Analysis of the known NO-donor, SNAG **19** confirmed what has been observed in the literature that in the presence of copper ions (Cu^+) the release of nitric oxide is accelerated compared with its relative release under thermal conditions. Under our experimental conditions it was found that photochemical release produced a greater quantity of NO compared to thermal and copper catalysed release, however it took slightly longer to do so. Comparatively in terms of NO-donor capabilities the cupferron derivatives **98-105** produce more NO per mM of compound than SNAG **19** did.

2.2.4- References

1. A. Butler, and R. Nicholson, "Life, Death and Nitric Oxide", RSC paperbacks, The Royal Society of Chemistry, 2003.

2. P. H. MacArthur, S. Shiva and M. T. Gladwin, *J. Chromatogr. B*, 2007, **851**, 93-105

3. A. G. Pinder, S. C. Rogers, A. Khalatbari, T. E. Ingram and P. E. James, Redox-Mediated Signal Transduction- Chapter 2, 2009, Humana Press

4. J. McAinly, D. L. Williams, S. C. Askew, A. R. Butler and C. Russell, *J. Chem. Soc. Chem. Commun*, 1993, 1758-1759

5. R. J. Pearson, PhD thesis, University of St Andrews, 2001

6. D. L. Williams, *Acc. Chem. Res*. 1999, **32**, 869-876

7. J. S. Stamler, O. Jaraki, J. Osborne, D. I. Simon, J. Keaney, J. Vita, D. Singel, C. R. Valeri and J. Loscalzo, *Proc. Nat. Acad. Sci*. 1992, **89**, 7674-7677

8. H. M. S. Patel and D. L. H. Williams, *J. Chem. Soc. Perkin Trans 2*, 1990, 37-42

9. S. C. Askew, D. J. Barnett, J. McAninly and D. L. H. Williams, *J. Chem. Soc. Perkin Trans 2*, 1995, **4**, 741-745

10. M. M. Veleeparampil, U. K. Aravind and C. T. Aravidakumar, *Adv. Phys. Chem.*, 2009. 1-5

11. J. A. Hrabie and L. K. Keefer, *Chem. Rev.*, 2002, **102**, 1135-1154

12. J. R. Hu, C. S. Yau, S. C. Tsay and T. I. Ho. *Tetrahedron. Lett*. 1997, **38**, 52, 9001-9004

13. Y. Hou, W. Xie, A. J. Janczuk and P. G. Wang, *J. Chem. Org.*, 2000, **65**, 4333-4337

14. R. Fruttero, M. Crosetti, K. Chegaev, S. Guglielmo, A. Gasco, F. Berardi, M. Niso, R. Perrone, M. A. Panaro and N. A. Colabufo, *J. Med. Chem*, 2010, **53**, 5467-5475.

15. R. M. Paton, *Comprehensive Heterocyclic Chemistry I*, 1984, 393-426

16. S. Auricchio, A. Selva and A. M. Truscello, *Tetrahedron*, 1997, **53**, 51, 17407-17416

17. W. F. Nirode, J. M. Luis, J. F. Wicker and N. M. Wachter, *Bioorg. Med. Chem. Lett.*, 2006, **16**, 2299-2301

18. P. G. Wang, T. B. Cai and N. Taniguchi, Nitric oxide donors: For Pharmaceutical and Biological Applications, Science, John Wiley and Sons, 2005

19. R. M Paton, *Comprehensive Heterocyclic Chemistry II*, 1995, 229-265

20. G. N. Nikonov, and S. Bobrov, *Comprehensive Heterocyclic Chemistry III*, 2008, Vol.5, 315-394

21. M. Feelisch, K. Schonafinger and E. Noack, *Biochem. Pharmocol.,* 1992, **44**, 5, 1149-1157

22. J. Kaffy, R. Pontikis, D. Carrez, A. Croisy, C. Monneret and J. C. Florent, *Bioorg. Med. Chem.*, 2006, **14**, 4067-4077

2.3- Biological results

The furoxan ring was introduced into the combretastatin structure to increase the stability of the anti-tubulin agent and prevent its original alkene bond from isomerising *in vivo*. Furoxans capability to release nitric oxide, and therefore induce vasodilation, is an advantageous property for the combretafuroxans due to the cardiotonic side effects associated with combretastatin and can therefore work as a dual purpose compound. To assess the effectiveness as NO-donor compounds, collaborators at Kingston University were sent samples of compounds from the combretafuroxan series to test their effectiveness as vasodilators. Using rings of rat aorta submerged in organ baths the success of each compound was determined by the percentage relaxation that occurred on pre-contracted aortic rings. Contraction of aortic rings was induced before experimentation using methoxamine **202**, a known and industry used vasoconstricting agent.

202
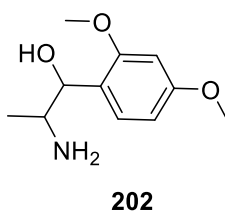
Figure 78: Methoxamine **202**, a chemical agent used to induce vasoconstriction.

The following compounds were tested for their effectiveness as vasodilators and produced varying results which are presented and discussed in the following section.
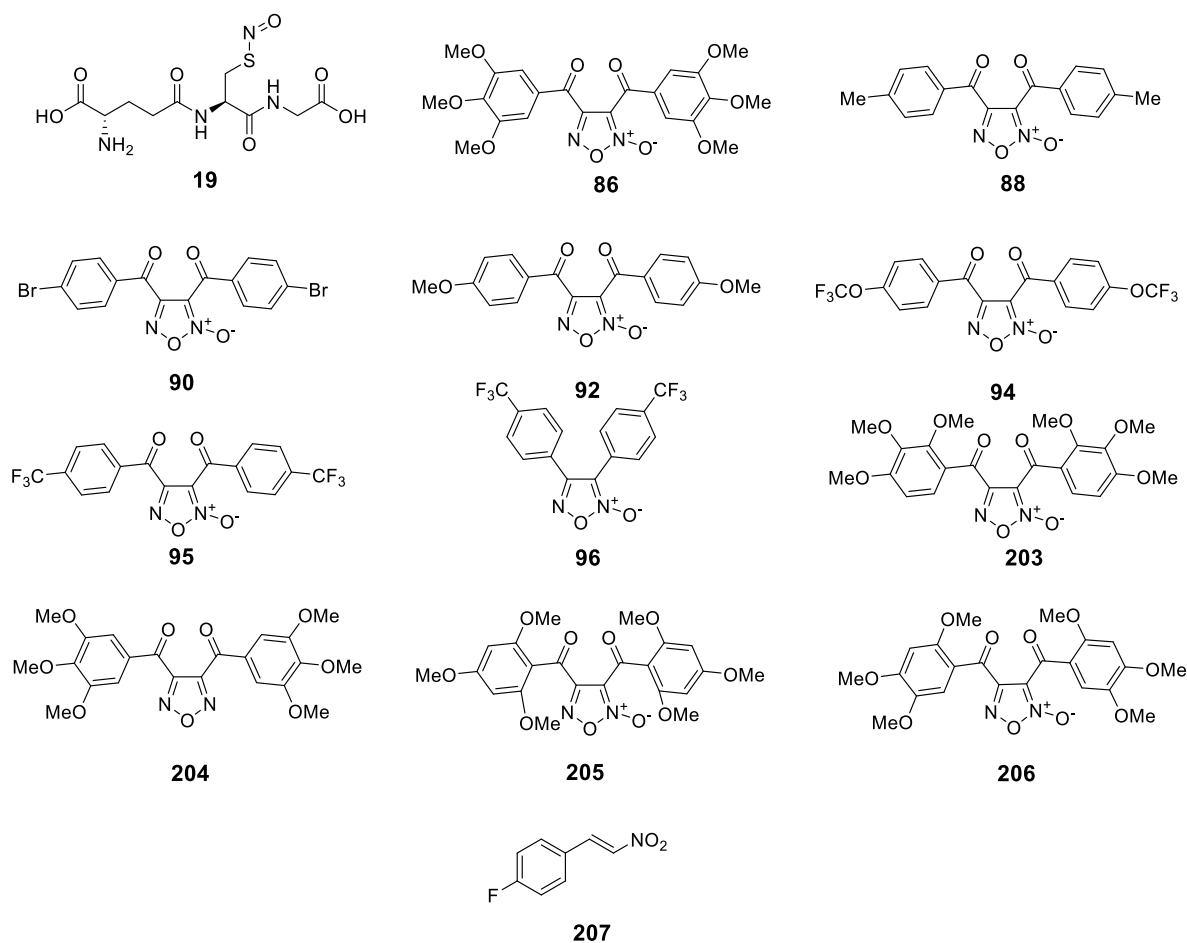
Figure 79: Combretafuroxans, GSNO, a nitroalkane and a combretafuarzan used in the vasodilatory study using contracted rat aorta.

Each compound was tested for its ability to induce relaxation on the aortic smooth muscle, which was pre-contracted with methoxamine (Fig.78). Dimethyl sulphoxide (DMSO) was used a reference compound due to all samples being dissolved in this organic solvent. DMSO produces minimal to no relaxation of the aorta and therefore any response seen can be attributed to the testing compound and not that of the solvent.

% Contraction of rat aorta for compounds **86, 203 and 206**
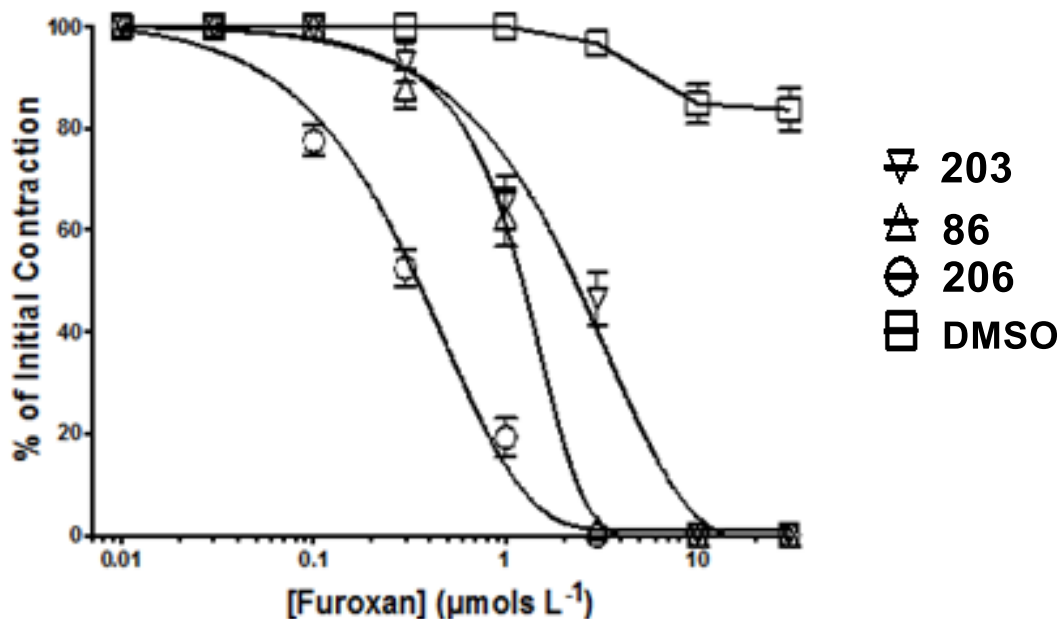
Graph 11: Initial vasodilatory investigations of furoxans on rat thoracic aorta, graphically grouped according to compound potency and comparing effect to compound vehicle, dimethyl sulfoxide (DMSO). (n= 4-6 animals).

Graph 11 shows the initial relaxation results for compound **86**, **203** and **206** on rat aortic rings. In this initial study the furoxan compounds tested were all substituted with a tri-methoxy unit decorating the aryl ring in various positions. All compounds were able to reverse contraction by 100%, with compound **206** only requiring 0.3 µM to induce half of the maximal response. Comparatively speaking, **206** is 3 and 8 times more potent than **86** and **203** respectively. This suggests that the tri-methoxy subunit and specifically methoxy (OMe) groups in the 2, 4 and 5 positions are important in NO-release and the induction of vasorelaxation.

% Contraction of rat aorta of compounds **88, 94 and 205**
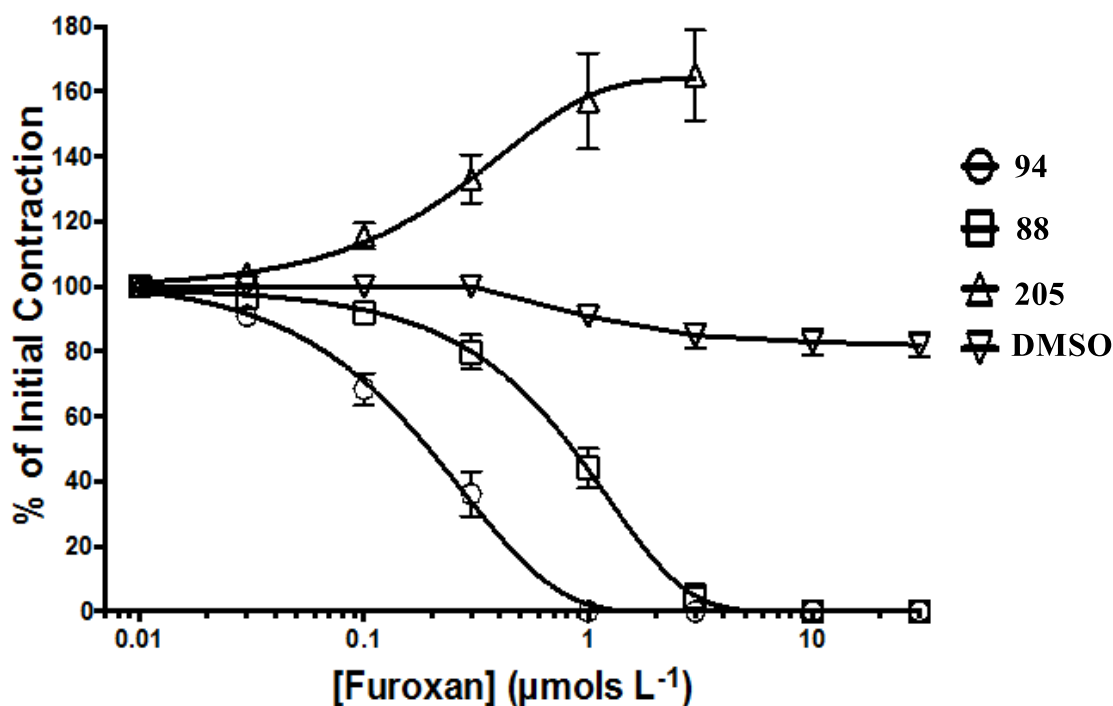
Graph 12: Initial vasodilatory investigations of furoxans on rat thoracic aorta, graphically grouped according to compound potency and comparing effect to compound vehicle, dimethyl sulfoxide (DMSO). The compound **205** causes the unexpected effect of contracting the aorta further than the maximum obtained from use of methoxamine. (n= 4-6 animals).

Graph 12 shows the initial relaxation test for compounds **88**, **94** and **205**, with DMSO used as a control. Compound **205** displays an interesting profile in that it increases the percentage contraction of the aortic rings compared to the other furoxan compounds tested in this study (**88** and **94**). This phenomenon suggests that **205** in fact acts more as a vasoconstrictor rather than a vasodilator possibly giving scope for its use as a lead compound based upon combretastatin, which depletes tumour cells by disrupting the vascular structure supplying the tumour with blood.[1] Out of the compounds tested in this relaxation study, compound **205** is the only one with a substituent in the 2 and 6-position on the aryl rings. This observation suggests that having substituents in both the 2 and the 6 positions of the aryl rings flanking the furoxan disrupts NO-release in some manner and instead increases their potential for vasoconstriction by hindering NO release.

% Contraction of rat aorta of compounds **94, 88**
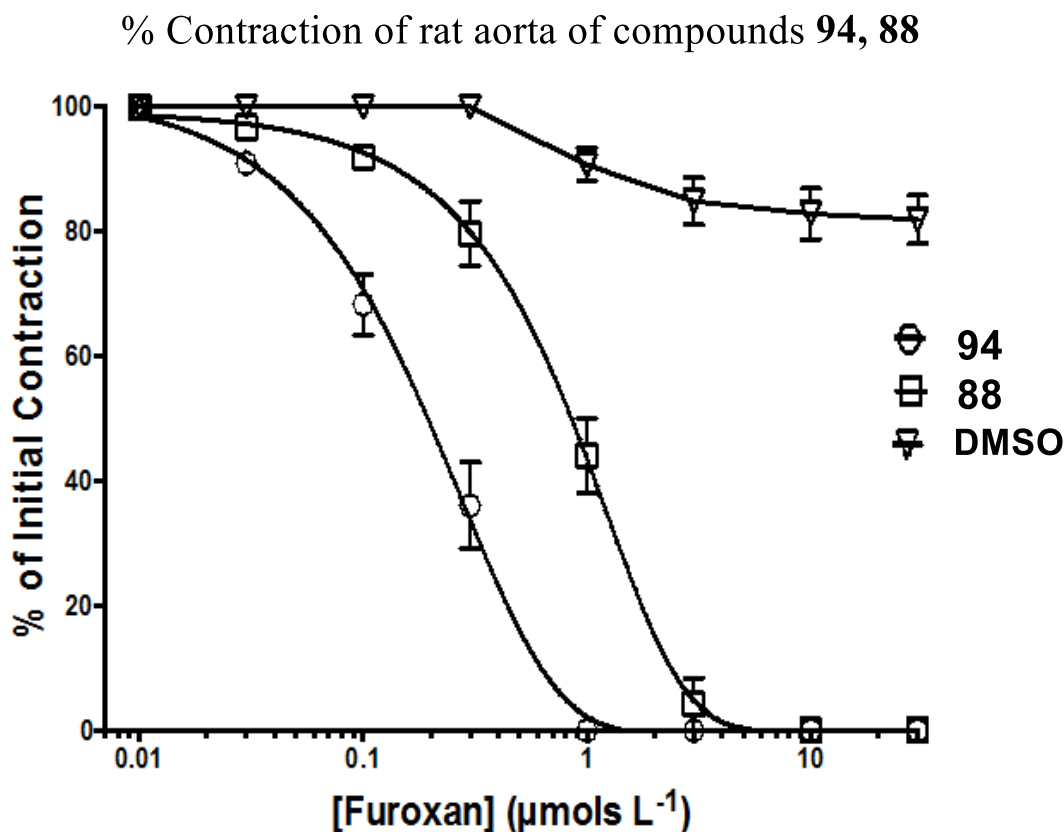
Graph 13: Initial vasodilatory investigations of furoxans on rat thoracic aorta, graphically grouped according to compound potency and comparing effect to compound vehicle, dimethyl sulfoxide (DMSO) – without compound **205**. (n= 4-6 animals).

Graph 13 shows the percentage relaxation for compounds **88** and **94**, this time without the outlier compound **205**. This graph shows more clearly that compound **94** is a potent vasodilator inducing 100% reversal in contraction at a remarkably low concentration (IC$_{50}$: 0.25 µM) compared with the furoxan compounds seen already (**86**, **88**, **203**, **205** and **206**). Compound **88** has a methyl group in the *para* position of the aryl rings flanking the furoxan, whereas compound **94** is substituted with a trifluromethoxy (OCF$_3$) in the para positon (as shown in Fig. 79). This observation suggests that an electron withdrawing group present in the furoxan structure increases its ability to release nitric oxide and induce vasodilation.

% Contraction of rat aorta of compounds **92**, **95** and **207**
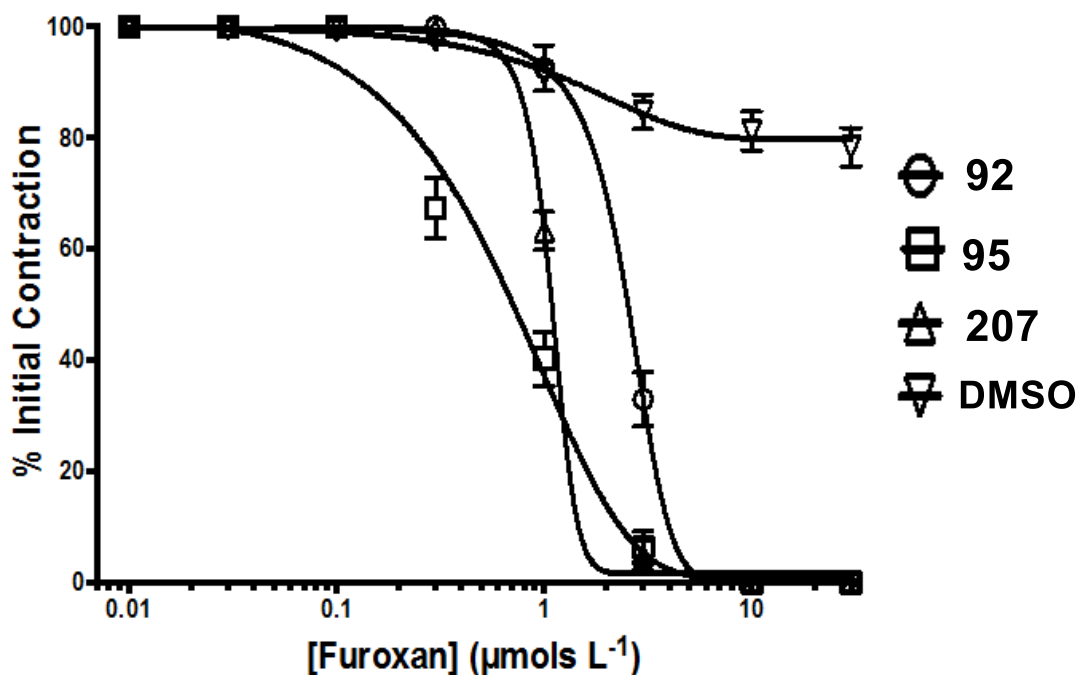
Graph 14: Initial vasodilatory investigations of furoxans on rat thoracic aorta, graphically grouped according to compound potency and comparing effect to compound vehicle, dimethyl sulfoxide (DMSO). (n= 4-6 animals).

Graph 14 shows another comparative study for the relaxation potential of compounds **92**, **95** and **207** (their structures can be seen in Fig. 79). Compound **95** is substituted with a trifluromethyl (CF_3) group and appears to produce relaxation in a more sigmoidal profile compared to that of **92** and **207**. Compound **207** is a nitro alkene (Fig. 79) and successfully produces 100% relaxation however in a much more concentration dependent way. There is no relaxation in concentrations lower than 1 µM but there is almost an instant relaxation at 1 µM. Compound **92** also produces a sigmoidal curve but is a lot less potent than either **95** or **208**. Compound **92** contains a methoxy (OMe) substituent and its lack in potency compared to **95** which has the more electron withdrawing group, $CF_{3,}$ suggests that electronegativity again plays a key role in the relaxation potential of the furoxan compounds, as already seen in graph 13 with compound **94**.

From the graphs shown above (11-14), it can be seen that there is a range of relaxation activity produced from the compounds tested. This can also be seen in Table 6, which displays the relative IC_{50} for each compound. An IC_{50} is defined as the effective concentration of a drug or compound that produces half of the maximal response[2].

Compound Number	IC_{50} value (µM)
86	1.131
88	0.9839
90	15.5364
92	3.1502
94	0.2562
95	0.8423
96	23.565
203	2.991
204	20.51
206	0.3420
207	1.1537

Table 6: IC_{50} values for the panel of furoxan compounds tested on rat thoracic aorta. All concentrations are reported in µM.

The relative IC_{50} data indicate that compound **94** (OCF_3) is the most potent compound, reversing contraction by 100% and producing a IC_{50} of 0.25 µM. Converting the OCF_3 group to CF_3 invokes a 3 fold loss in potency suggesting that the oxygen is somehow key to the mechanism of relaxation seen for compound **94**. It appears as you increase the electron donating potential of the substituent, the potency with respect to vasodilation, decreases. This is especially the case within the mono-substituted compounds. Which can be seen clearly by compound **88** (*p*-Me) and **92** (*p*-OMe), having

an IC$_{50}$ of 0.98 µM and 3.15 µM respectively. For the tri-MeO substituted compounds, the most potent vasodilator was the 2,4,5-trimethoxy furoxan **207**, closely followed by the 3,4,5-trimethoxy **86** and then the 2,3,4-trimethoxy **203** all with IC$_{50}$'s below 5 µM. The 2,4,5-trimethoxy **206** compound producing an IC$_{50}$ of 0.34 µM. This shows that the trimethoxy substituent is a beneficial functionality in terms of vasodilation with the majority (**86** and **206**) producing sub 2.0 µM potency. It appears that the relative position of the methoxy group does however affect the IC$_{50}$ value. Comparing **203** and **206**, one methoxy group has been moved from the 5-position (**206**) to the 3-position (**203**) of the benzene ring. This change in position causes a significant drop in potency from 0.34 µM to 2.99 µM. Removing the *ortho* methoxy group completely and changing the substitution pattern to the three, four and five positions (**86**) changes the IC$_{50}$ to 1.13 µM. This suggests that a methoxy group in the five position induces more relaxation as both **86** and **206** both contain this substituent and have sub 3 µM IC$_{50}$'s. However, having a methoxy group in both *ortho* positions (2 and 6) alters the relaxation profile totally. Compound **205** was the only compound not to induce relaxation and instead induced an increase in the contraction of the rat aorta. Comparing **205** with the other trimethoxy substituted compounds **86**, **203** and **206**, it is the only compound tested that has a methoxy substituted in the 6 position of the aromatic ring. This suggests that having a substituent in both the two and six position of these symmetrical combretafuroxan compounds impedes the release of NO in some manner. The lack of relaxation from compound **205** correlates with findings from the ovarian cancer cell line studies. Previous work[3] on symmetrical combretafuroxans found that compound **205** was a potent anti-tubulin agent producing an IC$_{50}$ of 3.64 µM against the A2780 ovarian cancer cell line as well as sub 100 µM activity against several others. Anti-tubulin agents work by restricting the blood flow to the tubulin cells, causing oxygen deprivation and eventually cell death, so it is no surprise that compound **205** did not cause any relaxation. Instead it acts as an effective vasoconstricting agent.

An interesting observation from the initial biological testing is that there is a stark difference between the relaxation ability of compound **95** and compound **96**. Both of these compounds are substituted in the *para* position with a trifluromethyl group; however compound **96** lacks the two carbonyl groups

bridging the furoxan ring and the aryl groups. It appears that without the carbon spacer present, there is around a 30 fold loss in potency with **96** producing an IC_{50} of 23.5 μM compared to **95**'s IC_{50} of 0.84 μM. This can potentially be explained by the mechanism that each compound uses to release nitric oxide. Both furoxan compounds will release NO in the presence of thiols, however due to the presence of the carbonyl groups, compound **95** can undergo rearrangement upon release of NO to produce the isoxazole ring as already seen in scheme 67 (page 163). Without the carbonyl group present adjacent to the furoxan, this new ring formation cannot occur and therefore the resulting compound post NO release for compound **96**, may not be as stable and therefore the process may not be as energetically favourable as the decomposition of **95**. Depending on the exact mechanism of NO release within the aortic rings, compound **95** may also interact differently with endogenous thiol groups as it can form additional non-covalent interactions with amino acid residues along the aortic wall. These interactions may also stimulate nitric oxide to be produced by NOS enzymes and stimulate the relaxation mechanism from the aortic cells therefore creating a summative relaxation and hence the much lower IC_{50}.

Compounds **90** and **96** were the least effective in these relaxation studies with IC_{50}'s of 15.5 and 23.5 μM respectively. Compound **204** is similar to the combretafuroxan compounds **86, 203,** and **205** and **207** but instead contains a furazan ring. A furazan ring is chemically similar to the furoxan ring but lacks the ability to release nitric oxide, as it lacks the N-oxide functionality and therefore should not be able to induce relaxation. Compound **204** produced an IC_{50} of 20.5 μM, which was much lower than initially expected due to the inability to release nitric oxide. The observation that **204** still produces relaxation may suggest that relaxation is not entirely induced by the release of nitric oxide and another factor may be involved that enables the compounds tested to cause vasodilation.

2.3.1- Lead compound isolation and further analysis

From the derived IC_{50}'s, compound **94** was determined to be the most potent compound, resulting in the collaborators choosing it as their lead compound for further biological analysis. It has been established from both NO release data using the NOA apparatus and initial biological experiments that compound **94** is capable of producing nitric oxide and to a high enough concentration to promote 100% relaxation. Although the most potent furoxan compound in the initial studies (graph 11-14) the question arose, how does this compare to other NO-donors. Sodium nitrosoprusside (SNP) as, aforementioned in chapter 1, is a known NO-donor, commercially available in the BNF[4], and is considered as the 'gold standard' in NO release despite its unfavourable metabolites such as cyanide and cyanoheamaglobin.[5]

Samples of compound **94** and SNP **9** were studied alongside each other to test their relative relaxation effects. Aortic rings were pre-contracted with methoxamine **202** (Fig.78) before the appropriate testing compound was introduced.

Comparison of lead compound **94** with SNP **9**
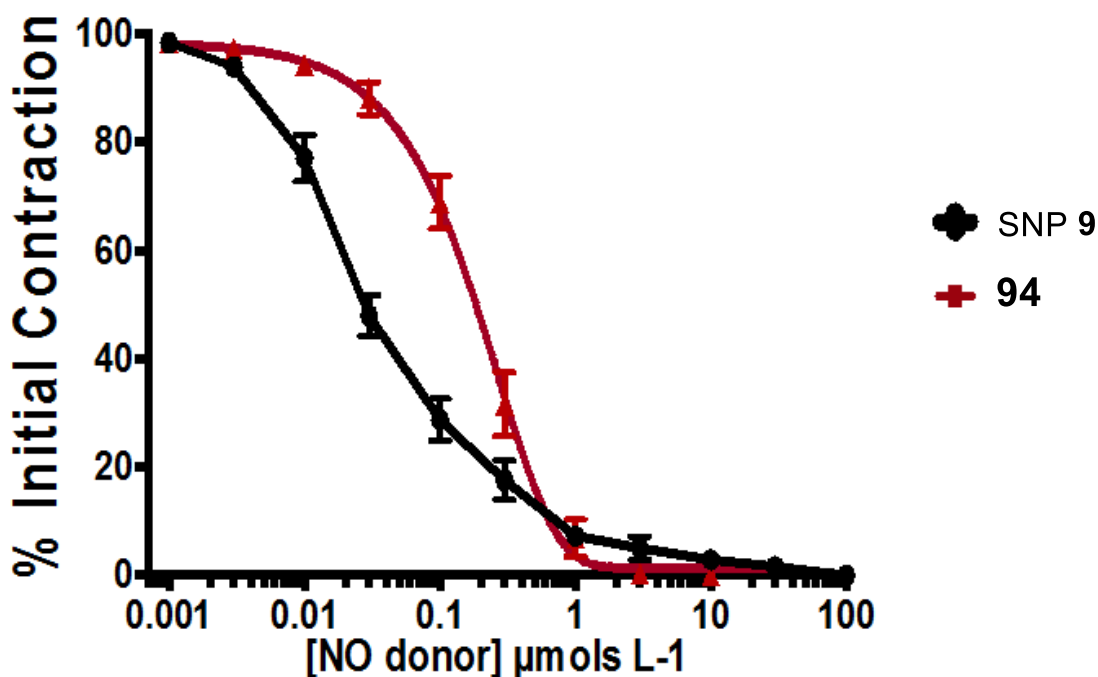
Graph 15: A direct comparison between the vasodilatory effects of compound **94** against SNP, **9**. It can be seen that SNP is the more potent compound; however, compound 94 appears to be able to reverse a methoxamine induced α-1 contraction the greatest. (n=4-6).

Sodium nitrosprusside (SNP) is clearly a more potent vasodilator than compound **94** inducing relaxation with an IC_{50} of 0.05 µM compared to 0.25 µM for compound **94**. However although less potent in terms of IC_{50} value, compound **94** appears to be able to fully reverse methoxamine induced contraction at a concentration of 1 µM whereas it takes nearly 10 times more SNP **9** to produce the same effect.
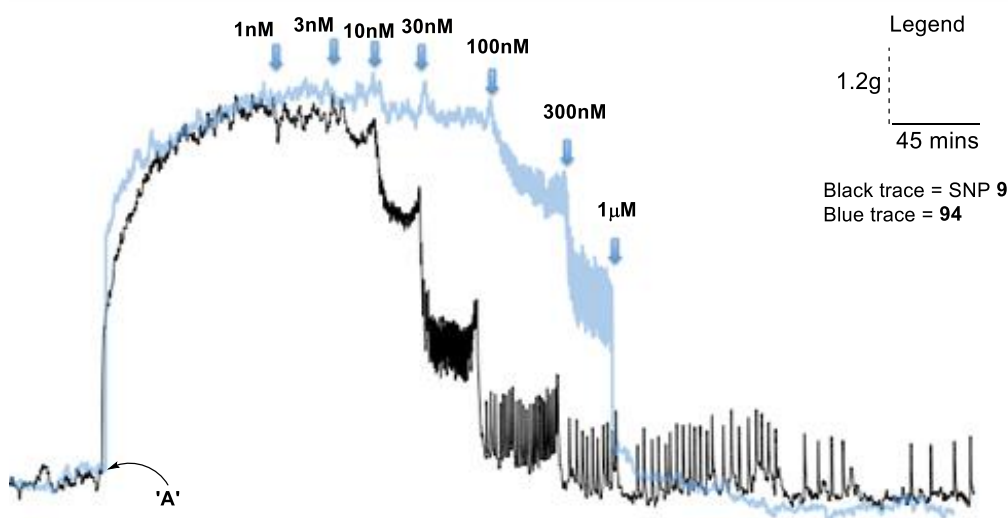
Graph 16: A representative trace showing the effects of cumulative concentrations of both sodium nitroprusside (SNP, black trace) and compound **94** (blue trace). The concentration additions are from the left: 1 nM, 3 nM, 10 nM, 30 nM, 100 nM, 300 nM, 1 µM.

A vascular pressure gauge (graph 16) was constructed to analyse compound **94** and SNP's **9** relaxation profile in terms of reducing the pressure observed upon contraction. Aortic rings were pre-contracted with 10 µM methoxamine (Fig. 78) as shown by point 'A' on graph 16. The contraction of the aortic ring increased the pressure measured on the gauge and hence the rise in peak line. Increasing concentrations of both SNP **9** and **94** were then injected and their effect on contracted aorta was observed over 45 minutes. As the concentration of SNP **9** increased from 1 nM towards

1 µM, the aorta relaxed at a greater rate. Compound **94** was shown to be the less potent of the two compounds but it elicits a more sustained relaxation with no fluctuations in vascular tone when compared to SNP, once the vessel became fully relaxed.
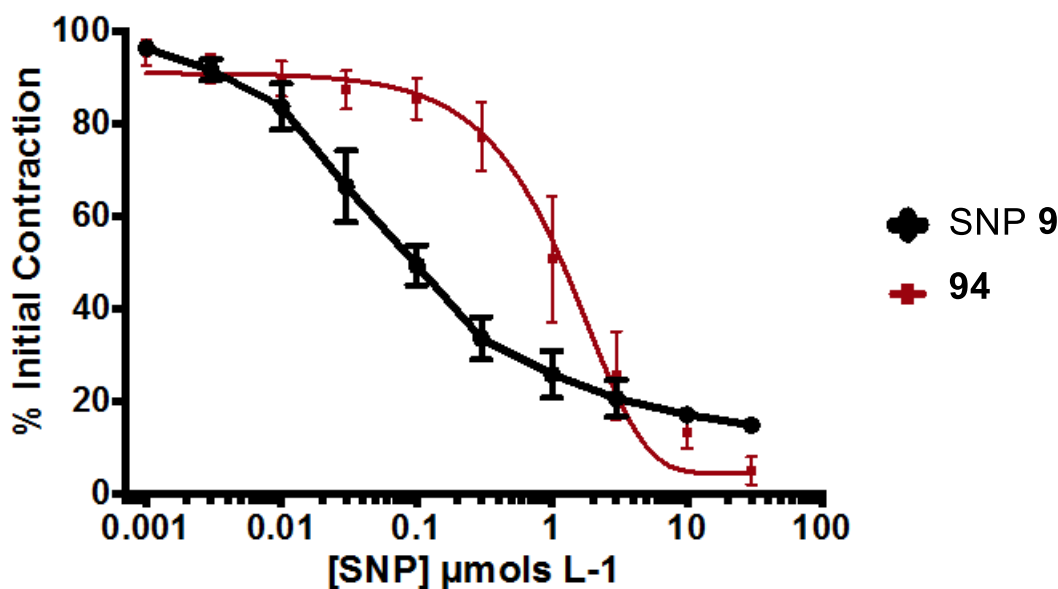
Graph 17: Comparison of effect between SNP and 94 in vasodilation of pulmonary arteries. SNP is a more potent vasodilator in pulmonary artery, however, it appears from the data available that compound **94** has a greater V_{max} (SNP – 83.6 ± 0.98% and **94**= 94.86 ± 3.42 %. Data are means ± SEM. (n= 6-8).

SNP's **9** potency when compared against compound **94** is not just isolated to the aortic vessel. Graph 17 shows the action of SNP and compound **94** upon pre-contracted pulmonary arteries. SNP **9** produces a lower IC_{50} value of 0.1 µM where compound **94** has an IC_{50} of 2.0 µM (a slight reduction in relaxation potential). Despite SNP **9** producing relaxation at a faster rate, it only ever induces up to 80% relaxation; this is where compound **94** performs better. Although a higher concentration of **94** is needed, almost 100% relaxation of the pulmonary artery is possible; this is consistent with the results seen within the aortic vessel.

Mechanistically, vasodilation *in vivo* is said to occur through activation of soluble guanylate cyclase's (sGC) heam centre by nitric oxide.[6,7] It is this activation that induces the cascade of biochemical reactions that result in vasodilation and the increase of blood flow. In an attempt to establish the mechanism by which compound **94** was acting, and if in fact it works by binding and activating sGC, an inhibitory experiment was set-up. ODQ or [1H-[1,2,4]oxadiazolo-[4,3-a]quinoxalin-1-one] **208** (Fig. 80) is a known inhibitor of guanylate cyclase[8] and was introduced to the rat aorta rings 10 minutes prior to contraction with methoxamine.

208
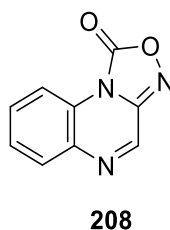
Figure 80: The industry used sGC inhibitor, [1H-[1,2,4]oxadiazolo-[4, 3-a]quinoxalin-1-one] or ODQ **208**. Which can help assess the mechanism of action of lead compound **94**.

Both SNP **9** and compound **94** were then injected into the aorta and analysed for their ability to reverse relaxation under identical conditions. The results from this study are depicted in graph 18.

SNP **9** and lead compound **94** in the presence of ODQ inhibitor
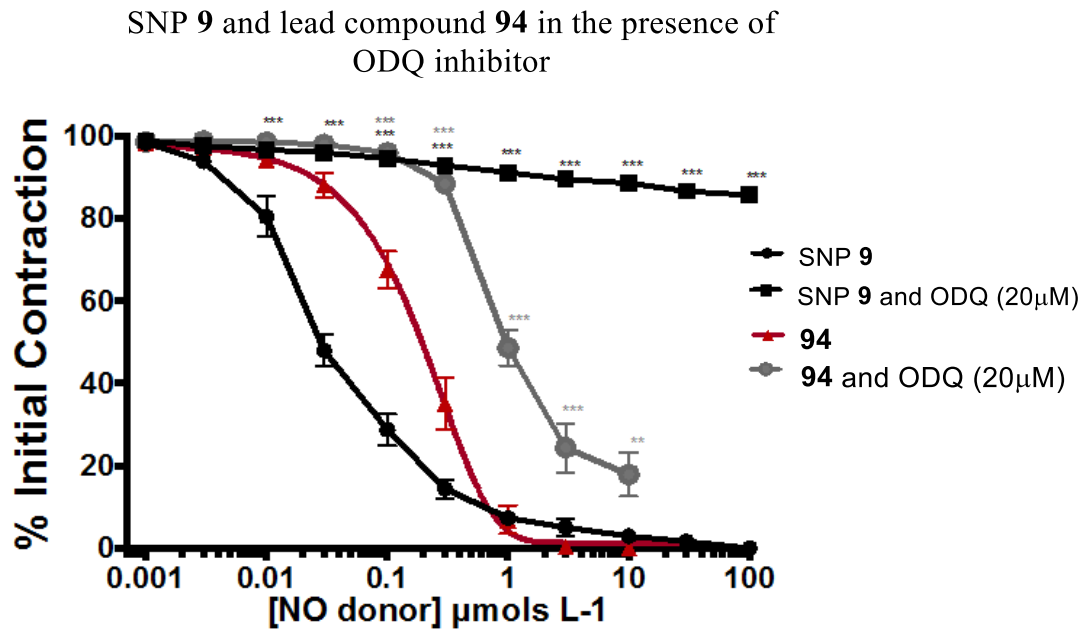
Graph 18: Comparison of dose-effect of sodium nitroprusside (SNP) and **94** in pre-contracted rat thoracic aorta, both with and without incubation with ODQ (20 µM) for ten minutes before contracting the vessel. Aorta rings were pre-contracted with 10^{-5} M methoxamine. Data are means ± SEM. Statistical analysis was conducted and significance is shown by $P < 0.05 = *$; $P < 0.01 = **$; $P < 0.001$. (n=6-7).

Graph 18 shows the profile of SNP with and without the ODQ inhibitor. Without ODQ inhibition, SNP reproduces its profile from graph 16, however upon inhibition of sGC its effectiveness as a vasodilator is greatly reduced causing only 5% relaxation and essentially very little vasodilation occurs. In contrast compound **94** in the presence of the ODQ inhibitor still induces around 80% relaxation of aortic muscle suggesting activation of sGC is not its primary route to vasodilation and is therefore producing relaxation by another means.

Comparison of different concentrations of ODQ inhibitor on lead compound **94**

94 and ODQ (100μM)   **94** and ODQ (20μM)

94 alone
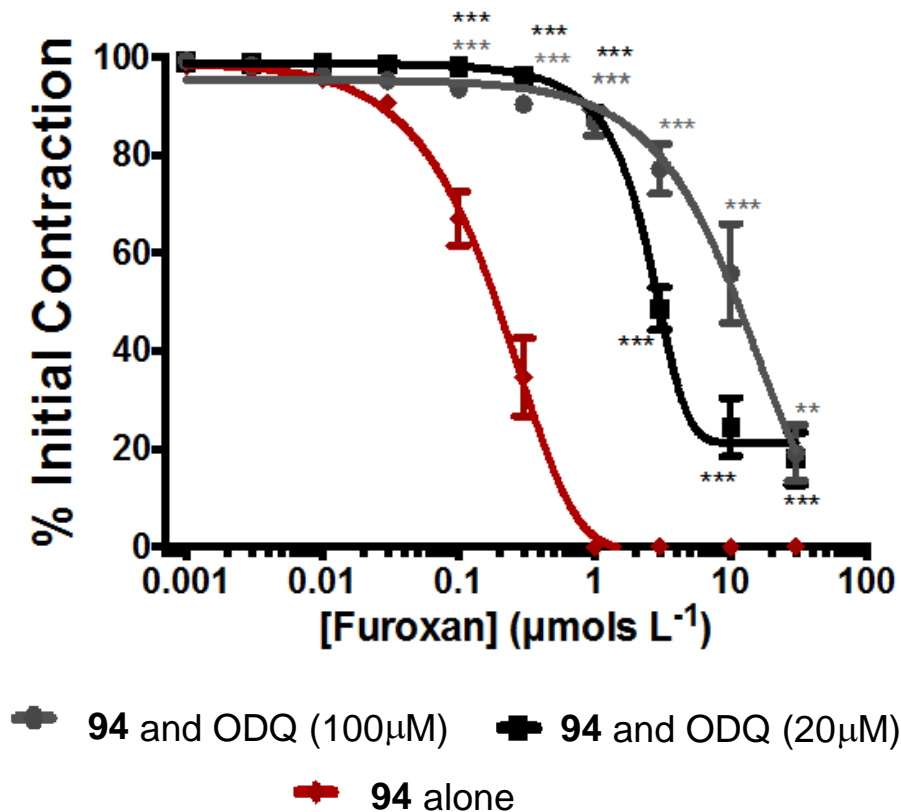
Graph 19: Comparison of 20 µM ODQ and 100 µM of ODQ **209** on inhibition of vasodilation in rat thoracic aorta. ODQ was allowed to incubate in the vessels for ten minutes before contraction. Aorta rings were pre-contracted with 10^{-5} M methoxamine. Data are means ± SEM. Statistical analysis was conducted using two-way ANOVA and significance when compared to compound **94** is shown by P $<0.05 = *$; P $<0.01 = **$; P $<0.001 = ***$. A student's t-test indicates that the effects of the two ODQ concentrations are not significantly different. (P = 0.7845). (N=7).

Increasing the concentration of sGC inhibitor fivefold to 100μM still has minimal effect on the action of compound **94** on aortic relaxation, increasing the IC_{50} from 0.2 µM to 10 µM. Compound **94** still produces around 80% relaxation suggesting that an alternative relaxation mechanism is being utilised to reverse the contraction of aortic smooth muscle and therefore an alternative experiment is needed to assess compound **94**'s mechanism of action.

Haemoglobin is a known scavenger of nitric oxide[6, 9, 10], with the ferric centre of haemoglobin readily able to bind to nitric oxide *in vivo*. Introducing a NO scavenger into the experiment (graph 20) could assess what overall action NO release from **94** has on the vessel if it is not acting via the sGC activation pathway.

The effects of haemaglobin on NO-donors SNP and lead compound 94
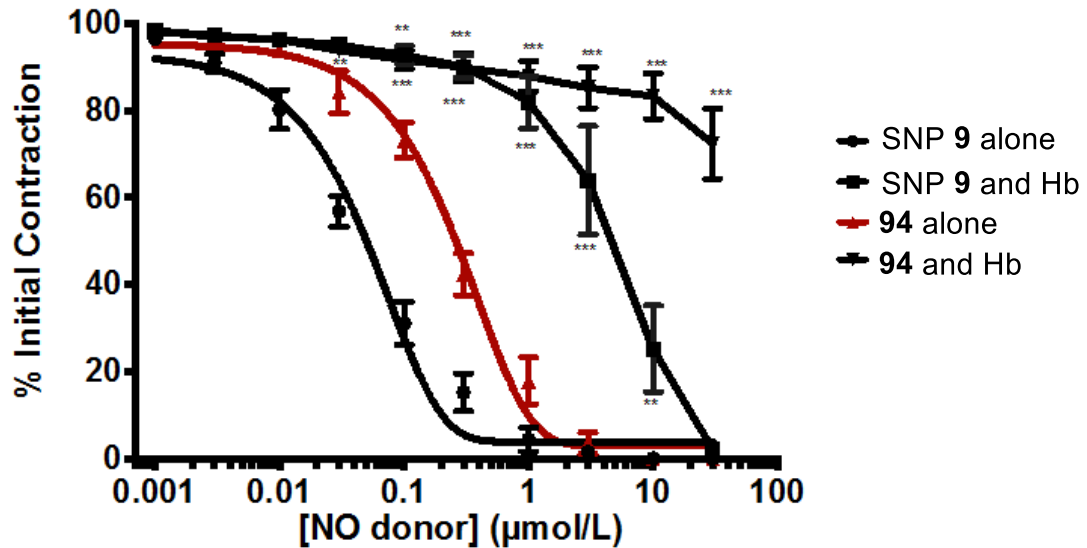
Graph 20: Effect of 10 μM haemoglobin on nitrovasodilator effect. Haemoglobin was added prior to addition of methoxamine. All vessels were pre-contracted with 10^{-5} M methoxamine before addition of compound **94** or SNP (**9**). Data are means ± SEM. Statistical analysis was conducted and significance is shown by P <0.05 = *; P <0.01 = **; P <0.001. A student's *t*-test shows that the effect of haemoglobin on SNP and compound 94 is significant (*P*=0.0042 and 0.0078 respectively). (n= 5-7).

Graph 20 shows the effect of haemoglobin (Hb) on SNP **9** and compound **94**. It appears that SNP **9** is not greatly affected by the scavenging properties of haemoglobin as almost 100% relaxation still occurs; the effect of vasodilation in the presence of haemoglobin is probably due to the NO release saturating haemoglobin and then surplus NO being free to bind to sGC and promote relaxation. When compound **94** is exposed to haemoglobin the effect is much more drastic. The relaxation profile of compound **94** is completely reversed upon NO scavenging with only 20% relaxation being brought about, even at concentrations close to 100 μM, a 200 fold increase in concentration from the IC$_{50}$ of compound **94** with Hb. The fact that very little relaxation occurs in the presence of Hb confirms that compound **94** works by the release of nitric oxide, consistent with what was observed using the nitric

oxide analyser. This observation suggests that NO release from compound **94** is more of a causative agent that induces a vasodilation cascade rather than directly causing relaxation.

One explanation of why compound **94** is able to observe an effect upon relaxation when sGC has been inhibited with ODQ, is that compound **94** is interacting with eNOS enzymes present in the aortic ring and perhaps stimulating them to produce more NO and therefore combat the inhibition of sGC. To test this theory, L-NAME and Indomethacin, two known NOS inhibitors aforementioned in chapter 1 were introduced to the pre-inhibited aortic rings, to see if compound **94**'s relaxation profile changed from Graph 18.

Group comparison of molecular inhibitors on the effect of lead compound **94**

Legend:
- **94** + Indomethacin (10 μM)
- **94** + L-NAME(100 μM)
- **94** + ODQ (20 μM)
- **94** alone
- DMSO
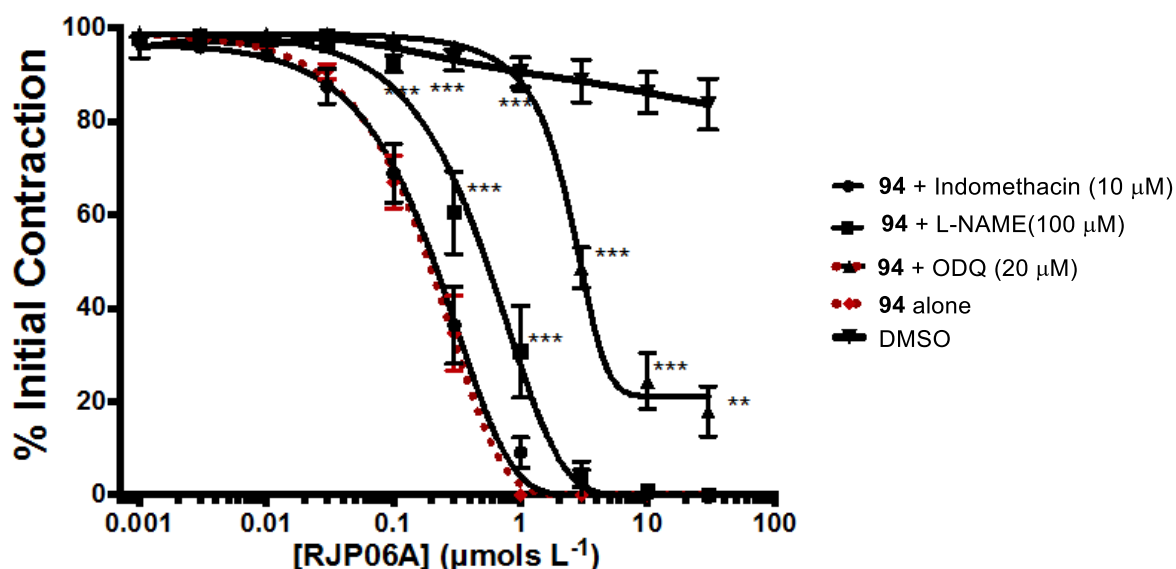
Graph 21: A group comparison of molecular inhibitors used on the effect of compound **94**. Inhibitors were added ten minutes prior to the addition of methoxamine to allow time to act. Aorta rings were pre-contracted with 10^{-5} M methoxamine Data are means $\pm$ SEM. Statistical analysis was conducted comparing inhibitors with control compound **94** and significance is shown by $P <0.05$ = *; $P <0.01$ = **; $P <0.001$ = ***. (n = 5-7 animals).

Graph 21 shows that inhibition of the NOS enzymes present in the aortic vessel has no effect on the relaxation profile of compound **94** and therefore indicates that there is no interaction between the furoxan compound and the NOS enzymes. This therefore suggests that relaxation of the aortic smooth muscle occurs by an alternative mechanism to that of SNP. In the presence of L-NAME there is only

a small loss of potency of compound **94**, shifting the sigmoidal profile slightly to the right, but still producing 100% relaxation. This suggests that the presence of the NOS inhibitor does not affect the relaxation potential of compound **94** and that in fact the NOS inhibitor is more likely disrupting any NO being produced by the aortic endothelium itself. To further account for any endogenous NO interfering with the relaxation profiles, and to attempt to explain the mechanism of action, the endothelium was removed from the aortic ring entirely. The removal of this layer of cells should remove any endogenous NO affecting the results as eNOS will no longer be present in the experiment. This was also compared to eNOS inhibited with L-NAME aortic muscle.

Graph 22: A group comparison of molecular inhibitors used on the effect of compound 94. Inhibitors were added ten minutes prior to the addition of methoxamine to allow time to act. Aorta rings were pre-contracted with 10^{-5} M methoxamine Data are means ± SEM. Statistical analysis was conducted comparing inhibitors with control compound **94** and significance is shown by P <0.05 = *; P <0.01 = **; P <0.001= ***. (n = 5-7 animals).

Graph 22 shows that with the endothelium layer removed and no endogenous nitric oxide being produced, there is still 100% relaxation when the aortic rings are treated with compound **94**. Almost identical profiles can be seen with the inclusion of a NOS inhibitor, confirming that compound **94** works independently to that of endogenous NO production and the relaxation seen from compound **94** is solely from the furoxan rings decomposition of this ring. The difference in the two profiles can be used to calculate how much NO endogenous contributes to the relaxation of aortic smooth muscle when compound **94** is applied. It can be concluded that compound **94** does produce relaxation of aortic smooth muscle in an independent process to that of SNP and with a larger V_{max}.

2.3.2- Is relaxation induced through potassium channels?

The data for compound **94**, upon inhibition of sGC (graph 18) and scavenging with Hb (graph 20), indicates that an alternative pathway to relaxation via a direct NO route is in operation here. Potassium channels have been shown to be involved in NO-mediated vasodilation.[11-13] Potassium channels are found in most cell types and are involved in a number of other physiological processes such as neurotransmission and endocrine function, to which NO is also known to contribute. In these processes involving potassium channels there are four main classes[14]: Voltage-gated potassium channel (K_v), ATP-sensitive potassium channel (KATP), large conductance calcium-activated K channels (BK) and inward rectifier K channel (KIR). Voltage-gated potassium channels are by far the largest class, and are frequently used by biologists for experimentation and were hence used in this analysis.
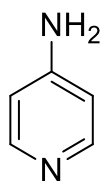
209
4-aminopyridine (4-AP)
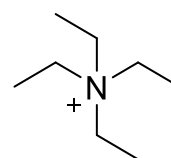
210
Tetraethylammonium (TEA

Figure 81: 4-Amino pyridine **209** and tetraethylammonium **210**, two common potassium channel blockers that were used to assess the potential mechanism that compound **94** operates through in order to bring about the vasodilatory profiles seen previously.

To test the hypothesis that compound **94** was inducing relaxation by synergistically working with potassium channels, two different channel blockers (Fig. 81) were utilised. If no or less relaxation occurs when the potassium channels are blocked then it suggests that compound **94** induces dilation through the use of these channels. 4-Amimpyridine (4-AP) **209** and tetraethylammonium (TEA) **210** are two commonly used potassium channel blockers, and were utilised in this experiment. 4-AP **209** is known to block voltage-gated K^+ channels and TEA is a known inhibitor of calcium dependent K^+ channels.
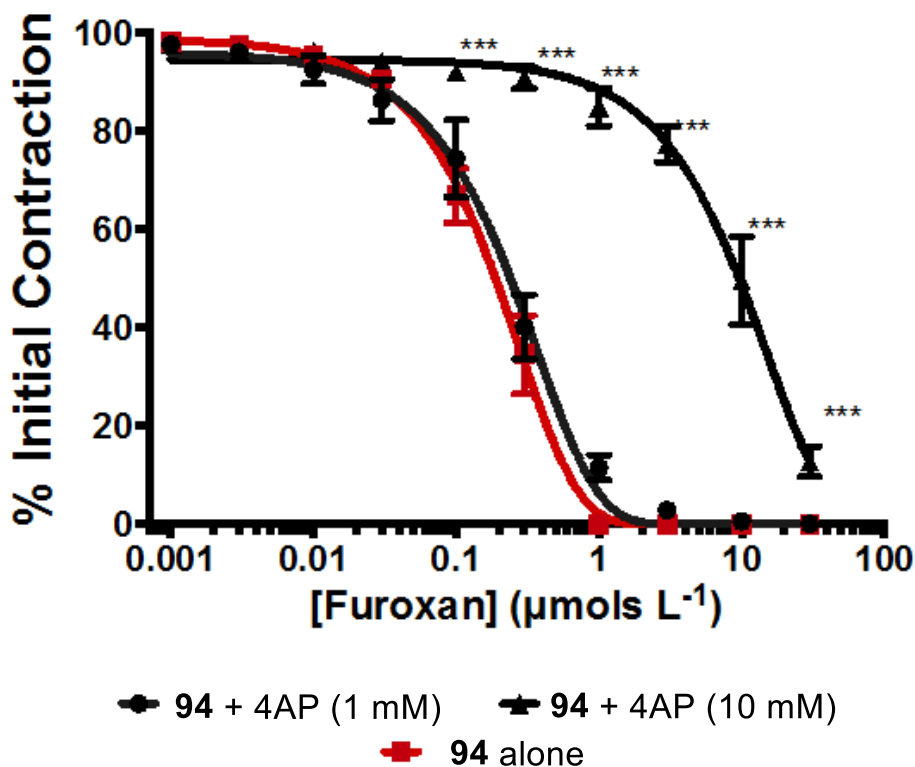
Graph 23: Comparison of different concentrations of the K_v channel blocker 4-aminopyridine **210**. The channel blocker was allowed to incubate in the vessels for ten minutes before contraction. Aorta rings were pre-contracted with 10^{-5} M methoxamine. Data are means ± SEM. Statistical analysis was conducted and significance is shown by P <0.05 = *; P <0.01 = **; P <0.001. According to a paired student's *t*-test, the difference between the effect of the two concentrations is significant (*P*=0.0114). (n= 6-8 animals).

In the presence of 1 mM of 4-AP **209**, there appears to be no effect on the relaxation profile of compound **94**. It takes a 10 fold increase in K^+ channel inhibitor to cause a difference in the relaxation profile. With a 10 mM concentration of 4-AP **209** inhibiting all potassium channels, it requires 10µM of compound **94** to induce vasodilation. This suggests that there is a correlation between furoxan-mediated vasodilation and the voltage-gated potassium channel (K_v). This paradigm was confirmed by introduction of the second potassium channel blocker, TEA (graph 24).

At a concentration of 10 mM TEA **211** produced a similar effect on relaxation to that of 4-AP **209**. Compound **94**'s IC_{50} in the presence of TEA is 10 µM compared to an IC_{50} of 0.2 µM without the presence of a K^+ blocker. Combining both K^+ channel blockers, prompted a dramatic effect on compound **94** induced relaxation increasing the IC_{50} to upwards of 50 µM. The action of two different potassium channel blockers indicates that compound **94** causes vasodilation from interaction with both voltage-gated and calcium dependent potassium channels.

Comparison of each K^+ channel blockers on the releaxation potential of **94**

● **94** + 4-AP (10 mM)   ◆ **94** alone
■ **94** + TEA (10 mM)   ▲ **94** + 4-AP (10 mM) and TEA (10 mM)
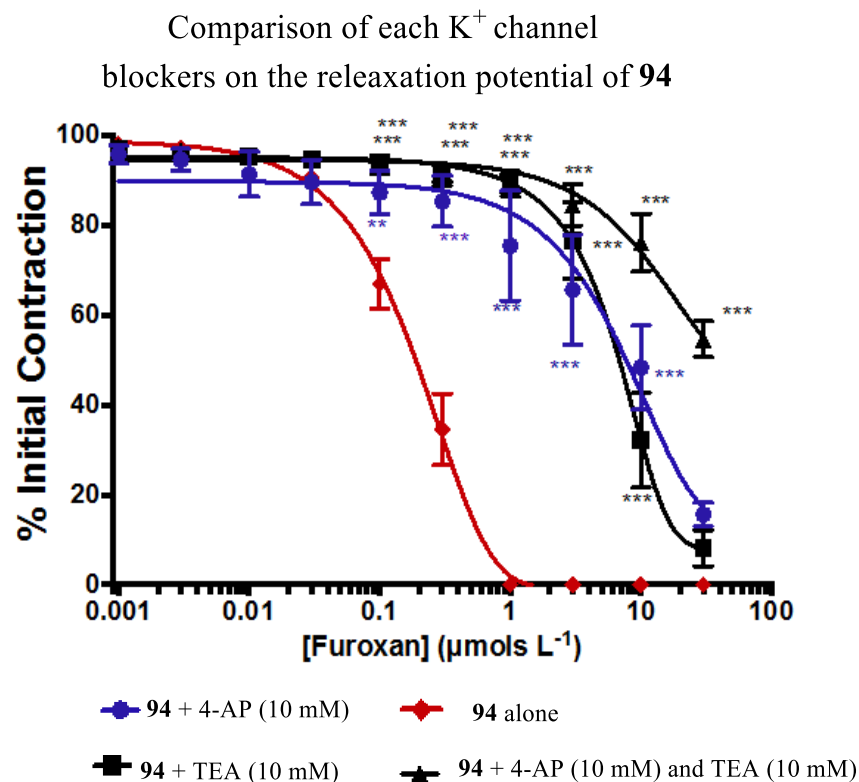
Graph 24: Comparison of each of the potassium channel blockers used in this investigation to elucidate which, if any potassium channels are implicated in compound 94-mediated vasodilation. Channel blockers were allowed to incubate in the vessels for ten minutes before contraction. Aorta rings were pre-contracted with 10^{-5} M methoxamine. Data are means ± SEM. Statistical analysis was conducted and significance is shown by $P < 0.05 = *$; $P < 0.01 = **$; $P < 0.001$ (N=6-8 animals).

Rat aorta rings were pre-contracted with methoxamine and left to incubate with the appropriate potassium channel inhibitor for 10 minutes before introduction of compound **94**. Graph 24 shows that compound **94** is capable of reversing the inhibition of potassium channels and producing around 80% relaxation of the aortic vessel, however this requires a large increase in concentration of the furoxan compound, upwards of 10 μM and 100% relaxation is still not observed. As vasodilation occurs in all blood vessels and not just the aorta, compound **94**'s relaxation potential was tested against two other vessels and compared to the previous finding within the rat aorta.
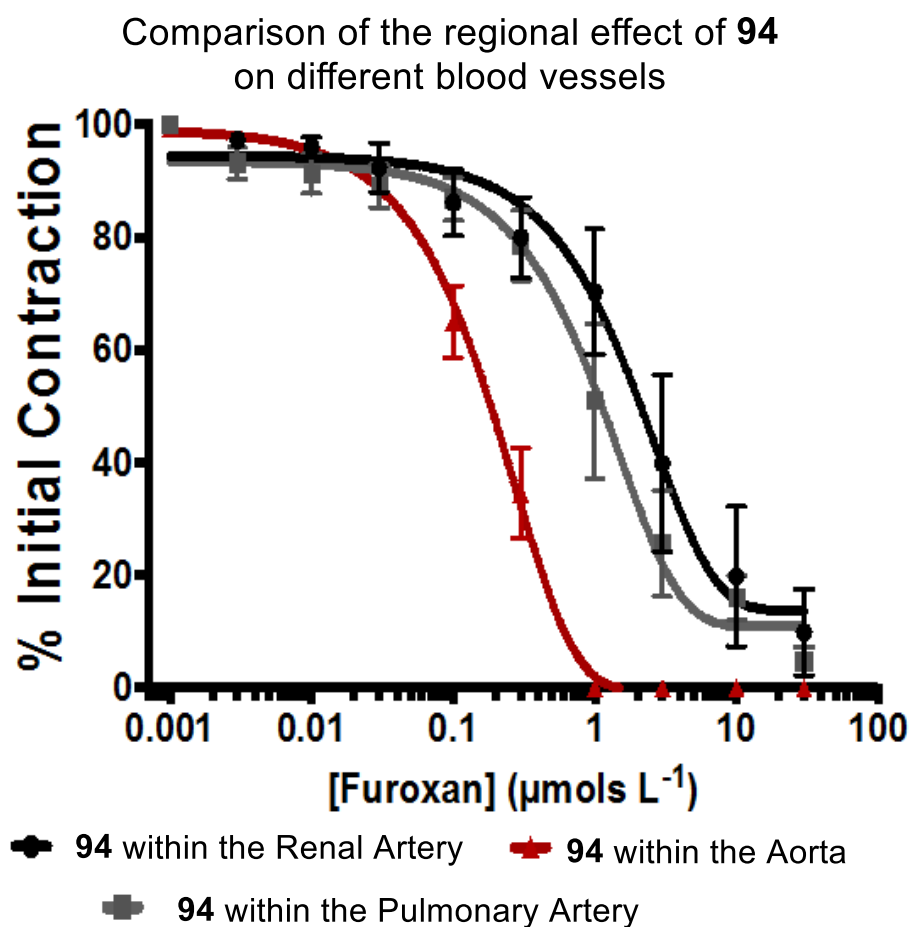
Graph 25: A comparison of the regional effect of compound **94** in different vessels. All vessels were pre-contracted with 10^{-5} M methoxamine before addition of **94**. These data were not obtained concurrently; renal and pulmonary artery results were obtained simultaneously on a myograph and the aorta data were obtained using organ baths. Data are means ± SEM (n= 5-7).

Graph 25 shows that compound **94** does produce effective relaxation in all three blood vessels. However, only 100% relaxation is seen for the aortic smooth muscle with the renal and pulmonary only being relaxed by 18 and 15% respectively. This effect may be due to the size of the respective blood vessels; the renal and pulmonary are considerably smaller in diameter than the aortic muscle and therefore have a slightly different vasculature. Smaller vessels contain other endothelium-derived vasodilators such as prostacyclin and endothelium derived hyperpolarising factor (EDHF).[15-17] It can therefore be said that compound **94** is a more potent vasodilator for larger diameter vessels, which suggests potential applications linked to cardiac arrest for example.

To be an effective pharmaceutical compound, the effects of compound **94**-mediated vasodilation on blood vessels, needs to be assessed in even greater detail. Ideally its mode of action will be reversible and allow for repeated use once the initial effects have worn off. A common comparison compound is the effect of carbon monoxide (CO) on haemoglobin, an irreversible reaction which renders the protein out of action. To assess this potential, a two-curve protocol was used. Aortic vessels were contracted with methoxamine and re-dilated using 1 µM of compound **94** until its maxima was reached. The organ bath was then washed out and re-contracted at different time intervals. The results for this experiment are shown in graph 26.

**Time dependent effects showing the reversibility
of vasorelaxation induced by lead compound 94 .**
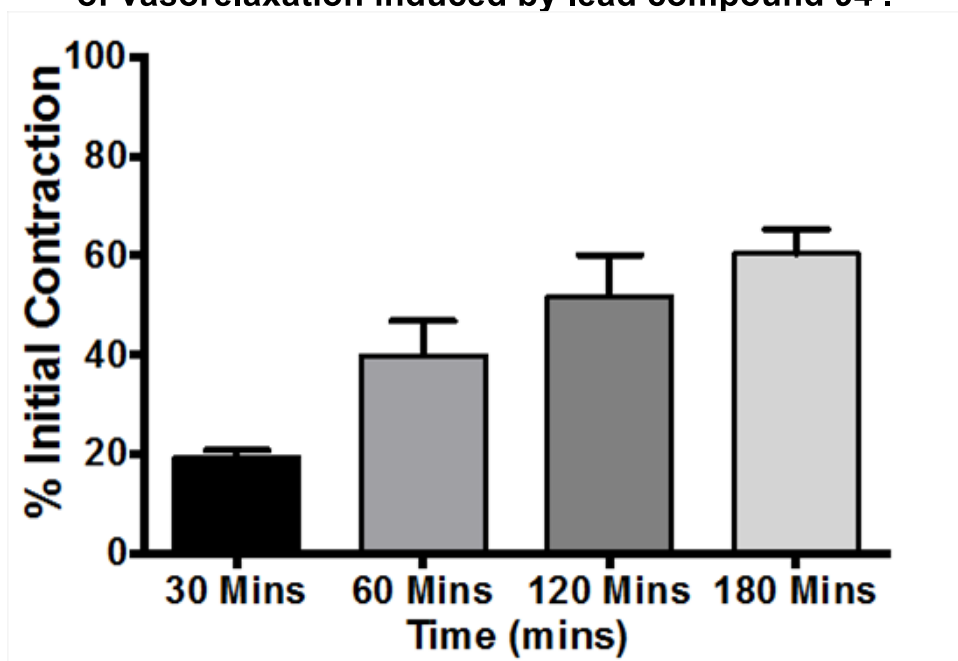
Graph 26: Comparison between first and second response curves; initially contracting the aorta with methoxamine and relaxing with 1 µM of **94**, and then allowing the vessel to rest for set periods of time before attempting to re-contract using methoxamine again.

Graph 26 indicates that the process of vasodilation caused by compound **94** is a reversible one. Thirty minutes after the initial contraction and subsequent relaxation with compound **94** only 20% contraction was observed upon re-contraction with methoxamine **202**. As more time passes towards that of 180 minutes, the ability of the smooth muscle to re-contact increases to that of 60%, suggesting that there is a lag time of at least 180 minutes before the aortic smooth muscle can be fully contracted again by methoxamine **202**.

 Biological tests conducted on compounds shown in Fig. 79 found that the majority of compounds induced vasodilation to some degree. Out of the compounds tested, all except compounds **90, 96** and **204**, managed to produce 100% reversal on the aortic rings that were pre-contracted with methoxamine. Compound **205** was found to be an effective vasoconstricting agent instead of inducing relaxation but is supported by the data found in the anti-cancer studies[3]. There is good evidence, in combination with the results from the NO release studies (chapter 2.2), that the

synthetically produced NO-donors are capable of releasing nitric oxide and in concentrations high enough to induce a biological effect.

Isolation of the lead compound **94** enabled further insight into the potential mechanism of action of these furoxan based NO-donors. Results shown in graphs 18-20 indicate that relaxation does not occur by the sGC pathway as inhibition of this route still produced 100% relaxation by compound **94**. In the presence of a nitric oxide scavenger such as haemoglobin (Hb), **94**'s activity was greatly diminished, only producing 20% relaxation. This observation confirms that **94** does induce vasodilation through the release of nitric oxide, but through an alternative mechanism to that of SNP **9** and the sGC pathway. Further experiments alluded to the idea that relaxation is stimulated through the use of K^+ channels. Graphs 23 and 24 indicate that with inhibition of these potassium channels, the effects of compound **94** are far less potent, needing 50x more furoxan to bring about full relaxation. Evidence was also found to suggest that the potency of compound **94** is vessel dependent, as **94** performed 10x better in the aortic vessel than it did in the renal and pulmonary arteries. However, this may be due to the relative size of the vessel but is nevertheless and interesting observation.

When compared to an existing NO-donor, such as SNP **9**, the results are interesting. Graphs 15-17 show that SNP **9** is a better vasodilator under the conditions used, but compound **94** produces 100% relaxation at much lower concentrations than SNP (graph 15) in the aortic vessel. In the pulmonary artery (graph 17) SNP **9** fails to bring about 100% relaxation, whereas 10 μM of compound **94** completely reverses methoxamine induced contraction.

As SNP is the 'gold standard' NO donor used by our collaborators, compound **94**'s relaxation profile is impressive. Although (as seen in graph 16) it is less potent than SNP, compound **94** produces a more sustained relaxation over time, suggesting that although a slightly higher concentration is needed initially, sequential doses may be needed less frequently. Compound **94**'s relaxation profile was also found to be highly reproducible and reversible as shown in graph 26. After initial relaxation of the aortic vessel with compound **94**, aortic cells were washed out and left for allotted time periods before being successfully re-contracted with methoxamine **202.** This showed that over time

relaxation could be achieved again as the induction of vasorelaxation by compound **94** does not occur through a damaging process, and is in fact reversible and reproducible giving further scope to its use as a lead compound for any future biological work.

2.3.3- References

1. G. Nagaiah and S.C. Remick, *Future Oncol.*, 2010, **6**, 8, 1219-1228

2. Compendium of Chemical Terminology, IUPAC, 2014, version 2.3.3- web address: http://goldbook.iupac.org/PDF/goldbook.pdf. Date accessed 27/10/2015

3. M. E. Richardson, PhD thesis, Keele University, 2012

4. Joint Formulary Committee. British National Formulary. 64 ed. London: BMJ Group and Pharmaceutical Press; 2012. Page 110

5. J. A. Friederich and J. F. Butterworth IV, *Anesthesia and Analgesia*, 1995, **81**, 152-162

6. A. Butler, and R. Nicholson, "Life, Death and Nitric Oxide", RSC paperbacks, The Royal Society of Chemistry, Cambridge, 2003.

7. C. Napoli, and L. J. Ignarro, *Nitric Oxide*, 2001, **5**, 88-97

8. M. Feelisch, P. Kotsonis, J. Siebe, B. Clement and H. H. H. W. Schmidt, *Molecular Pharmcol.*, 1999, **56**, 2, 243-253

9. A.R. Butler, I. L. Megson and P. G. Wright, *Biochemica et Biophysica Acta*, 1998, **1425**, 168-176

10. J. O, Dreier, K. Korner, N. Ebert, A. Gorner, I. Rubin, T. Back, U. Lindauer, T. Wolf, A. Villringer, K. M. Einhauol, M. Lauritzen and U. Dirnagl, *J. Cereb. Blood. Flow*, 1998, **18**, 978-990

11. T. J. Jentsch, *Nature reviews: Neurosci.*, 2000, **1**, 21-30

12. M. V. Soldovieri, F. Miceli and M. Taglialatela, *Physiol.*, 2011, **26**, 365-376

13. T. A. Jepps, S. P. Olesen and I. A. Greenwood, *Br. J. Pharmacol.*, 2013, **168**, 19-27

14. J. B. Stott, T. A. Jepps and I. A. Greenwood, *Drug Discov. Today*, 2014, **19**, 413-424

15. M. R. Miller and I. L. Megson, *Br. J. Pharmacol.*, 2007, **151**, 305-321

16. D. J. Green, J. H. Walsh, A. Maiorana, A. Burke, R. R. Taylor and J. G. O'Driscoll, *J. Appl. Physiol.*, 2004, **97**, 2, 749-755

17. S. Kawashima and M. Yokoyama*, Arterioscler. Thromb. Vasc. Biol.*, 2004, **24**, 998-1005

Chapter 3.0- Conclusions

Conclusions drawn on results presented in chapter 2.0

The aim of this project was to discover a method to successfully moderate the levels of nitric oxide in attempt to provide suitable compounds for the application of a variety of medical conditions known to be affected by the concentration of nitric oxide, such as angina, ischemia and Alzheimer's disease. The synthesis of compounds that release nitric oxide under a variety of conditions was largely successfully. Furoxan compounds substituted in a logical and systematic way were synthesised using a combination of acetic acid and dilute nitric acid along with a catalytic amount of sodium nitrite ($NaNO_2$). Furoxan compounds **86-128** were analysed for their ability to release NO using a Siever's nitric oxide analyser (NOA); all compounds were found to release NO under both photochemical and oxidative conditions. The furoxan compounds appear to be photosensitive, releasing the majority of NO in the presence of light (254 nm) and as well as under conditions of ambient light.

Collaborators at Kingston University tested the furoxan compounds for their ability to reverse methoxamine induced constriction of aortic, pulmonary and renal arteries. It was observed that all compounds bar **205** induced vasodilation of the vascular structure and produced IC_{50}'s ranging from 0.25-20.5 μM. Compound **205** in fact increased the constriction of the blood vessel passed that of methoxamine, and can therefore be considered of a vasoconstriction agent similar to that of combretastatin. Compound **94** substituted with an OCF_3 group in the *para* position, produced an IC_{50} of 0.25 μM. This led to its use as a lead compound in further biological tests and was found to induce 100% relaxation of aortic smooth muscle and produced a more sustained relaxation compared to that of the BNP listed SNP. Analysis also showed that compound **94**'s action on aortic smooth muscle is a reversible one, as with a suitable lag time (180 minutes) and introduction of methoxamine, re-contraction could be brought about. This is obviously an advantageous attribute of compound **94** as it means that the vascular tone is not permanently changed in the presence of **94**.

The stabilisation of the industry chelator cupferron **56** was also successful using simple alkylation chemistry. Serendipitous crystallisation also afforded the isolation of a single crystal structure of compound **103**. This led to the confirmation that the site of alkylation was in fact on the terminal oxygen (shown in Fig. 54 in section 2.1.2.1, page 116) of cupferron as predicted. NO release work established that the alkylation chemistry had stabilised cupferron, with all compounds releasing less NO under the experimental conditions than the parent compound. Compound **103** was the most stable at both 25 and 37°C when compared to cupferron. All cupferron derivatives **99-101** and **103-105** were capable of releasing nitric oxide under both photochemical and thermal conditions. The classic alkylation chemistry used, not only provided the desired cupferron derivatives but also produced evidence of some very interesting by-products. The intramolecular ring closure reaction produced the 8, 10 and 12 membered heterocycles (shown in Fig. 57 and 58 in section 2.1.2.1, page 118). The isolation of these ring systems had not been reported previously but was confirmed through the use of HRMS. In terms of increasing the levels of nitric oxide, a variety of novel NO-donors that are capable of producing nitric oxide under thermal, oxidative and photochemical conditions and therefore are a set of tailorable NO-donors, have been successfully synthesised. Biologically the NO-donors tested were efficient in producing vasodilation in pre-contracted blood vessels. The cupferron series are yet to be tested as anti-cancer or vasodilatory agents but their comparison to the furoxan series will be very interesting.

Reducing the levels of nitric oxide using NOS inhibitors remains a viable and relevant avenue to further explore. The rationale developed from the three-dimensional work in the KAVE (Keele Active Virtual Environment) is certainly very robust and compelling, especially with regard to the potential for hydrogen bonding interactions between nNOS inhibitors and the propionic acid functionality of the enzyme's heam centre. An interesting literature precedent, using phenyl lithium to deprotonate the *ortho* position of trimethylpyridine has been successfully found and tested producing a successful alkylation albeit in low yield. With further optimisation of this reaction the nNOS inhibitors shown in section 1.3 can by synthesised. With the successful synthesis and purification of these inhibitors, further docking studies and testing can be conducted which may

allude to the key structural features being uncovered and ultimately allow an improvement in the potency and selectivity of nNOS inhibitors of this type.

Chapter 4.0- Experimental

Synthesis, purification and characterisation of compounds

All commercial solvents were purchased from either Sigma Aldrich or Ficher Scientific and unless otherwise stated were used without further purification. THF was distilled using sodium benzophenone under anhydrous conditions. Diethyl ether was stirred for 24 hours over calcium hydride under anhydrous conditions and used directly. *N,N*-Dimethylformamide was purchased in anhydrous form. TLC plates used were silica gel 60 F_{254} (Merck) and detection was conducted using UV light or vanillin stain. Melting point determination was completed using a Bibby Stuart Scientific Melting point apparatus (uncorrected).

IR spectra were recorded using Thermo Nicolet FT-IR Nexus with an Avatar Smart Omni Sampler and diamond crystal. Scan rate was set at a minimum of 32 scans. ^{1}H NMR and ^{13}C NMR spectra were obtained using Bruker Avance 300 operating at frequencies 300.13 and 75.47MHz respectively and referenced using the following internal standards. δ_H $CDCl_3$: 7.24 ppm, DMSO: 2.50 ppm, δ_C $CDCl_3$: 77.36 ppm, DMSO: 40.45 ppm. ^{19}F NMR spectra were obtained using a Bruker Avance 400 operating at 376. 41 MHz and using the internal standard, δ_F CF_3Cl: -28.6 ppm

Accurate mass spectrometry data was obtained from NMSF (EPSRC National Mass Spectrometry Facility). The instrument used to obtain accurate mass data is noted after the mass data. LTQ Orbitrap refers to Thermofisher LTQ Orbitrap XL (High resolution instrument giving accurate mass measurement over the full mass range in electrospray), MAT 95 refers to Finnigan MAT 95 XP (EI, CI, LSIMS, ESI and APCI capability), ASAP refers to Atmospheric-pressure Solids Analysis Probe.

3-(4-Iodophenyl)-4-(2,4,6-trimethoxyphenyl)-1,2,5-oxadiazole 2-oxide[1], **80**
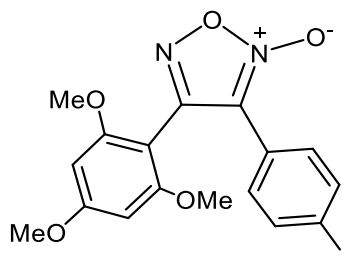
80

To a stirred solution of (1*E*,2*E*)-1-(4-iodophenyl)-2-(2,4,5-trimethoxyphenyl)ethane-1,2-dione dioxime (0.119g, 0.26mmol) in acetonitrile (10ml) copper (II) chloride (0.1g, 0.78mmol) and sodium perchlorate (0.19g, 1.56mmol) were added turning the solution green and then gradually turned a pale brown over the course of 12 hours. The resulting brown solution was poured into a separating funnel and upon standing revealed a green oil, which was then separated. This oil was dissolved in distilled water (5ml) before aqueous ammonia (30ml) was added, causing the solution to immediately turn a deep blue colour. The blue solution was left to stir vigorously for 3 hours before being extracted with chloroform (4 x 20ml). The combined organic layers were dried over MgSO$_4$ and concentrated to give the title compound as a pale yellow solid, 0.2 g, 16%. δ_H (300 MHz, CDCl$_3$) 4.19-4.10 (m, 9H), 7.46 (dd, *J* = 5.56, 3.37 Hz, 2H), 7.64 (dd *J* = 5.55, 3.33 Hz, 4H).

3,4-Bis(3,4,5-trimethoxybenzoyl)-1,2,5-oxadiazole-2-oxide[2, 3, 4,] **86**

86
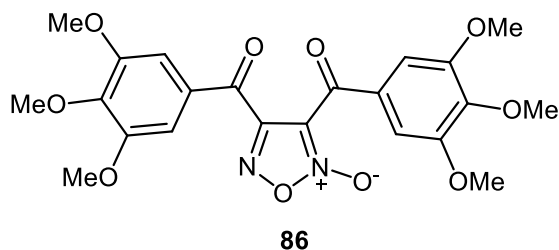
To a solution of 3,4,5-trimethoxyacetophenone, (5.0 g, 23.7 mmol) in glacial acetic acid (30ml.) dilute nitric acid (8 mL in 15ml H_2O) was added drop-wise over the course of 30 minutes. A catalytic amount of $NaNO_2$ was then added to the solution which was then heated to 60°C for 2 hours. TLC showed an incomplete conversion so the reaction was maintained at 60°C for a further 2 hours. The reaction was then cooled to room temperature and a small amount of ice was added to quench the reaction and to encourage precipitation. No precipitate formed, so the solution was extracted with DCM (3 x 30 mL). The combined extracts were washed with water (25 mL), brine (25 mL), and dried over $MgSO_4$. The combined extracts were combined and reduced to give a red solid (3.23g), this was then purified by column chromatography (hexane:ethyl acetate 10:1 to 1:1, followed by 100% ethyl acetate) to yield the title compound as red/orange solid 1.01 g, 9.0%, R_f: 0.86 (petroleum ether :ethyl acetate, 1:1) Mp: 117.3-119.8°C (Lit Mp: 116-118°C[4]), IR (cm^{-1}), 3099 C-H (Ar), 2943 C-H (Ar), 2839 C-H (Methyl), 2659 C-H (Methyl), 1675 (C=O), 1606 (C=N), 1455 (C=N^+-O^-), 1331 (Methyl), 1120 (C-O-Me), δ_H NMR (300 MHz, $CDCl_3$) 3.75-3.94 (m, 18H), 7.01 (s, 1H), 7.36 (s, 1H), 7.41 (s, 2H), δ_C NMR (75 MHz, $CDCl_3$) 56.2 (2 x OCH_3), 56.3 (2 x OCH_3), 60.9 (2 x OCH_3), 101.1 (2 x Ar-C), 111.9 (C=N^+-O^-), 128.5 (2 x Ar-C), 128.7 (Ar-C), 144.5 (Ar-C), 144.5 (C=N), 152.7 (2 x Ar-$\underline{C}OCH_3$), 153.1 (2 x Ar-$\underline{C}OCH_3$), 153.2 (2 x Ar-$\underline{C}OCH_3$), 179.0 (C=O), 180.3 (C=O). MS theoretical (m/z): 474.1270. Actual: 475.1347 ±0.0 ppm for $C_{22}H_{22}N_2O_{10}$.

3,4-Bis(4-ethylbenzoyl)-1,2,5-oxadiazole 2-oxide[2,3,4], **87**
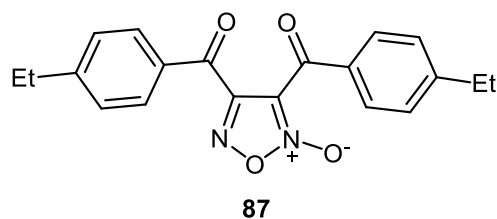
87

To a solution of 4-ethylacetophenone (2.9g, 20.0mmol) in acetic acid (30ml), dilute nitric acid (12.5 ml in 18ml H_2O) was added drop-wise over the course of 30 minutes. The reaction was slowly heated to 55°C and a catalytic amount of $NaNO_2$ was added causing the evolution of brown fumes and turning the solution an orange colour. The reaction was left to stir at 55°C for 2 hours, at which time more $NaNO_2$ was added and the reaction left for a further 2 hours. The reaction was then cooled to room temperature and then added drop-wise onto ice to produce a yellow precipitate of the title compound, 2.2g 29%. Mp: 78.8-79.6°C, IR (cm^{-1}): 2964, 2930, 2872, 1677, 1600 (C=N), 1457 (C=N$^+$-O$^-$), 1245, 895. δ_H (300 MHz, CDCl$_3$) 1.26 (dd, J = 6.8, 6.8 Hz, 6H), 2.73 (q, J = 7.62, 7.62, 7.62, 7.62 Hz, 4H), 7.51-7.02 (m, 4H), 7.84-7.73 (m, 2H), 8.12 (m, 2H) δ_C (75 MHz, CDCl$_3$) 14.9, 15.0, 29.2 (2C), 111.9 (C=N+-O-) 128.5 (2C), 128.8 (2C), 129.9 (2C), 130.8 (2C), 131.5, 131.6, 152.8, 153.0, 154.5 (C=N), 180.0 (C=O), 181.3 (C=O). MS: theoretical (m/z): 357.1159. Actual: 373.1157 ± 0.5 ppm corresponding to $C_{20}H_{18}N_2O_4$ +Na.

3,4-Bis(4-methylbenzoyl)-1,2,5-oxadiazole 2-oxide[2] **88**
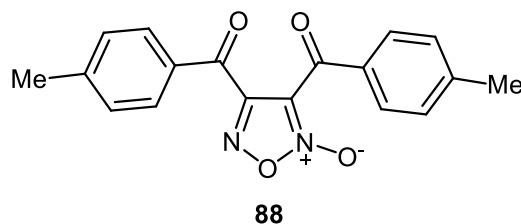
88

4-Methylacetophenone (5.0g, 37.3mmol) was dissolved in acetic acid (30 ml) and heated to 60°C under reflux conditions. Dilute HNO_3 (8ml in 20ml H_2O) was added drop-wise to the solution over the course of 30 minutes. A catalytic amount of $NaNO_2$ was added and the reaction was left to reflux for a further 2 hours. The reaction was then left to cool, but no precipitate formed so the solution was extracted with DCM and dried over $MgSO_4$, and concentrated *in vacuo*. The resulting solid was then purified further using flash column chromatography, 10:1 (petroleum ether:ethyl acetate) to give a yellow oil of the title compound, 0.26g, 2%. R_f: 0.93 (petroleum ether: ethyl acetate 1:1) Mp:110-114°C (Lit value[5]: 123-125°C), IR (cm^{-1}), 3271 C-H (Ar), 2923 C-H (Methyl), 2854 C-H (Methyl), 1674 (C=O), 1661 (C=O), 1602 (C=N), 1471 (C=N$^+$-O$^-$), 775 (C-H bend), 753 (C-H), δ_H (300 MHz, $CDCl_3$) 2.43 (s, 3H), 2.46 (s, 3H), 7.33 (dd, *J*= 8.04, 11.62 Hz, 4H), 7.78 (d, *J*= 8.25 Hz, 2H), 8.12 (d, *J*= 8.25 Hz, 2H) δ_C (75 MHz, $CDCl_3$) 21.9 (CH_3), 22.0 (CH_3), 111.9 (C=N$^+$), 129.7 (2C Ar-C), 129.8 (2C Ar-C), 129.9 (4C Ar-C), 130.7 (C-C=O), 131.4 (C-C=O), 146.8 (C-CH_3), 147.0 (C-CH_3), 154.5 (C=N), 180.0 (C=O), 181.3 (C=O). MS: theoretical (m/z) 324.1060, Actual: 323.1020 ±1.0ppm corresponding to $C_{18}H_{15}O_4N_2$.

3,4-bis(4-chlorobenzoyl)-1,2,5-oxadiazole 2-oxide[2,3] **89**

89

To a solution of 4-chloroacetophenone (3.0g, 19.5 mmol) in acetic acid (30ml), dilute nitric acid (12.5 ml in 18ml H_2O) was added drop-wise over the course of 30 minutes. The reaction was slowly heated to 55°C and a catalytic amount of $NaNO_2$ was added causing the evolution of brown fumes and turning the solution an orange colour. The reaction was left to stir at 55°C for 2 hours, cooled and poured drop-wise on to ice. A white solid was filtered off and recrystallized from DCM to give a fine white powder 1.37g 19.4%, R_f: 0.4 (1:1 petroleum ether:ethyl acetate), Mp: 116.4-117.8°C (Lit value[6]: 124°C), IR (cm^{-1}): 3093, 1680, 1661, 1584 (C=N), 1487 (C=N$^+$-O$^-$), 1239, 1088. δ_H (300 MHz, CDCl$_3$) 7.55-7.52 (m, 4H), 7.58-7.49 (m, 2H), 7.86-7.76 (m, 1H), 8.18 (m, 1H), δ_C (75 MHz, CDCl$_3$) 111.3 (C=N$^+$-O$^-$), 129.5 (2C), 129.7 (2C), 131.0 (4C), 131.9 (2C), 142.4 (2C), 154.0 (C=N), 179.1 (C=O), 180.1 (C=O).

3,4-Bis(4-bromobenzoyl)-1,2,5-oxadiazole 2-oxide[2,7] **90**
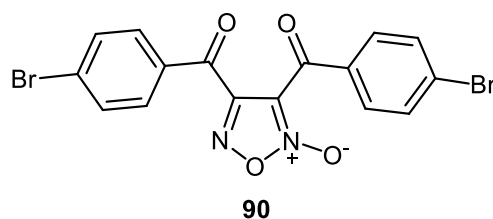
90

4-Bromoacetophenone (10.0g, 50.5mmol) was dissolved in acetic acid (53 ml) and heated to 80°C under reflux conditions. Dilute HNO_3 (11.9ml in 35ml H_2O) was added drop-wise to the solution over the course of 30 minutes. A catalytic amount of $NaNO_2$ was added and the reaction was left to reflux for a further 2 hours. The reaction was then left to cool, forming a precipitate which was then filtered off. The filtrate was extracted with DCM and dried over $MgSO_4$, and concentrated *in vacuo*. The resulting solid was then recrystallized from hot DCM, producing a white precipitate which corresponded to the by-product 4-bromobenzoic acid. The recrystallization was repeated a further four times but the TLC still showed two spots so the final filtrate was then reduced to yield a pale yellow solid and purified further using flash column chromatography, 8:1 (petroleum ether:ethyl acetate) to give white needles of the title compound 2.97g, 12%. R_f: 0.92 (petroleum ether:ethyl acetate, 1:1), Mp: 123.3-124.4°C (Lit value[7]: 128°C). IR (cm^{-1}) 2923 C-H (Ar), 1675 (C=O), 1651 (C=O) 1601 (C=N), 1470 (C=N^+-O^-), 1326 (N-O), 754 (C-Br). δ_H (300MHz, d_6-DMSO) 7.81 (d, J = 8.62 Hz, 2H), 7.88 (d, J = 8.66 Hz, 2H), 7.94 (d, J = 8.62 Hz, 2H), 8.08 (d, J = 8.67 Hz, 2H). δ_C (75MHz, d_6-DMSO) 112.4 (C=N^+-O^-), 129.9 (C-Br), 130.0 (Ar C-C), 131.4 (Ar C-C), 132.0 (Ar C-H, 2C), 132.34 (Ar C-H, 4C), 132.7 (Ar C-C, 2C), 132.8 (C-Br), 153.9 (C=N), 180.0 (C=O), 181.5 (C=O). MS (m/z) theoretical: 449.8851 MS (m/z) actual: 449.8845 ± 2.1 ppm corresponding to $C_{16}H_8O_4N_2Br_2$.

3,4-Bis(4-iodobenzoyl)-1,2,5-oxadiazole 2-oxide[2,3] **91**
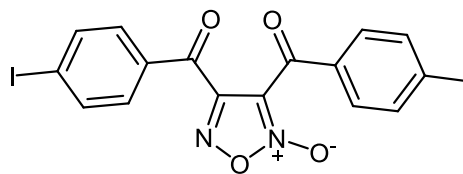
91

To a solution of 4-iodoacetophenone (3.3g, 12.2mmol) in acetic acid (30ml), dilute nitric acid (12.5 ml in 18ml H_2O) was added drop-wise over the course of 30 minutes. The reaction was slowly heated to 55°C and a catalytic amount of $NaNO_2$ was added causing the evolution of brown fumes and turning the solution an orange colour. The reaction was left to stir at 55°C for 2 hours, cooled and poured drop-wise on to ice. A pink solid was filtered off and washed with water (5ml) to give a yellow solid of the title compound, 1.1g. 15%. R_f: 0.94 (1:1 petroleum ether:ethyl acetate) IR (cm^{-1}): 3091, 1685, 1659, 1576 (C=N), 1469 (C=N$^+$O-), 1176, 794. δ_H (300MHz, CDCl$_3$) 7.61-7.45 (m, 4H), 7.92 (m, 4H) δ_C (75MHz, CDCl$_3$) 105.1, 105.2, 112.3 (C=N$^+$-O$^-$), 130.8, 131.5, 132.9 (2C), 133.0 (4C), 138.1 (2C), 153.94 (C=N), 180.3 (C=O), 181.8 (C=O).

3,4-Bis(4-methoxybenzoyl)-1,2,5-oxadiazole 2-oxide[2] **92**

92
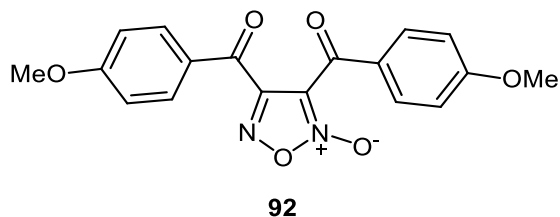
4-Methoxyacetophenone (5.0g, 30.0mmol) was dissolved in acetic acid (35 ml) and heated to 60°C under reflux conditions. Dilute HNO_3 (8ml in 20ml H_2O) was added drop-wise to the solution over the course of 30 minutes. A catalytic amount of $NaNO_2$ was added and the reaction was left to reflux for a further 2 hours. The reaction was then left to cool, but no precipitate formed so the solution was extracted with DCM and dried over $MgSO_4$, and concentrated *in vacuo*. The resulting crude yellow solid (4.54g) was then purified further using flash column chromatography, 10:1 (petroleum ether:ethyl acetate) to give a pale yellow solid of the title compound, 2.24g, 21% R_f: 0.88 (petroleum ether:ethyl acetate, 1:1), Mp: 127.0-128.0°C (Lit value[5]: 138°C), IR (cm^{-1}) 3298 (C-H Ar), 3045 (C-H Ar), 2938 (C-H Methyl), 2843 (C-H Methyl), 1653 (C=O), 1594 (C=N), 1439 (C=N$^+$-O$^-$), 1327 (NO), 1172 (C-O), 1163 (C-O). δ_H (300 MHz, CDCl$_3$) 3.92 (s, 3H), 3.94 (s, 3H) 7.02 (m, 2H), 7.83-7.91 (m, 4H), 8.24 (m, 2H). δ_C (300 MHz, CDCl$_3$) 55.7 (2 x OCH$_3$), 112.2 (C=N$^+$-O$^-$) 114.3, 114.6, 126.7 (2C Ar-C), 126.9 (2C Ar-C), 132.4(2C Ar-C), 133.2 (2C Ar-C), 154.8 (C=N), 165.4 (C-OCH$_3$), 165.5 (C-OCH$_3$), 178.8 (C=O), 179.9 (C=O), MS: theoretical (m/z) 354.0852, Actual: 355.0925 ±0.5ppm corresponding to C$_{18}$H$_{15}$O$_6$N$_2$.

3,4-Bis(4-ethoxybenzoyl)-1,2,5-oxadiazole 2-oxide **93**

93
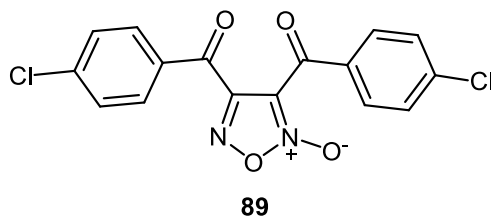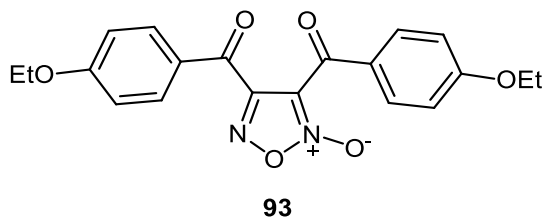
To a solution of 4-ethoxyacetophenone (3.3g, 20.0mmol) in acetic acid (30ml), dilute nitric acid (12.5 ml in 18ml H_2O) was added drop-wise over the course of 30 minutes. The reaction was slowly heated to 55°C and a catalytic amount of $NaNO_2$ was added causing the evolution of brown fumes and turning the solution an orange colour. The reaction was left to stir at 55°C for 2 hours, cooled and poured dropwise on to ice. No filterable solid was recovered so the aqueous solution was extracted with ethyl acetate (3 x 50ml), washed with brine (50ml) and dried over $MgSO_4$ and the solvent removed to give a crude orange gum (1.35g). This was then purified by silica-gel chromatography (petroleum ether : ethyl acetate, 10:1) to give a white solid of the titled compound 0.21g, 2.1%, R_f: (petroleum ether:ethyl acetate, 10:1), Mp: 132.0-133.0°C (Lit value[8]: 131-134°C), IR (cm^{-1}): 3062, 2976, 2890, 1674, 1648, 1615 (C=N), 1471 $(C=N^+-O^-)$, 1258, 1227, 1127. δ_H (300MHz, $CDCl_3$) 1.37 - 1.49 (m, 6 H), 4.05 - 4.17 (m, 4 H) 6.88 - 7.04 (m, 4 H), 7.82 (d, J=9.04 Hz, 2 H) 8.18 (d, J=9.04 Hz, 2 H), δ_C (75MHz, $CDCl_3$) 14.5 (2C), 64.1 (2C), 112.4 $(C=N^+-O^-)$, 114.7 (2C), 114.9 (2C), 126.5 (2C), 126.6 (2C), 132.4 (2C), 154.8 (C=N), 164.8 ($C-OCH_2$), 164.9 ($C-OCH_2$), 178.6 (C=O), 179.8 (C=O). MS: theoretical mass (m/z) 382.1238 Actual: 383.1236 ± 0.4 ppm corresponding to $C_{20}H_{19}N_2O_6$.

3,4-Bis(4-(trifluoromethoxy)benzoyl)-1,2,5-oxadiazole 2-oxide[3] **94**

94

To a solution of 4-trifluoromethoxyacetophenone, (5.0g, 24.5 mmol) in glacial acetic acid (30ml.) dilute HNO_3 (8 mL in 12ml H_2O) was added drop-wise over the course of 30 minutes. A catalytic amount of $NaNO_2$ was then added to the solution which was then heated to 60°C for 2 hours. TLC showed an incomplete conversion so the reaction was maintained at 60°C for a further 2 hours. The reaction was then cooled to room temperature and a small amount of ice was added to quench the reaction and to encourage precipitation. No precipitate formed, so the solution was extracted with DCM (3 x 30 mL). The combined extracts were washed with water (25 mL), brine (25 mL) and dried over $MgSO_4$. The combined extracts were concentrated to give a yellow oil (5.3g). The yellow oil was purified by column chromatography (hexane: ethyl acetate 10:1 to 1:1, followed by 100% ethyl acetate) to yield the title compound as a yellow oil 2.55g, 23%. R_f: 0.6 (hexane:ethyl acetate 1:1), Mp: 58°C, IR (cm^{-1}) 3116 (Ar-H), 2988, 2900, 1694 (C=O), 1693 (C=O), 1600 (C=N), 1475 (C=N$^+$-O$^-$), 1309, 1246, 1202 1155. δ_H (300 MHz, d$_6$-DMSO) 7.58 (dd, J = 19.71, 8.34 Hz, 4H), 8.16 (d, J = 7.42 Hz, 2H), 8.29 (d, J = 7.42 Hz, 2H). δ_C (d$_6$-DMSO, 75 MHz) 112.5 (C=N$^+$-O$^-$), 118.1(2C), 120.6 (2C), 120.9 (2C), 120.9 , 121.5, 131.6, 132.2 (2C), 132.8 (2C), 152.9, 153.9 (C=N), 179.5, 181.5, δ_F {^{1}H} (CDCl$_3$, 376 MHz) -57.5 (6F). MS (m/z) theoretical: 462.0286. MS (m/z) actual: 463.0351 ± 5.0 ppm correlating to $C_{18}H_9F_6N_2O_6$.

3,4-Bis(4-(trifluoromethyl)benzoyl)-1,2,5-oxadiazole 2-oxide[3] **95**

95
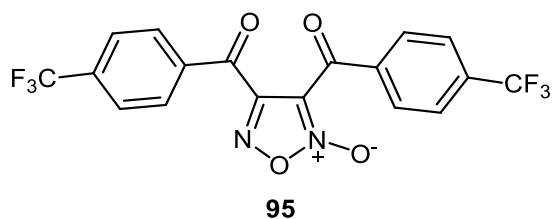
To a solution of 4-trifluoromethylacetophenone, (5.0g, 27.7 mmol) in glacial acetic acid (30ml), dilute nitric acid (8 mL in 15ml H_2O) was added drop-wise over the course of 30 minutes. A catalytic amount of $NaNO_2$ was then added to the solution which was then heated to 60°C for 2 hours. TLC showed an incomplete conversion so the reaction was maintained at 60°C for a further 2 hours. The reaction was then cooled to room temperature and a small amount of ice was added to quench the reaction and to encourage precipitation. No precipitate formed, so the solution was extracted with DCM (3 x 30 mL). The combined extracts were washed with water (25 mL), brine (25 mL), and dried over $MgSO_4$. The combined extracts were purified by column chromatography (hexane: ethyl acetate 10:1 to 1:1, followed by 100% ethyl acetate) to yield the titled compound 2.3g, 20%. R_f: 0.8 (hexane:ether, 3:1), Mp: 76.0-77.9°C, IR (cm^{-1}) 1690 (C=O), 1677 (C=O), 1623 (C=N), 1515, 1470 (C=N$^+$-O$^-$), 1411, 1315. δ_H (300MHz, d$_6$-DMSO) 7.97 (dd, J = 8.38 Hz, J = 18.40 Hz, 4H), 8.21 (d, J = 8.10 Hz, 2H), 8.34 (d, J = 8.10 Hz, 2H)). δ_C (75MHz, d$_6$-DMSO) 112.45 (C=N$^+$-O$^-$), 126.0 (CF$_3$), 126.0 (CF$_3$), 130.2 (2x C=OC-$\underline{C}$H), 130.9 (2 xC=OC$\underline{C}$H), 133.9 (2x C-CF$_3$), 134.3 (4x Ar-C), 136.9 (C=O-$\underline{C}$), 137 (C=O-$\underline{C}$), 153.8 (C=N), 180.3 (C=O), 181.7 (C=O), δ_F {^{1}H} (CDCl$_3$, 376 MHz) –63.4 (3F), -63.3 (3F), MS (m/z) theoretical: 430.0388. MS (m/z) actual: 431.0461 ±5.0 ppm corresponding to $C_{18}H_9O_4N_2F_6$.

3,4-Bis(4-(trifluoromethyl)phenyl)-1,2,5-oxadiazole 2-oxide[9, 10] **96**

96
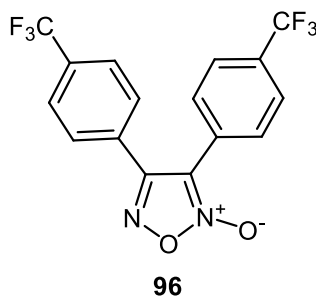
To a stirred solution of (*E*)-*N*-hydroxy-4-(trifluoromethyl)benzimidoyl chloride (0.93g, 4.17mmol) in dry diethyl ether (5ml), dry pyridine (0.34ml, 4.17mmol) was added. The reaction was monitored by TLC (7:3 petroleum ether:ethyl acetate) and left to stir overnight. The precipitate was filtered off and dried in air to give the title compound 0.09g, 5.8%, Mp: 96°C, IR (cm^{-1}): 1694 (C=O) 1599 (C=O), 1600 (C=N), 1470 (C=N$^+$-O$^-$), 1155 (C-O), δ_H (300 MHz, d$_6$-DMSO) 7.40-7.65 (m, 4H), 8.1 (d, *J* = 8.0 Hz, 2H), 8.3(d, *J* = 8.0 Hz, 2H). δ_C (75MHz, d$_6$-DMSO) 121.23 (C=N$^+$-O$^-$), 123.30 (2C, CF$_3$), 125.74 (4C), 129.97 (2C, C-CF$_3$), 130.59 (4C), 130.95 (2C, Ar-C), 160.46 (C=N). MS theoretical (m/z): 375.0563, Actual: 375.0560 ± 0.7 ppm corresponding to C$_{16}$H$_8$F$_6$N$_2$O$_2$.

<u>(<i>Z</i>)-2-Ethoxy-1-phenyldiazene oxide[11]</u> **98**
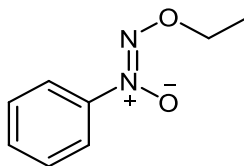
98

Cupferron (5.0g, 32.2 mmol) was dissolved in dry DMF (40ml) under nitrogen conditions and cooled to 0°C before 1-bromoethane (7.21ml, 96mmol) was injected. The resulting yellow solution was left to stir at room temperature in the dark for 3 days. The DMF was then removed via a cold finger apparatus resulting in a dark brown/black sludge which was purified using flash column chromatography in petroleum ether:ethyl acetate (1:1) to give a brown oil of the title compound 1.47g 27%, R_f: 0.57 (petroleum ether:ethyl acetate 1:1), δ_H NMR (300 MHz, CDCl$_3$) 0.76 (t, J = 7.12 Hz, 3H), 3.80 (q, J = 7.12 Hz, 2H), 6.96-6.59 (m, 3H), 7.31 (dd, J = 5.93, 1.57 Hz, 2H) δ_C (75MHz, CDCl$_3$), 13.9, 69.9, 120.3(2C), 128.4, 130.6 (2C), 142.6. MS: theoretical 166.1057 m/z. Actual: 167.0737 corresponding to C$_8$H$_{10}$N$_2$O$_2$.

<u>(Z)-2-Butoxy-1-phenyldiazene oxide[11]</u> **99**
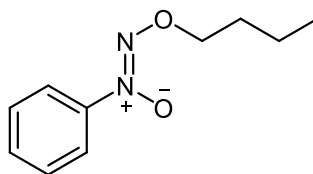
99

Cupferron (2.0g, 12.8 mmol) was dissolved in dry DMF (40ml) under nitrogen conditions and cooled to 0°C before 1-bromoebutane (4.08ml, 38mmol) was injected. The resulting yellow solution was left to stir at room temperature in the dark for 3 days. The DMF was then removed via a cold finger apparatus resulting in a dark brown/black sludge which was purified using flash column chromatography in petroleum ether:ethyl acetate (1:1) to give a brown oil of the titled compound 0.25g 10% R_f: 0.6 (petroleum ether:ethyl acetate 1:1). IR(cm^{-1}): 3095, 2983, 2900, 1471, 1436, 1033, 1021, 817, δ_H NMR (300 MHz, CDCl$_3$) 0.95 (t, J = 7.37 Hz, 3H) 1.82 (td, J = 14.68, 6.92, Hz, 2H), 1.54-1.35 (m, 2H), 4.44 (t, J = 6.78, 6.78 Hz, 2H), 7.56-7.34 (m, 3H), 7.96 (m, 2H) δ_C (75 MHz, CDCl$_3$) 13.7, 18.8, 30.9, 74.7, 121.0, 128.0 (2C), 131.1 (2C,) 143.1. MS: theoretical 195.1128, actual 196.1126 ± 1.0 ppm for C$_{10}$H$_{14}$N$_2$O$_2$.

(Z)-2-(hexyloxy)-1-phenyldiazene oxide[11] **100**
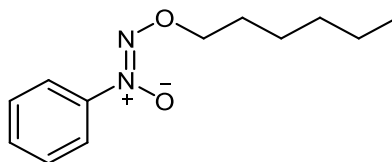
100

Cupferron (5g, 32 mmol) was dissolved in dry DMF (40ml) under nitrogen conditions and cooled to 0°C before 1-bromohexane (13.5ml, 96mmol) was injected. The resulting yellow solution was left to stir at room temperature in the dark for 3 days. The DMF was then removed leaving a dark brown/black sludge (4.56g) which was purified using flash column chromatography in petroleum ether:ethyl acetate (4:1) to give a yellow/brown oil of the title compound 2.57g, 36%, R_f: 0.35 (1:1 petroleum ether:ethyl acetate), IR(cm^{-1}): 3421 (Ar-H), 2937 (CH$_2$), 1681 (N=N), 1477 (N$^+$-O$^-$), 1033, 913, 744, δ_H (300 MHz, CDCl$_3$) 0.95-0.76 (m, 3H), 1.27-1.35 (m, 6H), 1.68-1.91 (m, 2H), 4.43 (t, J = 6.87 Hz, 2H), 7.67-7.14 (m, 3H), 7.97 (m, 2H), δ_C (75 MHz, CDCl$_3$) 13.9, 22.5, 25.2, 28.9, 31.4, 75.0, 121.0, 128.9 (2C), 131.1 (2C), 143.1,

(Z)-2-(Octyloxy)-1-phenyldiazene oxide[11] **101**
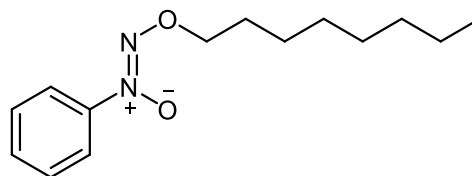
101

Cupferron (10.0g, 64.5mmol) was dissolved in dry DMF (40ml) under nitrogen and cooled to 0°C. To this suspension, 1-bromooctane (3.68ml, 21.3mmol) was injected forming a dark yellow/brown solution. The reaction was left to stir at room temperature for 3 days. The DMF was then removed using a cold finger apparatus resulting in a dark brown tar (6.81g). This was then purified using silica gel chromatography, petroleum ether:ethyl acetate (4:1), to give a dark brown oil of the title compound, 1.45g, 9.06%, Rf: 0.78 (1:1 petroleum ether: ethyl acetate), IR(cm^{-1}): 2925 (Ar-H), 2855 (CH$_2$), 1582, 1503 (N=N), 1476 (N$^+$-O$^-$), 1030, 1015, 764, δ_H (300 MHz, CDCl$_3$) 0.86 (d, J = 1.76 Hz, 3H), 1.33 (d, J = 46.24 Hz, 10H), 1.83 (s, 2H), 3.97-4.74 (m, 2H), 7.79-6.99 (m, 3H), 7.92 (m, 2H), δ_C (75 MHz, CDCl$_3$) 14.1, 22.6, 25.5, 29.0, 29.1, 29.2, 31.7, 75.0, 121.0, 128.9 (2C), 131.1 (2C), 143.2. MS: theoretical 251.1752 m/z, Actual: 251.1754 ±0.8 ppm for C$_{14}$H$_{23}$N$_2$O$_2$.

<u>(1Z,1'Z)-2,2'-(Butane-1,4-diylbis(oxy))bis(1-phenyldiazene oxide)[11] **103**</u>
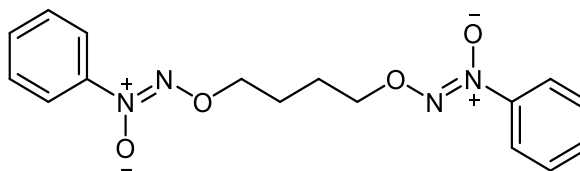
103

Cupferron (10.03g, 64.51mmol) was dissolved in dry DMF (85ml) under nitrogen and cooled to 0°C. To this suspension 1,6-dibromobutane (2.55ml, 20mmol) was injected forming a yellow solution. The reaction was left to stir at room temperature for 1 week resulting in a dark brown/red solution. The DMF was removed using a cold finger apparatus giving a dark brown sludge. This sludge was re-dissolved in DCM (30ml) and extracted with water (3 x 50ml). The organic layers were combined, dried over MgSO$_4$ and the solvent removed *in vacuo*. The product was then purified using flash column chromatography in 8:1 petroleum ether: ethyl acetate followed by 4:1 and 1:1 petroleum ether:ethyl acetate. This produced a brown oil, which was recrystallized from ethyl acetate yielding a light brown crystalline compound. 1.5g 7%, R$_f$: 0.67 (1:1 petroleum ether: ethyl acetate), Mp: 100.0-100.9°C, IR(cm^{-1}): 2952 (Ar-H), 2887 (Ar-H), 2358 (C-H), 1474 (N=N), 1436 (N$^+$-O$^-$), 1051, 1040, 768, δ_H (300 MHz, CDCl$_3$) 2.06 (t, *J* = 2.7, 4H), 4.33-4.43 (m, 4H), 7.65-7.33 (m, 6H), 7.98 (m, 4H). δ_C (75 MHz. CDCl$_3$) 25.4(2C), 74.2 (2C), 121.15 (4C), 129.0 (4C), 131.2 (2C), 143.2 (2C), ^{1}H-^{15}N HSQC (40MHz, CDCl$_3$) -22.5, 312.7, MS theoretical: 331.1401 m/z, Accurate: 331.1402 ± 0.04ppm corresponding to C$_{16}$H$_{19}$N$_4$O$_4$.

(1Z,1'Z)-2,2'-(Hexane-1,6-diylbis(oxy)bis(1-phenyldiazene oxide)[11] **104**
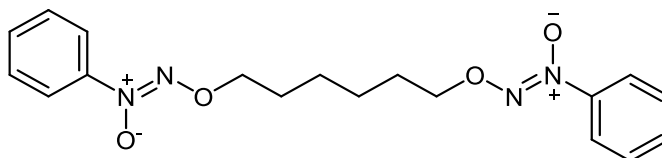
104

Cupferron (10.06g, 64.8mmol) was dissolved in dry DMF (85ml) under nitrogen and cooled to 0°C. To this suspension 1,6-dibromohexane (3.06ml, 20mmol) was injected forming a yellow solution. The reaction was left to stir at room temperature for 1 week resulting in a dark brown/red solution. The DMF was removed using a cold finger apparatus giving a dark brown sludge. This sludge was re-dissolved in DCM (30ml) and extracted with water (3 x 50ml). The organic layers were combined, dried over $MgSO_4$ and the solvent removed *in vacuo*. The product was then purified using flash column chromatography in 8:1 petroleum ether: ethyl acetate followed by 4:1 and 1:1 petroleum ether:ethyl acetate to give a dark brown oil 1.27g, 6.6%, IR(cm^{-1}): 2960 (Ar-H), 2920 (C-H) 1470 (N=N), 1424 (N$^+$-O$^-$), 1386, 1036, 1020, 769, δ_H (300 MHz, CDCl$_3$) 1.3 -1.50 (m, 4H), 1.94-1.77 (m, 4H), 3.63 (t, J = 6.45Hz, 2H), 4.44 (t, J = 6.73Hz, 2H), 7.40-7.56 (m, 6H), 7.97 (m, 4H), δ_C (75 MHz, CDCl$_3$) 25.4 (2C), 28.9 (2C), 74.8 (2C), 121.1 (2C), 128.9 (4C), 131.2 (4C), 143.1 (2C), MS (m/z) theoretical: 359.1714, Actual: 359.1714 ± 0.1 ppm corresponding to $C_{18}H_{23}N_4O_4$.

(1Z,1'*E*)-2,2'-(Octane-1,8-diylbis(oxy)bis(1-phenyldiazene oxide)[11] **104**
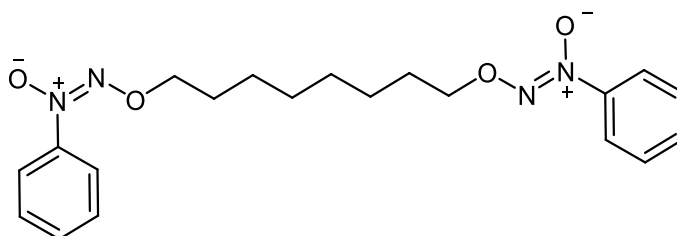
105

Cupferron (10g, 64mmol) was dissolved in DMF (40ml) under nitrogen and cooled to 0°C. To this suspension 1,8-Dibromooctane (3.9ml, 21.3mmol) was injected giving a dark brown solution. This solution was left to stir for 3 days before the DMF was removed using a cold finger apparatus to yield a dark brown gum (3.8g). This was then purified using silica-gel chromatography 9:1 petroleum ether:ethyl acetate to give a brown oil of the titled compound 0.45g, 1.8%. R_f: 0.73 petroleum ether:ethyl acetate (9:1), δ_H (300 MHz, CDCl$_3$) 1.30-1.57 (m, 8H), 1.78-1.97 (m, 4H), 4.45 (t, *J* = 6.81Hz, 4H), 7.38-7.62 (m, 6H), 8.00 (m, 4H), δ_C (75 MHz, CDCl$_3$) 25.4 (2C), 28.8 (2C), 29.0 (2C), 74.9 (2C), 120.9 (2C), 128.9 (4), 131.1 (4C), 143.0 (2C). MS: theoretical 387.2027, Actual: 387.2027 $\pm$ 0.0ppm corresponding to $C_{20}H_{27}N_4O_4$.

(*Z*)-2-(8-Bromoethoxy)-1-phenyldiazene oxide[11] **113**


113
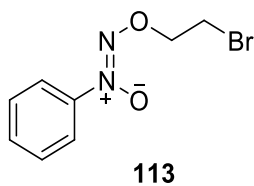
Cupferron (5.0g, 32.3 mmol) was dissolved in dry DMF (40ml) under nitrogen conditions and cooled to 0°C before dibromoethane (7.21ml, 96mmol) was injected. The resulting yellow solution was left to stir at room temperature in the dark for 3 days. The DMF was then removed via a cold finger apparatus resulting in a dark brown/black sludge which was purified using flash column chromatography in petroleum ether:ethyl acetate (1:1) to yield the title compound as a brown oil, 0.35g, 2.05%, δ_H (300 MHz, CDCl$_3$) 3.66 (t, J = 6.78Hz, 2H), 4.70 (t, J = 6.78, 6.78 Hz, 2H), 7.54-7.45 (m, 3H), 7.97 (m, 2H), δ_C (75 MHz, CDCl$_3$) 27.8, 73.4, 121.1, 129.0 (2C), 131.5 (2C), 143.0. MS: theoretical 244.9920, actual 244.9922 ± 0.7 ppm corresponding to C$_8$H$_9$N$_2$O$_2$Br.

(*Z*)-2-(8-Bromobutoxy)-1-phenyldiazene oxide[11]

114
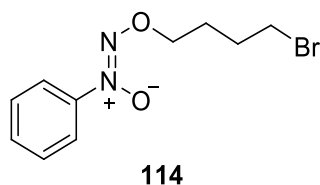
Cupferron (10.03g, 64.8mmol) was dissolved in dry DMF (85ml) under nitrogen and cooled to 0°C. To this suspension 1,6-dibromobutane (2.55ml, 20mmol) was injected forming a yellow solution. The reaction was left to stir at room temperature for 1 week resulting in a dark brown/red solution. The DMF was removed using a cold finger apparatus giving a dark brown sludge. This sludge was re-dissolved in DCM (30ml) and extracted with water (3 x 50ml). The organic layers were combined, dried over $MgSO_4$ and the solvent removed *in vacuo*. The product was then purified using flash column chromatography in 8:1 petroleum ether:ethyl acetate followed by 4:1 and 1:1 petroleum ether:ethyl acetate to yield the title compound as a brown/yellow gum 0.7g, 20%. δ_H (300 MHz, $CDCl_3$) 1.77-1.86 (m, 4H), 3.28 (t, J = 6.25Hz, 2H), 4.28 (t, J = 6.02 Hz, 2H), 7.11-7.40 (m, 3H), 7.79 (m, 2H), δ_C NMR (75 MHz, $CDCl_3$) 27.5, 28.7, 33.2, 73.6, 120.9, 128.9 (2C), 131.2 (2C), 142.9, MS: theoretical 272.0233 (m/z) Actual: 273.0235 ± 0.7 ppm corresponding to $C_{10}H_{14}N_2O_2Br$.

(*Z*)-2-(8-Bromohexyloxy)-1-phenyldiazene oxide[11]

115

Cupferron (10.0g, 64.8mmol) was dissolved in dry DMF (85ml) under nitrogen and cooled to 0°C. To this suspension 1,6-dibromohexane (3.06ml, 20mmol) was injected forming a yellow solution. The reaction was left to stir at room temperature for 1 week resulting in a dark brown/red solution. The DMF was removed using a cold finger apparatus giving a dark brown sludge. This sludge was re-dissolved in DCM (30ml) and extracted with water (3 x 50ml). The organic layers were combined, dried over $MgSO_4$ and the solvent removed *in vacuo*. The product was then purified using flash column chromatography in 8:1 petroleum ether: ethyl acetate followed by 4:1 and 1:1 petroleum ether:ethyl acetate to give a dark brown oil of the title compound, 0.7g 3.6%, δ_H (300 MHz, CDCl$_3$) 1.12-1.41 (m, 4H), 1.58-1.77 (m, 4H), 3.26 (t, *J* = 6.69 Hz, 2H), 4.30 (t, *J* = 6.60 Hz, 2H), 7.17-7.46 (m, 1H), 7.91 (m, 2H) δ_C (75 MHz, CDCl$_3$) 24.8, 27.7, 28.7, 32.5, 33.9, 74.9, 121.0, 129.0 (2C), 131.4 (2C), 143.0.

(*Z*)-2-(8-Bromooctyloxy)-1-phenyldiazene oxide[11]
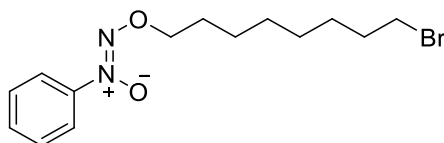
116

Cupferron (10.0g, 64.8mmol) was dissolved in DMF (40ml) under nitrogen and cooled to 0°C. To this suspension 1,8-dibromooctane (3.9ml, 21.3mmol) was injected giving a dark brown solution. This solution was left to stir for 3 days before the DMF was removed using a cold finger apparatus to yield a dark brown gum (3.8g). This was then purified using silica-gel chromatography 9:1 petroleum ether:ethyl acetate to give a brown oil of the title compound 0.91g, 4.3%, δ_H (300 MHz, CDCl$_3$) 0.90-1.22 (m, 6H), 1.27 (d, J = 5.79 Hz, 2H), 1.54 (m, 2H), 1.73 (d, J = 2.33 Hz, 2H), 3.33 (t, J = 6.19 Hz, 2H), 4.15 (t, J = 6.34 Hz, 2H), 7.00-7.26 (m, 3H), 7.69 (d, J = 7.52 Hz, 2H), δ_C (75MHz, CDCl$_3$) 25.2, 25.5, 28.7, 28.8, 29.0, 29.0, 32.4, 74.7, 120.7, 128.7 (2C), 131.0 (2C), 142.8.

<u>(3-Iodobenzyl)triphenylphosphonium bromide[12]</u>
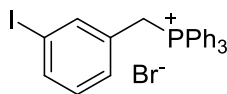
117

3-Iodobenzyl bromide (5.0g, 16.0mmol) was dissolved in dry THF (25ml) under an atmosphere of nitrogen before, triphenylphosphine (5.74g, 21.0mmol) in dry THF (15ml) was added. The resulting milky solution was allowed to reflux at 55°C for 24 hours. A white precipitate formed, which was filtered off and washed with ice cold hexane (5ml) and diethyl ether (5ml), and dried under vacuum to give a white powder 10.1g 86%, Mp: 286.5°C, IR(cm^{-1}):3052 (Ar-H), 2852 (Ar-H), 2775 (Ar-H), 1483 (P-Ph), 1434 (P-Ph), 1108 (P-Ph), 723, 694 δ_H (300 MHz, CDCl$_3$) 5.53 (d, J = 14.63 Hz, 2H), 6.90 (t, J = 7.82, Hz, 1H), 7.07 (s, 1H), 7.44 (d, J = 7.76 Hz, 1H), 7.52 (d, J = 7.87 Hz, 1H), 7.65 (m, 8H), 7.80 (m, 7H) δ_C (75 MHz, CDCl$_3$) 29.7, 30.3, 94.4, 117.0, 118.2, 130.0 (7C), 130.2 (7C), 134.4 (2C), 134.5, 137.7 (2C), 137.7.

<u>(4-Iodobenzyl)triphenylphosphonium bromide[12]</u>
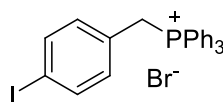
118

4-Iodobenzyl bromide (5.0g, 16.0mmol) was dissolved in dry THF (25ml) under an atmosphere of nitrogen, triphenylphosphine (5.74g, 21.0mmol) in dry THF (15ml) was then added. The resulting milky solution was allowed to reflux at 55°C for 24 hours. A white precipitate formed, which was filtered off and washed with ice cold hexane (5ml) and ether (5ml), and dried under vacuum to give a white powder, 10.3g, 88%, Mp: 270.9-271.1°C, IR(cm^{-1}): 3319 (Ar-H), 3008 (Ar-H), 2900 (Ar-H), 2790 (Ar-H), 1487 (P-Ph), 1436 (P-Ph), 1109 (P-Ph), 1074 (P-Ph), 761, 529. δ_H (300 MHz, CDCl$_3$) 5.55 (d, J = 14.78 Hz, 2H), 6.93 (dd, J = 8.39, 8.40 Hz, 2H), 7.42 (d, J = 8.30 Hz, 2H), 7.64 (m, 6H), 7.84-7.73 (m, 9H) δ_C (75 MHz, CDCl$_3$) 29.7, 30.4, 94.4 (C-I), 117.1, 118.2, 130.0 (7C), 130.2 (7C), 134.4 (2C), 134.5, 137.7 (2C), 137.7.

<u>(4-Bromobenzyl)triphenylphosphonium bromide[12]</u>
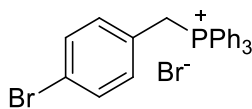
119

4-Bromobenzyl bromide (10.0g, 54.0mmol) was dissolved in dry THF (60ml) under an atmosphere of nitrogen, triphenylphosphine (23.3g, 54.0mmol) in dry THF (15ml) was then added. The resulting milky solution was allowed to reflux at 55°C for 24 hours. A white precipitate formed, which was filtered off and washed with ice cold hexane (5ml) and ether (5ml), and dried under vacuum to give a white powder, 10.3g, 88%, Mp: 265.4-266.1°C, IR (cm^{-1}) 3061 (Ar-H), 3008 (Ar-H), 2901 (Ar-H), 2791 (C-H), 1488 (P-Ph), 1437 (P-Ph), 1109 (P-Ph), 692 (C-Br), δ_H (300 MHz, CDCl$_3$) 5.53 (d, J=14.88 Hz, 2 H) 6.99 - 7.09 (m, 2 H) 7.13 - 7.22 (m, 2 H) 7.53 - 7.65 (m, 7 H) 7.68 - 7.83 (m, 8 H), δ_C (75 MHz, CDCl$_3$) 29.5, 116.9, 117.8, 122.5 (C-Br), 122.5 (C-P, 3C), 130.0 (6C), 130.1, 131.6, 133.1, 133.2. 134.2, 134.3, 134.9 (6C)

_E/Z_)-1-(3-Iodostyryl)-2,4,5-trimethoxybenzene[13]
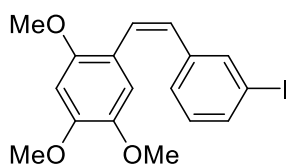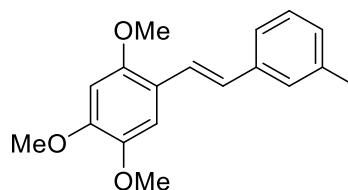
120 Z   **120 E**

To a stirred solution of 3-iodobenzyl triphenylphosphonium bromide (1.99, 6.49mmol) in dry THF (15ml), _n_-BuLi (0.73ml, 7.78mmol) was added at -15°C and left to stir for 20 minutes. 2,4,5-Trimethoxybenzaldehyde, (1.27g, 6.49mmol) in dry THF (5ml) was injected and the resulting solution was left to stir at room temperature for 1 hour and then treated with water (10ml). The reaction was allowed to cool and extracted with diethyl ether (3 x 20ml). The organic layers were washed with water (2x 10ml) and brine (2x 10ml) and concentrated in _vacuo_ to give a yellow oil. This was purified through flash column chromatography with a 3:1 (petroleum ether:ethyl acetate) system to give a mixture of _cis_:_trans_ (4:1 ratio) 0.04g. R_f: 0.52 and 0.36 (3:1 petroleum ether:ethyl acetate). IR (cm^{-1}) 3517 (Ar-H), 2994 (Ar-H), 2937 (Methyl), 2830 (Methyl), 1516, 508 (C-I), δ_H (300 MHz, CDCl$_3$) 3.43 (s, 3H), 3.71 (s, 3H), 3.81 (s, 3H), 6.36 (d, J = 12.13 Hz, 2H, _cis_ isomer), 6.60 (d, J = 15.00 Hz 2H, _trans_ isomer), 6.93 (d, J = 8.33 Hz, 2H), 7.20 (m, 2H), 7.44 (d, J = 8.34 Hz, 2H). δ_C (75 MHz, CDCl$_3$) 55.7, 55.8, 56.2, 91.8, 96.8, 97.2, 109.0, 112.8, 116.5, 125.8, 127.4, 127.8, 130.5, 136.9, 142.2, 149.1, 151.5.

(Z/E)-1-(4-Iodostyryl)-2,4,5-trimethoxybenzene[13]
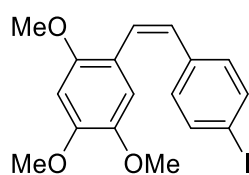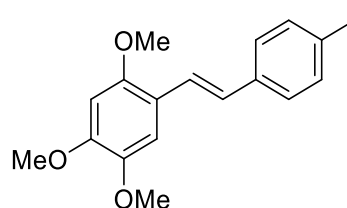
121 Z   **121 E**

To a stirred solution of 4-iodobenzyl triphenylphosphonium bromide (2.03g, 3.39mmol) in dry THF (15ml), *n*-BuLi (0.38ml, 4.06mmol) was added at -15°C and left to stir for 20 minutes. 2,4,5-Trimethoxybenzaldehyde, (0.66, 3.39mmol) in dry THF (5ml) was injected and then left to stir at room temperature for 1 hour before being treated with water (10ml). The resulting solution was allowed to cool and extracted with diethyl ether (3 x 20ml). The organic layers were combined and washed with water (2x 10ml) and brine (2x 10ml) and concentrated *in vacuo* to give a yellow oil. This was purified through flash column chromatography with a 3:1 petroleum ether:ethyl acetate system to give a mixture of the *cis* and *trans* isomers as a pale white gum. (0.3g, 22%) (3:1 ratio, *cis:trans*) R_f: 0.70 and 0.53 (3:1 petroleum ether:ethyl acetate, 54mm). IR (cm^{-1}) 2993 (Ar-H), 1509 (C=C), 1479 (C-O), 534 (C-I), δ_H (300 MHz, CDCl$_3$) 3.70 (s, 3H), 3.77 (s, 3H), 2.79-3.83 (m, 3H), 6.35 (d, *J*=12.24 Hz, 1H, *cis* isomer), 6.41 (s, 1H), 6.57 (s, 1H), 6.60 (d, *J*=12.24 Hz, 1H, *cis* isomer) 6.78 (d, *J*=16.39 Hz, 1H, *trans* isomer), 6.92, (d, *J*=8.29 Hz, 2H), 7.12-7.19 (m, 2H), 7.34 (d, *J*=16.39 Hz, 1H, *trans* isomer) δ_C (75 MHz, CDCl$_3$) 56.0, 56.5, 56.6, 91.9, 97.3, 109.1 (2C), 117.6, 123.7, 125.5, 128.0, 137.6, 137.6, 143.3, 149.8, 151.7, 151.8. MS: theoretical 397.0295, Actual 397.0284 ± 2.8 ppm for C$_{17}$H$_{18}$O$_3$I.

(*Z/E*)-2-(4-Iodostyryl)-2, 4, 6-trimethoxybenzene[13]
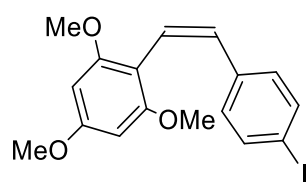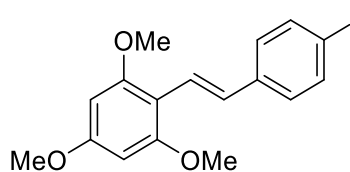
122 *Z*   **122 *E***

To a stirred solution of 4-iodobenzyl triphenylphosphonium bromide (2.03g, 3.39mmol) in dry THF (15ml), n-BuLi (0.76ml, 4.06mmol) was added at -15°C and left to stir for 20 minutes. 2,4,6-trimethoxybenzaldeyhde (0.66g, 3.39mmol) in dry THF (5ml) and left to stir at room temperature for 1 hour and then treated with water (10ml). The resulting solution was allowed to cool and extracted with diethyl ether (3 x 20ml). The organic layers were combined and washed with water (2x 10ml) and brine (2x 10ml) then concentrated in *vacuo* to give a yellow oil. This was purified through flash column chromatography with a 3:1 petroleum ether:ethyl acetate system to give a mixture 0.5g. (3:1 ratio, *trans:cis*) R_f: 0.5 and 0.4 δ_H (300 MHz, CDCl$_3$) 3.49 (s, 3 H) 3.71 (s, 3 H) 3.74 - 3.78 (m, 3 H) 6.01 (d, *J*=15.82 Hz, 2 H, *trans*), 6.06 (s, 2H), 6.34 (d, *J*=12.43 Hz, 1H, *cis*) 6.45 (d, *J*=12.06 Hz, 1H, *cis*) 7.14 (d, *J*=8.29 Hz, 2 H) 7.51 (d, *J*=8.29 Hz, 2 H), δ_C (75 MHz, CDCl$_3$) 55.3, 55.4, 55.7, 119.9, 120.7 (2C), 122.0, 126.2, 126.6, 128.0, 128.4, 128.5, 129.8, 129.8, 136.7, 137.4. 159.6. MS: theoretical 397.0295, Actual 397.0285 ± 2.6 ppm for C$_{17}$H$_{18}$O$_3$I.

<u>(*Z/E*)-3,5-Dibromo-5-(3-iodostyryl)benzene</u>[13]

123 *Z*   **123 *E***

To a stirred solution of 3-iodobenzyl)triphenylphosphonium bromide, (2g, 3.5mmol) in dry THF (15ml), *n*-BuLi (0.8ml) was added at -15°C and left to stir for 20 minutes. 3,5-Dibromobenzaldehyde, (0.9 g, 3.5mmol) in dry THF (5ml) was injected and the reaction was left to stir at room temperature for 1 hour and then treated with water (10ml). The resulting solution was allowed to cool and extracted with diethyl ether (3 x 20ml). The organic layers were washed with water (2x 10ml) and brine (2x 10ml) and concentrated in *vacuo* to give a yellow oil. This was purified through flash column chromatography with 100:1 petroleum ether:ethyl acetate system to give a pale yellow oil 0.69g. R_f: 0.53 and 0.46 (100:1 petroleum ether:ethyl acetate), IR (cm^{-1}) 3059 (Ar-H), 2917 (Ar-H), 1577 (C=C), 1541 (C=C), 1466 (C=C-H), 741 (C-I), 681 (C-Br), 663 (C-Br), δ_H (300 MHz, CDCl$_3$) 6.86 (d, *J*=16.20 Hz, 1 H, *trans* isomer) 6.89 (d, *J*=16.58 Hz, 1 H, *trans* isomer) 7.04 (t, *J*=7.91 Hz, 1 H) 7.19 (s, 1 H) 7.34 - 7.39 (m, 1 H) 7.48 (s, 2 H) 7.53 - 7.58 (m, 1 H) 7.78 (t, *J*=1.70 Hz, 1 H), δ_C (75 MHz, CDCl$_3$) 94.4, 122.8, 126.8, 128.3 (2C), 130.4 (2C), 131.0, 132.8 (2C), 136.8 (2C), 137.7, 140.1

NB: *cis* isomer *J* value of 12 Hz not found.

<u>(*Z/E*)-3,5-dibromo-5-(4-iodostyryl)benzene[13]</u>

124 *Z*   **124 *E***

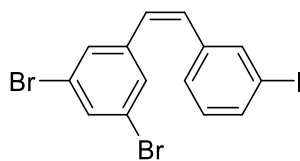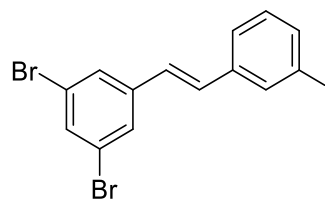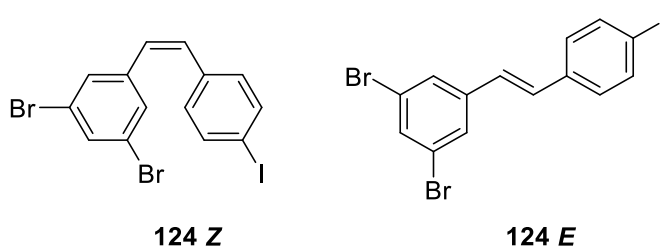To a stirred solution of 4-iodobenzyltriphenylphosphonium bromide, (2.50g, 4.40mmol) in dry THF (15ml), *n*-BuLi (0.5ml) was added at -15°C and left to stir for 20 minutes. 3,5dibromobenzaldeyhde, (1.17g, 4.4mmol) in dry THF (5ml) was then injected and the reaction was left to stir at room temperature for 1 hour before then being treated with water (10ml). The resulting solution was allowed to cool and extracted with diethyl ether (3 x 20ml). The organic layers were washed with water (2x 10ml) and brine (2x 10ml) and concentrated in *vacuo* to give a yellow oil. This was purified through flash column chromatography with 100:1 petroleum ether: ethyl acetate system to give a mixture of inseparable isomers 0.86g. (13:1 ratio, *trans:cis*) R_f 0.59, 0.50 (100:1 petroleum ether:ethyl acetate). δ_H (300 MHz, CDCl$_3$) 6.44 (d, *J*=12.43 Hz, 1 H, *cis* isomer) 6.71 (d, *J*=12.43 Hz, 1 H, *cis* isomer) 6.95 (d, J=18.84 Hz, 2 H, *trans* isomer) 7.21 (d, *J*=8.29 Hz, 2 H) 7.32 (s, 1 H) 7.61 (d, *J*=8.29 Hz, 2 H) 7.71 (d, *J*=8.29 Hz, 2 H), δ_C (75 MHz, CDCl$_3$) 93.6, 122.4, 122.9, 125.9, 126.4, 127.7, 128.0, 129.9 (2C), 132.5, 135.3 137.2, 137.5, 140.1

(Z)-1,2-Bis(4-bromophenyl)ethane[13], **125**

125
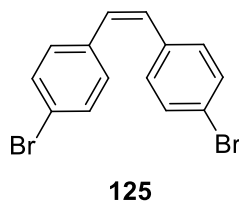
(4-Bromobenzyl)triphenylphosphonium bromide (11.1g, 25.8mmol) was dissolved in dry THF (40ml) under anhydrous conditions, to which *n*-Buli (7.16ml, 77.4mmol) was injected at -20°C. The resulting red solution was left to stir for half an hour at -20°C and then brought to room temperature before 4-bromobenzaldehyde (4.73g, 25.8mmol) was added. The solution was then left to stir for 2 hours before being quenched by addition of water (10ml) and then extracted with diethyl ether (3 x 20ml). The organic layers were washed with water (2x 10ml) and brine (2x 10ml) and concentrated in *vacuo* to give a brown oil (2.71g). This was purified through flash column chromatography with 20:1 petroleum ether:ethyl acetate system to give the title compound as a yellow oil, 0.2g, 2.3%, Rf: 0.71 (20:1 petroleum ether:ether acetate), δ_H (300 MHz, CDCl$_3$) 6.47 (s, 2 H) 6.98 - 7.04 (m, 4 H) 7.25 - 7.32 (m, 4 H), δ_C (75 MHz, CDCl$_3$) 121.2 (2C), 129.7 (2C), 130.4 (4C), 131.5 (4C), 135.6 (2C).

Synthesis of 3-acetyl-1,2,5-oxadiazole-2-oxide[8]

126
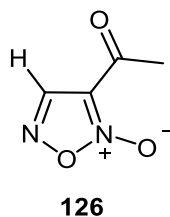
Aqueous NaNO$_2$ (34.0g, 0.449mol, 3.5eq) was added drop-wise to a stirred solution of crotonaldehyde (10.0g, 0.142mol) in acetic acid. During the addition the temperature of the reaction was kept at 14°C. The resulting yellow solution was left to stir for one hour, diluted with water (200ml) and then extracted with DCM (250ml) to yield a crude orange solid (5.45g). This was purified with flash column chromatography using DCM:petroleum ether (10:1) as an eluent to yield

a viscous, pale yellow oil, 4.19g, 23%, R_f: 0.74 (petroleum ether:ethyl acetate, 1:1) IR (cm^{-1}): 3362, 2980, 1660, 1578 (C=N), 1470 (C=N$^+$-O$^-$)m 1244, 1006, δ_H (300 MHz, CDCl$_3$) 2.13 (s, 3H), 9.84 (s, 1H). δ_C (75 MHz, CDCl$_3$ 18.83 (methyl), 110.35 (C=N$^+$-O$^-$), 154.35 (C=N), 198.73 (C=O). MS: theoretical (m/z): 129.0295. Actual: 129.0291± 2.9+ ppm for C$_4$H$_5$N$_2$O$_3$.

3,4-Diphenyl-1,2,5-oxadiazole-2-oxide[14]
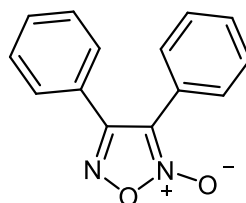
128

To a warm solution (50-60°C) of acetic acid (6ml) and 1,4-dioxane (15ml), *trans* stilbene (10.0g, 0.05mol) was added and left to stir for 10 minutes to ensure a homogenous mixture before solid NaNO$_2$ (26.0g, 0.38mol) was also added. The reaction was then allowed to proceed with stirring at 55°C for 6.5 hours and then quenched by the addition of ice water (100ml). The mixture was extracted with ethyl acetate (2 x 60ml) and dried over MgSO$_4$, to yield a brown oil. Purification was attempted by column chromatography (3:1 hexane: petroleum ether) to no effect. The oil was then recrystallized from hot hexane to yield orange crystals 0.12g, 1% in the first crop. The recrystallization process was repeated 6 times and all crystals were combined (0.8g, 6%) and the final remaining red oil was columned for a second time (10:1 hexane: petroleum ether). Further purification of the two spots from the TLC was not possible. Orange crystals were shown to be a mixture of furoxan and a nitrated starting material. Diagnostic signals consistent with furoxan formation were identified, and are as follows: Mp: 89.5-97.5°C, IR (cm^{-1}), 3316 C-H (Ar), 3064 C-H (Ar), 1657 (C=N), 1449 (C=N$^+$-O$^-$), 1246, C-H (Ar), 1209 C-H (Ar), δ_C (75 MHz,CDCl$_3$) 114.3 (C=N$^+$-O$^-$), 122.8, 126.6, 128.32, 128.7, 128.9, 129.0, 129.2 (2C), 129.9, 130.5, 131.0, 131.1, 156.2 (C=N), MS: theoretical (m/z): 239.0815 Actual: 239.0814 ± 0.4 ppm for C$_{14}$H$_{11}$N$_2$O$_2$. Signals corresponding to nitrated material are MS: 226.0862 (low res) corresponding to C$_{14}$H$_{12}$NO$_2$.

(*E*)-1-(4-Bromophenyl)-3-(2,4,5-trimethoxyphenyl)prop-2-en-1-one[15]
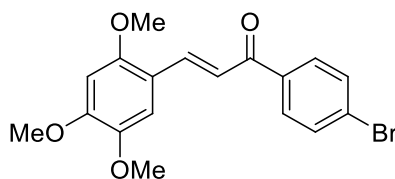
130

To a stirred solution of 2,4,5-trimethoxybenzaldehyde (10.0g 0.05mol) and 4-bromoacetophenone, (10.0g 0.05mol) in methanol (100ml) 5% NaOH (25ml) solution was added and the resulting yellow solution was left to stir at room temperature for 24 hours. This was worked up with the addition of water (100ml) which led to a bright yellow precipitate (7.14g). This was then recrystallized from hot ethanol to give a bright yellow powder 4.47g, 23%, M.p. 156.5°C, IR (cm^{-1}) 536 (C-Br), 1201 (C-OMe), 1274 (C-OMe), 1290 (C-OMe), 1610 (C=C), 1651 (C=O), 2833 (C-H), 2952 (C-H). δ_H (300 MHz, CDCl$_3$) 3.92 (d, *J*= 1.24 Hz, 6H), 3.97 (s, 3H), 6.54 (s, 1H), 7.13 (s, 1H), 7.41 (d, *J*= 15.74 Hz, 1H), 7.64 (d, *J*= 8.61 Hz, 2H), 7.89 (d, *J*= 8.61 Hz, 2H), 8.10 (d, *J*= 15.76 Hz, 1H) δ_C (75 MHz, CDCl$_3$) 56.1, 56.3 , 56.5 , 96.6, 111.41 , 115.2 , 119.7 , 127.3 (C-Br) , 130.0 (2C), 131.7 (2C), 137.5, 140.8, 143.3, 152.7, 154.8, 190.1 (C=O), MS (m/z) theoretical: 377.0386 MS (m/z) actual: 377.0386 ± 0.8 ppm corresponding to C$_{18}$H$_{18}$BrO$_4$.

1-(4-Iodophenyl)-2-(2,4,5-trimethoxyphenyl)ethane-1,2-dione[16]
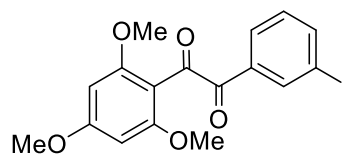
131

To a solution of (*E*)-1-(3-iodostyryl)-2,4,6-trimethoxybenzene (0.5g, 1.26mmol) in acetic anhydride (15ml), potassium permanganate (0.79g, 5mmol) was added that turned the solution a deep purple colour. This was left to stir for 1 hour, then reaction was cooled to 0°C before sodium sulphite (2g) was added resulting in a dark brown solution. The precipitate was filtered off and the filtrate was extracted with ethyl acetate (2x 25ml) then washed with $NaHCO_3$ (25ml) followed by brine (25ml) and then dried over $MgSO_4$. The solvent was removed resulting in a pale yellow solid of the title compound, 0.2g, 37%, IR(cm^{-1}) 2944 (Ar-H), 1812 (C=O), 1733 (C=O), 1220, 1209 (C-O), 1120 (C-H methyl), 1032 (C-H, methyl), 991, 588 (C-I), δ_H (300 MHz, CDCl$_3$) 3.70 (s, 3H) 3.88-3.89 (m, 6H), 6.02 (s, 2H), 7.29- 7.34 (m, 1H), 8.00-8.06 (m, 1H), 8.09-8.14 (m, 1H), 8.47 (t, *J*= 1.7, 1H), δ_C (75 MHz, CDCl$_3$) 56.0 (3C), 90.1 (2C), 99.9 (C-I), 130.9, 132.7,134.9, 138.6 (2C), 144.1, 164.1 (2C, C-OMe), 169.2 (C-OMe), 187.9 (C=O), 189.9 (C=O).

(1*E*,2*E*)-1-(4-Iodophenyl)-2-(2,4,5-trimethoxyphenyl)ethane-1,2-dione dioxime[16]
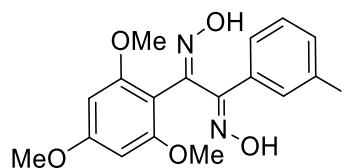
132

To a solution of 1-(3-iodophenyl)-2-(2,4,6-trimethoxyphenyl)ethane-1,2-dione (0.2g, 47mmol) in dry pyridine (10ml) and ethanol (20ml), an excess of hydroxylamine hydrochloride was added. The resulting solution was heated 90°C for 3 days and then diluted with ethyl acetate and washed with 2N sulphuric acid, water and brine. Removal of the solvent gave the title compound as a pale yellow oil 0.119g, 5.5%, IR (cm^{-1}) 3234 (OH), 2922 (Ar-H), 2852, 1678 (C=N), 1561 (C=N), 1260 1229, 1209, 528 (C-I), δ_H (400 MHz, CDCl$_3$) 3.81 - 3.92 (m, 9 H) 6.07 (s, 2 H) 7.05 - 7.15 (m, 1 H) 7.92 (d, *J*=7.09 Hz, 1 H) 7.99 - 8.11 (m, 1 H) 8.43 (s, 1 H), δ_H (75 MHz, CDCl$_3$) 56.1 (3C), 90.3 (2C), 93.8 (C-I), 129.3, 129.7, 130.0, 130.1, 139.0, 142.2, 151.4 (C=N), 154.3, 163.8 (3C).

(*E*)-*N*-hydroxy-4-(trifluoromethyl)benzimidoyl chloride[9]
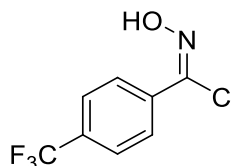
133

To a stirred solution of 3-trifluromethyl-benzamidoxime (5.0g, 24.5mmol) in hydrochloric acid (12.5ml), NaNO$_2$ (2.02g, 29mmol) was added portion-wise to the solution causing it to turn orange. The reaction was left to stir for 30 minutes causing an orange precipitate to form, which was then filtered off and purified by flash column chromatography with petroleum ether:ethyl acetate 7:3 to yield the title compound as a colourless oil. 1.34g 24%. (300 MHz, CDCl$_3$) 7.66 (d, *J* = 7.77 Hz, 2H), 7.81 (d, *J* = 7.78 Hz, 2H), δ_C (75 MHz, CDCl$_3$) 121.6, 121.7, 125.3, 125.8, 129.1, 129.2, 134.2, 149.6, MS theoretical (m/z): 223 MS actual: 221.3 and 223.3 for C$_8$H$_5$F$_3$NOCl^{35+} and C$_8$H$_5$F$_3$NOCl^{37+} respectively.

(*E*)-4-Chlorobenzaldehyde oxime[17]
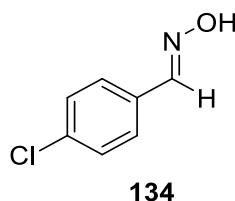
134

4-Chlorobenzaldehyde, (2.0g, 14.2mmol), hydroxylamine. HCl (1.16g, 16.8mmol) and sodium hydroxide (0.67, 16.8mmol) were ground together using a pestle and mortar. To this silica (2.0g) was added and the four solids ground for 10 minutes at room temperature. The fine powder was then ground every 15 minutes for 2 hours and then washed with water and allowed to dry in air to yield a pale white solid. 2.9g, 83% δ_H (300 MHz, CDCl$_3$) 7.39 (d, J = 8.54 Hz, 2H), 7.53 (d, J = 8.51 Hz, 2H), 8.13 (s, 1H). δ_C (75 MHz, CDCl$_3$) 128.2, 129.1, 130.3 (2C), 133.6, 136.0 (C-Cl), 149.3 (C=N).

(*E*)-4-Chlorobenzaldehyde oxime[17]

134
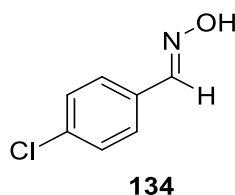
4-Chlorobenzaldehyde (2.0g, 14.2mmol), hydroxylamine. HCl (1.16g, 16.8mmol) and sodium hydroxide (0.64g) was added at the same time to a pestle and mortar and ground continuously for 10 minutes forming a 'wet dough' consistency. This mixture was then ground intermittently over the course of 2 hours and then washed with water and dried in air to give a cream solid of the titled compound 1.3g, 59% δ_H (300 MHz, CDCl$_3$) 7.39 (d, J = 8.54 Hz, 2H), 7.54 (d, J = 8.50 Hz, 2H), 8.13 (s, 1H), δ_C (75 MHz, CDCl$_3$) 128.2, 129.1, 130.3 (2C), 133.6, 136.0 (C-Cl), 149.3 (C=N).

(*E*)-4-Chlorobenzaldehyde oxime[18]

134
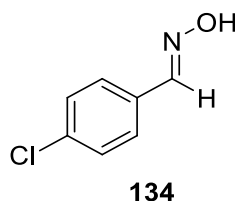
To a stirring solution of 4-Chlorobenzaldehyde (2.0g, 14.2mmol) in diethyl ether (30ml), aqueous hydroxylamine. HCl (1.16g (16.8mmol) and sodium hydroxide (0.55g, 13,7mmol) was added at room temperature. This was then stirred vigorously for 2 hours. The reaction was then diluted with water (50ml) and extracted with diethyl ether (100ml) to produce a white solid of the titled compound 1.9g, 87% δ_H (300 MHz, CDCl$_3$) 7.39 (d, J = 8.56 Hz, 2H), 7.55 (d, J = 8.56 Hz, 2H), 8.13 (s, 1H), δ_C (75 MHz, CDCl$_3$) 128.2, 129.1, 130. 3 (2C), 133.6, 136.0 (C-Cl), 149.3 (C=N).

(*Z*)-4-Chloro-*N*-hydroxybenzimidoyl chloride[19]

135
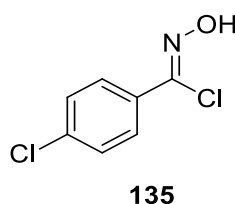
To a solution of (*Z*)-4-chlorobenzaldehyde oxime (1.8g, 11.6mmol) in THF (30ml) at room temperature, *N*-chlorosuccinamide (1.54g, 11.6mmol) was added and the resulting yellow solution allowed to stir for 2 hours before water (25ml) and diethyl ether (25ml) were added. The organic layer was extracted and washed with brine (20ml) to yield pale yellow flakes, of the titled compound 2.0g, 88.6% R$_f$: 0.83 (1:1 petroleum ether:ethyl acetate), Mp: 102.9-103.8°C δ_H (300 MHz, CDCl$_3$) 7.71 (d, J = 8.83 Hz, 2H), 7.32 (d, J = 8.83 Hz, 2H).

(*Z*)-4-Chloro-*N*-hydroxybenzimidoyl chloride[19]

135
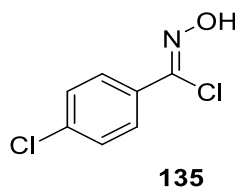
To a solution of (*Z*)-4-chlorobenzaldehyde oxime, (1.2g, 7.7mmol) in THF (30ml), *N*-chlorosuccinamide (1.03g, 7.7mmol) was added at room temperature. The resulting yellow solution was left to stir for 2 hours. After stirring water (25ml) and ether (25ml) were added and the organic layer was washed with brine (25ml) and dried over $MgSO_4$ to yield a pale yellow solid, 1.4 g, 96% R_f: 0.83 (1:1 petroleum ether:ethyl acetate), Mp: 102.9-103.8°C, δ_H (300 MHz, $CDCl_3$) 7.39 (d, *J* = 8.75 Hz, 2H), 7.78 (d, *J* = 8.78 Hz, 2H), δ_C (75 MHz, $CDCl_3$) 68.06, 128.2, 128.3, 128.7, 129.1, 129.4, 149.18 (C=N).

4-Bromobenzoic acid
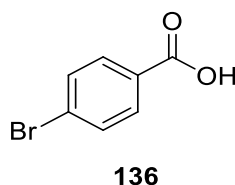
136

4-Bromoacetophenone (10.0g, 50.5mmol) was dissolved in acetic acid (53 ml) and heated to 80°C under reflux conditions. Dilute HNO_3 (11.9ml in 35ml H_2O) was added drop-wise to the solution over the course of 30 minutes. A catalytic amount of $NaNO_2$ was added and the reaction was left to reflux for a further 2 hours. The reaction was then left to cool, forming a precipitate which was then filtered off. The filtrate was extracted with DCM (3 x50ml) and dried over $MgSO_4$, and concentrated in *vacuo*. The resulting solid was then recrystallized from hot DCM, producing a white precipitate which corresponded to the by-product 4-bromobenzoic acid, 0.99g, 9.8%, Mp: 245-247°C (Lit: 247-250°C[20]), δ_H (300 MHz, d_6-DMSO) 7.67 (d, *J* = 8.47 Hz, 2H), 7.85 (d, *J* = 8.51 Hz, 2H), 13.21 (s, 1H), δ_C (75 MHz, d_6-DMSO) 126.8, 129.9, 131.2 (2C), 131.6 (2C), 166.5 (C=O).

4-(Trifluoromethoxy)benzoic acid

137

To a solution of 4-trifluoromethoxyacetophenone, (5.0g, 24.5 mmol) in glacial acetic acid (30ml.) dilute HNO_3 (8 mL in 12ml H_2O) was added drop-wise over the course of 30 minutes. A catalytic amount of $NaNO_2$was then added to the solution which was then heated to 60°C for 2 hours. TLC showed an incomplete conversion so the reaction was maintained at 60°C for a further 2 hours. The reaction was then cooled to room temperature and a small amount of ice was added to quench the reaction and to encourage precipitation. No precipitate formed, so the solution was extracted with DCM (3 x 30 mL). The combined extracts were washed with water (25 mL), brine (25 mL) and dried over $MgSO_4$. The combined extracts were concentrated to give a yellow oil (5.3g). The yellow oil was purified by column chromatography (hexane: ethyl acetate 10:1 to 1:1, followed by 100% ethyl acetate) to yield the title compound as a fine white powder, 0.19g, 3.6%, Rf: 0.46 (10:1 petroleum ether:ethyl acetate) Mp: 138.9-139.7°C (Lit: 150-152°C, hexane[21]) δ_H (300 MHz, d_6-DMSO) 7.48 (d, J=7.91 Hz, 2 H) 8.06 (t, J=8.85 Hz, 2 H), 13.19 (s, 1H), δ_H (75 MHz, d_6-DMSO) 120.7, 129.7 (CF_3), 130.6 (2C), 131.6 (2C), 151.3, 166.1 (C=O).

4-Methoxybenzoic acid[22]
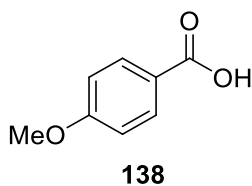
138

4-Methylacetophenone (5.0g, 37.3mmol) was dissolved in acetic acid (30 ml) and heated to 60°C under reflux conditions. Dilute HNO_3 (8ml in 20ml H_2O) was added drop-wise to the solution over the course of 30 minutes. A catalytic amount of $NaNO_2$ was added and the reaction was left to reflux for a further 2 hours. The reaction was then left to cool, but no precipitate formed so the solution was extracted with DCM and dried over $MgSO_4$, and concentrated *in vacuo*. The resulting solid was then purified further using flash column chromatography, 10:1 (petroleum ether:ethyl acetate) to give a yellow oil of the title compound, 1.44g, 25.3%, Mp: 175.2-175.6°C , δ_H (300 MHz, CDCl$_3$) 3.89 (s, 3 H) 6.89 - 7.09 (m, 2 H) 8.00 - 8.14 (m, 2 H) δ_C (75 MHz, CDCl$_3$) 55.7, 113.7, 114.3, 121.6, 132.3, 133.2, 164.0 (C-OMe), 171.6 (C=O).

4-Iodobenzoic acid[23]
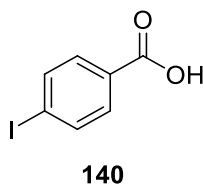
140

To a solution of 4-iodoacetophenone (3.3g, 12.2mmol) in acetic acid (30ml), dilute nitric acid (12.5 ml in 18ml H_2O) was added drop-wise over the course of 30 minutes. The reaction was slowly heated to 55°C and a catalytic amount of $NaNO_2$ was added causing the evolution of brown fumes and turning the solution an orange colour. The reaction was left to stir at 55°C for 2 hours, cooled and poured drop-wise on to ice forming a white precipitate, and was isolated to yield the title compound as a colourless oil, 0.62g, 20.5%, δ_H (300 MHz, d$_6$-DMSO), 7.68 (d, *J*=8.67 Hz, 2 H) 7.87 (d, *J*=8.48 Hz, 2 H), δ_C (75 MHz, d$_6$-DMSO) 101.1 (C-I), 130.1, 131.1 (2C), 137.5 (2C), 166.9 (C=O).

4-Ethylybenzoic acid[24]
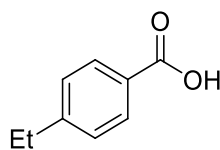
141

To a solution of 4-ethylacetophenone (2.9g, 20.0mmol) in acetic acid (30ml), dilute nitric acid (12.5 ml in 18ml H_2O) was added drop-wise over the course of 30 minutes. The reaction was slowly heated to 55°C and a catalytic amount of $NaNO_2$ was added causing the evolution of brown fumes and turning the solution an orange colour. The reaction was left to stir at 55°C for 2 hours, at which time more $NaNO_2$ was added and the reaction left for a further 2 hours. The reaction was then cooled to room temperature and then added drop-wise onto ice to produce a yellow precipitate. The filtrate was then extracted with DCM (2 x50ml), dried over $MgSO_4$ and reduced to give a colourless oil of the title compound, 0.64g, 21%, δ_H (300 MHz, $CDCl_3$) 1.06 - 1.18 (m, 3 H) 2.52 - 2.64 (m, 2 H) 7.16 (d, J=8.10 Hz, 2 H) 7.90 (d, J=8.10 Hz, 2 H) 12.25 (br. s., 1 H), δ_C (75 MHz, $CDCl_3$) 15.1, 29.0, 126.6, 128.0 (2C), 130.4 (2C), 151.0, 172.7 (C=O).

<u>2, 4, 5-Trimethoxy-5-nitrobenzene</u>
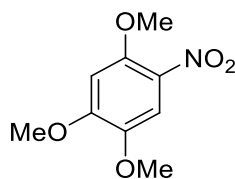
142

To a solution of 2,4,5-trimethoxyacetophenone, (5.0g, 24.0 mmol) in glacial acetic acid (30ml.) dilute nitric acid (8 mL of conc. nitric acid in 15ml H_2O) was added drop-wise over the course of 30 minutes. A catalytic amount of sodium nitrite was then added to the solution which was then heated to 60°C for 2 hours. TLC showed an incomplete conversion so the reaction was maintained at 60°C for a further 2 hours. The reaction was then cooled to room temperature and a small amount of ice was added to quench the reaction and to encourage precipitation. No precipitate formed, so the solution was extracted with DCM (3 x 30 mL). The combined extracts were washed with water (25 mL), brine (25 mL), and dried over $MgSO_4$. The combined extracts were combined and reduced to give a red solid (3.23g), this was then purified by column chromatography (hexane:ethyl acetate 10:1 to 1:1) to give the titled compound as a bright orange solid, 0.42g, 8%, R_f: 0.56 (1:1 petroleum ether:ethyl acetate), Mp:112.9-113.7°C (Lit: 123-124°C[25], acetone), δ_H (300 MHz, CDCl$_3$) 3.91 (s, 3H), 3.99 (s,3H), 4.00, (s, 3H), 6.57 (s, 1H), 7.60 (s, 1H) δ_C (75 MHz, CDCl$_3$) 56.4, 56.5, 57.1, 97.3, 108.8, 130.7, 142.3, 150.4, 154.7 MS theoretical: 214.0708 m/z Actual: 2.14.0710 ±0.9 corresponding to $C_9H_{12}O_5N_1$.

2-(2,5-Dimethyl-1*H*-pyrrol-1-yl)-4,6-dimethylpyridine[26]
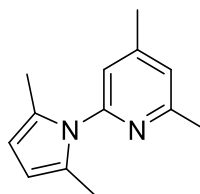
147

To a solution of 2,4-dimethylaminopyridine (25.7g, 21.08mmol) and acetonlyacetone (25.0g, 21.9mmol) in toluene (200ml) was added p-TsOH (0.40g, 2.10mmol). The resulting solution was refluxed under dean-stark conditions for 8 hour. The solvent was then removed and the crude product was purified via silica gel chromatography in 10:1 petroleum ether: ethyl acetate to give a pale yellow oil, 12.95g, 30.5% which upon standing crystallised to a yellow solid. R_f: 0.51 (petroleum ether: ethyl acetate, 10:1) Mp: 38.5°C (lit value 59°C[17]) IR (cm^{-1}): 2959 (Ar-H), 2925, 1607 (C=N), 1570, 839. δ_H (300 MHz, CDCl$_3$) 2.15 (s, 6H), 2.41 (s, 3H), 2.58 (s, 3H), 5.90 (s, 2H), 6.88 (s, 1H), 7.03 (s, 1H). δ_C (75 MHz, CDCl$_3$) 13.1 (2C), 20.9, 24.1, 106.6, 119.7, 122.9, 128.3 (2C), 149.4, 151.4, 158.0

2,4-Dimethyl-6-propylpyridine
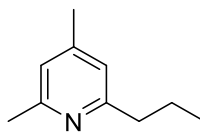
148

A solution of 2,4-dimethylaminopyridine (1.0g, 8mmol) in THF (25ml) was cooled to -78°C and *n*-BuLi (0.85ml, 9mmol) was added and stirred for 20 minutes. TMEDA* (1.3ml, 9mmol) was added drop-wise and the solution was left to stir for a further 10 minutes before warming the solution to 0°C for 1 hour. To the orange solution bromoethane (0.59ml, 8mmol) was added and left to stir for 30 minutes. The reaction was quenched with a molar equivalent of NH₄Cl. The solution was then extracted with DCM, (50ml) dried over MgSO₄ and the solvent removed. No product was obtained for this reaction. *TMEDA was distilled over calcium hydride prior to use.

2,4-Dimethyl-6-propylpyridine[27]
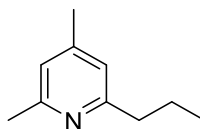
148

Phenyl lithium (3.4g 41mmol) was added at -78°C to a solution 2,4,6-trimethylpyridine (5g, 41mmol) in dry diethyl ether (40ml) under anhydrous conditions. The resulting red solution was stirred at -78°C for half an hour then at room temperature for 30 minutes. To this red solution, bromoethane (4.42, 41mmol) was injected and the resulting mixture was then refluxed at 40°C for 4 hours and then poured onto ice (25g). The organic layer was extracted with diethyl ether (100ml) and reduced to give a brown/dark yellow oil which was then purified by flash column chromatography (10:1, petroleum ether:ethyl acetate) to give the title compound as a pale yellow oil, 0.3g, 4%. δ_H (300 MHz, CDCl3) 0.89 (t, J = 7.35 Hz, 3H), 1.65 (qd, J = 14.92, 7.42, 7.42, 7.42 Hz, 2H), 2.21 (s, 3H), 2.43 (s, 3H), 2.63 (m, 2H), 6.73 (s, 2H), δ_C (75 MHz, CDCl₃) 13.9, 20.8, 23.4, 24.2, 40.3, 120.5, 121.4, 147.3, 157.3, 161.4.

2,4-Dimethyl-6-propylpyridine[27]
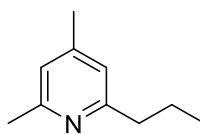
148

Phenyl lithium (3.4g 41mmol) was added at -78°C to a solution 2,4,6-trimethylpyridine (5g, 41mmol) in dry THF (40ml) under anhydrous conditions. The resulting red solution was stirred at -78°C for half an hour then at room temperature for 30 minutes. To this red solution, bromoethane (4.42, 41mmol) was injected and the resulting mixture was then refluxed at 40°C for 4 hours and then poured onto ice (25g). The organic layer was extracted with diethyl ether (100ml) and reduced to give a brown/dark yellow oil which was then purified by flash column chromatography (10:1, petroleum ether:ethyl acetate) to give the title compound as a pale yellow oil, 0.1g, 2%. δ_H (300 MHz, CDCl3) 0.97 (t, J=7.35 Hz, 3 H) 1.72 (m, 2 H) 2.28 (s, 3 H) 2.50 (s, 3 H) 2.63 - 2.76 (m, 2 H) 6.80 (d, J=4.90 Hz, 2 H), δ_C (75 MHz, CDCl$_3$) 13.9, 20.8, 23.4, 24.2, 40.3, 120.5, 121.4, 147.3, 157.3, 161.4.

1,5-Bis(6-(2,5-dimethyl-1*H*-pyrrol-1-yl)-4-methylpyridin-2-yl)pentan-3-ol[26]
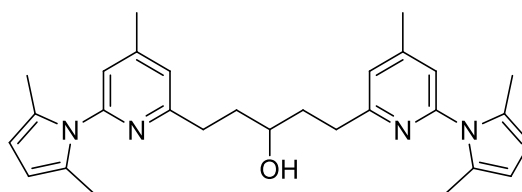
149

2-(2,5-Dimethyl-1*H*-pyrrol-1-yl)-4,6-dimethylpyridine (0.5g, 2.5mmol) was dissolved in dry THFl ether (40ml) and cooled to -78°C, where *n*-butyl lithium (1.17ml, 12.5mmol) was injected dropwise. . The resulting orange solution was left to stir for 1 hour at -78°C and then brought to 0°C for 30 minutes when 1,3-dibromo-2-propanol (0.26g, 1.25mmol) was added and the reaction left to stir for 1 hour. The reaction was quenched with addition of water (10ml). The THF was then removed under reduced pressure to give a brown/yellow oil. Only starting material was recovered, this was confirmed by GCMS and ^{1}H NMR spectroscopy.

6-Bis(6-(2,5-dimethyl-1*H*-pyrrol-1-yl)-4-methylpyridin-2-yl)hexane-3,4-dione[26]
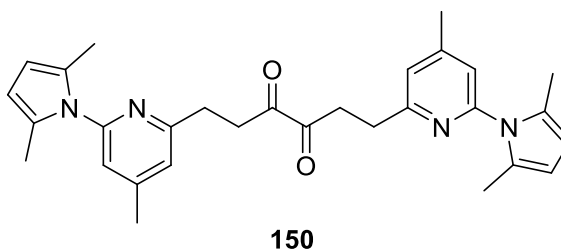
150

2-(2,5-Dimethyl-1*H*-pyrrol-1-yl)-4,6-dimethylpyridine (7.0g, 35mmol) was dissolved in dry diethyl ether (40ml) and cooled to -78°C, where phenyl lithium (3.87ml, 38mmol) was injected dropwise. The resulting bright red solution was left to stir for 1 hour at -78°C and then brought to room temperature. The solution was slowly warmed to 45°C, where 1,4-dibromo-2,3-butandione (9.38g, 38mmol) was injected and the solution left to reflux for a further 4 hours. The resulting solution was poured onto ice (25g) and the phases extracted with diethyl ether (3x 100ml), dried over $MgSO_4$ and the solvent removed to give a brown oil. No product was obtained from this reaction this was confirmed by GCMS and ^1H NMR spectroscopy.

1,2-Bis((6-(2,5-dimethyl-1*H*-pyrrol-1-yl)-4-methylpyridin-2-yl)methyl)benzene[26]
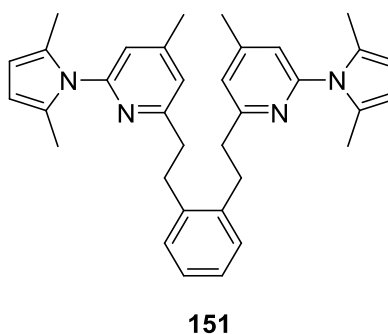
151

2-(2,5-Dimethyl-1*H*-pyrrol-1-yl)-4,6-dimethylpyridine (7.0g, 35mmol) was dissolved in dry diethyl ether (55ml) and cooled to -78°C, where phenyl lithium (3.87ml, 38mmol) was injected drop-wise. The resulting bright red solution was left to stir for 1 hour at -78°C and then brought to room temperature. The solution was slowly warmed to 45°C, where α,α'-dibromo-o-xylene (4.7ml, 35mmol) was injected and the solution left to reflux for a further 4 hours. The resulting solution was

poured onto ice (25g) and the phases extracted with diethyl ether (3x 100ml), dried over MgSO₄ and the solvent removed to give a brown oil. No product was obtained from this reaction; this was confirmed by GCMS and ^{1}H NMR spectroscopy.

(*E*)-1,4-Bis(6-(2,5-dimethyl-1*H*-pyrrol-1-yl)-4-methylpyridin-2-yl)but-2-ene[26]
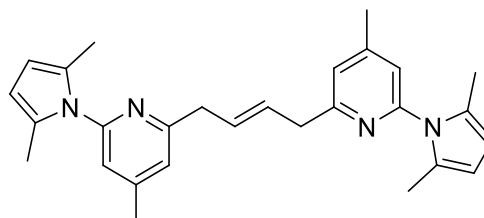
152

2-(2,5-dimethyl-1H-pyrrol-1-yl)-4,6-dimethylpyridine (0.5g, 2.5mmol) was dissolved in dry THF (20ml) and cooled to -78°C, where *n*-BuLi (0.58ml, 6.2mmol) was injected dropwise. The resulting orange solution was left to stir for 1 hour at -78°C and then brought to 0°C for 30 minutes when 1,4-dibromobut-2-ene (0.26g, 1.25mmol) was added and the reaction left to stir for 1 hour. The reaction was quenched with addition of water (110µl). The THF was then removed under reduced pressure to give a brown/yellow oil. Only starting material was recovered.

2-Amino-5-(1-(carboxymethylamino)-3-(nitrosothio)-1-oxopropan-2-ylamino)-5-oxopentanoic acid (GSNO)[28]
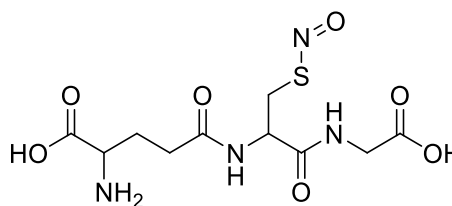
19

To an ice cold solution of glutathione (5.0g, 16.2mmol) in water (40ml) containing 2N HCl (10ml), sodium nitrite (1.0g, 14.4mmol) was added in one portion. The resulting solution was stirred for 40 minutes at 5°C until the solution turned red. At this point acetone (10ml) was added and the reaction was stirred for a further 10 minutes. The resulting light pink solid was filtered off and washed with

ice cold water (5ml), acetone (10ml), and diethyl ether (10ml) to afford the title compound (4.5g, 82%). Compound was used directly upon isolation.

S-Nitroso-1-thio-2,3,4,6-tetra-*O*-acetyl-β-D-glucopyranose (SNAG)[29]
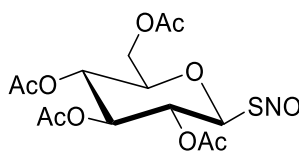
153

1-Thio-2,3,4,6-tetra-*O*-acetyl-β-D-glucopyranose (75mg, 0.25mmol) was dissolved in ethanol (5ml). The solution was then kept in the dark, while nitrous fumes were bubbled through the solution. These were generated by reacting concentrated HCl with solid $NaNO_2$ in an attached, adjacent flask. The orange solution was then filtered off and the ethanol volume corrected back to 5ml to account for evaporation. Compound was used directly upon isolation.

Acidic triiodide solution for conversion of nitrite and use in the NOA[30]

Potassium iodide (2.0g, 12.0mmol) and iodine (1.3g, 10.3mmol) was dissolved in a combination of distilled water (40ml) and glacial acetic acid (140ml). The dark brown solution was sonicated to insure all particulates were dissolved. Aliquots of this solution was then used to measure nitrite formation in the nitric oxide analyser (NOA) apparatus.

Acidified vanadium (III) chloride solution for conversion of nitrate and use in the NOA[31]

Vanadium (III) chloride (0.5g, 5.0mmol) was weighed into a pre-dried conical flask. To this 1M HCl (100ml) was added very carefully, turning the solution a vibrant blue colour. Inversion of the flask was completed several times before the solution was ready to use. Aliquots of this solution were used to measure nitrate levels in the nitric oxide analyser (NOA) apparatus. NB: Before use in an NOA machine, the solution must be filtered to remove any undissolved VCl_3.

4.1- References

1. O. Das, S. Paria and T. K. Paine, *Tetrahedron Letters*, 2008, **49**, 5923-5927.

2. W. Nirode, J. M. Luis, J. F. Wicker and N.M. Wachter, *Bioorg. Med. Chem.*, 2006, 229-2301.

3. H.R. Snyder and N.E. Boyer, *J. Am. Chem. Soc* 1955, **77**, 4233-4237.

4. M. E. Richardson, PhD thesis, Keele University, 2012

5. A.F. Holleman, *Recueil des Travaux Chimiques des Pays-Bas*, 1891, **10**, 218-222.

6. A.R. Daniewski, M. Witanowski and T. Urbanski, *J. Org. Chem*, 1967, **32**, 4650-4652.

7. T. Okuda, *Yakugaku Zasshi*, 1958, **78**, 808-809.

8. R. Fruttero, B. Ferrarotti, A. Serafino, A. Di Stilo and A. Gasco, *J. Heterocylcic.*, 1989, 1345-1347

9. V. Yarovenko, S. A. Kosarev, I.V Zavazin and M.M Krayushkin, *Russian Chem. Bulletin*, 2002, 1387-1391.

10. I. M. Mills, Mpharm report, Keele University, 2013

11. Y. Hou, W. Xie, A. J. Janczuk and P. G. Wang, *J. Chem. Org.,* 2000, **65**, 4333-4337.

12. J. D. Olszewski, M. Marshalla, M. Sabat and R. J. Sundberg. *J. Org. Chem.,* 1994, **59**,(15), 4285-4296.

13. J.A. Woods, J.A Hadfield, G.R. Pettit, B.W. Fox and A.T McGown, *British Journal of Cancer*, 1995, **71**, 705-711.

14. C. Velazquez, P.N. Praveen Rao, R. McDonald and E.K. Knaus, *Bioorg. Med. Chem*, 2005,**13**, 2749-2757.

15. D. I. Batovska and I.T. Todorova, *Curr. Clin. Pharmacol*, 2010, **1**, 1-4

16. G. Tron, F. Pagliai, E. Del Grosso. A. A. Genazzani and G. Sorba, *J. Med.Chem*, 2005, **48**, 3260-3268

17. I. Damljanovic, M. Vukicevic and R. D. Vukicevic, *Monatshefte für Chemie*, 2006, **137**, 301-305.

18. K.C. Liu, B.R. Shelton and R. K. Howe, *J. Org. Chem*, 1980, **45**, 3916-3918.

19. Kwang-Jin Hwang, Y. C. Park, H. Jin Kim, and J. H. Lee, *J. Biochem.,* 1998, **62**, 9, 1693-1697.

20. M. Uyanik and K. Ishihara, *Org., Synth.*, 2012, **89**, 105-114

21. E. Castagnetti, M. Schlosser, *Eur. J. Org. Chem*, 2001, 691-695

22. L. Huang, N. Teumelsan, X. Huang, *J. Chem. Eur*, 2006, **12**, 5246-5252

23. L. Niu, H. Zhang, H. Yang and H. Fu, *Synlett*, 2014, **25**, 07, 995-1000

24. A. Modvig, T. L. Anderson, R. H. Taaning, A. T. Lindhardt and T. Skrydstrup. *J. Org. Chem.*, 2014, **79**, 12, 5861-5868

25. N. K. Downer and Y. A. Jackson, *Org. Biomol. Chem.,* 2004, **2**, 3039-3043

26. Q. Jing andR. B. Silverman, *J. Bioorg. Med. Chem.*, 2013, **21**, 5323-5331.

27. C. Osuch and R. Levine*, J. Am. Chem. Soc.*, 1956, 1723-1725.

28. T.W. Hart, *Tetrahedron Letters*, 1985, **26**, (16), 2013-2016

29. R. J. Pearson, PhD thesis, University of St. Andrews, 2001

30. P. H. MacArthur, S. Shiva and M. T. Gladwin, *J. Chromotogr. B.,* 2007, **851**, 93-105

31. Nitric oxide analyser™ 280i operation and matainence manual, 2000, Sievers Instruments Inc.

Appendices

AP01-Single crystal raw data for compound 103

A. Crystal Data

Empirical Formula	$C_{16}H_{18}N_4O_4$
Formula Weight	330.34
Crystal Colour, Habit	colourless, prism
Crystal Dimensions	0.200 X 0.200 X 0.200 mm
Crystal System	triclinic
Lattice Type	Primitive
Lattice Parameters	a = 7.2312(8) Å
	b = 7.8356(9) Å
	c = 8.4677(9) Å
	α = 64.604(9) °
	β = 66.847(10) °
	γ = 73.147(12) °
	V = 394.24(9) Å^3
Space Group	P-1 (#2)
Z value	1
D_{calc}	1.391 g/cm^3
F_{000}	174.00
μ(MoKα)	1.023 cm^{-1}

B. Intensity Measurements

Diffractometer	XtaLAB P200
Radiation	MoKα (λ = 0.71075 Å) multi-layer mirror monochromated
Voltage, Current	45kV, 66mA
Temperature	-180.0$^{\text{O}}$C
Detector Aperture	83.8 x 70.0 mm
Data Images	1441 exposures
□ oscillation Range (□=54.0, □=0.0)	-75.0 - 105.0$^{\text{O}}$
Pixel Size	0.172 mm
2□$_{max}$	50.7$^{\text{O}}$
No. of Reflections Measured	Total: 5339 Unique: 1422 (R_{int} = 0.0693)
Corrections	Lorentz-polarization Absorption (trans. factors: 0.501 - 0.980) Secondary Extinction (coefficient: 3.23000e-002)

C. Structure Solution and Refinement

Structure Solution	Direct Methods (SIR2011)
Refinement	Full-matrix least-squares on F^2
Function Minimized	$\Sigma \, w \, (F_o^2 - F_c^2)^2$
Least Squares Weights	$w = 1/ [\, \sigma^2(F_o^2) + (0.0629 \cdot P)^2 + 0.0824 \cdot P \,]$ where $P = (Max(F_o^2,0) + 2F_c^2)/3$
$2\theta_{max}$ cutoff	50.7^o
Anomalous Dispersion	All non-hydrogen atoms
No. Observations (All reflections)	1422
No. Variables	110
Reflection/Parameter Ratio	12.93
Residuals: R1 ($I > 2.00\sigma(I)$)	0.0504
Residuals: R (All reflections)	0.0554
Residuals: wR2 (All reflections)	0.1494
Goodness of Fit Indicator	1.181
Max Shift/Error in Final Cycle	0.000
Maximum peak in Final Diff. Map	$0.27 \, e^-/\text{Å}^3$
Minimum peak in Final Diff. Map	$-0.30 \, e^-/\text{Å}^3$

Table 1. Atomic coordinates and B_{iso}/B_{eq}

Atom	X	Y	Z	B_{eq}
O1	0.6342(2)	0.6840(2)	0.2209(2)	1.82(4)
O8	0.2796(2)	0.72819(19)	0.4219(2)	1.47(3)
N1	0.5174(3)	0.5659(2)	0.2687(3)	1.26(4)
N7	0.3315(3)	0.5715(2)	0.3702(2)	1.37(4)
C1	0.5930(3)	0.4072(3)	0.2005(3)	1.27(4)
C2	0.4985(3)	0.2449(3)	0.2918(3)	1.54(4)
C3	0.5715(4)	0.1007(3)	0.2189(3)	1.69(4)
C4	0.7372(4)	0.1191(3)	0.0606(3)	1.70(4)
C5	0.8327(4)	0.2806(3)	-0.0254(3)	1.65(4)
C6	0.7585(3)	0.4278(3)	0.0447(3)	1.49(4)
C9	0.0707(3)	0.7279(3)	0.5415(3)	1.60(4)
C10	0.0071(3)	0.9099(3)	0.5837(3)	1.48(4)

$B_{eq} = 8/3\ \pi^2(U_{11}(aa^*)^2 + U_{22}(bb^*)^2 + U_{33}(cc^*)^2 + 2U_{12}(aa^*bb^*)\cos\gamma + 2U_{13}(aa^*cc^*)\cos\beta + 2U_{23}(bb^*cc^*)\cos\alpha)$

Table 2. Atomic coordinates and B_{iso} involving hydrogen atoms

Atom	x	y	z	B_{iso}
H2	0.38661	0.23273	0.40133	1.844
H3	0.50778	-0.01072	0.27770	2.033
H4	0.78563	0.02063	0.01068	2.036
H5	0.94840	0.29087	-0.13176	1.980
H6	0.82113	0.53987	-0.01419	1.786
H9A	0.06006	0.61482	0.65655	1.915
H9B	-0.01828	0.72375	0.47967	1.915
H10A	0.10651	0.91775	0.63316	1.778
H10B	-0.12687	0.90406	0.68030	1.778

Table 3. Anisotropic displacement parameters

Atom	U_{11}	U_{22}	U_{33}	U_{12}	U_{13}	U_{23}
O1	0.0194(10)	0.0161(8)	0.0338(10)	-0.0050(7)	-0.0035(7)	-0.0118(7)
O8	0.0164(9)	0.0142(8)	0.0259(9)	0.0016(6)	-0.0047(7)	-0.0120(7)
N1	0.0139(11)	0.0120(9)	0.0215(10)	0.0014(7)	-0.0063(8)	-0.0070(7)
N7	0.0174(11)	0.0130(9)	0.0230(10)	0.0019(7)	-0.0076(9)	-0.0093(8)
C1	0.0154(12)	0.0132(10)	0.0218(12)	0.0031(8)	-0.0093(10)	-0.0084(9)
C2	0.0153(13)	0.0176(10)	0.0240(12)	-0.0005(9)	-0.0051(10)	-0.0082(9)
C3	0.0195(13)	0.0149(10)	0.0321(13)	-0.0006(9)	-0.0103(11)	-0.0094(9)
C4	0.0230(13)	0.0183(11)	0.0275(13)	0.0038(9)	-0.0118(11)	-0.0129(9)
C5	0.0208(13)	0.0204(11)	0.0201(12)	0.0022(9)	-0.0068(10)	-0.0090(9)
C6	0.0197(13)	0.0149(10)	0.0208(12)	-0.0010(9)	-0.0078(10)	-0.0050(9)
C9	0.0147(13)	0.0179(11)	0.0252(12)	-0.0003(9)	-0.0029(10)	-0.0095(9)
C10	0.0157(12)	0.0175(11)	0.0227(12)	0.0026(9)	-0.0064(10)	-0.0097(10)

The general temperature factor expression: $\exp(-2\pi^2(a^{*2}U_{11}h^2 + b^{*2}U_{22}k^2 + c^{*2}U_{33}l^2 + 2a^*b^*U_{12}hk + 2a^*c^*U_{13}hl + 2b^*c^*U_{23}kl))$

Table 4. Bond lengths (Å)

Atom	Atom	Distance	Atom	Atom	Distance
O1	N1	1.263(3)	O8	N7	1.380(3)
O8	C9	1.451(2)	N1	N7	1.280(2)
N1	C1	1.467(3)	C1	C2	1.388(3)
C1	C6	1.374(3)	C2	C3	1.390(4)
C3	C4	1.388(3)	C4	C5	1.389(3)
C5	C6	1.395(4)	C9	C10	1.517(4)
C10	C10[1]	1.526(3)			

Symmetry Operators:

(1) -X,-Y+2,-Z+1

Table 5. Bond lengths involving hydrogens (Å)

Atom	Atom	Distance	Atom	Atom	Distance
C2	H2	0.95	C3	H3	0.95
C4	H4	0.95	C5	H5	0.95
C6	H6	0.95	C9	H9A	0.99
C9	H9B	0.99	C10	H10A	0.99
C10	H10B	0.99			

Table 6. Bond angles (^{o})

Atom	Atom	Atom	Angle	Atom	Atom	Atom	Angle
N7	O8	C9	107.22(18)	O1	N1	N7	126.4(2)
O1	N1	C1	119.25(16)	N7	N1	C1	114.3(2)
O8	N7	N1	108.25(19)	N1	C1	C2	120.41(18)
N1	C1	C6	117.08(19)	C2	C1	C6	122.5(2)
C1	C2	C3	118.35(19)	C2	C3	C4	120.2(2)
C3	C4	C5	120.3(2)	C4	C5	C6	119.98(19)
C1	C6	C5	118.6(2)	O8	C9	C10	107.2(2)
C9	C10	C10^1	113.3(2)				

Symmetry Operators:

(1) -X,-Y+2,-Z+1

Table 7. Bond angles involving hydrogens (^{o})

Atom	Atom	Atom	Angle	Atom	Atom	Atom	Angle
C1	C2	H2	120.8	C3	C2	H2	120.8
C2	C3	H3	119.9	C4	C3	H3	119.9
C3	C4	H4	119.8	C5	C4	H4	119.8
C4	C5	H5	120	C6	C5	H5	120
C1	C6	H6	120.7	C5	C6	H6	120.7
O8	C9	H9A	110.3	O8	C9	H9B	110.3
C10	C9	H9A	110.3	C10	C9	H9B	110.3
H9A	C9	H9B	108.5	C9	C10	H10A	108.9
C9	C10	H10B	108.9	C10^1	C10	H10A	108.9
C10^1	C10	H10B	108.9	H10A	C10	H10B	107.7

Symmetry Operators:

(1) -X,-Y+2,-Z+1

Table 8. Torsion Angles(^{o})

(Those having bond angles > 160 or < 20 degrees are excluded.)

Atom 1	Atom 2	Atom 3	Atom 4	Angle	Atom 1	Atom 2	Atom 3	Atom 4	Angle
N7	O8	C9	C10	-174.73 (15)	C9	O8	N7	N1	-178.17 (16)
O1	N1	N7	O8	-0.9(3)	O1	N1	C1	C2	159.35 (19)
O1	N1	C1	C6	-20.8(3)	N7	N1	C1	C2	-22.4(3)
N7	N1	C1	C6	157.48 (19)	C1	N1	N7	O8	-179.03 (16)
N1	C1	C2	C3	178.0 (2)	N1	C1	C6	C5	-179.15 (19)
C2	C1	C6	C5	0.7(4)	C6	C1	C2	C3	-1.8(4)
C1	C2	C3	C4	1.1(4)	C2	C3	C4	C5	0.6(4)
C3	C4	C5	C6	-1.8(4)	C4	C5	C6	C1	1.1(4)
O8	C9	C10	C10^1	67.4(2)	C9	C10	C10^1	C9^1	180.00 (18)

Symmetry Operators:

(1) -X,-Y+2,-Z+1

Table 9. Intramolecular contacts less than 3.60 Å

Atom	Atom	Distance	Atom	Atom	Distance
O1	O8	2.4801(19)	O1	C2	3.589(3)
O1	C6	2.744(3)	O8	C1	3.518(3)
O8	C10^1	2.982(2)	N1	C9	3.414(3)
N7	C2	2.735(3)	N7	C6	3.515(3)
C1	C4	2.747(4)	C2	C5	2.788(3)
C3	C6	2.788(3)			

Symmetry Operators:

(1) -X,-Y+2,-Z+1

Table 10. Intramolecular contacts less than 3.60 Å involving hydrogens

Atom	Atom	Distance	Atom	Atom	Distance
O1	H6	2.448	O8	H10A	2.532
O8	H10A[1]	3.336	O8	H10B	3.241
O8	H10B[1]	2.653	N1	H2	2.656
N1	H6	2.574	N7	H2	2.478
N7	H9A	2.535	N7	H9B	2.457
C1	H3	3.248	C1	H5	3.242
C2	H4	3.264	C2	H6	3.276
C3	H5	3.265	C4	H2	3.269
C4	H6	3.272	C5	H3	3.265
C6	H2	3.275	C6	H4	3.268
C9	H10A[1]	2.728	C9	H10B[1]	2.728
C10	H9A[1]	3.387	C10	H9B[1]	2.704
H2	H3	2.351	H3	H4	2.334
H4	H5	2.337	H5	H6	2.356
H9A	H10A	2.407	H9A	H10A[1]	3.598
H9A	H10B	2.325	H9B	H10A	2.868
H9B	H10A[1]	2.52	H9B	H10B	2.422
H9B	H10B[1]	2.951	H10A	H10A[1]	2.865
H10A	H10B[1]	2.377	H10B	H10B[1]	2.865

Symmetry Operators:

(1) -X,-Y+2,-Z+1

Table 11. Intermolecular contacts less than 3.60 Å

Atom	Atom	Distance	Atom	Atom	Distance
O1	O8[1]	3.4504(19)	O1	N7[1]	3.241(3)
O1	C3[2]	3.158(3)	O1	C4[2]	3.275(3)
O1	C5[3]	3.590(3)	O1	C9[1]	3.582(3)
O8	O1[1]	3.4504(19)	O8	N1[1]	3.196(2)
O8	C1[1]	3.322(3)	O8	C2[1]	3.492(4)
O8	C3[2]	3.514(3)	N1	O8[1]	3.196(2)
N1	N1[1]	3.519(3)	N1	N7[1]	3.290(3)
N1	C4[4]	3.572(3)	N1	C5[4]	3.509(4)
N7	O1[1]	3.241(3)	N7	N1[1]	3.290(3)
N7	N7[1]	3.542(3)	N7	C4[4]	3.546(3)
N7	C5[4]	3.210(4)	C1	O8[1]	3.322(3)
C1	C6[4]	3.519(4)	C1	C9[1]	3.537(4)
C2	O8[1]	3.492(4)	C3	O1[5]	3.158(3)
C3	O8[5]	3.514(3)	C4	O1[5]	3.275(3)
C4	N1[4]	3.572(3)	C4	N7[4]	3.546(3)
C5	O1[3]	3.590(3)	C5	N1[4]	3.509(4)
C5	N7[4]	3.210(4)	C6	C1[4]	3.519(4)
C9	O1[1]	3.582(3)	C9	C1[1]	3.537(4)

Symmetry Operators:

(1) -X+1,-Y+1,-Z+1   (2) X,Y+1,Z

(3) -X+2,-Y+1,-Z   (4) -X+1,-Y+1,-Z

(5) X,Y-1,Z

Table 12. Intermolecular contacts less than 3.60 Å involving hydrogens

Atom	Atom	Distance	Atom	Atom	Distance
O1	H2^1	3.47	O1	H3^2	2.483
O1	H4^2	2.728	O1	H5^3	2.854
O1	H9A^1	2.858	O8	H2^1	3.439
O8	H3^2	2.575	O8	H4^4	3.486
O8	H5^4	3.524	N1	H3^2	3.331
N1	H9A^1	3.16	N7	H3^2	3.52
N7	H5^4	3.068	N7	H9B^5	3.217
C1	H9A^1	3.122	C1	H10A^1	3.051
C2	H3^6	3.292	C2	H6^4	3.51
C2	H9B^5	3.239	C2	H10A^1	2.968
C2	H10B^5	3.118	C3	H2^6	3.218
C3	H10A^1	2.992	C3	H10B^5	2.992
C4	H4^7	3.195	C4	H5^7	3.321
C4	H10A^1	3.092	C5	H4^7	3.073
C5	H6^3	3.386	C5	H9A^8	3.127
C5	H9B^4	3.554	C5	H10A^1	3.156
C6	H6^3	3.024	C6	H9A^8	3.129
C6	H9A^1	3.141	C6	H10A^1	3.155
C9	H2^5	3.089	C9	H5^9	3.445
C9	H5^4	3.592	C9	H6^9	3.321
C10	H2^5	3.288	C10	H3^2	3.571
C10	H3^5	3.394	C10	H6^9	3.464
H2	O1^1	3.47	H2	O8^1	3.439
H2	C3^6	3.218	H2	C9^5	3.089
H2	C10^5	3.288	H2	H2^6	3.499
H2	H3^6	2.793	H2	H9A^5	3.257
H2	H9B^5	2.426	H2	H10A^{10}	3.109
H2	H10A^1	3.444	H2	H10B^5	2.825
H3	O1^{10}	2.483	H3	O8^{10}	2.575
H3	N1^{10}	3.331	H3	N7^{10}	3.52
H3	C2^6	3.292	H3	C10^{10}	3.571
H3	C10^5	3.394	H3	H2^6	2.793
H3	H10A^{10}	3.228	H3	H10A^1	3.491
H3	H10B^5	2.562	H4	O1^{10}	2.728
H4	O8^4	3.486	H4	C4^7	3.195
H4	C5^7	3.073	H4	H4^7	2.963
H4	H5^7	2.718	H4	H10A^{11}	3.398

Table 12. Intermolecular contacts less than 3.60 Å involving hydrogens (continued

Atom	Atom	Distance	Atom	Atom	Distance
H4	H10B^{11}	3.086	H5	O1^3	2.854
H5	O8^4	3.524	H5	N7^4	3.068
H5	C4^7	3.321	H5	C9^8	3.445
H5	C9^4	3.592	H5	H4^7	2.718
H5	H6^3	3.22	H5	H9A^8	2.541
H5	H9B^8	3.559	H5	H9B^4	2.834
H6	C2^4	3.51	H6	C5^3	3.386
H6	C6^3	3.024	H6	C9^8	3.321
H6	C10^8	3.464	H6	H5^3	3.22
H6	H6^3	2.562	H6	H9A^8	2.549
H6	H9A^1	3.11	H6	H10B^8	2.916
H9A	O1^1	2.858	H9A	N1^1	3.16
H9A	C1^1	3.122	H9A	C5^9	3.127
H9A	C6^9	3.129	H9A	C6^1	3.141
H9A	H2^5	3.257	H9A	H5^9	2.541
H9A	H6^9	2.549	H9A	H6^1	3.11
H9A	H9B^5	3.438	H9B	N7^5	3.217
H9B	C2^5	3.239	H9B	C5^4	3.554
H9B	H2^5	2.426	H9B	H5^9	3.559
H9B	H5^4	2.834	H9B	H9A^5	3.438
H9B	H9B^5	3.314	H10A	C1^1	3.051
H10A	C2^1	2.968	H10A	C3^1	2.992
H10A	C4^1	3.092	H10A	C5^1	3.156
H10A	C6^1	3.155	H10A	H2^2	3.109
H10A	H2^1	3.444	H10A	H3^2	3.228
H10A	H3^1	3.491	H10A	H4^{12}	3.398
H10B	C2^5	3.118	H10B	C3^5	2.992
H10B	H2^5	2.825	H10B	H3^5	2.562
H10B	H4^{12}	3.086	H10B	H6^9	2.916

Symmetry Operators:

(1) -X+1,-Y+1,-Z+1

(2) X,Y+1,Z

(3) -X+2,-Y+1,-Z

(4) -X+1,-Y+1,-Z

(5) -X,-Y+1,-Z+1

(6) -X+1,-Y,-Z+1

(7) -X+2,-Y,-Z

(8) X+1,Y,Z-1

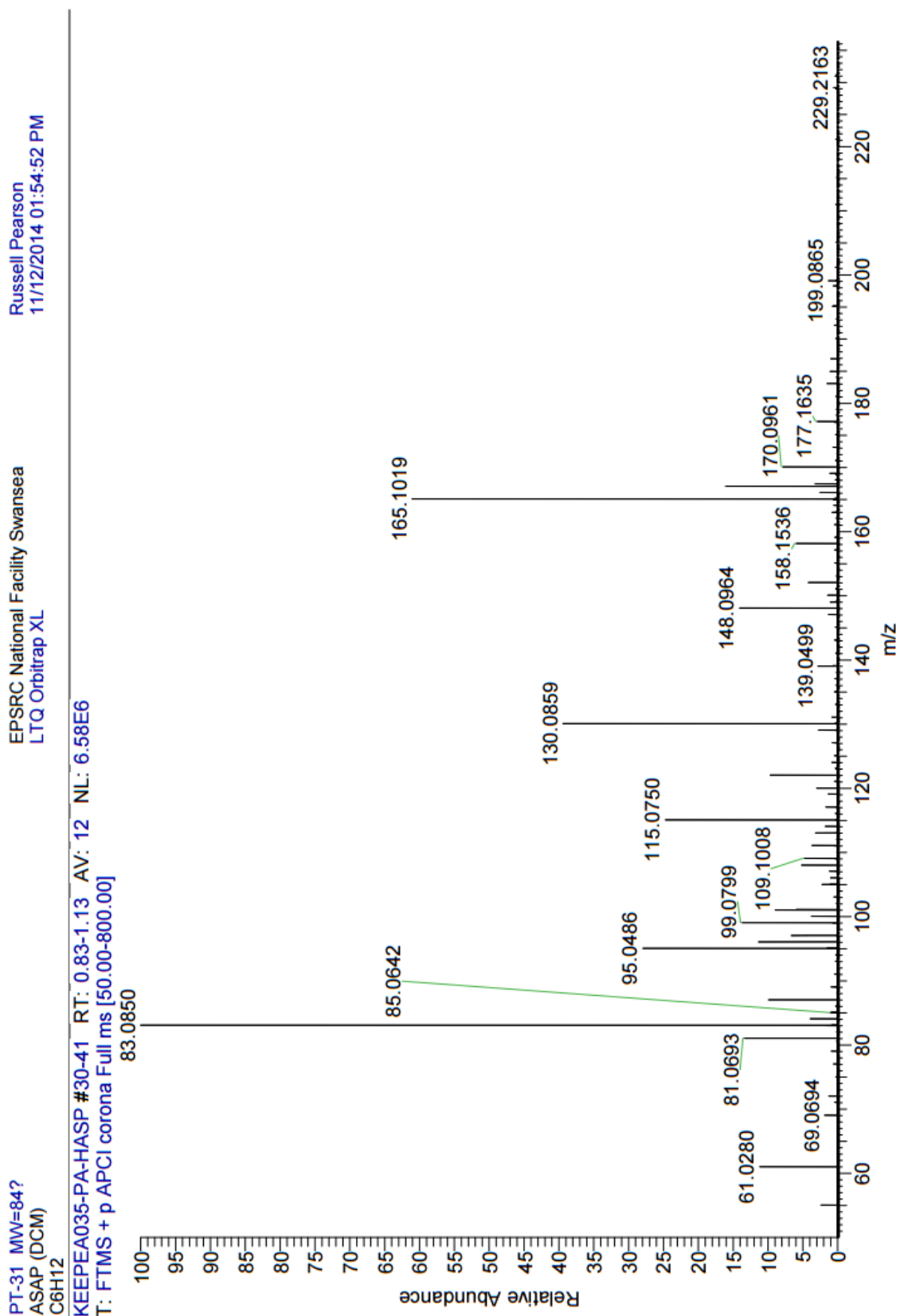(9) X-1,Y,Z+1

(10) X,Y-1,Z

(11) X+1,Y-1,Z-1

(12) X-1,Y+1,Z+1
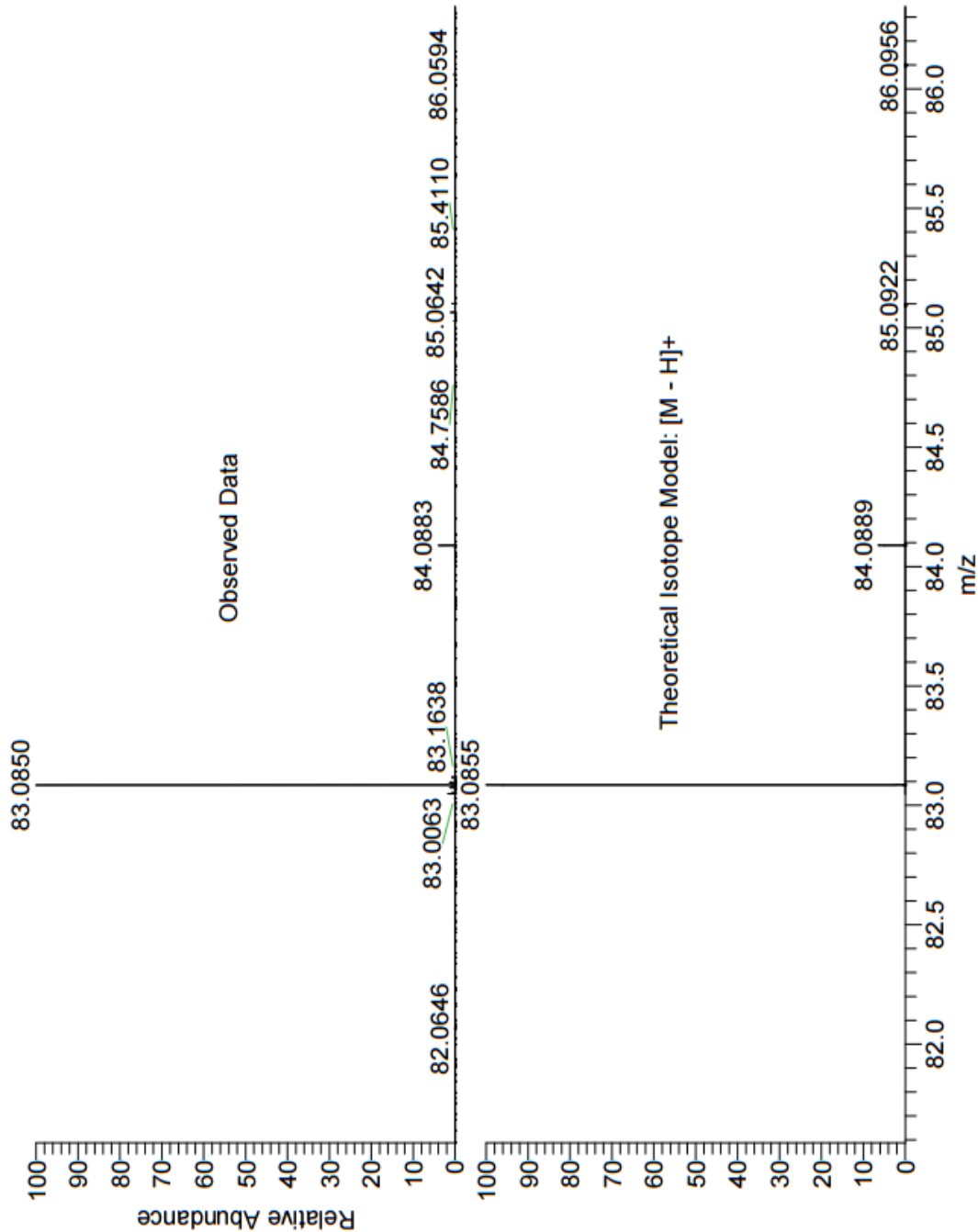
AP02- HRMS of cyclohexane, formed from 104 decomposition

PT-31 MW=84?
ASAP (DCM)
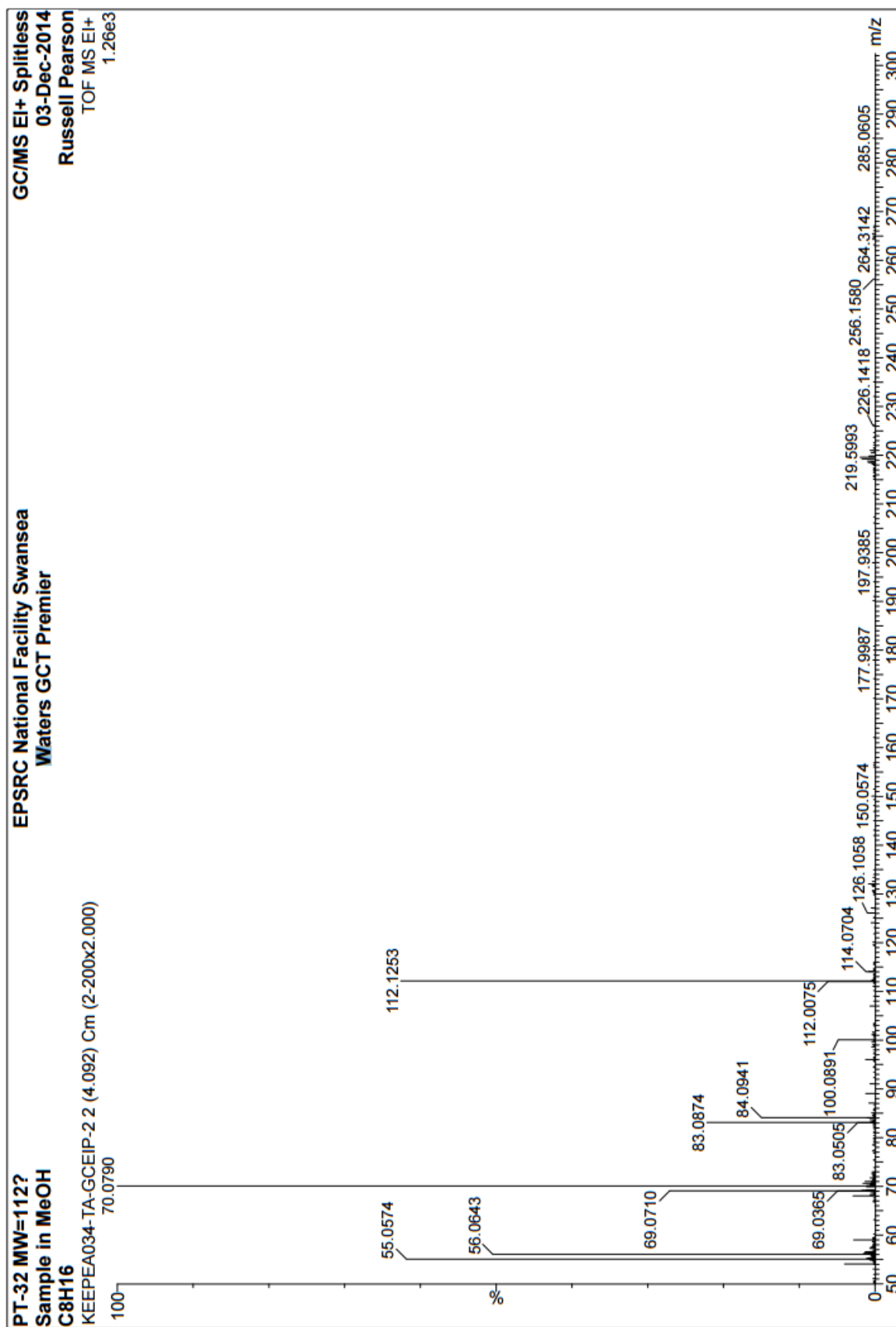C6H12

EPSRC National Facility Swansea
LTQ Orbitrap XL

Russell Pearson
11/12/2014 01:54:52 PM

KEEPEA035-PA-HASP #30-41   RT: 0.83-1.13   AV: 12   NL: 6.58E6
T: FTMS + p APCI corona Full ms [50.00-800.00]

AP03- HRMS of cyclooctane, formed from 105 decomposition

Elemental Composition Report

Single Mass Analysis

Tolerance = 10.0 mDa / DBE: min = -1.5, max = 50.0
Element prediction: Off

Monoisotopic Mass, Odd and Even Electron Ions
14 formula(e) evaluated with 1 results within limits (up to 150 best isotopic matches for each mass)
Elements Used:
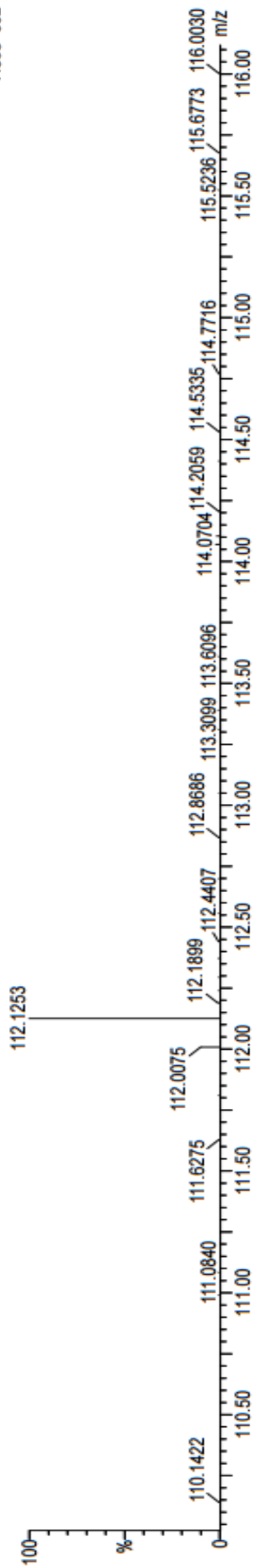C: 0-500   H: 0-1000   O: 0-200

PT-32 MW=112?
Sample in MeOH
C8H16
KEEPEA034-TA-GCEIP-2 2 (4.092) Cm (2-200x2.000)

EPSRC National Facility Swansea
Waters GCT Premier

GC/MS EI+ Splitless
03-Dec-2014
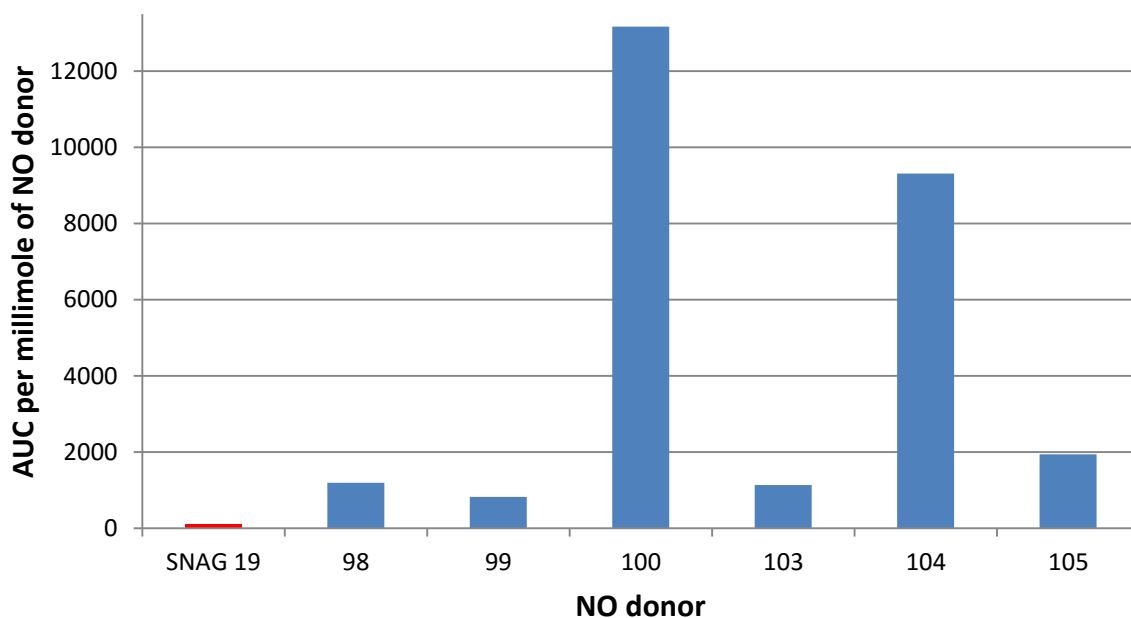Russell Pearson
TOF MS EI+
7.86e+002

| Minimum: | | | | -1.5 | | |
Maximum:		10.0	10.0	50.0		
Mass	Calc. Mass	mDa	PPM	DBE	i-FIT	Formula
112.1252	112.1252	0.0	0.0	1.0	326.2	C8 H16

AP04- Comparison of SNAG and cupferron compounds

Comparison of SNAG and Cupferron derivatives in the presence of light (254nm) at 37°C

Graph 27: Comparison of SNAG and cupferron compounds 98-105 in the presence of light (254nm) NB: Under these conditions the parent cupferron compound 56 produced too much NO for the instrument to detect and is hence not included on the graph. The AUC measured has been divided by the concentration of the initial NO-donor solution to obtain the y axis.

Comparison of SNAG 19, Cupferron and its derivatives 98-105 under thermal conditions (37°C)
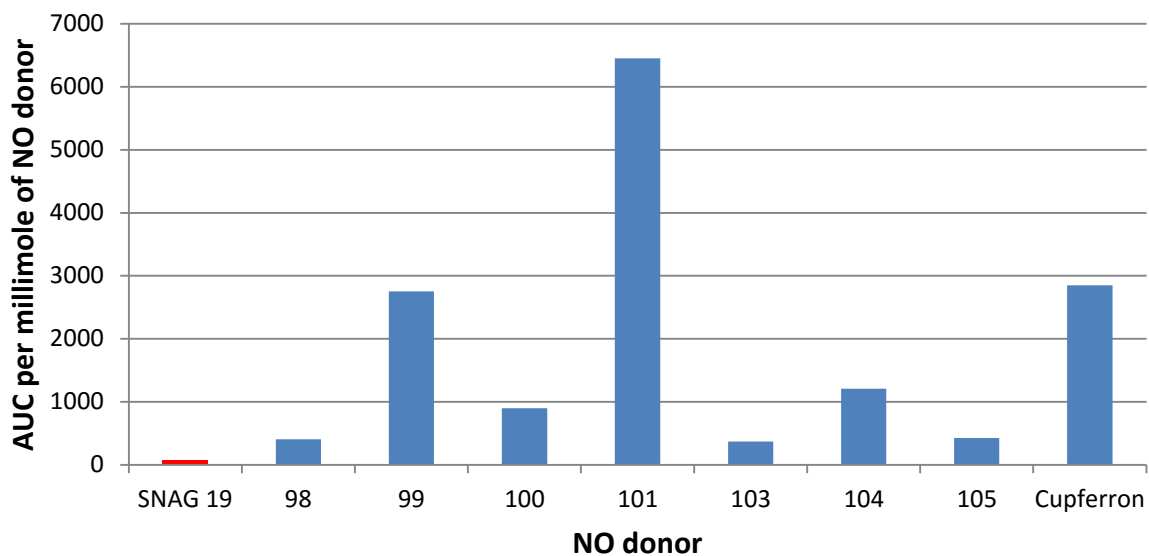
Graph 28: Comparison of SNAG **19** with cupferron and its alkylated derivatives **99-105** at 37°C. The AUC measured has been divided by the concentration of the initial NO-donor solution to obtain the y axis.